ABCB5 and the regulation of $p16^{INK4a}$ by non-coding RNA

Paul Braker

A Thesis presented for the degree of
Doctor of Philosophy

2014

Supervisors:
Prof. Kenneth Linton
Dr. Cleo Bishop

Centre for Cutaneous Research
The Blizard Institute
Barts and The London School of Medicine and Dentistry
Queen Mary, University of London

The universe is no narrow thing and the order within it is not constrained by any latitude in its conception to repeat what exists in one part in any other part. Even in this world more things exist without our knowledge than with it and the order in creation which you see is that which you have put there, like a string in a maze, so that you shall not lose your way. For existence has its own order and that no man's mind can compass, that mind itself being but a fact among others."

Cormac McCarthy "Blood Meridian; or, the Evening of Redness in the West"

Statement of originality

I, Paul Braker, confirm that the research included within this thesis is my own work or that where it has been carried out in collaboration with, or supported by others, that this is duly acknowledged below and my contribution indicated.

I attest that I have exercised reasonable care to ensure that the work is original, and does not to the best of my knowledge break any UK law, infringe any third party's copyright or other Intellectual Property Right, or contain any confidential material. I accept that the College has the right to use plagiarism detection software to check the electronic version of the thesis. I confirm that this thesis has not been previously submitted for the award of a degree by this or any other university.

Paul Braker

01/07/2014

Abstract

$p16^{INK4a}$ (p16) traps the cell at the restriction point of the cell cycle by binding to cyclin-dependent kinase 4/6 thus preventing the phosphorylation of the retinoblastoma protein (pRB). As p16 accumulates the cell stops dividing and becomes senescent. This study investigates the modulation of p16 function by the putative membrane protein ABCB5 and a group of five putative oncogenic microRNAs (oncomiRs).

ABCB5 is a poorly characterised member of the B-subfamily of human ATP Binding Cassette transporters. *ABCB5* is reportedly transcribed into four transcripts, one of which could potentially encode a full-length transporter (*ABCB5fl*) whilst a second could encode a half-transporter (*ABCB5β).* The other two transcripts (*ABCB5α* and *ABCB5γ*) could only encode short polypeptides. Exogenous expression of ABCB5fl and ABCB5β was achieved in HEK293T cells, but the recombinant protein expressed poorly and localised to the endoplasmic reticulum. Point mutations introduced into the ATP catalytic domain failed to improve expression levels suggesting that protein function was not deleterious to the cell. Exogenous expression in HEK293T cells also allowed commercial antibodies purportedly raised against ABCB5 isoforms to be tested. Several were found not to recognise ABCB5 necessitating re-interpretation of published data. However, one antibody recognised both ABCB5fl and ABCB5β, and was subsequently used to evaluate protein expression levels in other cell types.

siRNA knockdown of *ABCB5* in human mammary epithelial cells (HMECs) caused a concomitant reduction in p16 expression and an increase in cellular proliferation. Differential siRNAs and RT-qPCR analyses demonstrated *ABCB5β* to be the relevant transcript with respect to the reduction in p16 expression; however, no native ABCB5β protein was detected in HMECs. Together these data lead to the hypothesis that the *ABCB5β* transcript may act as a long non-coding RNA to regulate p16.

Exogenous expression of each of five distinct putative oncomiRs in HMECs was found to increase cellular proliferation and, surprisingly, increase p16 expression. These results mirror a phenotype commonly observed in p16-positive basal-like breast cancer (BLBC), an aggressive form of breast cancer with poor prognosis and few treatment options. Bioinformatic analysis of the predicted target genes for these oncomiRs identified multiple transcriptional regulators of pRB. These predictions, together with the work performed in a cellular model of p16-positive BLBC, suggest that the oncomiRs may cause unrestricted cell proliferation by indirectly reducing transcription of the pRB gene, *RB1*. In the absence of pRB, p16 expression is induced via a previously reported oncogene-induced senescence-like positive feedback loop. These data, and previously published observations, suggest that a similar mechanism may explain the basis of p16-positive BLBC.

Acknowledgements

I would like to thank Kenny Linton and Cleo Bishop for allowing me to be a part of their groups for the last few years. Your continued guidance and support has been invaluable throughout the course of my degree, and you have been essential in helping me push through even the most difficult times during the projects. Thank you.

A big thank you is required for everyone else in both Linton and Bishop groups for making this a great place to work. For all the knowledge, help, advice and food provided over the years to aid the passing of all the 'problematic' experiments.

To all my friends who have kept me going, but especially George, Joe, Marc and Michael. Thank you for giving me a constant distraction that I can escape to. From Alaska to The Vatican, you have been instrumental (ha) in helping me get through the hard parts.

Finally, I want to say a huge thank you to all of my family. Ruth, Jez, David and Su, without all of your constant support and encouragement I doubt this would have been possible. You have all provided me with the resolve I needed to get through. I am forever grateful.

Presentations

Public presentations, which contained parts of the data reported within this thesis, are as follows:

Oral Presentations

Blizard Institute Graduate Studies Day, Blizard Institute, London. Braker, P.J., Gillet, JP., Gottesman, M.M., Beach, D.H., Bishop, C.L., Linton, K.J. (2013). ABCB5 and p16: a membrane protein and the cell cycle.

UK ABC Researchers' Spring Meeting, Rothamsted Research, Harpenden. Braker, P.J., Gillet, JP., Gottesman, M.M., Beach, D.H., Bishop, C.L., Linton, K.J. (2013). ABCB5: A potential link to the cell cycle.

Poster Presentations

William Harvey Day, St Bartholomew's Hospital, London. Braker, P.J., Gillet, JP., Gottesman, M.M., Beach, D.H., Bishop, C.L., Linton, K.J. (2012). Knockdown of ABCB5 in HMECs causes a concomitant reduction in the tumour suppressor $p16^{INK4a}$.

Blizard Institute Graduate Studies Day, Blizard Institute, London. Braker, P.J., Gillet, JP., Gottesman, M.M., Beach, D.H., Bishop, C.L., Linton, K.J. (2012). ABCB5 and the effect of its expression on the tumour suppressor gene $p16^{INK4a}$.

4th FEBS Special Meeting, ATP-Binding Cassette Proteins: From Multidrug Resistance to Genetic Diseases. *Innsbruck*. Braker, P.J., Gillet, JP., Gottesman, M.M., Beach, D.H., Bishop, C.L., Linton, K.J. (2012). ABCB5 and the effect of its expression on the tumour suppressor gene $p16^{INK4a}$.

William Harvey Day, St Bartholomew's Hospital, London. Braker, P.J., Gillet, JP., Gottesman, M.M., Beach, D.H., Bishop, C.L., Linton, K.J. (2011). ABCB5 expression and knockdown in Human Mammary Epithelial Cells.

Nomenclature

3'-UTR	3' untranslated region
5'-UTR	5' untranslated region
4-PB	sodium 4-phenylbutyrate
ABC	ATP binding cassette
ADAR	adenosine deaminases acting on RNA
Ago2	Argonaute-2
ANOVA	analysis of variance
antimiR	anti-miRNA
ATP	adenosine triphosphate
BLBC	basal-like breast cancer
BSA	bovine serum albumin
CDK	cyclin-dependent kinase
cDNA	complementary DNA
C. elegans	*Caenorhabditis elegans*
ChIP	chromatin immunoprecipitation
CK	cytokeratin
CML	chronic myelogenous leukaemia
DAPI	4',6-diamidino-2-phenylindole
DMEM	Dulbecco's modified Eagle's medium
D/P	Drosha/Pasha complex
DPBS	Dulbecco's phosphate buffered saline
dsDNA	double stranded DNA

E. coli	*Escherichia coli*
EDTA	ethlyenediaminetetraacetic acid
EGF	epidermal growth factor
EGFR	epidermal growth factor receptor
EGFP	enhanced green fluorescent protein
ER	endoplasmic reticulum
FBS	fetal bovine serum
fl	full-length
GWAS	genome-wide association studies
HDAC	histone deacetylase
HEK293	human embryonic kidney 293 cells
HEK293T	human embryonic kidney 293 cells expressing the SV40 large T antigen
HEPES	4-(2-hydroxyethyl)-1-piperazineethanesulphonic acid
HER2	human epidermal growth factor receptor 2
HMEC	normal 184 human mammary epithelial cells
HRP	horseradish peroxidase
IF	immunofluorescence
INK/ARF	*INK4b-ARF-INK4a*
LB	lysogeny broth
LDH	lactate dehydrogenase
lncRNA	long non-coding RNA
LSC	limbal stem cell
MAPK	mitogen-activated protein kinase
MDR	multidrug resistance
MEBM	mammary epithelial basal medium

MEGM	mammary epithelial grown medium
miRISC	miRNA induced silencing complex
miRNA	micro RNA
MMIC	malignant melanoma initiating cells
mRNA	messenger RNA
ncRNA	non-coding RNA
OIS	oncogene-induced senescence
oncomiR	oncogenic miRNA
OR	oestrogen receptor
p16	$p16^{INK4a}$
p21	$p21^{CIP1}$
P4	passage 4
P5	passage 5
P6	passage 6
P10	passage 10
P11	passage 11
P20	passage 20
P28	passage 28
PACT	protein activator of PKR
PBS	phosphate buffered saline
PcG	polycomb group
PCR	polymerase chain reaction
PEI	polyethyleneimine
PFA	paraformaldehyde
PR	progesterone receptor

pre-miRNA	precursor miRNA
pri-miRNA	primary miRNA
qPCR	quantitative PCR
RT-qPCR	reverse transcription quantitative PCR
RBP	RNA-binding protein
RIP	RBP immunoprecipitation
RISC	RNA induced silencing complex
RLC	RISC loading complex
RNAi	RNA interference
RNA-seq	RNA sequencing
RPMI	Roswell Park Memorial Institute
r-point	restriction point
RT	room temperature
RT-PCR	reverse transcription PCR
SASP	senescence-associated secretory phenotype
S. cerevisiae	*Saccharomyces cerevisiae*
SCC	squamous cell carcinoma
SCF	seed compliment frequency
SD	standard deviation
SDS	sodium dodecyl sulphate
SDS-PAGE	sodium dodecyl sulphate polyacrylamide gel electrophoresis
shRNA	short hairpin RNA
siRISC	siRNA induced silencing complex
siRNA	small interfering RNA
TBRP	Tar RNA binding protein

TBS	Tris buffered saline
TBS-T	Tris buffered saline supplemented with 0.2% Tween 20
TdT	terminal deoxynucleotidyl transferase
TMH	transmembrane helix
TNBC	triple-negative breast cancer
tRNA	transfer RNA
UTR	untranslated region
UV	ultraviolet
V5-6His	V5 and 6-histidine tag
VEGF	vascular endothelial growth factor

Contents

List of Figures

List of Tables

Chapter One

1 Introduction

1.1 The ABCs of ABCs

ATP Binding Cassette (ABC) proteins are a superfamily of integral membrane proteins, which use energy derived from the hydrolysis of ATP to perform a variety of functions in cells, but are primarily concerned with the transport of molecules across membranes (Linton and Holland, 2011). ABC proteins have been found in all organisms studied to date (Higgins, 1992), and often play crucial roles in organism survival. For example, Rad50 plays a key role in the repair of double strand breaks in *Saccharomyces cerevisiae* (*S. cerevisiae*) (Hopfner et al., 2000), and a wide array of proteins such as the ABC importer Znu (Desrosiers et al., 2010) are important for bacterial cell growth.

1.2 Mammalian ABC proteins

Humans have 48 ABC transporters genes, split between seven distinct subfamilies (Dean et al., 2001), most of which are currently believed to translocate molecules across the cell and intracellular membranes (Linton and Holland, 2011). ABC transporters in humans are mostly primary active pumps that comprise, minimally, four domains: two transmembrane domains (TMDs) each with six transmembrane helices that span the membrane and often impart specificity for the transport substrate, and two nucleotide binding domains (NBDs) that reside in the cytosol and hydrolyse ATP to drive the transport mechanism (Zolnerciks et al., 2011). Many of the human ABC transporters are important in normal physiology, and as such, their dysregulation or mutation can have health consequences, such as cystic fibrosis, which most commonly arises as a result of a deletion of codon 507 in ABCC7 (Bobadilla et al., 2002).

1.3 The ABCB subfamily of proteins

The ABCB subfamily of ABC transporters is unusual in that in contains both full- and half-transporters (Dean et al., 2001), and is the third largest subfamily, containing a total of 11 proteins (ABCB1 – ABCB11). Members of the subfamily are localised throughout the cell, with ABCB1, ABCB4 and ABCB11 in the plasma membrane (Thiebaut et al., 1987, Buschman et al., 1992, Gerloff et al., 1998), ABCB2 and ABCB3 in the endoplasmic reticulum (ER) (Lankat-Buttgereit and Tampé, 2002), ABCB6, ABCB7, ABCB8 and ABCB10 all within the mitochondria (Zutz et al., 2009), and ABCB9 found in the lysosomal compartments (Zhang et al., 2000).

ABCB1 plays an important role in multidrug resistance (MDR) in cancer, as it can transport a wide array of chemically diverse molecules, such as anthracyclines, epipodophyllotoxins and taxanes (Ambudkar et al., 1999). ABCB2 (TAP) and ABCB3 (TAP2) are half-transporters that dimarise to form the TAP1/2 (ABCB2/ABCB3) heterodimer, which also transports a wide array of antigenic peptides into the ER lumen for loading onto the major histocompatibility complex class I molecules, which is an essential process for antigen presentation (Lankat-Buttgereit and Tampé, 2002). ABCB4 and ABCB11 are both involved in bile secretion from the gall bladder in the liver, and transport phosphatidyl choline and bile salts (van Helvoort et al., 1996, Gerloff et al., 1998), respectively. ABCB6, ABCB7, ABCB8 and ABCB10 are thought to transport to molecules involved with Fe-S biosynthesis and iron metabolism (Zutz et al., 2009), and ABCB9 is highly expressed in testes although its function is, as of yet, unknown (Zhang et al., 2000).

One of the most recently discovered members of the ABCB subfamily is ABCB5, which was first identified in 2001 based upon its sequence homology to the other ABCB family members (Dean and Allikmets, 2001).

1.4 *ABCB5*

The *ABCB5* gene is located on chromosome 7p21, has 28 exons, and spans 141.8 kb of DNA. All of the ABCB full transporters originated from a single gene with a common ancestor in non-vertebrates that can be examined as far back as *Caenorhabditis elegans (C. elegans),* and yeast (Moitra et al., 2011). The only non-mammalian *ABCB5* can be found in *Xenopus*, suggesting that the gene may have been lost in some linages (Moitra et al., 2011). This same study also identified high levels of selection in both the TMDs and NBDs of *ABCB5*, signifying that these domains have kept their functional significance throughout evolution (Moitra et al., 2011).

1.5 *ABCB5* isoforms

From the *ABCB5* gene, four isoforms are known to be transcribed: full-length (ABCB5fl; NM_001163941.1); alpha (ABCB5α; NM_001163942.1); beta (ABCB5β; NM_178559.5); and gamma (ABCB5γ; NM_001163993.2; Figure 1-1; Figure 1-2; Figure 1-3). Of the four isoforms, ABCB5fl and ABCB5β are reported to be active transporters (see Section 1.7.2).

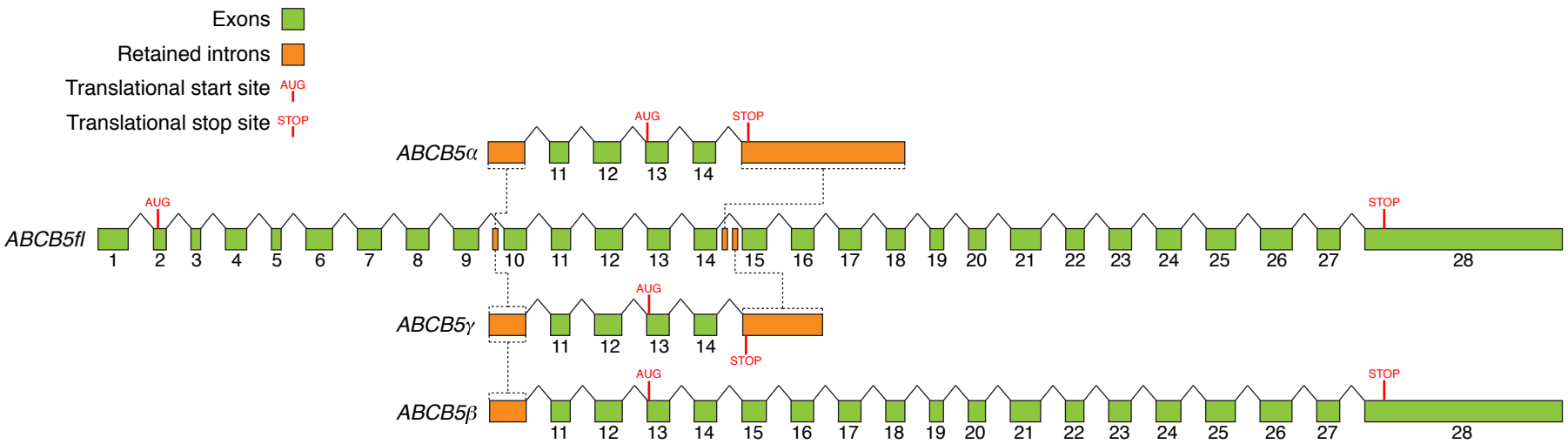

Figure 1-1. Exon and intron arrangement of the four *ABCB5* isoforms.

Cartoon showing the relative sizes of each of the 28 main exons (green) giving rise to ABCB5fl, and the mixture of introns (orange) and exons that comprise ABCB5α, ABCB5β and ABCB5γ. Translational start sites are denoted by (AUG), translational stop sites are marked by (STOP). Distance between exons is not indicative of intron length.

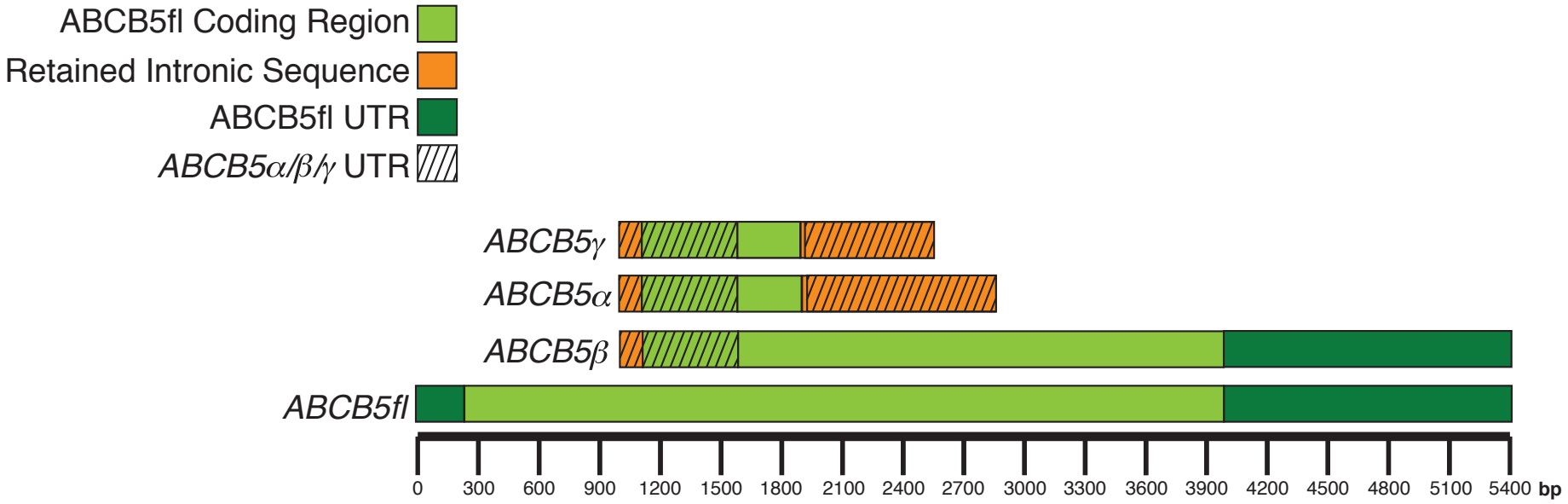

Figure 1-2. Relative mRNA size of the four *ABCB5* isoforms.

Cartoon illustrating the relative mRNA sizes of each of the *ABCB5* isoforms.

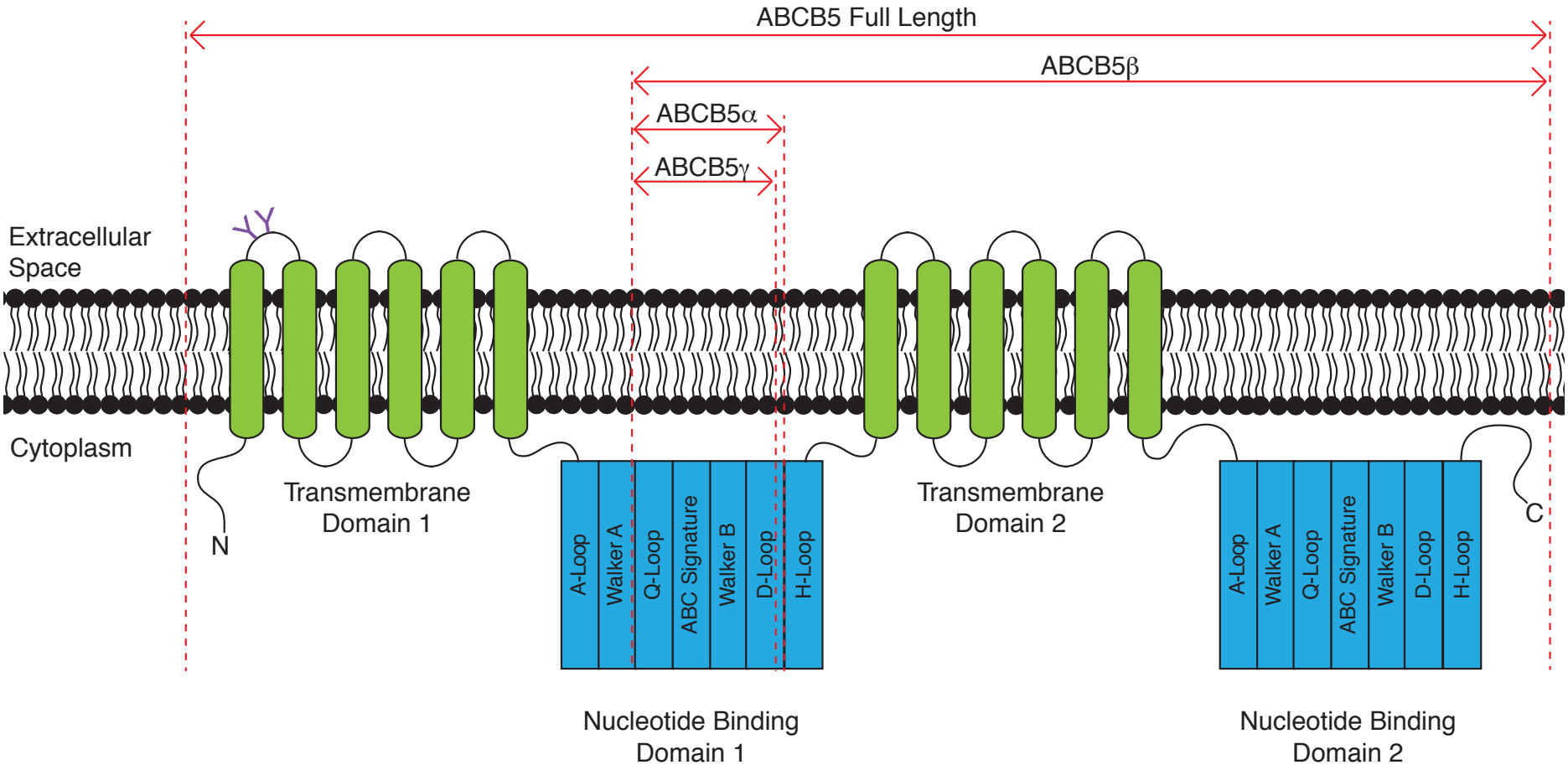

Figure 1-3. Topography of the four ABCB5 isoforms.

Transmembrane regions and nucleotide binding domains (NBDs) are represented in green and blue, respectively. Each NBD contains seven distinct and highly conserved motifs for nucleotide binding and hydrolysis. Red lines indicate the coding sequence of ABCB5α, ABCB5β, and ABCB5γ isoforms, compared to ABCB5fl. Purple 'Y's represent predicted glycosylation sites.

1.5.1 ABCB5fl

The 5401 nt mRNA of *ABCB5fl* is generated when the full 28 exons of the *ABCB5* gene are spliced together (Figure 1-1; Figure 1-2). This mRNA is then translated to create a protein of 1257 amino acids (Figure 1-3). The ABCB5fl protein has two TMDs and two NBDs, providing it with a structure similar to ABCB1, ABCB4 and ABCB11. Each of the TMDs contains six predicted transmembrane helices, and each of the NBDs contains the seven motifs required for effective ATP binding and hydrolysis: A-loop, Walker A. Q-loop, ABC signature, Walker B, D-loop and H-loop.

In order to gain a better appreciation of the structure of ABCB5fl, the three-dimensional structure was predicted using the crystal structure of the *Mus musculus* homologue of ABCB1, Abcb1a, as a template (Figure 1-4). This was carried out by uploading the amino acid sequence of ABCB5fl (NP_001157413.1) to the I-TASSER protein structure prediction server[I], alongside Abcb1a. In the predicted three-dimensional structure both NBDs appear more disorganised than in Abcb1a, although this is likely due to an imperfect prediction algorithm.

1.5.1.1 Nucleotide binding domains of ABCB5fl

ABCB5fl would contain two NBDs, both of which include the seven conserved motifs present in the majority of ABC proteins (Figure 1-5) (Kerr, 2002). Each NBD is split into two subdomains. The F1-type 'core' subdomain contains the Walker A (GxxGxGKS[S/T]) and Walker B (hhhhDE) motifs (where x is any amino acid, and h is

[I] The I-TASSER protein structure prediction server can be found at http://zhanglab.ccmb.med.umich.edu/I-TASSER/ (accessed April 2011).

any hydrophobic amino acid), along with the A- Q- D- and H- loops. The α-helical subdomain contains the ABC signature motif (LSGGQ), which aligns with the Walker A motif of the opposite NBD when both NBDs come together in a head-to-tail arrangement to bind ATP (Zolnerciks et al., 2011). Together, the presence of all of the

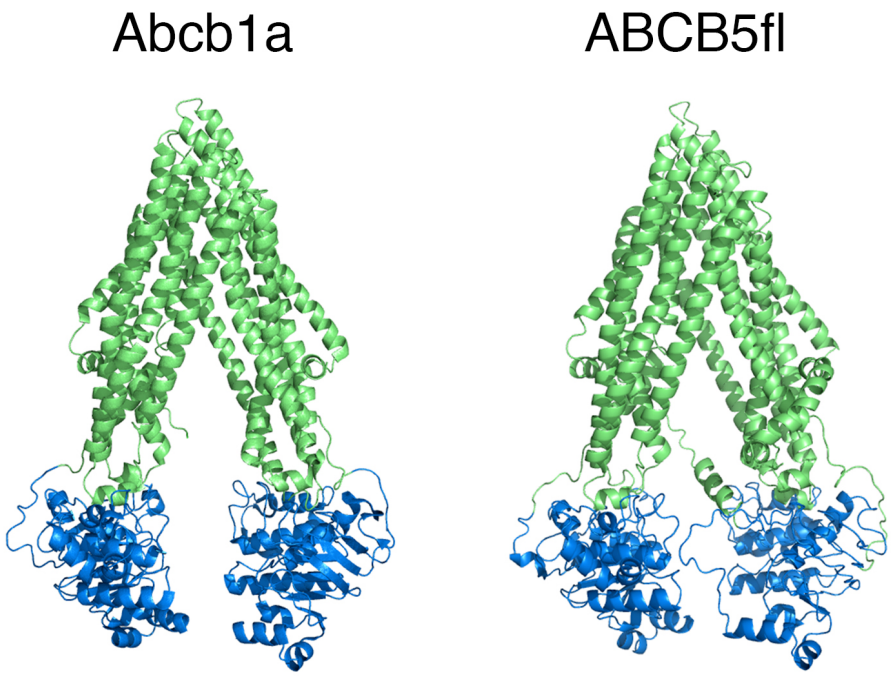

Figure 1-4. Predicted three-dimensional structure of ABCB5fl.

ABCB5fl three-dimensional model, based on the crystal structure of the ABCB1 mouse homologue Abcb1a (PDB number: 3D5U), generated using I-TASSER protein structure prediction server (Roy et al., 2010)[I]. Blue – nucleotide binding domains; green – transmembrane regions.

essential motifs on the two NBDs suggest that ABCB5fl should be able to bind and hydrolyse ATP to power substrate transport.

1.5.1.1 Transmembrane domains of ABCB5fl

ABCB5fl is predicted to include 12 transmembrane helices (TMHs), grouped into two transmembrane domains of six helices each (Moitra et al., 2011). The aforementioned

[I] The I-TASSER protein structure prediction server can be found at http://zhanglab.ccmb.med.umich.edu/I-TASSER/ (accessed April 2011).

predicted structure of ABCB5fl (Figure 1-4) shows that the TMHs are likely to be arranged in a similar manner to those of Abcb1a.

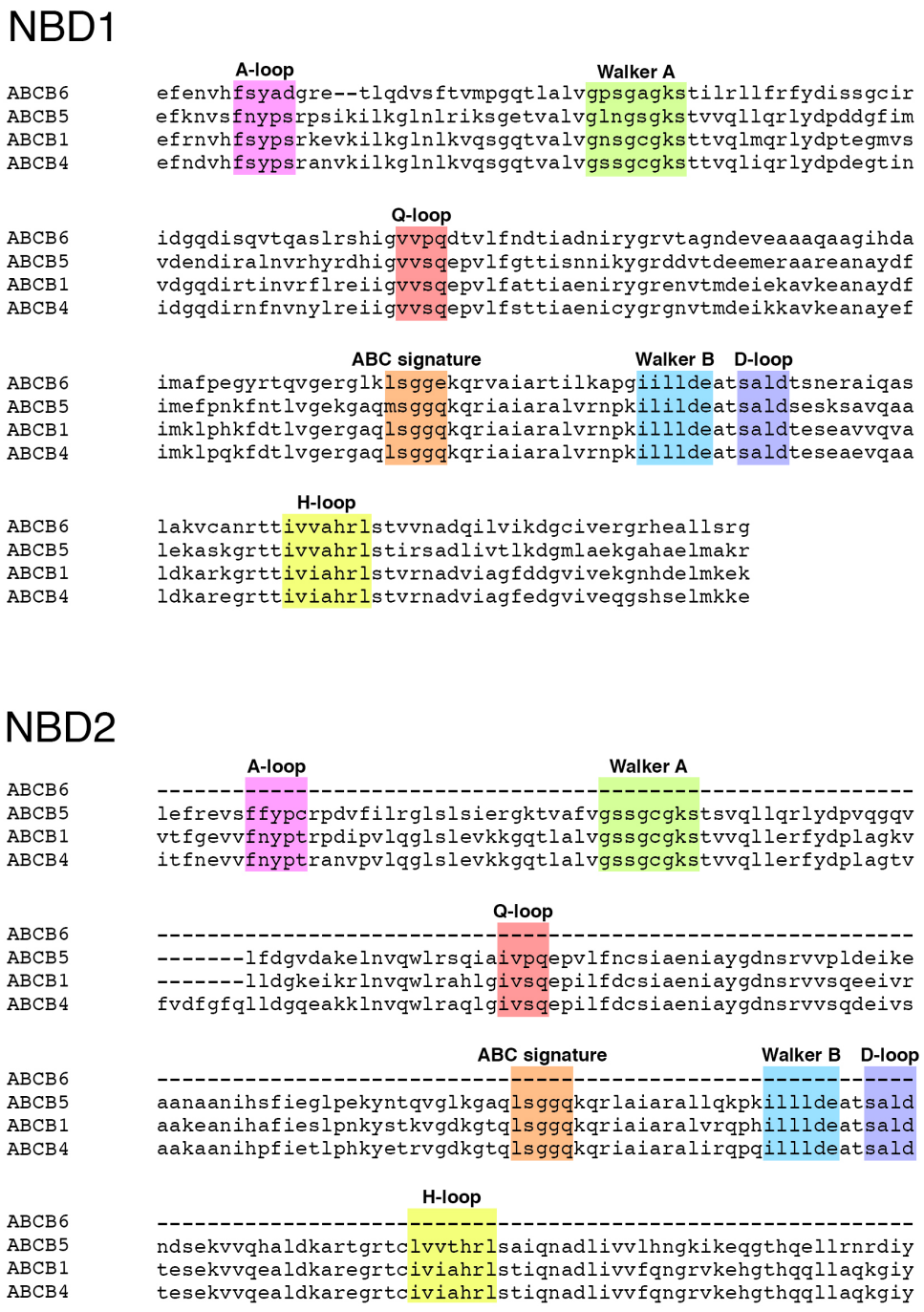

Figure 1-5. Conserved motifs in the nucleotide binding domains of ABCB transporters.

The Walker A (green), Q-loop (red), ABC signature (orange), Walker B (blue), D-loop (purple) and H-loop (yellow) motifs are conserved across ABCB family transporters. ABCB6 is a half-transporter and therefore does not have a second NBD.

1.5.1.2 Glycosylation of ABCB5fl

Glycosylation is known to be important for correct trafficking and function in multiple ABC transporters (Wojtowicz et al., 2012, Beers et al., 2013), and other membrane proteins (Hoosdally et al., 2009). ABCB5fl has two potential N-linked glycosylation sites present in the first extracellular loop (Figure 1-3). Because of the nature of its truncation, ABCB5β does not have these two potential glycosylation sites. There are multiple alternative sites throughout the protein, however none of these are predicted to be extracellular and so are unlikely to be available for glycosylation.

1.5.2 ABCB5α

ABCB5α is generated when a 306 nt section of intron 9 is spliced to exons 11, 12, 13 and 14 and a 1328 nt section of intron 14 (Figure 1-1). This splicing event creates an mRNA of 2247 nt (Figure 1-2), which could then be translated to produce a protein of 131 amino acids (Figure 1-3). The resulting protein would contain the Q-loop, ABC signature motif, Walker B, and D-Loop of NBD1, but no transmembrane helices. Without any transmembrane helices this protein would be unable to act as a half-transporter, or even attach to a membrane. This small protein was originally suggested to play a role by interacting with either mRNA or proteins (Gottesman, 2004, Chen et al., 2005a), although, as of yet, there is no empirical data to support this postulation.

1.5.3 ABCB5β

ABCB5β is just over half the length of ABCB5, arising from a splicing of the same 306 nt section of intron 9 found in ABCB5α, to exons 11 – 28 (Figure 1-1). The resulting mRNA sequence (4375 nt; Figure 1-2) could encode an 812 amino acid, C-terminal portion of the full-length protein with NBD1 (minus the Walker A motif), TMD2 and NBD2 present (Figure 1-3). The truncation of the N-terminal end would position the Q-

loop of NBD1 at the N-terminus (Chen et al., 2005). Due to its size and domain composition, ABCB5β has been suggested to function as a half-transporter, which could dimerise to produce a functional transporter, similar to the drug efflux pump ABCG2 (Woodward et al., 2011, Moitra et al., 2011) and the peptide transporters ABCB2 and ABCB3 (Lankat-Buttgereit and Tampé, 2002). Indeed, some published studies have claimed to measure transport function in ABCB5β$^+$ cells (see Section 1.7.2).

1.5.4 ABCB5γ

ABCB5γ is formed when the same 306 nt section of intron 9 present in ABCB5α and ABCB5β is spliced to exons 11, 12, 13 and 14, and an 805 nt section of intron 14 (unrelated to the section of intron 14 present in ABCB5α; Figure 1-1). This pattern of splicing creates an mRNA of 1724 nt, which potentially encodes a protein of 126 amino acids. This potential protein encodes a similar section of ABCB5fl to ABCB5α, including the Q-loop, ABC signature, Walker B and D-loop motifs of NBD1, although with a shorter amino acid sequence after the D-loop. As of yet, no suggestions as to the function of this protein have been made, although if translated, it is likely that it could act in a similar manner to ABCB5α given the near identical sequence.

1.6 *ABCB5* tissue expression pattern

Compared to many other genes, *ABCB5* is expressed at relatively low levels, and in only within certain compartments of the body. At present *ABCB5β* and *ABCB5α* expression has only been detected in normal melanocytes, placenta, retinal pigment and epithelial cells (Chen et al., 2005a, Volpicelli et al., 2014). High expression in melanoma cells however has been reported multiple times (Frank et al.,

2003, Chen et al., 2005a, Frank et al., 2005, Schatton et al., 2008, Lin et al., 2013), and it has been suggested that because expression of *ABCB5α* or *ABCB5β* is usually specific to pigment cells, that it may be involved in melanogenesis (Chen et al., 2005a). It should be noted that although the *ABCB5α* transcript would be unlikely to encode an ABC protein, it was the most common isoforms of *ABCB5* found expressed in a human melanoma cDNA library (Chen et al., 2005a).

1.7 Cancer treatment and chemotherapy resistance

Throughout history surgical resection has been the first choice for cancer treatment (Daviel and Parsons, 1755, Papavramidou et al., 2010), as it is provides rapid relief from tumour bulk for the patient (Zabel and Debus, 2004), and is commonly a very effective course of action (Cushing et al., 1999, Simmonds et al., 2006). However, tumours that cannot be treated surgically (such as leukaemia), tumours that have characteristically undefined edges (such as glioblastoma multiforme) (Lacroix et al., 2001), and tumours that have metastasised pose problems for this course of action. Treatment with toxic xenobiotic compounds (chemotherapy) and radiation (radiotherapy) are often therefore utilised instead of, or, in addition to, surgery.

The treatment of cancer with chemotherapy also has problems associated with it, such as the commonly known adverse side effects associated with treatment. One of the most difficult issues to overcome with chemotherapy is the multi-drug resistance (MDR) of some tumours (Baguley, 2010). MDR in cancer arises when the chemical compounds used to kill tumour cells are no longer effective, often because they are removed from, or compartmentalised within, the cancer cells by ABC transporter activity (Szakács et al., 2006), thus protecting the cell from damage.

1.7.1 ABC proteins in multi-drug resistance

ABC transporters were first recognised as having an important role in MDR, when Dano (1973) recognised the extrusion of daunomycin from MDR Ehrlich ascites tumour cells. Further study showed that it was the transport function of ABCB1 which was removing the compound from the cells (Juliano and Ling, 1976).

Since this original finding, several other ABC transporters have been linked to MDR in specific tumours, such as ABCG2 in breast cancer (Maciejczyk et al., 2012), while others are found more ubiquitously, such as ABCB1 (Scherf et al., 2000). Currently ABCA2 (Boonstra et al., 2004), ABCB1 (Ambudkar et al., 1999), ABCB5 (Frank et al., 2003, Frank et al., 2005), ABCC1 (Borst et al., 2000), ABCC2 (Cui et al., 1999, Borst et al., 2000), ABCC4 (Borst et al., 2000, Chen et al., 2001), and ABCG2 (Staud and Pavek, 2005) are reported to be up-regulated in cancer cell lines selected for MDR. Additionally, ABCB11 (Childs et al., 1998), ABCC3 (Borst et al., 2000), ABCC5 (Borst et al., 2000), ABCC6 (Belinsky et al., 2002), ABCC10 (Hopper-Borge et al., 2004), and ABCC11 (Guo et al., 2003) have all been described as conferring drug resistance to transfected cells.

All of these proteins are reported to transport multiple xenobiotic compounds including drugs from different chemical classes. As such, their expression in response to one chemotherapy regime can also render others ineffective. In an effort to combat MDR as a result of ABC transporter expression, inhibitors have been trialled in patients diagnosed with drug resistant cancers, however nearly all of these trials were found to be unsuccessful, either due to the tolerable doses of inhibitor being too low to produce

an effect (O'Brien et al., 2010), or due to the adverse side effects in participating patients (Dalton et al., 1995).

1.7.2 Evidence for ABCB5fl and ABCB5β in MDR

Although ABCB5 is one of the least well-characterised members of the B-subfamily, some experiments have been carried out with the objective of elucidating the function of the two largest isoforms. Due to their similarity with the other ABCB family transporters, it was postulated that both ABCB5fl and ABCB5β would be able to transport chemotherapeutic substrates, with ABCB5β dimerising to form a full transporter (Moitra et al., 2011).

The majority of research into the function of these proteins has been carried out in cell lines with endogenous ABCB5β expression. The first study was carried out in tandem with MCF-7 cells transfected with ABCB5β, and G3361 melanoma cells that endogenously expressed ABCB5β, but not ABCB5fl (as evaluated by antibody binding) (Frank et al., 2003, Frank et al., 2005). These studies reported that ABCB5β could efflux both rhodamine-123 and doxorubicin from the cells, and also suggested a role in the regulation of progenitor cell fusion (see Section 1.8).

Subsequently, two separate groups carried out studies into the function of ABCB5fl and ABCB5β, with exogenously expressed protein. Both concluded that ABCB5β was unable to transport the previously tested substrates from the transfected cells (Chen et al., 2009, Gillet et al., 2009, Kawanobe et al., 2012). One of these groups additionally found that ABCB5fl expression in naive cells could confer resistance to a variety of

chemotherapeutic compounds, such as anthracyclines, epipodophyllotoxins, and taxanes (Kawanobe et al., 2012).

1.8 ABCB5β, progenitor cell fusion, and membrane potential

The first two papers to report the function of ABCB5β also described a link to the fusion of progenitor cells, and the regulation of membrane potential in expressing cells (Frank et al., 2003, Frank et al., 2005). Initial characterisation of G3361 melanoma cells found that a small subset of the cells expressed ABCB5β, and this was found to coincide with CD133 expression, a known marker of stem and progenitor cells (Corbeil et al., 2000, Sanai et al., 2005). These ABCB5β$^+$ and CD133$^+$ cells were commonly observed to be binucleate or polynucleate, and through experimentation using differentially labelled cells (labelled with DiI and DiO), this was found to be due to the fusion of the ABCB5β$^+$ progenitor cells (Frank et al., 2003).

To further investigate the role of ABCB5β in progenitor cell fusion, the group assessed whether the function of ABCB5β regulated the membrane potential of these cells, as it had previously been shown that membrane potential is critical in cell fusion (Liu et al., 2003). When cells were treated with an antibody targeting ABCB5β, there was a significant increase in depolarised cells within the population (Frank et al., 2003, Frank et al., 2005), suggesting that ABCB5β functions to maintain membrane potential.

1.9 ABCB5β in cancer stem cells

After the small population of ABCB5β$^+$ cells in the G3361 melanoma cell lines was first suggested to mark progenitor cells (Frank et al., 2003), much of the following

studies carried out have been concerned with using ABCB5β expression to mark CSCs (cancer stem cells) in different tumours. The majority of these studies have investigated the expression of ABCB5β in the CSC-like sub-population of melanoma cells, namely the malignant melanoma initiating cells (MMICs).

These studies reported that by targeting the small subset of ABCB5β^+ cells within the tumour, tumours growth could be inhibited, and that these MMICs had a higher tumourogenic capacity than ABCB5- bulk tumour cells when used as a xenotransplant into NOD/SCID mice (Schatton et al., 2008, Gazzaniga et al., 2010, Vásquez-Moctezuma et al., 2010). The ABCB5β^+ MMICs were also identified as being able to evade the host anti-tumour immune system, and were suggested to play a critical role in melanoma immune evasion via immunomodulation, advancing tumour growth and therapeutic resistance (Schatton and Frank, 2009). ABCB5β^+ MMICs have also been found circulating in the peripheral blood of melanoma patients, which is reported to correlate with disease recurrence and progression (Ma et al., 2010, Cigna et al., 2011, Freeman et al., 2012, Reid et al., 2013).

ABCB5β expression has also been reported to mark a higher risk population in patients with acute leukaemia (Farawela et al., 2014, Yang et al., 2012), and oral squamous cell carcinoma (Richard et al., 2013). In one study, *ABCB5* was found to be significantly down-regulated in breast carcinoma, compared to normal breast tissue controls. This work did not distinguish between the different isoforms. More intriguingly however, up-regulation in *ABCB5* in breast carcinoma was found to correlate with the ability of the tumour to metastasise to the lymph nodes (Viktor Hlavac, Czech Republic National Institute of Public Health, personal communication)

In addition to marking CSCs and possible roles in MDR, *ABCB5* has been linked to the regulation of the cell cycle, in particular, the switch between a proliferative and senescent phenotype.

1.10 The cell cycle

The eukaryotic cell cycle is described by the series of stages that a cell goes through leading up to its division (Figure 1-6 panel A), and is controlled by a large regulatory network, with many features being conserved from yeast to humans (Bertoli et al., 2013). The five stages of the cycle are most commonly referred to as Gap 1 (G_1), DNA synthesis (S), Gap 2 (G_2), Mitosis (M), and quiescence, otherwise known as Gap 0 (G_0). Progression through the cell cycle is regulated by changes in gene expression as a result of the specific activities of cyclin-dependent kinases (CDKs), which are differentially expressed throughout the cell cycle (Lim and Kaldis, 2013). These changes in gene expression cause the various cyclins to accumulate at different points in the cycle (Figure 1-6 panel B), thus they regulate CDK activity, and control progression through the cell cycle.

The activity of CDKs indirectly regulate the expression of many genes which are important for cellular processes that occur in the subsequent phase of the cell cycle. In the majority of eukaryotes, the transcription of these genes occurs in three waves (Bähler, 2005) at the main phase transition points during the cell cycle, G_1 to S, G_2 to M, and M to G_1, where new expression profiles of genes are required for the next phase (Wittenberg and Reed, 2005).

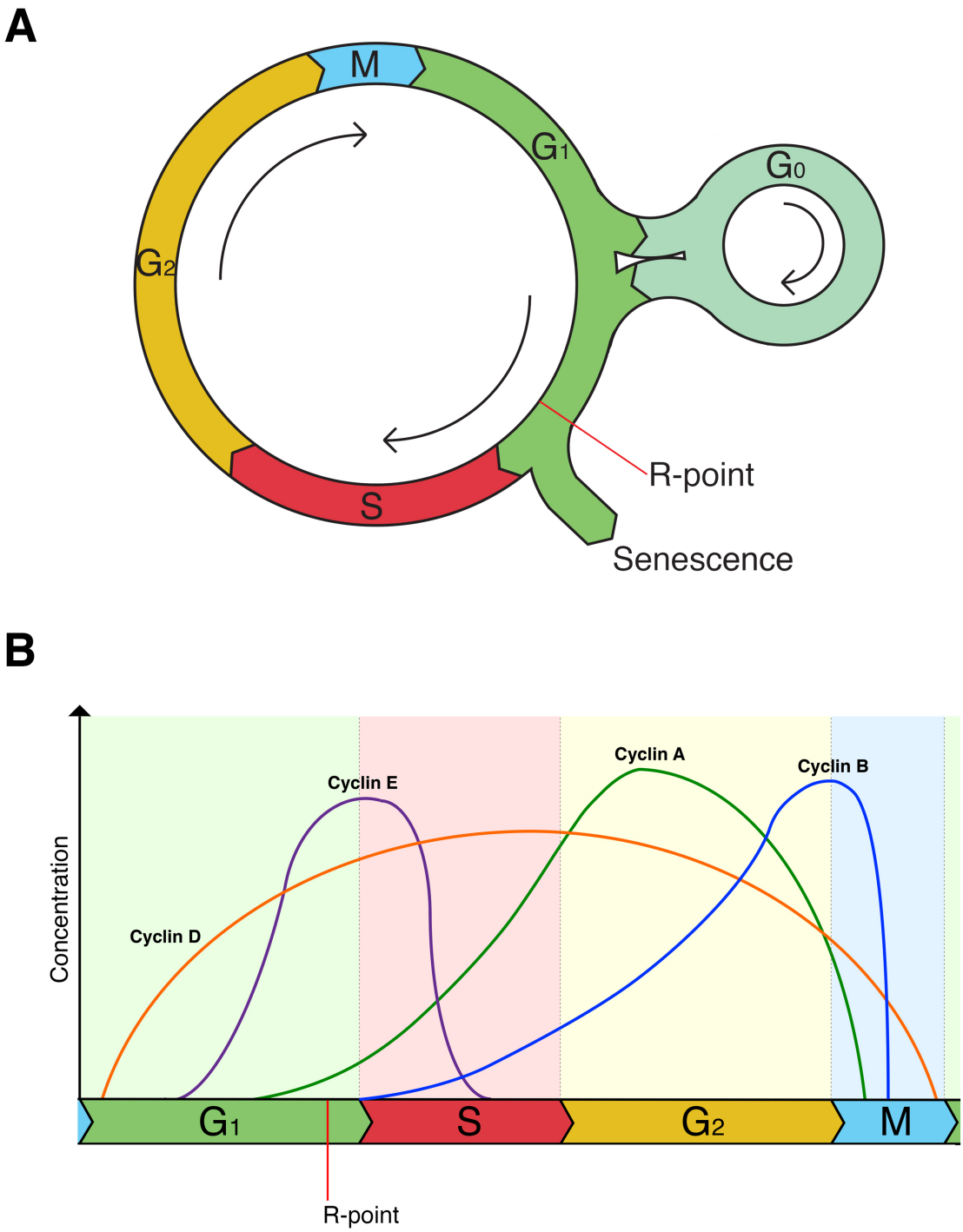

Figure 1-6. The cell cycle.

A. The cell cycle consists of four main sections, G_1 (Gap 1); S (DNA Synthesis); G_2 (Gap 2); and M (Mitosis), and one subsection, G_0 (Quiescence, or Gap 0). The R-point (red line) controls the cells passage from G_1 to S phase, with certain conditions causing the cell to enter senescence. B. Expression of the different cyclins drives the cell cycle at different points. Cyclin D (orange line) is present throughout the cell cycle, with the exception of the M to G_1 phase transition peaking in late S phase. Cyclin E (purple line) is present in G_1 and S phase, reaching its maximum level at the phase transition. Cyclin A (green line) expression increases steadily from mid – late G_1 to peak at early – mid G_2, and then drops rapidly during the transition from G_1 to M phase. Cyclin B (blue line) expression increases from the beginning of S phase until the G_2 to M phase transition, after which it declines sharply.

Uninhibited cell cycling, with unrestricted growth is common, and gives rise to tumourous cells, the majority of which are cleared by the immune system before they become an issue for the host organism (Jewett et al., 2012). The derepression of genes associated with enhanced cellular proliferation is a hallmark of cancer, and is commonly the first step in the cancer pathway. It is therefore important for the cell to closely regulate the cell cycle, and this is achieved through the use of checkpoints and CDK inhibitors.

1.11 Cell cycle regulation

There are three important points in cell cycle regulation, two DNA damage checkpoints, and a 'restriction point' (R-point), after which the cell is committed to complete the cycle independently of external signals from the environment (Johnson and Skotheim, 2013). At the DNA damage checkpoints, the structure of the DNA is assessed to ensure that correct cellular function and viability is maintained (Elledge, 1996). If this system finds genetic faults, the G_1 or G_2 phases can be stalled whilst the damage is repaired, or else the cell will enter apoptosis (Massagué, 2004, Bertoli et al., 2013). The importance of these checkpoints can be easily illustrated by the high frequency of mutations found in the constituent regulatory proteins after oncogenesis has occurred (Lukas et al., 1996).

1.11.1 The restriction point

The R-point is close to the point of G_1 to S phase transition, at which time the cell must either commit to entering the cell cycle and complete cell division, or stop cycling and senesce. In order for the cell to carry out DNA replication in the S phase, various genes related to the process must first be transcribed. The transcription of these genes is controlled by the E2F family of transcriptional regulators, some of which act as

transcriptional activators (E2F1, E2F2, and E2F3A), whilst others act as transcriptional repressors (E2F3B, E2F4, E2F5, E2F6, E2F7 and E2F8) (Chong et al., 2009). The action of these proteins is controlled by the pocket proteins, which include pRB, p107, and p130, and act by binding to, and inhibiting, the expression of the E2F target genes (Helin et al., 1993, Graña et al., 1998).

During most of the cell cycle the activator E2F proteins are bound and inhibited by hypo-phosphorylated pRB (Figure 1-8). At the R-point pRB is hyper-phosphorylated by the complex of cyclin depended kinase 4 or 6 and cyclin D (D-CDK4/6) (Helin et al., 1993). Once pRB is released, the transcription of S phase genes by the activator E2F proteins can commence, resulting in an 'all or nothing switch' that commits the cell to complete a cycle (Eser et al., 2011). This 'all or nothing switch' is achieved by the expression of cyclin-E as one of the first events following pRB release, as this forms a positive feedback loop leading to a large increase in E-CDK2 activity, thus amplifying the signal to enter S phase from G_1. This rapid amplification in the signal telling the cell to continue with the cell cycle results in a strong amplification of all S phase genes, allowing the cell to progress in a timely manner (Eser et al., 2011).

1.11.2 Inhibitors of cyclin-dependent kinases

In much the same way as pRB negatively regulates the activator E2F proteins, CDK inhibitors (CKIs) restrain CDK activity by negatively regulating their association with cyclins, preventing the downstream phosphorylation of their targets (Lim and Kaldis, 2013). CKIs are divided into two separate classes, depending on their structure and CDK specificity. The INK4 family members $p15^{INK4b}$, $p16^{INK4a}$ (p16), $p18^{INK4c}$ and $p19^{INK4d}$ target CDK4 and CDK6, whilst the CIP/KIP family members $p21^{CIP1}$ (p21),

$p27^{KIP1}$ and $p57^{KIP2}$ have a broad specificity, targeting complexes containing cyclins A, B, D and E (Sherr and Roberts, 1999).

1.12 p16 structure

p16 was first identified as a protein with a molecular weight of approximately 16 kDa containing four ankyrin repeats (Figure 1-7), and was named after its molecular weight and its targeting of CDK4 (Serrano et al., 1993). Ankyrin repeats are motifs of 33 amino acids, comprising two α-helices separated by loops, which commonly fold together to form ankyrin repeat domains (Breeden and Nasmyth, 1987, Lux et al., 1990). Ankyrin repeats have been identified as one of the most common structural motifs in proteins, and are known to mediate protein–protein interactions in bacteria, archaea and eukaryota (Mosavi et al., 2004).

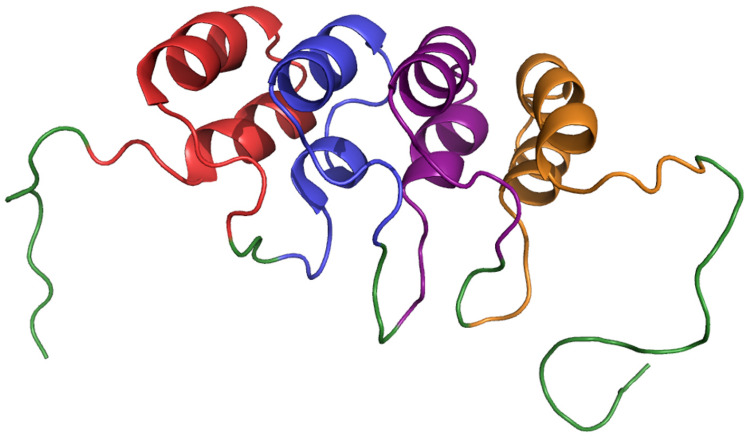

Figure 1-7. Three-dimensional structure of p16.

Solution NMR structure of p16 (PDB: 2A5E) (Byeon et al., 1998). Ankyrin repeats are shown in red, blue, purple and orange. Image generated from PDB entry 2A5E using PyMol (Schrödinger, DE).

1.13 p16 function

p16 is an important CKI which negatively regulates the cell cycle, controlling cell passage through the R-point of G_1 (Serrano et al., 1993, Gil and Peters, 2006). In the

absence of p16, pRB is hyper-phosphorylated by D-CDK4/6, allowing the cell to proceed past the R-point of the cell cycle via the release of the activator E2F proteins (Ishida et al., 2001, Müller et al., 2001, Cobrinik, 2005).

In the presence of p16, the cell cycle is blocked, causing senescence. This occurs by the protein binding to CDK4/6, preventing its association with cofactor cyclin D, therefore stopping the cyclin D-CDK4/6 complex from forming a kinase (Figure 1-8). The cell cannot pass the R-point due to the lack of E2F activity and the cell becomes senescent. Although senescent cells remain metabolically active, they stop reacting to mitogenic stimuli; they can be identified by the expression of markers such as p16 and β-galactosidase, and become enlarged and flattened.

Although the main role of p16 is to inhibit the kinase activity of CDKs, recent studies have uncovered novel p16-interacting proteins. For example, p16 interacts directly with the proliferating cell nuclear antigen, an accessory protein for DNA polymerase δ (Souza-Rodrígues et al., 2007). This interaction inhibits DNA polymerase activity and effectively prevents DNA replication, presenting an alternative route to p16-mediated cell cycle arrest. p16 has also been found to bind directly to mini-chromosome maintenance proteins 6 and 7 (MCM6/7), which are important subunits of the DNA helicase complex MCM, involved in DNA replication initiation. This binding has been shown to prevent the assembly of MCM7 onto chromatin during G_1 (Braden et al., 2006) and it has been suggested that the interaction of p16 and MCM6 may have the same effect (Braden et al., 2006, Souza-Rodrígues et al., 2007).

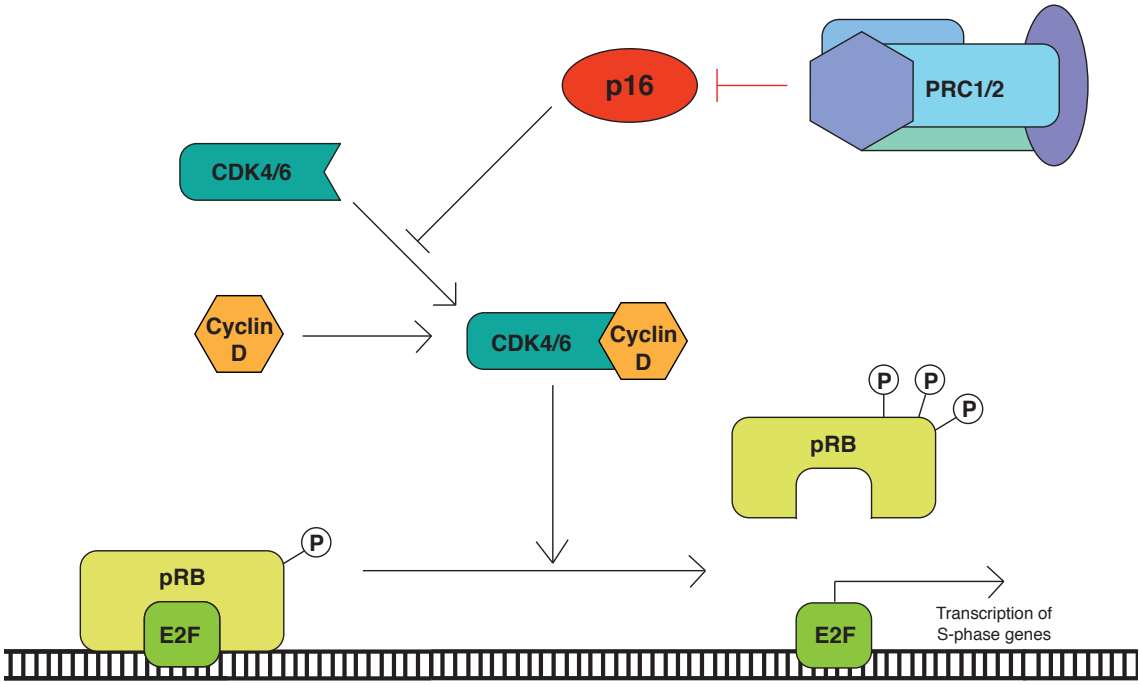

Figure 1-8. Action of p16 within the cell.

During G_1 of the cell cycle, the hypo-phosphorylated form of pRB negatively regulates the E2F transcriptional activators. The D-CDK4/6 complex of cyclin D and CDK4/6 hyper-phosphorylates pRB at the R-point, releasing the E2F transcription factors and allowing transcription of the S phase genes. When expressed, p16 prevents the association of cyclin D and CDK4/6, preventing downstream phosphorylation of pRB, and subsequent transcription of S phase genes. p16 expression is in turn negatively regulated by polycomb repression complexes 1 and 2 (PRC1/2), which epigenetically regulate the *INK/ARF* locus, from which p16 in transcribed. Red lines represent epigenetic repression.

1.14 *p16* expression

1.14.1 The *INK4b-ARF-INK4a* locus

The *p16* gene is encoded on the *INK4b-ARF-INK4a* (*INK/ARF*) locus of chromosome 9p21 (Figure 1-9), along with two other major tumour suppressor genes: $p15^{INK4b}$, which is induced by transforming growth factor beta and also acts on CDK4/6; and $p14^{ARF}$ ($p19^{ARF}$ in mice), which is translated from an alternative reading frame on the locus. $p14^{ARF}$ acts to inhibit the E3 ubiquitin ligase MDM2, which targets p53 for degradation; $p14^{ARF}$ therefore has a stabilising effect on the tumour suppressor p53 (Hannon and

Beach, 1994, Stott et al., 1998). It is thought that *p16* and *p15*^{INK4b} arose by tandem duplication of the *p15*^{INK4b} gene, explaining the similarity of these proteins in both sequence and function (Gil and Peters, 2006).

In addition to the three tumour suppressor genes in the locus, the lncRNA (long non-coding RNA) *ANRIL* is also encoded. *ANRIL* binds to the polycomb group (PcG) protein CBX7, found in polycomb repressor complex (PRC) 1, and SUZ12, a component of PRC2 (see Section 1.14.3). The binding of *ANRIL* to these complexes is thought to act as a scaffold allowing the correct association of the component proteins (see Section 1.20) (Yap et al., 2010).

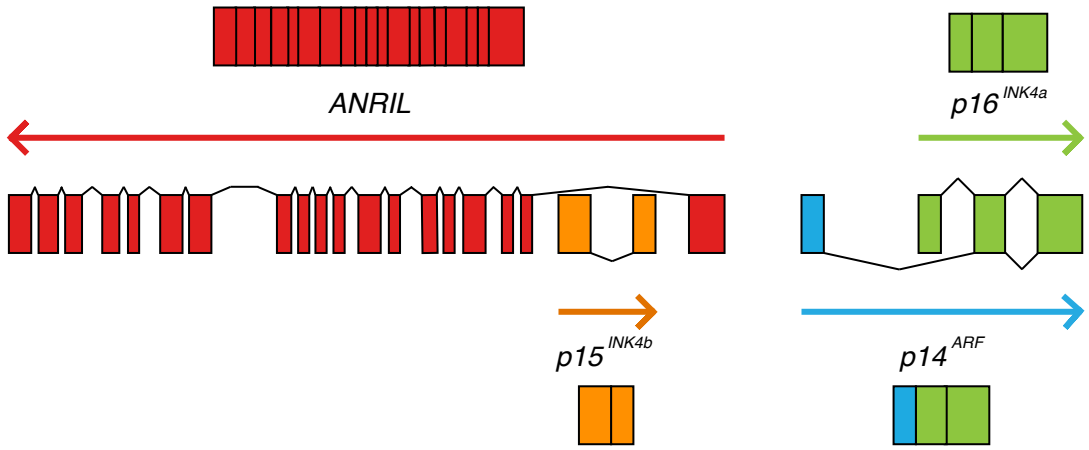

Figure 1-9. Genes of the *INK/ARF* locus.

The genes of the *INK/ARF* locus encode three tumour suppressor genes *p16*^{INK4a} (green), *p15*^{INK4b} (orange) and *p14*^{ARF} (blue/green). Although the first exons of *p16*^{INK4a} and *p14*^{ARF} are different, they share two 3' exons, although they are transcribed from different reading frames. The lncRNA *ANRIL* (red) is transcribed from the locus in the antisense direction and spans 126 kb.

1.14.2 Activation of p16 expression

p16 expression is often provoked in response to DNA damage, and can be induced by several transcription factors such as ID, ETS2 and MYC (Gil and Peters, 2006, Irelan et al., 2009). One of the best-understood pathways to p16 expression is the RAF-MEK-

ERK kinase-signalling cascade in response to activated H-RAS. The mutant form of BRAF found in human naevi and melanoma has also been found to strongly activate p16 via this pathway (Michaloglou et al., 2005).

1.14.3 Repression of p16 expression by polycomb proteins

The *p16* gene, along with the rest of the locus, is tightly regulated at the level of gene expression by the polycomb repressor complexes, PRC1 and PRC2 (Jacobs et al., 1999, Gil et al., 2004). PRC2 acts by di- and trimethylating lysine 27 the H3 histones present along stretches of DNA that contain CpG islands (areas of DNA which contain a high frequency of cytosine – guanine repeats) (Riising et al., 2014). These trimethylations are recognised by PRC1, which binds to, and forms polycomb bodies on the chromatin that further prevent gene transcription (Wang et al., 2004, Simon and Kingston, 2009).

Although both PRCs contain a small number of core subunits, in humans there are a wide variety of auxiliary subunits that can affect function. The exact composition of these complexes is thought to be different depending on the target gene (Gil and Peters, 2006, Simon and Kingston, 2009). One of the PcG proteins within PRC1 is the oncogene BMI1, which has repeatedly been found to play an important role in controlling p16 expression and senescence (Jacobs et al., 1999, Li et al., 2013b). Similarly, expression of the PcG protein CBX7 has also been found to down regulate p16 expression, although it does not appear to require BMI1 to function (Gil et al., 2004), suggesting that both these PcG proteins are independently important for epigenetic suppression of the *INK/ARF* locus. In addition to the PcG proteins that act to repress the *INK/ARF* locus, the lncRNA (see Section 1.20) *ANRIL* has also been found acting in concert with PRC1 (Yap et al., 2010), to increase function of CBX7, and repress the *INK/ARF* locus.

1.15 Senescence

1.15.1 Replicative senescence

Much of the research carried out to date on senescence has been concerned with normal human fibroblasts. Senescence was first identified by Hayflick and Moorhead, who observed that serially passaged human fibroblasts only divided a finite number of times (Figure 1-10 panel A) (Hayflick and Moorhead, 1961). In normal cells, the telomeric structures of the chromosomes are shortened after each mitotic cell division. This constant degradation eventually renders cell division impossible, leading to replicative senescence (Harley et al., 1990). Senescence is commonly believed to be an irreversible cellular state, although genomic mutations and epigenetic changes can cause cells to spontaneously escape senescence and develop a more tumourous phenotype (Romanov et al., 2001).

Senescent cells have a mixture of both phenotypic, and genetic changes, when compared to their proliferative selves. When senescent, cells are commonly recognised to have an enlarged and flattened appearance with prominent nucleoli and cytoplasmic granules (Chandler and Peters, 2013). As senescent cells contain many lysosomes, the cells can be assayed for senescent associated β-galactosidase activity (Dimri et al., 1995), although critics have shown that false positive results can be observed in quiescent cells, casting the efficacy of this assay into doubt (Yegorov et al., 1998). The major genetic changes in senescence are the activation of the two primary tumour suppressor pathways, the p53/p21 and p16/pRB pathways (Campisi, 2013), which restrict cellular proliferation. As such, expression of p16 is now commonly used as the gold standard of marking senescent cells as it is often undetectable in normal cells (Collins and Sedivy, 2003).

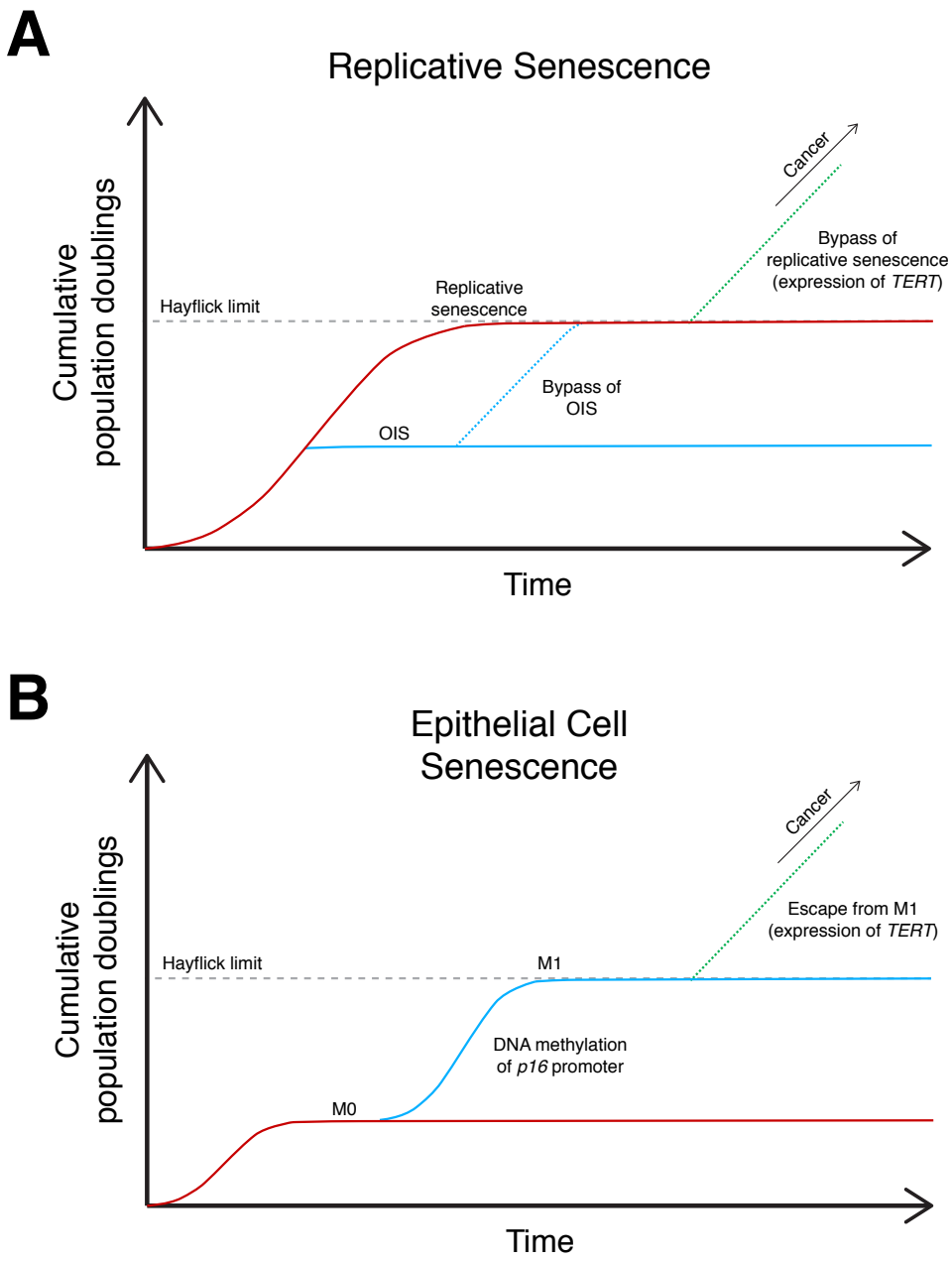

Figure 1-10. The Hayflick limit and senescence.

A. Normal cells grow undergo a period of exponential replication until a situation, such as critically short telomere length occurs, after which cells become senescent (red). Replication ceases, but metabolism remains active. An oncogenic event, such as the induction of *TERT* expression can allow the cells to escape senescence completely leading to unrestricted proliferation, and cell immortalisation (green). Oncogenic stimuli, such as the mutation of a tumour suppressor gene or activation of an oncogene, can cause proliferating cells to enter senescence prematurely, termed oncogene-induced senescence (OIS; blue). Further mutations can allow cells to bypass OIS and continue growth until they enter replicative senescence as a result of telomere shortening. B. Epithelial cells undergo a two-step pattern of senescence, with a first stage (M0) caused by p16 activity (red), which is escaped by epigenetic silencing of the *p16* gene (blue). A second senescence is entered when telomeres become critically short (M1), this in turn can be escaped via TERT activity, leading to unrestricted proliferation, and cell immortalisation (green).

Additionally, senescent cells secrete a variety of chemicals collectively described as the senescence-associated secretory phenotype (SASP), which include cytokines, growth factors, chemokines, extracellular matrix proteins and proteases (Coppé et al., 2010). The wide array of released SASP factors have been suggested to convey both beneficial and negative effects to surrounding cells. The SASP has been found to stimulate proliferation (Bavik et al., 2006), and angiogenesis (Coppé et al., 2006), as well as signalling other cells to also enter senescence (Liu et al., 2007). Other research has suggested that the SASP may be important in paracrine senescence across tissues, increasing the senescence footprint of pre-cancerous lesions and promoting clearance by the immune system within these areas (Acosta et al., 2013). This study also showed that some cells are more susceptible to paracrine senescence, with the concentration of extracellular growth factors playing an important role in how each cell will respond to the pro-senescence SASP signal.

1.15.2 Epithelial cell senescence

Unlike fibroblasts, which commonly enter senescence as a result of telomere shortening, epithelial cells exhibit a two-step pattern of senescence, where cells senesce once after an initial growth phase (termed M0), and again following a second limited phase of proliferation, at which point the Hayflick limit is reached (termed M1; Figure 1-10 panel B) (Huschtscha et al., 1998, Romanov et al., 2001).

During M0, the cells exhibit the hallmarks of senescent cells, i.e. the expression of *p16* whilst becoming enlarged and flattened. Cells in M0 senesce in response to activation of the p16/pRB pathway, but not the p53/p21 pathway. The cells can only escape senescence as a result of loss-of-p16 activity, commonly caused by specific hypermethylation of the *p16* promoter ($p15^{INK4B}$ is not affected) (Huschtscha et al.,

1998). The cells subsequently continue to divide until the telomere length becomes critical (Kiyono et al., 1998). Experiments in human mammary epithelial cells have shown that inactivation of p53 does not aid the cell in passing M0, although its loss can result in massive cell death when the critical telomere length is met (Garbe et al., 2007). $p53^{+}$ epithelial cells can only escape M1 if the barrier of critical telomere length is overcome, either by activation of TERT or a viral oncoprotein such as E6 (Kiyono et al., 1998, Romanov et al., 2001).

1.15.3 Oncogene-induced senescence

In addition to the "natural" causes, such as telomere shortening, senescence can be caused prematurely in response to oncogenic signals, such as strong or unbalanced mitogenic signals, often termed oncogene-induced senescence (OIS; Figure 1-10 panel A) (Blagosklonny, 2003). The first study of OIS showed that an oncogenic H-RAS mutant, which permanently stimulated the mitogen-activated protein kinase (MAPK) pathway, would induce senescence (Serrano et al., 1997). Other components of the MAPK pathway, such as MEK (Lin et al., 1998), BRAF (Michaloglou et al., 2005) and RAF, (Zhu et al., 1998) have subsequently also been shown to produce a similar effect when mutated or overexpressed. Induction of senescence due to unrestrained proliferation also often occurs following the loss of a tumour suppressor protein, such as PTEN (Chen et al., 2005b, Vredeveld et al., 2012), from the cell.

Some early studies suggested that OIS was a purely *in vitro* phenomenon, resulting from cellular stresses attributed to cell culture with non-human serum, on plastic dishes, and with supraphysiological levels of pO_2 (Sherr and DePinho, 2000). It was postulated that OIS was not representative of the situation found *in vivo*, however, subsequent research has found many oncogenes, which when induced produce the senescence

phenotype (Jacobs et al., 2000, Shvarts et al., 2002). Moreover, nearly all tumours have been found to feature mutations in the p53/p21 and p16/pRB pathways, which let the tumour to bypass OIS i*n vivo* to allow unrestricted cell growth (Sherr and McCormick, 2002).

1.16 Expression of p16 in ageing

1.16.1 Expression of p16 in murine ageing

Studies in mice have shown that p16 expression and the associated senescence of cells is important in a number of age-related disorders such as type 2 diabetes mellitus (Krishnamurthy et al., 2006a, Chen et al., 2011) and atherosclerosis (Kuo et al., 2011). In one important study, transgenic mice were engineered to clear all p16-expressing cells by drug-induced caspase activity (Baker et al., 2011). Upon administration of the drug to old mice, they became significantly healthier, showing increased muscle fibre diameter and increased fat deposition, both phenotypes associated with healthy mice. Life-long clearance of these senescent cells delayed the onset of age-related phenotypes, while delayed administration of the drug until later in life attenuated the progression of age-related disorders that had already become established. This single study demonstrates how important the role of p16-mediated senescent cells are in normal ageing, and also how they can be detrimental to health.

1.16.2 Expression of p16 in human ageing

As in mice, expression of *p16* has been found to increase with age in a variety of tissues. Expression in infants is limited to the thymus, occasionally pancreatic epithelial cells (Nielsen et al., 1999, Kanavaros et al., 2001). With increasing age, expression of *p16* is observed across a host of cell types throughout the body (Nielsen et al., 1999),

although this is especially notable within the kidney, with the renal cortex often found to have high expression in older patients (Chkhotua et al., 2003, Melk et al., 2004). In addition to the kidney, increasing expression has been observed in the breast duct, cervix, salivary gland, pancreas and testis (Nielsen et al., 1999), and is thought to be associated with a wide array of age-related disorders.

1.16.3 Association of p16 with age-related disorders

Recent genome-wide association studies (GWAS) have identified a host of diseases that are linked to the *INK/ARF* locus, including many age-related disorders (Jeck et al., 2012), such as Alzheimer's Disease (Züchner et al., 2008), atherosclerosis (Liu et al., 2009), coronary artery disease (Pasmant et al., 2011), myocardial infarction (Ogawa et al., 2010), stroke (Helgadottir et al., 2008), type 2 diabetes mellitus (Chen et al., 2011), glaucoma (Osman et al., 2012), aneurysms (Helgadottir et al., 2008), and endometriosis (Nyholt et al., 2012). Together, these human genetic studies, and those performed in mice, provide a strong argument for research into p16-mediated senescence with a view to modulation of this system, in order to attenuate disease.

1.17 Expression of p16 in cancer

1.17.1 Expression of p16 in murine cancer

Both mice and humans have the *INK/ARF* locus, but the relative importance of its constitutive genes are different in the two species. For example, in mice $p19^{ARF}$ ($p14^{ARF}$ in humans) holds the most crucial role of the *INK/ARF* genes in the suppression of tumour formation (Sharpless et al., 2004), where as this falls to p16 in humans (Hussussian et al., 1994). Knockout mouse models of both *p16* and $p19^{ARF}$ are found to grow spontaneous tumours at higher frequencies than their wild type counterparts

(Sharpless et al., 2001, Krimpenfort et al., 2001), although the *p19*^{ARF}-null mice are found to generate them at higher rates (Sharpless et al., 2004). *p16*-null mice were not found to grow tumours in early life, suggesting that in mice this gene plays a more active tumour-supressing role in later life (Krimpenfort et al., 2001).

1.17.2 Expression of p16 in human cancer

Expression of *p16* in humans is essential for protection against tumourogenesis, and is one of the most influential proteins in causing the cell to enter OIS. As such, *p16* is one of the most commonly mutated, deleted, or epigenetically down regulated genes in human cancers (Esteller et al., 2001, Forbes et al., 2006). Its inactivation is therefore thought to be one of the most important steps in the bypass of OIS, and subsequent development of many human tumours (Kamb et al., 1994, Ruas and Peters, 1998). Mutations and deletions of p16 have been catalogued in a wide array of both haematological and solid tumours, with incidences of deletion widely ranging from 1% (thyroid cancer) and 2% (breast cancer) to 58% (T-cell acute lymphoblastic leukaemia), depending on the cancer (Ruas and Peters, 1998).

1.18 Breast cancer

Breast carcinomas are a highly heterogeneous group of cancers, with variable behaviour, treatment response, and prognosis (Payne et al., 2008). Currently there are three major prognostic markers used to classify breast cancers: oestrogen receptor (OR), progesterone receptor (PR), and human epidermal growth factor receptor 2 (HER2).

The OR is currently the most important of the three markers, as its expression signifies a lower mortality risk tumour (Dunnwald et al., 2007), which can be treated using oestrogen antagonist or aromatase inhibitors, which prevent the conversion of

androgens to oestrogen (Fisher et al., 1988, Anderson et al., 2001). The OR is expressed in around 70% of all breast tumours, meaning that the 30% of tumours which lack expression cannot be targeted using hormone therapy (Osborne, 1998), and therefore must be treated with generic chemotherapy that is susceptible to multidrug resistance, often mediated by ABCG2 (breast cancer resistance protein) (Doyle and Ross, 2003). PR expression is also commonly used to assess whether the OR pathway is active, as it is also regulated by oestrogen (Horwitz et al., 1978). Much like the OR, expression of the PR is thought to mark a less aggressive tumour phenotype that may be responsive to hormonal therapy, even in OR-negative cancers (EBCTCG, 1998).

HER2 is a tyrosine kinase and important for the differentiation, adhesion and motility of cells (Hanna et al., 1999). Overexpression of the gene is observed in around 20% of breast tumours (Slamon et al., 1987), with HER2 positivity being associated with a poor prognosis, due to higher grade tumours, lymph node involvement and higher rates of recurrence and mortality (Payne et al., 2008), Expression on HER2 in breast cancers does however identify tumours which can be treated with trastuzumab (commonly referred to as Herceptin, one of its trade names), a monoclonal antibody for HER2, which binds to the receptor, and inhibits the proliferation of the cancer cell (Hudis, 2007).

1.18.1 Basal-like breast cancer

Basal-like breast cancer (BLBC) is a clinically aggressive subtype of breast cancer that accounts for around 15 – 20% of all breast cancers (Fulford et al., 2006). The majority of these tumours also belong to the triple negative breast cancer (TNBC) subtype, so called as they lack expression of OR, PR, and HER2 (Abd El-Rehim et al., 2004, Nielsen et al., 2004, Abd El-Rehim et al., 2005). BLBCs are also characterised by the

expression of CK 5/6 and 17, EGFR, VEGF and c-kit (Nielsen et al., 2004, Brenton et al., 2005, Linderholm et al., 2009).

One significant problem with BLBCs is that they cannot be treated with traditional targeted therapies for breast cancer, such as trastuzumab, tamoxifen, or aromatase inhibitors, as they do not express OR or HER2. This currently leaves surgical resection, radiotherapy and generic chemotherapy as the current best available treatments.

1.18.2 p16 expression in basal-like breast cancer

Unlike nearly all other tumours, expression of *p16* in BLBCs is commonly observed, and its overexpression is consistently found to correlate with a poor patient prognosis (Hui et al., 2000, Milde-Langosch et al., 2001). Higher expression of *p16* is also suggested to mark a more homogenous subgroup of BLBC, which could potentially be targeted (Abou-Bakr and Eldweny, 2013).

It has been hypothesised that the lack of a functional p16/pRB pathway may play an important role in the biology of this tumour subtype (Gauthier et al., 2007), through the widespread inactivation of pRB, rendering the high expression of p16 redundant (Subhawong et al., 2009). Although there is currently strong evidence that p16 expression in BLBC suggests a poor prognosis, any underlying mechanism behind this, and its relevance to disease aggressiveness are, as of yet, unknown.

1.19 RNA interference

During this study, one of the main methods of investigation was RNA interference (RNAi) by both short interfering RNA (siRNA) and microRNA (miRNA). The system of RNAi was first described in *C. elegans* by Fire et al. (1998), although some

components of the pathways were previously known under other names. RNAi is a powerful tool, which can be utilised to help understand the roles of specific genes within the cell by simulating loss of function. This system is commonly utilised through the introduction of exogenous miRNAs (see Section 1.19.1), anti-miRNA (antimiRs), or siRNAs (see Section 1.19.2). There are many pitfalls, which have to be navigated when RNAi is being utilised, however, if due care and attention are paid when planning experiments, there are few techniques as potent for interrogating the impact of single genes within the context of the cell.

1.19.1 miRNA

miRNAs are endogenously expressed, single stranded RNA molecules which act to repress gene expression (Bartel, 2004). Unlike the focus of siRNAs, which ideally serve to target only a single gene, miRNAs actively target hundreds or thousands of genes, depending on their sequence (Baek et al., 2008). A major functional difference between siRNAs and miRNAs is that the miRISC complex, which comprises the RNA induced silencing complex (RISC; described below) and miRNA, can destabilise or translationally inhibit mRNA in addition to targeting them for degradation (Eulalio et al., 2008). A wide array of cellular pathways are known to be affected by miRNAs, with their role in oncogenesis being especially prominent (Lu et al., 2005, He et al., 2007, Kumar et al., 2007).

miRNA coding sequences are commonly found in gene introns, gene antisense strands or in between genes, and are often found in clusters with multiple miRNA genes tightly packet into a section of the genome. They are transcribed by RNA polymerase II or III, to create primary miRNAs (pri-miRNAs), of which the pri-miRNAs generated by RNA

polymerase II are commonly polyadenylated and capped, much like mRNAs (Cai et al., 2004). The transcription of miRNAs can be controlled by many factors, including transcription factors (He et al., 2007) and promoter methylation (Saito et al., 2006), allowing for miRNAs to be regulated independently of one another, even within the same cluster (Song and Wang, 2008).

The pri-miRNA is cleaved in the nucleus by the Drosha/Pasha microprocessor complex (Lee et al., 2003), comprised of the RNase III enzyme Drosha, and the RNA binding protein Pasha (commonly called DGCR8), both of which are essential for miRNA processing (Gregory et al., 2004). pri-miRNAs contain a ~33 bp hairpin structure with a terminal loop and a single-stranded stem at each end which is essential for Pasha binding and Drosha cleavage (Han et al., 2006). The 5' and 3' arms of the pri-miRNA are cleaved by the RNase activity of Drosha (Han et al., 2006), leaving the hairpin loop structure intact, now termed the precursor miRNA (pre-miRNA).

pri-miRNAs and pre-miRNAs can be edited by adenosine deaminases acting on RNA (ADARs) to cause adenosine (A) to inosine (I) base changes within the pri-miRNA sequence, potentially altering subsequent processing and targeting of the mature miRNA (Yang et al., 2006, Kawahara et al., 2007).

The pre-miRNA is exported from the nucleus by the Exportin-5 and Ran-GTP complex (Yi et al., 2003), which recognises the processed pre-miRNAs irrespective of sequence (Lund et al., 2004, Zeng and Cullen, 2004). For the pre-miRNAs to be properly utilised, a they must first be processed again to their mature form, and loaded into the RISC

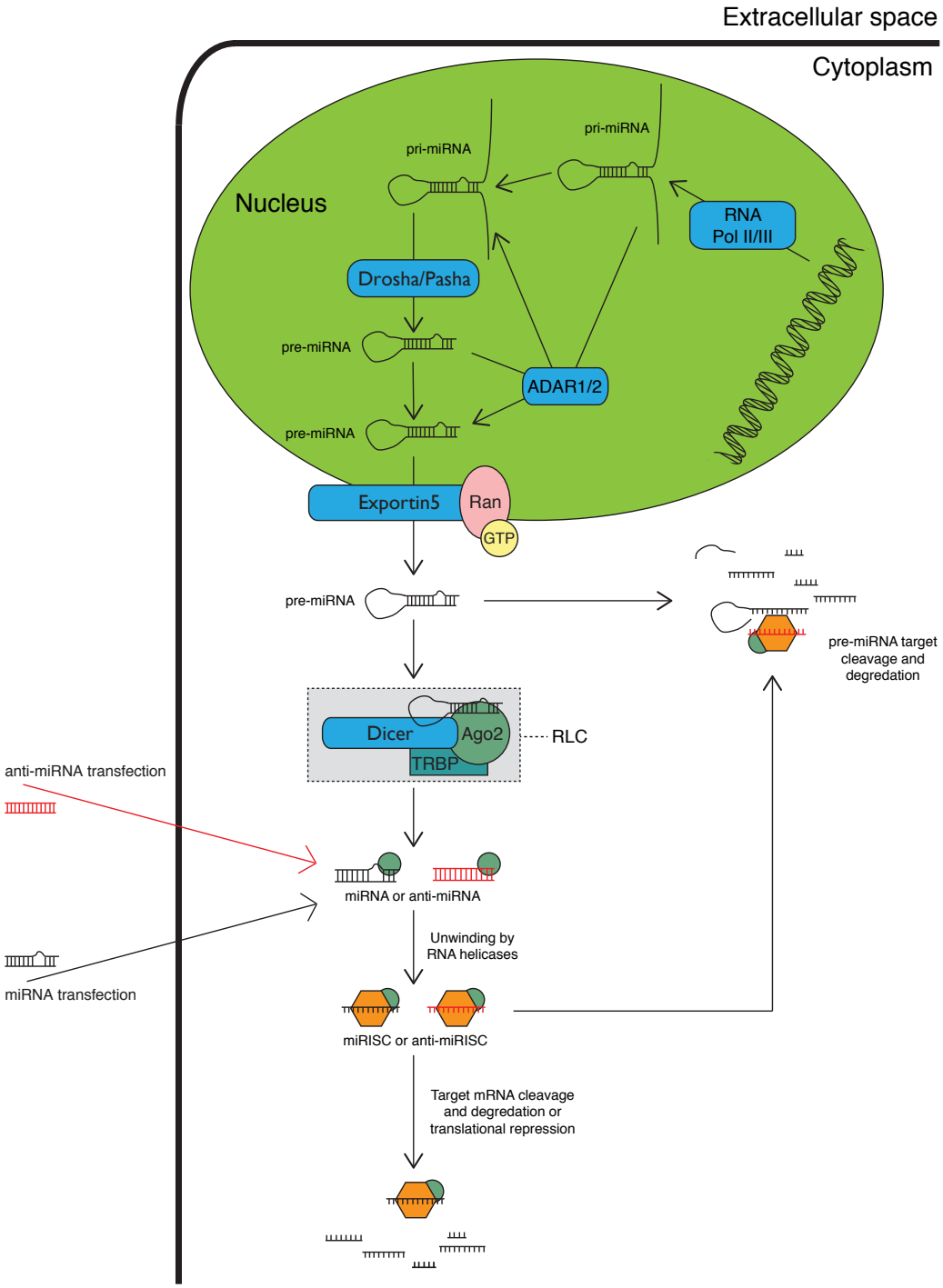

Figure 1-11. Mammalian pathways of miRNA mediated RNA interference.

miRNA molecules involved in RNAi are endogenously transcribed from the genome by RNA polymerase II/III in the nucleus. The tails of the resulting pri-miRNA are cleaved by the Drosha/Pasha complex to produce pre-miRNA. Pre-miRNAs are then either exported from the nucleus by Exportin5 in complex with Ran:GTP, or modified by ADAR1/2 and then exported. In the cytosol, the pre-miRNAs are cleaved by Ago2 activity of RLC to produce a mature miRNA. Mature miRNAs or anti-miRNAs can be introduced into the cell by transfection. miRNAs or anti-miRNAs in complex with Ago2 associate into RISC to form miRISC or anti-miRISC. miRISC will target mRNAs using the guide strand resulting in their degradation or repression of translation. anti-miRISC will act to degrade targeted pre-miRNAs before they are incorporated into RLC.

assembly. pre-miRNA processing in the cytoplasm and loading onto RISC is carried out by the multi-protein RISC loading complex (RLC). RLC contains the RNase Dicer, RNA-binding proteins TRBP (Tar RNA binding protein) and PACT (protein activator of PKR), and the core component Argonaute2 (Ago2) (MacRae et al., 2008). Although TRBP and PACT are not essential for pre-miRNA processing by RLC, they do increase its efficiency and facilitate the recruitment of Ago2 (Chendrimada et al., 2005, Lee et al., 2006).

Once the pre-miRNA is loaded into the RLC complex, the RNase activity of Dicer cleaves off the loop section of the hairpin, leaving a ~22 bp section of double stranded RNA (Hutvágner et al., 2001). After the miRNA has been fully processed Dicer, TRBP and PACT dissociate from the miRNA complex, and an RNA helicase, such as RNA helicase A, is recruited to unwind the double-stranded RNA (Robb and Rana, 2007), which the Ago2 subunit of RISC facilitates by dissociating from the passenger strand (Rand et al., 2005). Although the miRNA duplex could produce two different mature miRNAs, this is usually not the case, as one of the strands is used for targeting whilst the other is degraded (Schwarz et al., 2003). The strand which the RISC complex chooses depends on the thermodynamic stability of the base pairs at each end of the miRNA duplex; where the strand with the least thermodynamically stable 5' end is typically loaded as the targeting strand (Khvorova et al., 2003).

Once the final steps of processing and unwinding are complete, the miRISC complex is available for mRNA targeting, where upon binding the Ago2 subunit can degrade or translationally inhibit the mRNA (Bagga et al., 2005, Chendrimada et al., 2007, Eulalio et al., 2008). The majority of miRNAs target the 3' UTR of mRNAs, with the seed

region (nucleotides 2-7) of the miRNAs being the most important region for target recognition (Lewis et al., 2003). As the seed region is only 6 nt, and perfect binding of the rest of the miRNA to the target mRNA is not required for Ago2 action, miRNAs can have a wide array of target genes with diverse sequences.

1.19.2 siRNA

Exogenously introduced siRNAs utilise the endogenous cellular RNAi machinery to knockdown genes according to their target sequence (Figure 1-12) (Sigoillot and King, 2011). siRNAs are composed of a guide strand – the targeting sequence of the siRNA – and the passenger strand – the guide strand's complementary sequence. This use of the endogenous machinery can explain to some extent, why off-target effects can be observed in siRNA experiments – due to close but imperfect sequence identity, or the overloading of the RNAi machinery. It is therefore critical to control for these off-target effects.

Sequence independent off-target effects are often due to the abnormally high levels of siRNA passing through the cellular RNAi pathways during these experiments. Unusually high levels of siRNA will displace the endogenous miRNAs that are the typical substrate of RISC. This displacement can change normal patterns of gene expression within the cell. It should also be noted that studies have found that transfecting cells with siRNA can up-regulate the expression of some miRNAs, again possibly causing a change in gene expression patterns (Khan et al., 2009).

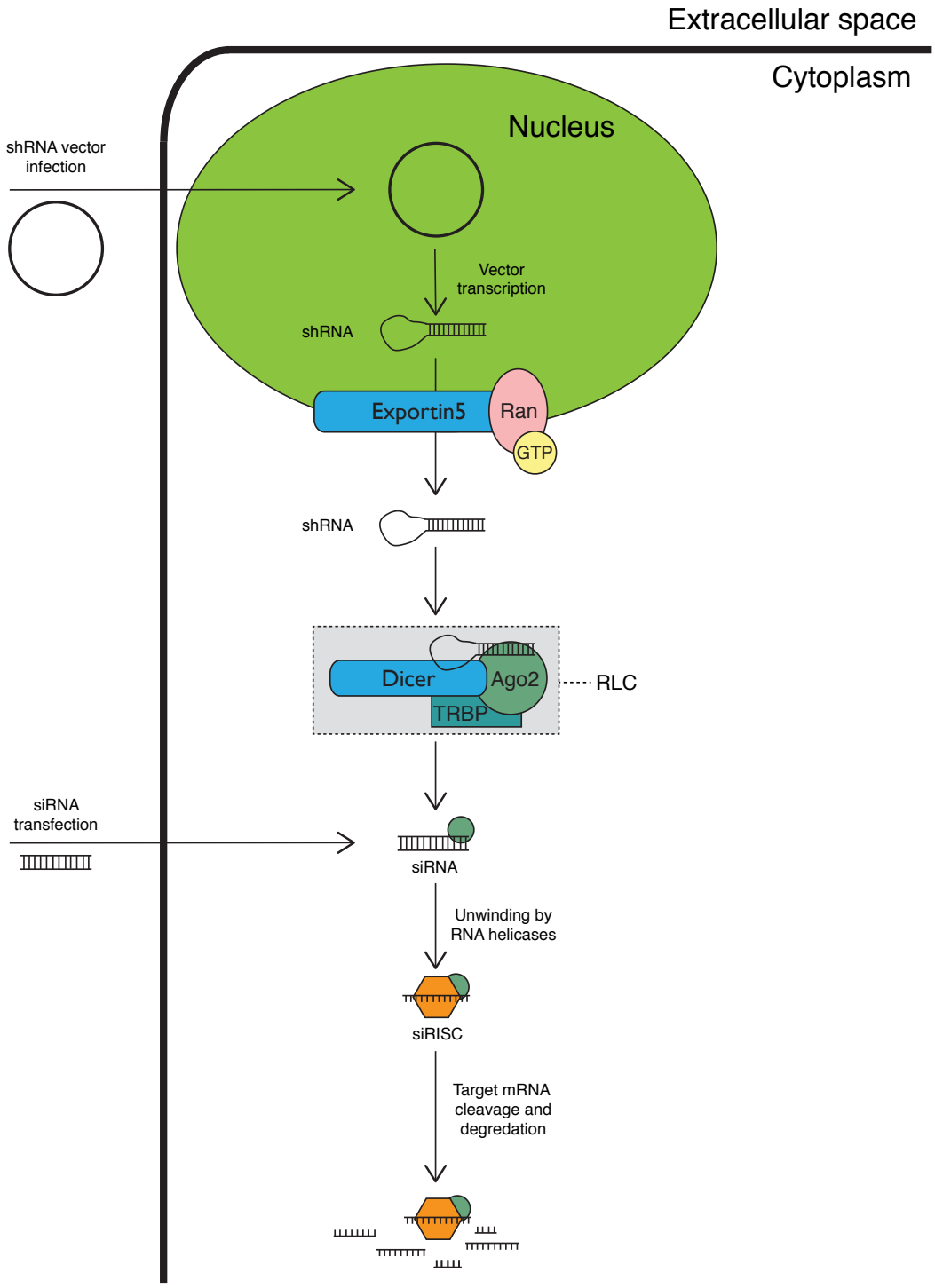

Figure 1-12. Mammalian pathway of siRNA-mediated RNA interference.

RNA molecules involved in RNAi can be introduced by transfection (siRNA) or infection (shRNA encoded by a lentiviral vector). The coding sequence for the shRNA is transcribed in the nucleus and transported by Exportin5 in complex with Ran GTP into the cytoplasm where Ago2 activity in complex with Dicer and TRBP cleaves it into its mature form: siRNA. RISC forms a complex with a Ago2 bound single strand of siRNA; this then targets mRNA for cleavage and degradation.

Furthermore, introduction of exogenous siRNA has been shown to provoke a cell-stress response when used at high concentrations (Persengiev et al., 2004), thus, it is important to use the lowest concentration of siRNA possible to produce effective knockdown of the target mRNA.

Sequence dependent off-target effects can also be a problem. Exogenously introduced siRNAs can act in a similar manner to endogenous miRNAs; either through perfect base pairing and cleavage of the regulated mRNA by the Ago2 subunit of RISC, or by the interaction of the seed region (bases 2 – 8 of the guide strand) of the siRNA with target sequences, in a similar manner to miRNA (see Section 1.19.1) (Doench et al., 2003). As the length of the sequence identity required for the latter mechanism of action is relatively small – seven bases for some siRNAs – (Jackson et al., 2003), there is a large potential for each siRNA to non-specifically down regulate hundreds of different genes within the cell (Doench et al., 2003, Burchard et al., 2009, Sigoillot and King, 2011). Transcriptional profiling has shown that each siRNA has a distinct pattern of effect within the cell, and even though the target gene is down regulated, other genes can also be affected by as much as 1.5 – 4 fold (Jackson et al., 2003). More recently, it has been confirmed that the seed region of the siRNA is important in causing these off-target effects (Jackson et al., 2006). It is, therefore, important when designing oligonucleotides for RNAi to keep the seed complement frequency (SCF) to a minimum (Anderson et al., 2008).

Some level of off-target effect is almost unavoidable with RNAi experiments; therefore it is important to confirm that any subsequent changes in gene expression or phenotype

are not due to the panel of possible off-target effects described above. To address this, the use of multiple siRNAs, with different sequences, in independent experiments to target the same gene is standard practice. With proper validation of the results by establishing that both the mRNA and protein levels of the target gene are reduced by qPCR and western blotting respectively, confidence in the conclusion that the observed phenotype is due to the knockdown of the intended gene can be increased (Mohr et al., 2010, Jackson and Linsley, 2010).

1.20 lncRNA

A third type of regulatory RNA in the cell is the lncRNA. These are 200 bp to 100 kb ncRNAs which regulate cell function, through numerous mechanisms and actions (Wang et al., 2011, Geisler and Coller, 2013). It has been suggested that as the noncoding portion of the transcriptome is so large (~80%) (Bernstein et al., 2012) that a significant amount of it may comprise as of yet unknown lncRNAs (Geisler and Coller, 2013). Although only relatively few of the known lncRNAs have had functional roles assigned to them (Ponting et al., 2009), their implications are many, including: cell cycle regulation, pluripotency, meiotic entry, telomere length and transposon silencing (Wilusz et al., 2009).

Although lncRNAs have been found to have a multitude of effects within the cell, their modes of function are even more diverse (Geisler and Coller, 2013). One of the most common modes of action for lncRNAs (such as *ANRIL*) is functioning as a scaffold, onto which other RNAs and proteins can then join (Yap et al., 2010). Once in a complex with other RNAs or proteins the lncRNA can then act as part of a complex, with established roles so far including: regulation of mRNA transcription (Tsai et al., 2010,

Latos et al., 2012), regulation of mRNA processing (Tripathi et al., 2010), modulation of post-transcriptional modification pathways (Poliseno et al., 2010), regulation of protein activity (Kino et al., 2010), organization of protein complexes (Tsai et al., 2010, Yap et al., 2010) and signalling (Huang et al., 2013).

1.21 Aims

The aim of the first project was to further characterise the poorly understood human ABC transporter ABCB5, in terms of its expression and subcellular localisation within expressing cells utilising a transient transfection system to allow easy and fast genetic manipulation of the protein, In addition to this, the possible link between *ABCB5* knockdown and p16 expression levels was to be studied. The aim of this was to find a process by which p16-expressing senescence cells could be modulated, potentially using the plasma membrane localised ABCB5 as a target. The overall hypothesis for this work was that as ABCB5 is reportedly expressed at the plasma membrane, it could be used to target therapies for age-related disorders known to involve the expression of p16, a tumour suppressor protein that is known to act within the cell nucleus, and thus is not available for direct targeting.

The aim of the second project was to investigate the role of five putative oncogenic miRNAs in HMECs and $p16^+$ BLBC. The five miRNAs were previously suggested to invoke a phenotype of increased p16 expression and proliferation when transfected into HMECs, closely resembling the phenotype observed in $p16^+$ BLBC. As miRNAs can regulate hundreds or thousands of genes, the identity of their predicted downstream targets may provide clues as to the genetic changes involved in the formation of BLBC, and the importance in such genes in cancer progression and for potential diagnosis. The

hypothesis for this project was that as the five putative oncogenic miRNAs cause BLBC-like phenotype in HMECs, the targets giving rise to this change could be identified and then investigated as potential targets for targeted therapy against BLBCs.

The detailed aims of the two projects undertaken are more fully introduced at the beginning of their respective chapters.

Chapter Two

2 Materials and methods

2.1 Cell strains

2.1.1 XL10-Gold® Ultracompetent *E. coli* cells

Tet^r Δ(mcrA)183 Δ(mcrCB-hsdSMR-mrr)173 endA1 supE44 thi-1 gyrA96 relA1 lac HTE [F' proAB lacI^{q}ZΔM15 Tn10 (Tet^r) Amy Cam^r]

2.1.2 Mammalian cell lines

An overview of the mammalian cell lines used within this study is given below (Table 2-1), including known mutations that may be relevant to the study.

Cells	Cell Type	p16 status	p53 status	B-RAF status
HEK239T	Embryonic kidney	wt	wt/E1B55K	UN
WM1158	Melanoma	NM	wt	V600E
A375M	Melanoma	NM	wt	V600E
K562	Chronic myeloid leukaemia	Δ	NM	UN
A431	Squamous cell carcinoma	wt	Δ	wt
Mel224	Melanoma	UN	wt	wt
Mel505	Melanoma	UN	wt	wt
HMEC	Mammary epithelium	wt	wt	wt
MDA-MB-468	Breast carcinoma	wt	R273H	V600E

Table 2-1. Mammalian cell lines used in the investigation.

HMEC – human mammary epithelial cells; NM – nonsense mutation; Δ – deletion of gene; UN – unknown; E1B55K – adenovirus gene that represses p53 activation.

2.1.2.1 HEK293T

Human embryonic kidney 293 cells (Graham et al., 1977) stably and constitutively expressing the SV40 large T antigen (HEK293T) allowing for the expression of transfected plasmids containing the SV40 origin of replication were obtained from the Imperial Cancer Research Fund cell production unit (UK).

2.1.2.2 WM1158

The Wistar Institute Melanoma cell line 1158 (WM1158) was established from a human, stage II metastatic melanoma in 1985 by the laboratory of Dr. M. Herlyn at the Wistar Institute, Philidelphia, USA (Masters and Palsson, 1999). These cells were

kindly provided by Dr. Daniele Bergamaschi (Blizard Institute, London, UK). All WM1158 cells were used for experiments between passages 14 and 20.

2.1.2.3 A375M

The human A375M cell line was isolated from a lung metastasis in a nude mouse following injection of the parental human melanoma cell line A375 (Kozlowski et al., 1984). These cells were kindly provided by Dr. Daniele Bergamaschi (Blizard Institute, London, UK). All A375M cells were used for experiments between passages 11 and 20.

2.1.2.4 K562

The cell line K562 grows in suspension and was the first human immortalised myelogenous leukaemia line to be established. The line was derived from a 53-year-old female chronic myelogenous leukaemia (CML) patient in blast crisis in 1975 (Lozzio and Lozzio). These cells were kindly provided by Dr. Paul Allen (Blizard Institute, London, UK). All K562 cells were used for experiments between passages 18 and 25.

2.1.2.5 A431

The hypertriploid, human A431 cell line was established from a squamous cell carcinoma (SCC) in an 85 year old female patient (Giard et al., 1973). This cell line was kindly provided by Prof. Harry Navsaria (Blizard Institute, London, UK). All A431 cells were used for experiments between passages 14 and 20.

2.1.2.6 Mel224

These melanoma cells were kindly provided by Dr. Daniele Bergamaschi (Blizard Institute, London, UK). All Mel224 cells were used between passages 12 and 18.

2.1.2.7 Mel505

These melanoma cells were kindly provided by Dr. Daniele Bergamaschi (Blizard Institute, London, UK). All Mel505 cells were used between passages 12 and 18.

2.1.2.8 Human mammary epithelial cells

Normal 184 human mammary epithelial cells (HMECs; (Stampfer et al., 1980), were isolated from reduction mammoplasty tissue and were kindly provided by Dr. Martha Stampfer (Lawrence Berkeley National Laboratory, Berkeley, CA, USA). These cells exhibit a p16-mediated senescence in response to extended *in vitro* cell culture, providing an ideal platform on which the processes of normal human cell biology, aging, senescence and carcinogenesis can be studied. All HMEC cells were used for experiments between passage 4 and 13, the majority being at passage 6.

2.1.2.9 MDA-MB-468

The MDA-MB-468 cell line was isolated in 1977 from a pleural effusion of a 51 year old woman with metastatic adenocarcinoma of the breast (Cailleau et al., 1978), and lacks expression of HER2, OR and PR. These cells were purchased from AATC, VA, USA. MDA-MB-468 cells were used in experiments between passage 19 and 25.

2.2 Plasmids

The vectors used for the transformation of bacteria, and the transfection of mammalian cells are described in Table 2-2.

Vector	Resistance Marker	Size of insert (bp)	Source
pcDNA3.1 expressing V5-6His protein tag			
pcDNA3.1-V5-6His	Ampicillin	0	MG
pcDNA3.1-ABCB5fl-wt_V5-6His	Ampicillin	5401	MG
pcDNA3.1-ABCB5β-wt_V5-6His	Ampicillin	4375	MG
pcDNA3.1-ABCB5fl-E550Q_V5-6His	Ampicillin	5401	This study
pcDNA3.1-ABCB5fl-E1181Q_V5-6His	Ampicillin	5401	This study
pcDNA3.1-ABCB5fl-E550/1181Q_V5-6His	Ampicillin	5401	This study
pcDNA3.1-ABCB5β-E736Q_V5-6His	Ampicillin	4375	This study
pcDNA3.1 expressing EGFP protein tag			
pcDNA3.1-EGFP	Ampicillin	0	MG
pcDNA3.1-ABCB5fl-wt_EGFP	Ampicillin	5401	MG
pcDNA3.1-ABCB5β-wt_EGFP	Ampicillin	4375	MG
pcDNA3.1-ABCB5fl-E550Q_ EGFP	Ampicillin	5401	This study
pcDNA3.1-ABCB5fl-E1181Q_ EGFP	Ampicillin	5401	This study
pcDNA3.1-ABCB5fl-E550/1181Q_ EGFP	Ampicillin	5401	This study
pcDNA3.1-ABCB5fl-E736Q_ EGFP	Ampicillin	4375	This study
pcDNA3.1 expressing Venus protein tag			
pcDNA3.1-CD36_Venus	Ampicillin	4727	MS

Table 2-2. List of vectors used in the investigation.

The sequences of all vector inserts used in the investigation were confirmed by DNA sequencing. MG – Prof. Michael Gottesman (Bethesda, MD, USA); MS – Dr. Marjolein Snippe (London, UK).

2.3 Primers

A list of the oligonucleotides used in this investigation is provided in Table 2-3.

Name	Sequence (5' – 3')
Mutagenic Primers	
ABCB5fl_E550Q-F	CCAAGATTCTGATTTTAGATCAGGCTACGTCTGCCCTGG
ABCB5fl_E550Q-R	CCAGGGCAGACGTAGCCTGATCTAAAATCAGAATCTTGG
ABCB5fl_E1181Q-F	CCCAAAATTTTATTGTTGGATCAGGCCACTTCAGCCCTCG
ABCB5fl_E1181Q-R	CGAGGGCTGAAGTGGCCTGATCCAACAATAAAATTTTGGG
ABCB5β_E736Q-F	CCCAAAATTTTATTGTTGGATCAGGCCACTTCAGCCCTCG
ABCB5β_E736Q-R	CGAGGGCTGAAGTGGCCTGATCCAACAATAAAATTTTGGG
Sequencing Primers	
ABCB5_42F	TCAGAGAAATGGAACTGCAG
ABCB5_601F	GTGAAGGGCTGGAAACT
ABCB5_1041F	AACCTTCGCAATAGCCCGAG
ABCB5_1603F	ATTGCTCGTGCCTTAGTT
ABCB5_2177F	CCACATTAAAGCATGATGCAG
ABCB5_2742F	GCACAGATTATTGGAAGCTG
ABCB5_3268F	CGTTCCCAAATAGCAATC
ABCB5_3706F	ACTCATCAAGAGCTCCTGAG
ABCB5_161R	GGCTCCATTGACCAGTGATG
ABCB5_1781R	CAGCATTCCATCCTTTAGGG
Endpoint PCR Primers	
ABCB5-EPF	GTGAAGGGCTGGAAACT
ABCB5-EPR	ATGCCAAAATCCTTTGCA
5' RACE Primers	
RACE-GSP1	TCTTGACTAACCACTCCAA
RACE-GSP2	TCGATAATGCCGCACATTTA
RACE-GSP3	CGCACATTTAAAGCTCTGATG

Table 2-3. List of primers used in the investigation.

All primers were designed for the study using MacVector software (MacVector Inc, NC, USA). All primers listed were purchased from Sigma-Aldrich, UK.

2.4 TaqMan Gene Expression Assays

For TaqMan Gene Expression Assay (Life Technologies Ltd, UK) the following primers and probes were used Table 2-4.

Name	Forward (5' – 3')	Probe (5' – 3')	Reverse (5' – 3')	Type
Targeting Genes				
tmGAPDH	*proprietary*	*proprietary*	*proprietary*	PD
tmp16	*proprietary*	*proprietary*	*proprietary*	PD
tmABCB5	*proprietary*	*proprietary*	*proprietary*	PD
tmABCB5fl only	CACGTCTCCTCTTATAA TGGCTTCA	ATGACCATCC TAGAACATG	CCCAGCTTTGGAATA GGCACTTAT	CM
tmABCB5β only	TGTGTTCTTTTTTATTT GGTCATATCTTCCATTC	TAGGCTCACA GAGAGATATT	TCTTTCTGCAGTTATA TAAGAAAGACAATAGA	CM

Table 2-4. List of TaqMan primers and probes used in the investigation.

PD – pre-designed by the manufacturer; CM – custom made. Custom primers were designed by Life Technologies Ltd (UK), to target the 5' DNA coding sequence unique to ABCB5fl and the 5'-UTR sequence unique to ABCB5β (see Appendix I). All TaqMan products were purchased from Life Technologies Ltd (UK).

2.5 siRNAs

The siRNAs used in this project are detailed in Table 2-4

Name	Target mRNA	Target Sequence (5' – 3')	Supplier	Product Code	Type
siGLO	*Cyclophilin B*	GAGCCCAGAUC AACCUUUA	Dharmacon	D-001610-01-05	PD
GAPDH	*GAPDH*	proprietary	Ambion	103855	PD
CBX7	*CBX7*	GGGUAACACAC ACCAAGAGT	Ambion	137077	PD
p16	*p16*	TACCGTAAATGT CCATTTATA	Qiagen	SI02664403	PD
PLK1	*PLK1*	proprietary pool	Dharmacon	L-003290-00-0005	PD
KIF11	*KIF11*	GAGCCCAGAUC AACCUUUA	Dharmacon	J-003317-13-0005	PD
Ambion-1	*ABCB5fl, α, β, γ*	CCACCAUCAGUA ACAAUAUtt	Ambion	117801	PD
Ambion-2	*ABCB5fl, α, β, γ*	CGAUGAGAUUA AGACACUUtt	Ambion	117802	PD
Ambion-3	*ABCB5fl, β*	GCAAAGGUCGG ACUACAAUtt	Ambion	117803	PD
Beta-1	*ABCB5β*	GCCUAAACCAAU AAUUAUAtt	Ambion	298227	CM
Beta-2	*ABCB5β*	CAUUCUUUCUU ACCUAAUUtt	Ambion	298228	CM
Beta-3	*ABCB5β*	CUAUUGUCUUU CUUAUAUAtt	Ambion	298229	CM
Beta-4	*ABCB5β*	CUCUAAUAUCUC UCUGUGAtt	Ambion	446395	CM
Beta-5	*ABCB5β*	AUAUAACUGCAG AAAGAUAtt	Ambion	446396	CM
Beta-6	*ABCB5β*	UGCAGAAAGAUA AAUAUCAtt	Ambion	446398	CM

Table 2-5. siRNAs used in the investigation.

PD – pre-designed by the manufacturer; CM – custom made. Custom made siRNAs were designed by Life Technologies Ltd (UK), to target the 5'-UTR sequence unique to ABCB5β (see Appendix I).

2.6 miRNAs and anti-miRNAs

The details of the miRNAs and anti-miRNAs (antimiRs) used in this investigation can be found in Table 2-6.

Name	Type	Sequence	Product Code
miR-24	miRNA	UGGCUCAGUUCAGCAGGAACAG	HMI0410
miR-140-3p	miRNA	UACCACAGGGUAGAACCACGG	HMI0215
miR-221	miRNA	AGCUACAUUGUCUGCUGGGUUUC	HMI0398
miR-451	miRNA	AAACCGUUACCAUUACUGAGUU	HMI0583
miR-574	miRNA	UGAGUGUGUGUGUGUGAGUGUGU	HMI0794
Anti-24	anti-miRNA	proprietary	HSTUD0410
Anti-140-3p	anti-miRNA	proprietary	HSTUD0215
Anti-221	anti-miRNA	proprietary	HSTUD0397
Anti-451	anti-miRNA	proprietary	HSTUD0583
Anti-574	anti-miRNA	proprietary	HSTUD0794

Table 2-6. miRNAs and anti-miRNAs used in the investigation.

All miRNAs used were purchased from Sigma Aldrich (UK).

2.7 Bacterial cell culture

Bacterial medium (LB (lysogeny broth) liquid medium and agar) was prepared by suspending 20 g of LB powder, Lennox (1% (w/v) NaCl, 1% (w/v) tryptone, 0.5% (w/v) yeast extract; Fisher Scientific Ltd, UK) in 1 L of sterile water. For LB-agar plates, the medium was supplemented with 1.5% (w/v) bacto agar (BD Biosciences, UK) prior to autoclaving for 15 min at 15 psi and 121°C. Where necessary, the medium was allowed to cool to 55°C before 100 μg mL^{-1} ampicillin (Sigma-Aldrich, UK) was added. LB-agar plates were prepared using aseptic techniques and stored at 4°C for up to one month. Prior to use, plates were dried and equlibriated at 37°C in an incubator (Sanyo, UK).

2.7.1 SOC rich medium

SOC rich medium for bacterial transformations was prepared by adding 2% tryptone, 0.5% yeast extract, 10 mM NaCl, 2.5 mM KCl, 10 mM $MgCl_2$, 10 mM $MgSO_4$ and 20 mM glucose (Life Technologies Ltd, UK) to dH_2O and autoclaving.

2.8 Mammalian cell culture

2.8.1 Culture conditions

Cells were grown as monolayers on 75 cm^2 tissue culture flasks (VWR, UK) and maintained by biweekly passage in 15 mL of the appropriate medium unless otherwise stated.

Unless otherwise stated cells were split by washing the cells with 10 mL Dulbecco's phosphate buffered saline (DPBS; PAA Laboratories, UK) without calcium and magnesium for 1 min at room temperature (RT) before treatment with 3 mL TrypLE™ Express trypsin substitute (Life Technologes Ltd, UK) for 5 min at 37°C. TrypLE™ Express was quenched by addition of 7 mL of the appropriate serum containing medium. The resuspended cells were transferred to a 15 mL sterile centrifuge tube (Fisher Scientific Ltd, UK) and pelleted by centrifugation at 600 x *g* for 4 min. Cells were resuspended in the appropriate medium, and then plated into a new 75 cm^2 flask at the desired density.

Cells were grown under 5% CO_2 at 37°C with a water vapour saturated atmosphere (Galaxy 170S; New Brunswick Scientific, Edison, NJ). All manipulations were carried out in a sterile environment with disposable plasticware and glassware reserved specifically for the purpose.

2.8.1.1 HEK293T and A431 Culture

Cells were grown in "DMEM medium" (Dulbecco's Modified Eagle Medium (DMEM) with 4.5 mg L^{-1} glucose, 1 mM sodium pyruvate, 4 mM GlutaMAX™ and 40 nM phenol red, but not 4-(2-hydroxyethyl)-1-piperazineethanesulphonic acid (HEPES; Life Technologies Ltd, UK). DMEM was supplemented with 10% (v/v) Fetal bovine serum (FBS; Sigma-Aldrich, UK) and 2mM L-glutamine (Life Technologies Ltd, UK). Prior to treatment with TrypLE™ Express, A431 cells were washed with 6 mL Versene (Life Technologies Ltd, UK) at 37°C for 4 min. HEK293T cells were split at a ratio of 1:20 into a new flask, A431 at 1:10 and HeLa at 1:10.

2.8.1.2 WM1158, A375M, K562, Mel224 and Mel505 Culture

Cells were grown in "RPMI medium" (Roswell Park Memorial Institute 1640 (RPMI 1640), with 1 mM GlutaMAX™, 40 nM phenol red and 25mM HEPES (Life Technologies Ltd, UK) supplemented with 10% (v/v) FBS, 2 mM L-glutamine and 1x Non-essential amino acids (PAA Laboratories Ltd, UK). K562 cells were grown in suspension in 75 mL "RPMI medium" and split 1:3 every seven days. WM1158 cells were split at a ratio of 1:8 into a new flask, A375M at 1:8, Mel224 at 1:6 and Mel505 at 1:6.

2.8.1.3 HMEC Culture

Cells were grown in "M87A medium" (50% Mammary Epithelial Basal Medium (MEBM; Lonza Ltd, CH) supplemented with MEGM SingleQuot Kit Supplements and Growth Factors (excluding gentamycin; Lonza Ltd, CH), 5 μg/mL transferrin (Sigma-Aldrich, UK), 5 μM isoproterenol (Sigma-Aldrich, UK), 2 mM L-glutamine; 50% DMEM: Nutrient Mixture F-12 (DMEM/F12), with 2 mM L-glutamine and 40 nM phenol red, but no HEPES (Life Technologies Ltd, UK) supplemented with 10 μg/mL

insulin, (Sigma-Aldrich, UK) 5% (v/v) FBS, 100 ng/mL hydrocortisone (Sigma-Aldrich, UK), 10 nM 3,3',5-triiodo-L-thyronine (Sigma-Aldrich, UK), 10 nM β-estradiol (Sigma-Aldrich, UK) and 5 ng/mL epidermal growth factor (Life Technologies Ltd, UK); 0.1% (w/v) AlbuMAX™ I (Life Technolgies Ltd, UK) and 0.1 nM oxytocin (Bachem, CH). Cells were cultured from passage 4 (P4), seeded at a density of 5000 $^{cm-2}$, media changed every 1-2 days and split every four days. Cells were split by washing for 30 sec in DPBS at RT followed by incubation with 3 mL Trypsin-EDTA pre-warmed to 37°C for 7 min at 37°C. Trypsin-EDTA was quenched by addition of 7 mL "M87A medium" and cells were centrifuged at 600 x *g* for 4 min. Cells were resuspended in medium and counted (NucleoCounter® NC-100™; Chemometec, DM) before being plated into fresh 75 cm^2 flasks. Cells were transfected with siRNA at passage 6 (P6; see Section 2.11.1).

2.8.1.4 MDA-MB-468 Culture

Cells were grown in "BLBC medium" (DMEM with 4.5 mg L^{-1} glucose, 1 mM sodium pyruvate, 4 mM GlutaMAX™ and 40 nM phenol red (but not HEPES), supplemented with 10% (v/v) FBS, 2 mM L-glutamine and 1 mM sodium pyruvate (Sigma-Aldrich, UK)). Prior to splitting, cells were washed with 6 mL Versene for 4 min at 37°C. cells were counted (NucleoCounter® NC-100™; Chemometec, DM) and seeded at 10,000 cm^{-2} into fresh 75 cm^2 flasks.

2.9 Bacterial (XL10-Gold® Ultracompetent *E. coli*) transformation

XL10-Gold® Ultracompetent cells (Agilent Technologies, UK) were thawed on ice. For each sample to be transformed, 22.5 μL of bacteria were aliquoted into a 1.5 mL

Eppendorf microcentrifuge tube (Eppendorf, UK) prechilled on ice. The bacteria were treated with 1 μL XL10-Gold® β-mercaptoethanol mix, mixed gently, kept on ice for 10 min and mixed gently every 2 min. Afterwards, 5 ng of plasmid DNA from each sample to be transformed was added to separate aliquots of the ultracompetent cells, mixed gently and incubated on ice for 30 min. The bacteria were heat-shocked for 30 sec at 42°C and then incubated on ice for 2 min before 250 μL of preheated (42°C) SOC rich medium (see Section 2.7.1) was added to the tube. The cells were allowed to recover for 1 h at 37°C with shaking at 250 rpm (Innova 4000 Benchtop Incubator Shaker; New Brunswick Scientific, NJ) before the entire transformation was plated onto a LB-agar plates containing 100 μg/mL ampicillin. Plates were subsequently incubated at 37°C for > 18 h.

2.10 Mammalian cell plasmid transfection

2.10.1 HEK293T

2.10.1.1 For immunoblot analysis

HEK293T cells were seeded as a monolayer at 30,000 cells cm^{-2} on 6 round-well plates (ThermoFisher Scientific, MA, USA) in 2.5 mL complete DMEM medium (see Section 2.8.1.1) 24 h prior to transfection, to provide 60% - 70% confluency. For the transfection, 7.5 μg total plasmid DNA was added to 7.5 μL sterile water and 1 μL 5% (w/v) glucose in individual 1.5 mL Eppendorf microcentrifuge tubes (Eppendorf, UK). Subsequently, 1.5 μL polyethyleneimine (PEI) was added to each reaction and then incubated for 10 min at RT. During the 10 min incubation period, all medium was aspirated from each well and replaced with 1.5 mL fresh DMEM medium pre-warmed to 37°C. After the 10 min incubation, 1 mL of 37°C DMEM medium was added to each

tube and then applied to the cells. Cells were harvested 48 h post transfection for immunoblot analysis (see Section 2.23).

2.10.1.2 For immunocytochemistry analysis

HEK293T cells were seeded and transfected as in Section 2.10.1.1. 24 h post transfection, medium was aspirated from the wells and cells were washed with 1 mL DPBS. Cells were recovered from the wells by treatment with 500 µL TrypLE™ Express for 5 min at 37°C and 2 mL of DMEM medium was subsequently added to quench the TrypLE™ Express. Next, 1 mL of each cell suspension was added to a well of a new six round-well plate, each containing four sterile coverslips which had previously been treated with 100 µL 100 µg/ml^{-1} poly-L-lysine for 1 h at RT followed by three washes in 1 mL DPBS. Each well was topped up with 1.5 mL of fresh DMEM medium. The cells were cultured for a further 24 h in normal culture conditions and were fixed 48 h post transfection for immunocytochemistry analysis (see Section 2.27.3).

2.10.1.3 For cytotoxicity assay

HEK293T cells were seeded as a monolayer at 3 x 10^4 cells cm^{-2} on 96-well flat bottom plates (ThermoFisher Scientific, MA, USA) in 250 µL complete DMEM medium (see Section 2.8.1.1) 24 h prior to transfection, to provide 60% - 70% confluency. For the transfection, 0.625 µg total plasmid DNA was added to 1.25 µL sterile water and 0.125 µL 5% (w/v) glucose in individual 1.5 mL Eppendorf microcentrifuge tubes (Eppendorf, UK). Subsequently, 0.188 µL PEI was added to each reaction and then incubated for 10 min at RT. During the 10 min incubation period, all medium was aspirated from each well and replaced with 200 µL fresh DMEM medium pre-warmed to 37°C. After the 10 min incubation, 50 µL of 37°C DMEM medium was added to

each tube and then applied to the cells. Cells used 48 h post transfection for the cytotoxicity assay (see Section 2.26).

2.11 Mammalian cell siRNA/miRNA transfection

2.11.1 HMEC

2.11.1.1 For immunocytochemistry

HMECs were transfected with siRNA and miRNA in 384-well plates (ThermoFisher Scientific, MA, USA) at P6 using the reverse transfection method to replicate the conditions used in the previous study (Bishop et al., 2010). All conditions were set up in sextuplicate.

Wells for the transfection reagent only 'HiPerFect Only' condition were coated with MEGM (Lonza Ltd, CH) without supplements, plus 0.25 μL HiPerFect (QIAGEN, DE) in a total volume of 5 μL. Wells for conditions containing either siRNA or miRNA were coated with 5 μL HiPerFect containing supplement-free MEGM, plus 5 μL supplement-free MEGM, containing either siRNA or miRNA to give a final concentration of 30, 60 or 90 nM, depending on the experiments being carried out. The HiPerFect and si/miRNA mixtures were incubated for 90 mins at RT to allow transfection complexes to form. HMECs at P6 were plated at 10,000 cm^{-2} in 60 μL M87A medium (see Section 2.8.1.3), to give each well a total volume of 70 μL. The transfection plate was media changed 48 h post transfection by the replacement of 50 μL, from each well with 80 μL fresh medium. The plate was fixed 120 h post transfection for immunocytochemistry analysis (see Section 2.27.2).

2.11.1.2 For RT-qPCR analysis

HMECs for RT-qPCR analysis were reverse transfected in 6-well plates (Fisher Scientific Ltd, UK) at P6. For wells containing the transfection reagent only condition 'HiPerFect Only', wells were coated with supplement-free MEGM (Lonza Ltd, CH) plus 6.9 μL HiPerFect (QIAGEN, DE) in a total volume of 188.6 μL supplement-free MEGM. For wells containing siRNA, the wells were coated with 48.27 μL of 1 μM siRNA in supplement-free MEGM, plus 6.9 μL HiPerFect in a total volume of 188.6 μL supplement-free MEGM. The transfection mixture was incubated for 90 mins at RT to allow transfection complexes to form. HMECs at P6 were plated at 10,000 cm^{-2} in 1.379 mL M87A medium (see Section 2.8.1.3), to give each well a total volume of 1.6 mL and a final siRNA concentration of 30 nM. The transfection plate was harvested for RT-qPCR analysis 48 h post transfection (see Section 2.13).

2.11.2 MDA-MB-468

MDA-MB-468s were transfected with siRNA and miRNA in 384-well plates (ThermoFisher Scientific, MA, USA) between passage 20 (P20) and passage 28 (P28) using the reverse transfection method, in order to reduce the chance of pipetting error, and to replicate the conditions used in the previous study (Overhoff et al., 2014). All conditions were set up in sextuplicate.

Wells for the transfection reagent only 'HiPerFect Only' condition were coated with DMEM without supplements, plus 0.2 μL HiPerFect (QIAGEN, DE) in a total volume of 5 μL. Wells for conditions containing either siRNA or miRNA were coated with 5 μL HiPerFect containing supplement-free DMEM, plus 5 μL supplement-free DMEM (Sigma Aldrich, UK), containing either siRNA or miRNA to give a final concentration

of 60 or 90 nM. The HiPerFect and si/miRNA mixtures were incubated for 90 mins at RT to allow transfection complexes to form. MDA-MB-468s were plated at 30,000 cm^{-2} in 60 μL BLBC medium (see Section 2.8.1.4), to give each well a total volume of 70 μL. The transfection plate was media changed 48 h post transfection by the replacement of 50 μL, from each well with 80 μL fresh medium. The plate was fixed 120 h post transfection for immunocytochemistry analysis (see Section 2.27.2).

2.12 Isolation of plasmid DNA from XL10-Gold® *E. coli*

Small-scale (μg quantities) preparations of plasmid DNA were isolated from *E. coli* using the GenElute™ Plasmid Miniprep Kit (Sigma-Aldrich, UK) as described by the manufacturer. Large-scale (mg quantities) preparations of plasmid DNA were isolated from *E. coli* using the QIAGEN Plasmid Mega Kit (QIAGEN, NL) as described by the manufacturer. Slight modifications to both protocols are included within the methods outlined below.

2.12.1 Small-scale preparations

A single bacterial colony from a freshly streaked plate was used to inoculate a small culture of 5 mL LB broth containing 100 μg/mL ampicillin (see Section 2.7), in a sterile 50 mL Erlenmeyer flask and incubated overnight at 37°C with shaking at 250 rpm (Innova 4000 Benchtop Shaker; New Brunswick Scientific, Edison, NJ, USA). From the 5 mL culture, 2 mL was harvested by centrifugation for 2 min at 12,000 x *g*. The pellet was then resuspended in 200 μL Resuspension Solution, followed by 200 μL Lysis Buffer and the solution was mixed by inversion. The alkaline Lysis Buffer lyses the cells and causes the denaturation of nucleic acids and proteins within the lysate. After 5 min at RT, 350 μL Neutralization Solution was added, causing the aggregation

of insoluble genomic DNA and high molecular weight RNA, and the precipitation of protein-sodium dodecyl sulphate (SDS) complexes. The lysate was then centrifuged for 10 min at 12,000 x *g*, during which time the GenElute HP Miniprep Binding Columns were primed by adding 500 µL Column Preparation Solution and centrifuging for 1 min at 12,000 x *g*. The supernatant from the cell lysate was then added to the columns and incubated for 1 min at RT, before being centrifuged at 12,000 x *g* for 1 min. With the plasmid DNA then bound to the column, the flow through was discarded. Each column was washed by adding 500 µL Wash Solution, before centrifuging for 1 min at 12,000 x *g*. Eluted wash solution was discarded and the columns were again centrifuged as before to remove any remaining traces of Wash Solution. Plasmid DNA was eluted by adding 50 µL of 10 mM Tris buffer pH 8.8 to the column and incubating for 5 min at RT before being centrifuged at 12,000 x *g* for 1 min. The concentration and purity of the eluted plasmid DNA was determined by spectrophotometric analysis as described in Section 2.14 and stored at -20°C.

2.12.2 Large-scale preparations

A single bacterial colony from a freshly streaked plate was used to inoculate a starter culture of 5 mL LB broth containing 100 µg/mL ampicillin (see Section 2.12.1), in a sterile 50 mL Erlenmeyer flask and incubated for 8 h at 37°C with shaking at 250 rpm. The starter culture was then diluted 1:500 in a 500mL LB broth containing 100 µg/mL ampicillin, in a sterile 2 L baffled Erlenmeyer flask and incubated at 37°C with shaking at 250 rpm for 16 h. The cells were harvested by transferring the culture to a 500 mL bottle and spinning in a superspeed centrifuge (Sorvall 5C Plus, Thermo-Sorvall, CT) at 6,000 x *g* for 15 min at 4°C, before being resuspended in 50 mL Buffer P1. 50 mL of Buffer P2 was then added to lyse the cells and the bottle was vigorously inverted six times before being incubated at RT for 5 min. 50 mL of Buffer P3 (pre-chilled to 4°C)

was added and mixed through by six further vigorous inversions then the bottle was incubated on ice for 30 min. Following this the lysate was mixed briefly and centrifuged at 20,000 x *g* for 30 min at 4°C. Whilst the lysate was being centrifuged, a QIAGEN-tip-2500 column was equilibrated by applying 35 mL Buffer QBT and letting the column empty by gravity flow. After centrifugation, the supernatant containing the plasmid DNA was promptly removed from the bottle, added to the equilibrated column and allowed to enter the resin by gravity flow. Subsequently, 200 mL of Buffer QC was applied to the QIAGEN-tip 2500 to wash the column and remove contaminants from the plasmid DNA. The plasmid DNA was eluted with 35 mL Buffer QF into a 50 mL centrifuge tube (Scientific Laboratory Supplies, UK) by gravity flow. DNA was precipitated by addition of 24.5 mL of isopropanol, mixed gently and immediately centrifuged at 15,000 x *g* for 30 min at 4°C before carefully removing the supernatant. The plasmid DNA pellet was washed with 7 mL 70% ethanol and centrifuged again at 15,000 x *g* for 10 min. The supernatant was removed and the pellet air-dried for 10 – 20 min, before redissolving the plasmid DNA in 500 µL 10 mM Tris buffer pH 8.8. The concentration and purity of the eluted plasmid DNA was determined by spectrophotometric analysis as described in Section 2.14 and stored at -20°C.

2.13 Isolation of total RNA from human cells

Small-scale (µg quantities) preparation of total RNA from human cells was carried out using the QIAGEN RNeasy® Mini Kit (QIAGEN, NL) as described by the manufacturer. Slight modifications to the protocol are detailed in the method below.

Media was aspirated from the wells 48 h post transfection (see Section 2.11) and cells were washed with DPBS containing both magnesium and calcium (PAA Laboratories,

UK; H15-001). Cells were lysed by the addition of 600 µL Buffer RLT (supplemented with 1.0% β-mercaptoethanol) and a sterile, disposable cell scraper (Fisher Scientific Ltd, UK) was used to ensure that all cells were lysed. The lysate was removed to a 1.5 mL Eppendorf microcentrifuge tube (Eppendorf, UK) and mixed by pipetting, before being homogenised by centrifuging through a QIAshredder spin column (QIAGEN, NL; 79654) for 2 min at 14,000 x *g*. One volume of 70% ethanol (Sigma-Aldrich) was added to the homogenised lysate and mixed by pipetting six times. The sample, including any precipitate formed, was transferred to an RNeasy spin column (in a supplied 2 mL collection tube) and was centrifuged for 15 sec at 8,000 x *g*, after which the flow-through was discarded. The column with bound RNA was subsequently washed with 700 µL Buffer RW1 by centrifuging for 15 sec at 8,000 x *g* followed by two further 500 µL washes with Buffer RPE using the same spin conditions. In each case the flow-through was discarded. The column was transferred to a fresh 2 mL collection tube and spun for a further 1 min at 14,000 x *g* to remove and residual Buffer RPE from the last wash. Subsequently, the column was transferred to a new 1.5 mL Eppendorf microcentrifuge tube and 50 µL RNase-free water was added directly to the spin column before being centrifuged for 1 min at 14,000 x *g* to elute the bound RNA. The concentration and purity of the eluted RNA was determined by spectrophotometric analysis as described in Section 2.14 and stored at -80°C.

2.14 Determination of nucleic acid yield and quality

DNA and RNA concentrations in nucleic acid preparations were determined by spectrophotometry by measuring the absorbance at 260 nm (A_{260}) using the NanoDrop ND-1000 (ThermoFisher Scientific, MA, USA). The quality of nucleic is indicated by

the ratio between the absorbance at 260 and 280 nm. For pure DNA the A_{260}/A_{280} ratio should be ~1.8 and for pure RNA the ratio should be ~2.0. Smaller ratios usually indicate contamination by protein or organic chemicals. As a secondary measure of nucleic acid purity, the A_{260}/A_{230} ratio was also measured which should be in the range of 1.8 to 2.0 for DNA and 2.0 to 2.2 for RNA. Only nucleic acids that passed these criteria were used in downstream applications.

2.15 Reverse-transcription of mRNA to cDNA

cDNA synthesis was carried out using the GrandScript cDNA synthesis Kit (PCR Biosystems, UK) as per the manufacturer's instructions. Briefly, 1 μg RNA (see Section 2.13) was mixed with 4.0 μL 5x cDNA synthesis mix (proprietary) 1.0 μL reverse transcriptase (RTase; proprietary) and nuclease-free H_2O to a total volume of 20 μL before incubation at 42°C for 30 min, followed by incubation at 70°C for 10 min to denature the RTase. cDNA was stored at -20°C for up to one week or used immediately for downstream applications.

2.16 PCR of cDNA

PCR was carried out using *Taq* DNA Polymerase and ThermoPol Buffer (New England Biolabs, UK) on previously generated cDNA (see Section 2.15). Reactions were set up as described in Table 2-7 and run with the conditions detailed in Table 2-8.

Reagent	Volume	Final Concentration
10x ThermoPol Reaction Buffer	5 μL	1x
dNTPs (20 mM)	0.5 μL	200 μM
Forward Primer (20 μM)	0.5 μL	0.2 μM
Reverse Primer (20 μM)	0.5 μL	0.2 μM
Template cDNA	Variable	5 μg/μL
Taq DNA Polymerase	0.25 μL	1.25 Units
Nuclease-free water	To 50 μL	N/A

Table 2-7. Reaction mix used for PCR of cDNA with Taq DNA Polymerase.

10x ThermoPol Reaction Buffer and Taq DNA Polymerase – proprietary (New England Biolabs, UK); dNTPs – 5 mM dCTP, 5 mM dTTP, 5 mM dATP, 5 mM dGTP (Bioline, UK); Nuclease-free water was from Promega, UK. Forward and Reverse Primers used were dependent on the sequence to be amplified (see Section 2.3).

Time (Sec)	Temperature (°C)	No. Of Cycles	Step
30	95	1	Initial denaturation
20	95	30 – 50	Denaturation
30	55		Primer binding
60 per kb	68		Extension
300	68	1	Final extension
∞	4	N/A	Hold

Table 2-8. Cycling conditions for Taq DNA Polymerase PCR.

2.17 TaqMan qPCR of cDNA

The TaqMan quantitative PCR (qPCR) system (Life Technologies Ltd, UK) uses two target-specific primers, which bind at opposite ends of the section of the template to be amplified, much like standard qPCR. Unlike standard qPCR, TaqMan qPCR also requires a third sequence-specific oligonucleotide probe which binds to the middle of the section to be amplified. This probe is different to the primers in two ways. Firstly, the probe cannot be extended by the *Taq* polymerase, as it has no free hydroxyl group. Secondly, the probe is covalently bound to two other molecules: a fluorescent Reporter molecule at the 5' end, and a fluorescent Quencher molecule at the 3' end. When not bound to DNA, the probe curls back on itself, so that the 5' and 3' ends of the molecule are in close proximity to each other, meaning that the Reporter and Quencher molecules are next to each other. When the Reporter is excited in this state, the energy is

transferred to the Quencher by fluorescence resonance energy transfer, and the Reporter does not produce a fluorescent signal. During the extension stage of the PCR reaction, the exonuclease activity of the *Taq* polymerase will cleave the nucleotides of the probe bound to the template, but only where both the primers and the probe are all bound to the same section of DNA. The hydrolysation of the probe will permanently separate the Reporter and Quencher molecules from each other, allowing the Reporter to fluoresce at a level detectable by the instrument when it is excited. As one Reporter molecule will be released from every new PCR amplicon created, the fluorescence in the reaction will increase proportionally with the amount of specific product in the reaction.

cDNA from the reverse transcription of 1 μg mRNA extracted from cells (see Section 2.15) was diluted 1:2 in RNase-free water and used in the reaction, as detailed in Table 2-9. Each 20 μL reaction was transferred to a well of a 96-well reaction plate (Life Technologies Ltd, UK) and the plate was sealed using optical adhesive film (Life Technologies Ltd, UK). The plate was loaded onto the qPCR machine (Applied Biosystems 7500 Real –Time PCR System; Life Technologies Ltd, UK) and run with the conditions outlined in Table 2-10.

PCR reaction mix component	Volume per 20 μL reaction
20x TaqMan Gene Expression Assay	1.0 μL
2x TaqMan Gene Expression Master Mix	10.0 μL
cDNA template	2.0 μL
RNase-free water	7.0 μL

Table 2-9. Reaction mix used for the TaqMan qPCR system (Life Technologies Ltd, UK).

TaqMan Gene Expression Assay – contents dependent on gene to be analysed, see Table 2-4; TaqMan Gene Expression Master Mix – proprietary.

Time (sec)	Temperature (°C)	No. of Cycles	Step
120	50	1	
600	95	1	Initial denaturation
15	95	40	Denaturation
60	60		Extension

Table 2-10. Cycling conditions for TaqMan qPCR.

2.18 5' RACE PCR

5' RACE PCR was carried out using the 5' RACE System for Rapid Amplification of cDNA Ends, Version 2.0 kit (Life Technologies Ltd, UK). The reactions were carried out according to the manufacturer's instructions apart from a few minor changes, detailed below.

2.18.1 First strand cDNA synthesis

mRNA isolated from P5 HMECs (See Section 2.13) was subjected to first strand cDNA synthesis. A total of 5 μg mRNA was used with 2.5 pmol RACE-GSP1 (see Table 2-3 for details) in a volume of 15.5 μL. The mixture was incubated for 10 min at 70°C, followed by chilling on ice for 1 min. Subsequently, 2.5 μL 10x PCR buffer (proprietary), 2.5 μL 25 mM $MgCl_2$, 1 μL 10 mM dNTP mix and 2.5 μL 100 mM DTT were added to the reaction and the mix was incubated for 1 min at 42°C. Finally, 1 μL SuperScript™ II RT was added, followed by incubation for 30 min at 42°C and then 70°C for 15 min to terminate the reaction.

The mixture was placed at 37°C following a brief centrifugation and 1 μL RNase mix added and incubated for 30 min. Subsequently the reaction was collected by brief centrifugation and placed on ice.

2.18.2 Purification of cDNA

Excess nucleotides and RACE-GSP1 were removed from the first strand product by purification using the provided S.N.A.P. columns. To the reaction containing the first strand product, 120 μL binding solution (6 M NaI) was added at RT; the resulting mixture was transferred to a S.N.A.P. column and centrifuged at 13,000 x *g* for 20 sec. The flowthrough from the centrifugation was discarded and the column was washed three times with 400 μL 4°C 1x wash buffer by centrifugation at 13,000 x *g* for 20 sec. The column was washed a further two times with 400 μL 4°C 70 % ethanol by centrifugation at 13,000 x *g* for 20 sec. After removing the flowthrough the membrane was dried by spinning the column for a further 1 min at 13,000 x *g*. The cDNA was recovered from the column by the addition of 50 μL RNase-free water pre-heated to 65°C to the spin cartridge and centrifugation at 13,000 x *g* for 20 sec.

2.18.3 TdT tailing of cDNA and amplification

Terminal deoxynucleotidyl transferase (TdT) was used to an oligo-dC tail to the first strand cDNA generated in Section 2.18.1 and purified in Section 2.18.2. The TdT tailing reaction was set up as described in Table 2-11.

Reagents	Volume (μL)	Final Concentration
RNase-free water	4.5	N/A
5x tailing buffer	5	1x
2 mM dCTP	2.5	0.2 mM
Purified cDNA sample	12	Unknown

Table 2-11. Reaction mix used for TdT tailing reaction (Life Technologies Ltd, UK). 5x tailing buffer – proprietary.

The reaction mixture was incubated for 2 min at 94°C and then 1 min on ice, followed by the addition of 1 μL TdT. The sample was incubated at 37°C for 10 min for the reaction to occur and subsequently at 65°C for 10 min to inactivate the TdT. The contents of the reaction was collected by brief centrifugation and placed on ice.

2.18.4 Amplification of dC-tailed cDNA

dC-tailed cDNA obtained from 2.18.3 was amplified directly by PCR using the reagents detailed in Table 2-12 and the conditions found in Table 2-13.

Reagent	Volume (μL)	Final Concentration
RNase-free water	31.5	N/A
10x PCR buffer	5	1x
$MgCl_2$ (25 mM)	3	1.5 mM
dNTP mix (10 mM)	1	200 μM
RACE-GSP2 (10 μM)	2	200 nM
Abridged Anchor Primer (10 μM)	2	200 nM
dC-tailed cDNA	5	Unknown
Taq DNA polymerase	0.5	2.5 U

Table 2-12. Reaction mix used for PCR of dC-tailed cDNA.

10x PCR buffer – 200 mM Tris-HCl (pH 8.4), 500 mM KCl.

Time (sec)	Temp (°C)	Cycles	Step
60	95	1	Initial Denaturation
30	95	35	Denaturation
45	55		Annealing
60	72		Extension
420	72	1	Final Extension

Table 2-13. Cycling conditions for PCR of dC-tailed cDNA.

2.18.5 Nested amplification of dC-tailed cDNA

Following the first amplification of dC-tailed cDNA, not enough product was generated to undertake direct sequencing. To produce additional cDNA, the products from the original PCR were diluted and then re-amplified using the nested gene-specific primer RACE-GSP3 (See Table 2-3) and the provided abridged universal amplification primer. The PCR products from Section 2.18.4 were diluted by the addition of 495 μL TE buffer (10 mM Tris-HCl (pH 8.0), 1 mM EDTA) to 5 μL of the products. The reaction was then set up using the reagents detailed in Table 2-14, and ran with the conditions outlined in Table 2-15.

Reagent	Volume (μL)	Final Concentration
RNase-free water	33.5	N/A
10x PCR buffer	5.0	1x
$MgCl_2$ (25 mM)	3.0	1.5 mM
dNTP mix (10 mM)	1.0	200 μM
RACE-GSP3 (10 μM)	1.0	200 nM
Abridged universal anchor primer (10 μM)	1.0	200 nM
Dilution of PCR product	5.0	Unknown
Taq DNA polymerase	0.5	2.5 U

Table 2-14. Reaction mix used for nested amplification of dC-tailed cDNA.

10x PCR buffer – 200 mM Tris-HCl (pH 8.4), 500 mM KCl.

Time (sec)	Temp (°C)	Cycles	Step
60	95	1	Initial Denaturation
30	95	35	Denaturation
45	55		Annealing
60	72		Extension
420	72	1	Final Extension

Table 2-15. Cycling conditions for nested amplification of dC-tailed cDNA.

2.19 Agarose gel electrophoresis of DNA

Agarose gels [2% (w/v)], were prepared by melting the required amount of powdered agarose (DNA grade; Life Technologies Ltd, UK) in TAE buffer (40 mM Tris-acetate, 1 mM EDTA) by heating in a microwave oven (Sharp, UK) until dissolved. The melted solution was allowed to cool to 55°C before GelRed™ (Biotium, CA, USA; 41002) was added to 1x. The gel was then poured into the appropriate mould (Owl Separation Systems; Thermo Fisher Scientific, UK) and allowed to set. DNA fragments were separated by electrophoresis through a gel submerged in TAE buffer. Before loading onto the gel, the samples were mixed with the appropriate volume of 6x gel-loading buffer (2.5% Ficoll® 400, 11 mM EDTA, 3.3 mM Tris-HCl pH 8.0, 0.017% SDS, 0.15% Orange G; New England Biolabs, UK). The samples were loaded into the wells alongside a 100 bp DNA ladder (HyperLadder IV; Bioline, UK) and electrophoresed at 10 V cm^{-1} until the required resolution was achieved. The DNA was visualised using an ultraviolet (UV) transilluminator and images recorded using the MultiImage™ Light Cabinet (Alpha Innotech Corporation, CA, USA).

2.20 Site-directed mutagenesis

Oligonucleotide-directed mutations were introduced into both the V5-6His and EGFP tagged forms of pcDNA3.1-ABCB5fl-wt and pcDNA3.1-ABCB5β-wt (see Table 2-2) using the QuikChange II XL site-directed mutagenesis kit (Agilent Technologies, UK).

2.20.1 Mutagenic primer design

Mutagenic oligonucleotides were designed using the web-based QuickChange Primer Design Program available at http://www.stratagene.com/qcprimerdesign and purchased from Sigma-Aldrich (Table 2-3).

2.20.2 Mutant strand synthesis

Template plasmid DNA was amplified by PCR using a pair of mutagenic primers. The primer pairs are complementary to opposite strands of the template and span the site to be mutated, causing the PCR reaction to generate mutant DNA. Following amplification, *Dpn* I endonuclease digestion of methylated and hemi-methylated DNA is carried out by addition of 1 μL 10 U mL^{-1} *Dpn* I and incubation for 1 h at 37°C. Because the template plasmid DNA is generated in a dam^+ *E. coli* strain and therefore methylated, whereas the newly synthesised DNA is unmethylated, only the template DNA is susceptible to *Dpn*I digestion. This enables selection of the newly synthesised DNA containing the desired mutation to occur. The resulting plasmid DNA can subsequently be used to transform XL10-Gold® Ultracompetent Cells as described in Section 2.9.

Thermal cycling reactions were set up in thin-walled PCR tubes (Sigma-Aldrich, UK), to maximise temperature-cycling performance. Each reaction was set up as listed in Table 2-16 and cycled using the parameters outlined in Table 2-17.

QuickChange® Reaction Reagents	Volume	Concentration
Reaction Buffer (10x)	5 μL	1x
dsDNA Template	1 μL	0.2 ng/μL
Primer #1	1 μL	2.5 ng/μL
Primer #2	1 μL	2.5 ng/μL
dNTP Mix	1 μL	proprietary
QuikSolution	3 μL	proprietary
ddH_2O	To 50 μL final volume	
PfuTurbo DNA Polymerase (2.5 U/μL)	1 μL	2.5 Units

Table 2-16. Protocol for the QuickChange® XL site-directed mutagenesis kit (Stratagene, UK).

This protocol was used to introduce the required mutations to pcDNA3.1-ABCB5fl-wt and pcDNA3.1-ABCB5β-wt vectors expressing both V5-6His and EGFP tagged protein. Reaction buffer (1x): 200 mM Tris-HCl (pH 8.8), 20 mM $MgSO_4$, 100 mM KCl, 100 mM $(NH_4)_2SO_4$, 1% Triton® X-100, 1 mg/mL nuclease free bovine serum albumin; dNTP mix and QuikSolution composition: proprietary (Agilent Technologies, UK).

Time (sec)	Temperature (°C)	No. Of Cycles	Step
60	95	1	Initial denaturation
50	95	18	Denaturation
50	60		Annealing
540	68		Extension
420	68	1	Final extension

Table 2-17. PCR programme used to mutate ABCB5fl and ABCB5β.

The sequence of the entire mutant cDNA insert was confirmed as described in Section 2.21.

2.21 DNA Sequencing

2.21.1 Automated sequencing

Automated DNA sequencing was out-sourced and performed by LifeSciences (Source BioScience, UK).

2.21.2 In-house sequencing

In-house Sanger sequencing of DNA was carried out using BigDye® Terminator v3.1 Cycle Sequencing Kit (Life Technologies Ltd, UK).

2.21.2.1 Cycle sequencing of plasmid DNA

The BigDye® Terminator v3.1 Cycle Sequencing Kit provides the required reagents components for the sequencing reaction in a pre-mixed format. These reagents were used for performing fluorescence-based cycle sequencing reactions on single-stranded or double-stranded DNA templates and on PCR fragments.

Each reaction mixture was prepared as shown in Table 2-18.

Reagent	Volume	Concentration
Oligonucleotide	1.0 μL	320 fmol/μL
BigDye® Terminator Buffer (5x)	2.0 μL	1x
DNA Template	variable	0.1 μg/μL
Ready Reaction Premix (2.5x)	4 μL	1x
Nuclease-free water	To 10 μL final volume	

Table 2-18. Reaction mixture preparation for DNA sequencing.

BigDye® Terminator Buffer and Ready Reaction Premix composition: proprietary (Life Technologies Ltd, UK)

Cycle sequencing was performed in the Touchgene Gradient Thermal Cycler (Techne Ltd, UK) using the protocol outlined in Table 2-19.

Time (Sec)	Temperature (°C)	No. Of Cycles	Step
60	96	1	Initial denaturation
10	96	25	Denaturation
5	50		Annealing
240	60		Extension
∞	10	∞	Final Extension

Table 2-19. Thermocycling conditions for plasmid DNA sequencing.

2.21.2.2 Ethanol/EDTA precipitation of DNA

To ensure optimum results, unincorporated dye terminators (which can cause high levels of background fluorescent signal) were completely removed before electrophoresis.

Tubes containing the amplified products (in 10 μL volumes) were briefly spun to collect the sample before adding 2.5 μL of 125 mM EDTA (25 mM final; Sigma-Aldrich, UK) followed by 30 μL of 100% ethanol (Sigma-Aldrich, UK). The tubes were sealed, mixed by inverting four times, incubated at RT for 15 min and spun for 20 min at 17000 x *g* at 4°C in a fixed rotor centrifuge (Heraeus Fresco 17; ThermoFisher Scientific, MA, USA). The supernatant was discarded and 30 μL of 70% ethanol was added to each sample. Tubes were spun for 10 min at 17,000 x *g* at 4°C and the supernatant was discarded. Samples were allowed to air-dry for 30 min in the dark, resuspended in 10 μL Hi-Di™ Formamide (Applied Biosystems, UK) and loaded onto a MicroAmp® Optical 96-Well Reaction Plate (Life Technologies Ltd, UK).

2.21.2.3 Sample Electrophoresis

Before electrophoresis, the 96-well reaction plate was sealed and the samples were heated for 5 min at 96°C on a hot block (DRI Block® DB1.M; Techne Ltd, UK) to denature the DNA, then cooled rapidly for 1 min on ice.

Automated sample electrophoresis and sequencing analysis were performed using the instrument protocol "sequencing_600bp_POP7" and analysis protocol "3130 POP7_BDTU3-KB_DENOVO_V.5.2" on ABI Prism® 3130*xl* Genetic Analyser (Applied Biosystems, UK).

2.21.2.4 Sequencing data analysis

Analysis of the electropherograms was performed using the Sequence Scanner V1.0 (Applied Biosystems, UK).

2.22 Plasmid constructs

2.22.1 pcDNA3.1-ABCB5fl-wt and pcDNA3.1-ABCB5β-wt plasmids

Plasmids encoding human ABCB5fl or ABCB5β with either a C-terminal enhanced green fluorescent protein (EGFP) tag (pcDNA3.1-ABCB5fl-wt_EGFP and pcDNA3.1-ABCB5β-wt_EGFP, respectively) or a C-terminal 6-histidine (V5-6His) tag (pcDNA3.1-ABCB5fl-wt_V5-6His and pcDNA3.1-ABCB5β-wt_V5-6His, respectively) were kindly provided by Prof. Michael Gottesman (Bethesda, MD, USA).

2.22.2 Site directed mutagenesis

All ABCB5fl and ABCB5β mutants were derived from the appropriate WT plasmid using the QuikChange II XL site directed mutagenesis kit (see Section 2.20). The primers used to derive each mutant were: ABCB5fl_E550Q-F (c.1885G>C), ABCB5fl_E1181Q-F (c.3778G>C), ABCB5β_E736Q-F (c.2752G>C) and their reverse complements (see Table 2-3). Colonies from the mutagenesis reaction were picked and incubated overnight in 5 mL LB-amp liquid medium at 37°C with shaking at 250 rpm. Plasmid DNA was isolated from the cultures as described in Section 2.12.1.

2.22.3 Confirming veracity of mutagenesis

Each successful mutagenesis was confirmed either by automated DNA sequencing (see Section 2.21.1; Source BioScience, UK) or in-house sequencing (see Section 2.21.2). The primers used for sequencing were designed to cover the whole ABCB5fl or

ABCB5β cDNA. For ABCB5fl these were: ABCB5_42F, ABCB5_601F, ABCB5_1041F, ABCB5_1603F, ABCB5_2177F, ABCB5_2742F, ABCB5_3268F, ABCB5_3706F and ABCB5_161R. For ABCB5β these were: ABCB5_1603F, ABCB5_2177F, ABCB5_2742F, ABCB5_3268F, ABCB5_3706F and ABCB5_1781R (see Table 2-3).

2.22.4 pcDNA3.1-CD36_Venus plasmid

The pcDNA3.1-CD36_Venus plasmid encoding the human plasma membrane, scavenger receptor CD36 with a C-terminal fluorescent Venus protein (an improved version of yellow fluorescent protein, with reduced chloride sensitivity, faster maturation and increased brightness) tag was kindly provided by Dr. Marjolein Snippe (London, UK).

2.23 Preparation of whole-cell protein content

Total-cell extracts from mammalian cells for immunoblot analysis were prepared 48 h post plasmid transfection (see Section 2.10) or 120 h post siRNA transfection (see Section 2.11). Prior to lysis, cells were washed twice with DPBS containing both magnesium and calcium (PAA Laboratories, UK) and lysed in the cell culture dish on ice in 300 µL lysis buffer (150 mM NaCl, 1% IGEPAL® CA-630, 0.5% sodium deoxycholate, 0.1% SDS, 50 mM Tris pH 8.0 (Sigma-Aldrich, UK; R0278), 150 mM NaCl, 10 mM HEPES, 25 U/µL Benzonase® Endonuclease (Merck Millipore, DE) and 2x cOmplete™ Protease Inhibitor Cocktail (Roche, UK). Cells were treated with lysis buffer for 5 min on ice before samples were collected from the dish by vigorous cell scraping using a sterile, disposable cell scraper (Fisher Scientific Ltd, UK) and pipetting into a 1.5 mL Eppendorf microcentrifuge tubes (Eppendorf, UK). Samples were

centrifuged at 17,000 x g for 5 min at 4°C to remove any insoluble material, the supernatant was removed to fresh tubes and stored at -20°C.

2.24 Protein quantitation

Protein concentration of whole-cell extracts was determined using the Bio-Rad *DC* Protein Assay (Bio-Rad, UK). The Assay is based on the Lowry method (Lowry et al., 1951) and was carried out following the manufacturer's instructions. The reactions were performed in triplicate in 96-well microplates (ThermoFisher Scientific, MA, USA) and a range of bovine serum albumen (BSA) concentrations (0, 0.25, 0.5, 0.75, 1.0, 2.0, 3, 4. 6, 8 and 10 mg mL^{-1}) were used to produce a standard curve.

2.25 Analysis of protein expression

2.25.1 General reagents and buffers

The buffers used in this investigation for western blotting are detailed below in Table 2-20.

Buffer	Reagent	Concentration
SDS gel-loading buffer (6x)	Tris-HCl (pH 6.8)	350 mM
	DTT	250 mM
	Glycerol	60% (w/v)
	SDS	12% (w/v)
	Bromophenol blue	0.12% (v/v)
Running buffer (5x)	Tris	250 mM
	Glycine	250 mM
	SDS	1.0% (w/v)
Transfer buffer (10x)	Tris	195 mM
	Glycine	250 mM
	SDS	0.185% (w/v)
TBS (10x)	Tris-HCl (pH 7.6)	200 mM
	NaCl	1.4 M
Stripping buffer (1x)	PBS adjusted to pH 2.0 with HCl	1x
	SDS	1.0%

Table 2-20. List of buffers used for western blotting in the investigation.

DTT – dithiothreitol; PBS – phosphate buffered saline; SDS – sodium dodecyl sulphate. All reagents were supplied by Sigma-Aldrich, UK.

Running buffer, transfer buffer and TBS were all diluted to 1x with dH_2O. Transfer buffer was supplemented with 20% (v/v) methanol; both transfer and running buffer were only used once; TBS was supplemented with 0.2% (v/v) Tween-20 (Sigma-Aldrich, UK) to make TBS-T.

2.25.2 Antibodies

The antibodies used in this investigation for western blotting are detailed below in Table 2-21.

Antibody	Working Dilution	Species	Clonality	Source
Anti-ABCB5 (Atlas)	1:2,000	Rabbit	Polyclonal	Atlas Antibodies AB, SE
Anti-ABCB5 (Rockland)	1:500	Rabbit	Polyclonal	Rockland Inc. PA, USA
Anti-ABCB5 (Sigma)	1:500	Rabbit	Polyclonal	Sigma-Aldrich, UK
Anti-β-tubulin	1:100,000	Mouse	Monoclonal	EnoGene Biotech Ltd, NY, USA
HRP Anti-Rabbit	1:5,000	Goat	Polyclonal	Life Technologies Ltd, UK
HRP Anti-Mouse	1:1,000	Goat	Polyclonal	DAKO, UK

Table 2-21. List of antibodies used for western blotting in the investigation.

HRP – horseradish peroxidase.

2.25.3 Sodium dodecyl sulphate polyacrylamide gel electrophoresis (SDS-PAGE)

Gels were prepared using the discontinuous buffer system devised by Davis (1964), Ornstein (1964), and Laemmli (1970) in which the buffer in the sample and stacking gel contain Tris-Cl (pH 6.8), and the resolving gel contains Tris-Cl (pH 8.8).

All SDS-PAGE was performed using the Mini-PROTEAN® electrophoresis system from Bio-Rad (CA, USA) and Tris-glycine running buffer (see Section 2.25.1). Proteins were diluted in 6x SDS sample buffer (see Section 2.25.1) and denatured briefly (5 min at 95°C) before loading on a freshly made SDS-polyacrylamide resolving gel (7.5% when resolving for ABCB5 isoforms or 15% when resolving for p16 protein) with a 4%

stacking gel. For each sample, 0.5 μg of total protein extract (protein concentration was determined as described in Section 2.24) was loaded in each lane. A lane containing 10 μl of standard molecular weight marker (Precision Plus Protein All Blue Standards; Bio-Rad, UK) was loaded onto each gel to enable the subsequent determination of protein molecular weights. Proteins were initially separated using a constant voltage of 80 V until the molecular weight marker separation became evident. The voltage was then increased to 110 V, and the separation was continued until the dye-front reached the base of the gel.

2.25.4 Immunoblot analysis

Western blotting was originally devised by Towbin (1979) and Burnette (1981) and involves the transfer of electrophoretically separated proteins from an SDS gel to a solid support (nitrocellulose membrane) and probing with antibodies specific for particular amino acids sequences. The bound (primary) antibody is then detected by a secondary (horseradish peroxidase (HRP)-conjugated) antibody via chemiluminescence.

Following separation by SDS-PAGE, proteins were transferred onto a nitrocellulose membrane (Amersham Hybond ECL Nitrocellulose; GE Healthcare, NJ). The transfer was carried out for 1 h at 400 mA when probing for ABCB5 isoforms, and at 350 m A when probing for p16. After electroblotting, the nitrocellulose membrane was washed in the appropriate TBS-T (see Section 1 and blocked in 5% (w/v) milk (Marvel, UK) in the same TBS-T for 1 h at RT on a rocking platform. The membrane was probed overnight with the primary antibody in 10 mL 5% (w/v) milk in the appropriate TBS-T inside a 50 mL centrifuge tube (Scientific Laboratory Supplies, UK) at 4°C on a roller (Denley Spiramix 5; Thermo Denley, UK). The membrane was washed eight times for 5 min each with TBS-T before incubation (1 h at RT in a 50 mL centrifuge tube on a roller) with the appropriate secondary HRP-conjugated antibody in 10 mL 5% (w/v) milk in

the appropriate TBS-T. Following a further eight 5 min washes in the appropriate TBS-T, bound antibodies were visualised by chemiluminescence (Immobilon Western Chemiluminescent HRP Substrate; Millipore, UK) and exposed to Hyperfilm ECL (GE Healthcare, NJ, USA).

2.25.5 Densitometric analysis of western blotting

Western blots generated using the technique described in Section 2.25.4 were subjected to densitometric analysis in order to assess relative protein levels. Western blots were scanned at 800 dpi and the resulting images were loaded into ImageJ (Schneider et al., 2012) for analysis using the densitometry tool. The highest molecular weight bands for ABCB5fl and ABCB5β were studied, so that lower molecular weight degradation products were not included. The area under the intensity peak for each band was calculated relative to background intensity and plotted for statistical analysis (see Section 2.29).

2.26 Lactate dehydrogenase cytotoxicity assay

Cytotoxicity in HEK293T cells following plasmid transfection was measured as a function of lactate dehydrogenase (LDH) activity, carried out using the CytoTox 96® Non-Radioactive Cytotoxicity Assay kit (Promega, WI, USA). The assay was carried out according to the manufacturer's instructions, with minor alterations included within the method below.

HEK293T cells in 96-well format were transfected in triplicate 48 h prior to lysis by the addition of 25 μL Lysis Solution (10x; 9 % (v/v) Triton X-100) and incubation for 1 h at 37°C. Subsequently, 50 μL of the supernatant from each well was removed to a fresh

96-well plate, followed by the addition of 50 µL Substrate Mix (proprietary) and an incubation for 30 min at RT in the dark. To stop the reaction, 50 µL Stop Solution (1 M acetic acid) was added to each well of the plate. The absorbance across the plate was read at 490 nm.

2.27 Immunocytochemistry

2.27.1 Antibodies and cell stains

The antibodies and fluorescent stains used to stain cells by immunocytochemistry are detailed in Table 2-22.

Antibody Or Stain	Conjugate	Working Dilution	Species	Clonality	Source
Anti-p16	N/A	1:1,000	Mouse	Monoclonal	J. Koh, Duke University, NC, USA
Anti-KDEL	N/A	1:100	Mouse	Monoclonal	Merck Millipore, MA, USA
Anti-Mouse 488	Alexa Fluor® 488	1:500	Goat	Polyclonal	Life Technologies Ltd, UK
Anti-Mouse 555	Alexa Fluor® 555	1:500	Goat	Polyclonal	Life Technologies Ltd, UK
HCS Cell Mask Deep Red	N/A	1:2,500	N/A	N/A	Life Technologies Ltd, UK
DAPI	N/A	1:1,000	N/A	N/A	Life Technologies Ltd, UK

Table 2-22. Antibodies and cell stains used for fluorescence microscopy in the investigation.

2.27.2 Staining cells for high-content fluorescence microscopy

120 h post-transfection, all medium was pipetted from the wells and cells were washed with 75 µl DPBS containing both magnesium and calcium (PAA Laboratories, UK) and then fixed with 4% (w/v) paraformaldehyde (PFA) and 5% (w/v) sucrose in PBS (all from Sigma-Aldrich, UK), for 15 min at RT. Cells were washed with PBS before being permeablised with 0.1% (v/v) Triton X-100 (Sigma-Aldrich, UK) in PBS for 15 min at

RT. Cells were again washed with PBS and blocked in "blocking solution" [0.25% (w/v) BSA (Sigma-Aldrich, UK) in PBS] for 30 min at RT. After blocking, the cells were incubated with the primary antibody (anti-p16, JC2; see Section 2.27.1) for 2 h at RT in "blocking solution", and subsequently washed with "blocking solution" for 30 min at RT. Cells were then incubated with the second antibody conjugated to a fluorescent-dye, DAPI and HCS Cell Mask Deep Red in "blocking solution" for 2 h at RT in the dark. After incubation with the secondary antibody and stains, the cells were washed three times with "blocking solution" and then twice with PBS. Plates were stored with 80 μL PBS in each well at 4°C, and imaged as detailed in Section 2.28.2.

2.27.3 Staining cells for confocal microscopy

Cells on coverslips 140 μm ± 15 μm thick were fixed 48 h post-transfection by aspirating all media from the wells, washing cells twice with 2.5 mL DPBS containing both magnesium and calcium (PAA Laboratories, UK) and subsequently fixing with 4% (w/v) PFA and 5% (w/v) sucrose in PBS (all Sigma-Aldrich, UK), for 15 min at RT. Following two washes in PBS, the cells were permeablised using 0.1% (v/v) Triton X-100 (Sigma-Aldrich, UK) in PBS for 15 min at RT and subsequently washed in PBS. Cells were blocked for 1 h at RT in 5% (w/v) BSA (Sigma-Aldrich, UK) in PBS. After blocking, coverslips were removed from wells onto a sheet of Parafilm M (Pechiney Plastic Packaging Company, IL, USA) and incubated with 100 μL of the primary antibody (see Section 2.27.1) in 1% (w/v) BSA in PBS for 1 h at RT. Following incubation with primary antibody, the coverslips were returned to a fresh 6 round-well plate (ThermoFisher Scientific, MA, USA) before washing three times with 1 mL PBS. Coverslips were again removed onto a sheet of Parafilm M and probed with the appropriate secondary antibody conjugated to fluorescent-dye, and DAPI in 1% (w/v) BSA in PBS for 1 h at RT in the dark. Subsequently, coverslips were again returned to a

fresh 6 round-well plate and washed 3x in 2 mL PBS, before mounting onto microscope slides using FluorSave™ Reagent (Merck Millipore, DE). Slides were stored at 4°C in the dark. Cells were viewed using a Zeiss LSM710 confocal laser scanning microscope based on an Axiovert inverted microscope (Carl Ziess, DE) with a 20x air, 40x oil immersion or 63x oil immersion objective with numerical apertures of 1.3, 1.4 and 1.4, respectively. Laser lines 405 nm, 488 nm and 555 nm were used to excite DAPI, Alexa Fluor® 488 and Alexa Fluor® 555, respectively. The pinhole was set to 5 airy units for all experiments. Images were acquired with sequential scanning to allow cross-talk free DAPI, Alexa Fluor® 488 and Alexa Fluor® 555 images to be collected.

2.28 High-content fluorescence microscopy

2.28.1 System.

All high-content fluorescence microscopy images were captured using the IN Cell 1000 automated microscope (GE Healthcare, UK) at 10x magnification and analysed using Developer Toolbox 1.7 (GE Healthcare, UK).

2.28.2 Imaging

Cells in 384-well plates at 48 h post transfection (see Section 2.11.1.1) were imaged for Brightfield (150 ms exposure) and *siGLO* (535 nm excitation; 1500 ms exposure) at 10x magnification, with two images taken per well.

Cells fixed and stained in 384-well plates for high-content analysis were imaged for DAPI (360 nm excitation; 500 ms exposure), Alexa Fluor® 488 (475 nm excitation; 500

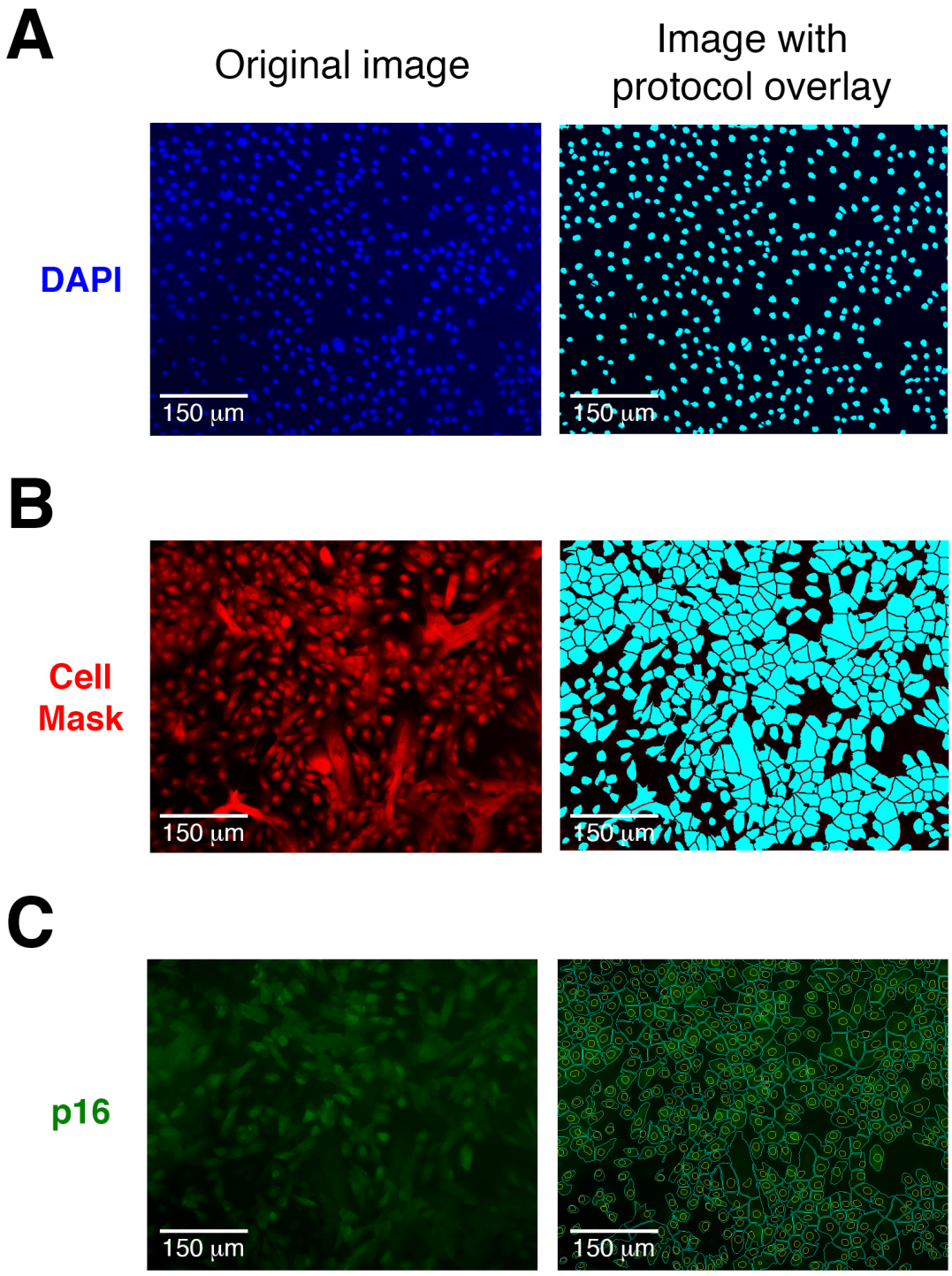

Figure 2-1. In Cell analysis protocol for transfected cells.

A. Nuclei stained with DAPI (blue) are selected by intensity, then counted and measured by the software (Developer Toolbox 1.7). Cyan overlay marks counted and measured nuclei. B. Cell Mask (red) staining is detected by the software and split into individual cells using the DAPI stain as a guide; the area of each cell was subsequently measured. Cyan overlay mark cells measured by the software. C. p16 intensity was measured in each nuclei is measured using the guide previously created using the DAPI staining. Yellow and cyan outlines represent previously marked nuclei and cells, respectively.

ms exposure) and HCS Cell Mask Deep Red (620 nm excitation; 10 ms exposure) at 10x magnification, with nine images acquired per well.

2.28.3 Analysis

Images taken for high-content analysis were examined using a protocol designed to examine multiple variables within the cell, namely: cell number; cell area; nuclear area; and nuclear green fluorescence (anti-p16 antibody) intensity.

Both cell number and nuclear area were measured using the DAPI staining of nuclei (Figure 2-1 panel A). The protocol was programmed to recognise the whole of each nuclei, whilst disregarding any background fluorescence, allowing the nuclei to be counted and measured at the same time.

The cellular area of each cell was measured using the HCS Cell Mask Deep Red, which stained all nucleic acid in each cell, allowing the area of each cell to be easily visualised against the background (Figure 2-1 panel B). However, as many of the cells were in contact, there was a requirement for the individual cells to be isolated, so the area of each could be accurately measured. To achieve this, the protocol was programmed to use the nuclei previously identified as markers for individual cells, and split the cell areas accordingly, so that each 'cell' contained a single nuclei.

Finally, the relative fluorescence intensity of p16 was measured in the nuclei of each cell (Figure 2-1 panel C). In order to carry out this measurement, the protocol was programmed to measure the relative green fluorescence within each area previously defined as a nuclei.

2.29 Statistical analysis of results

All experiments in this investigation were completed in triplicate unless otherwise stated in the text. All statistical analysis was performed using Prism v5.0d (GraphPad Software Inc, CA, USA).

2.29.1 Welch's t test

The unpaired two-tailed t test was used when the means of only two samples (with unequal variances) were to be compared.

2.29.2 One-way ANOVA

Performing multiple t-tests on a set of more than two samples can result in a 'statistical test theory type 1 error' (a false positive), where a hypothesis that should have been rejected, is in fact accepted. Therefore, the one-way analysis of variance (ANOVA) was used to statistically analyse data where three or more means had to be tested.

In many cases throughout this study, a Dunnett's multiple comparison follow up test was also used to compare individual conditions within an experiment to a control condition.

One problem with the ANOVA, is that it is impossible for the statistics software being used (Prism 5.0d; GraphPad Software Inc, CA) to calculate exact p values for this statistical test. Statistical significance is only accurately calculated as an arbitrary 'q value', which has no real meaning outside of the program. Approximate p values are however reported in the form, $p < 0.05$ or $p < 0.001$ etc. More information about this issue can be found at http://www.graphpad.com/support/faqid/189/ (accessed October 2013).

Chapter Three

3 Characterisation of ABCB5 isoforms at the protein level

3.1 Introduction

The *ABCB5* gene is predicted to encode an integral, dodecaspan membrane protein of the ABC superfamily of transport proteins. Members of the ABCB family of transporters are reported to efflux a wide variety of substrates across cellular membranes, ranging from chemotherapeutic agents (ABCB1) and peptides (ABCB2 and ABCB3), to lipids such as phosphatidylcholine (ABCB4; (Szakács et al., 2006). Of the four ABCB5 isoforms described (ABCB5fl, ABCB5α, ABCB5β and ABCB5γ), only the two longest isoforms, ABCB5fl and ABCB5β, are thought to encode active efflux transporters (Frank et al., 2005, Kawanobe et al., 2012). As neither ABCB5α nor ABCB5γ contain a TMD, and as both only have a partial NBD, they are highly unlikely to be able to act as transporters. It has been previously postulated, however, that the ABCB5α peptide could be involved in the regulation of transport, and that the *ABCB5α* mRNA could reduce expression of the *ABCB5* gene, or increase message stability of ABCB5fl or ABCB5β (Gottesman, 2004, Chen et al., 2005a).

Shortly after it was first described, ABCB5β was proposed to have a role in progenitor cell fusion (Frank et al., 2003), although this result has not been studied any further or reported since. More recently it has been reported that ABCB5β is highly expressed in the cancer stem cell-like malignant melanoma initiating cells (MMICs; (Frank et al., 2003, Schatton et al., 2008). As such, the majority of the research carried out since this discovery has been concerned with using antibodies – both commercially available, and in-house generated – purportedly against ABCB5β to mark MMICs (Ma et al., 2010, Schatton et al., 2010, Frank et al., 2011, Ramgolam et al., 2011, Wilson et al., 2011, Linley et al., 2012, Aldaz et al., 2013, Mathieu et al., 2014).

As a consequence, the other isoforms of ABCB5 are relatively uncharacterised both in terms of their structure and function. The limited research on characterisation has revolved around the postulation that ABCB5fl and ABCB5β would be able to transport chemotherapeutic drugs, due to their sequence similarity with ABCB1. The first published experiments to test this were carried out by the Frank Group (Harvard, MA, USA) in cells with endogenous ABCB5β expression, but no ABCB5fl expression (evaluated by antibody binding), and the authors reported that this truncated protein could transport both rhodamine-123 and doxorubicin (Frank et al., 2003, Frank et al., 2005). Subsequently, a separate group using exogenously expressed ABCB5β or ABCB5fl, reported that ABCB5β was unable to transport the previously reported substrates (Chen et al., 2009). ABCB5fl expression was, however, found to effectively confer drug resistance to multiple chemotherapeutic drugs including anthracycline, mitoxantrone, and epipodophyllotoxin (Gillet et al., 2009, Chen et al., 2009). In support of this latter finding, another group also found that ABCB5fl could confer resistance to anthracyclines and taxanes when stably expressed in HEK293 cells (Kawanobe et al., 2012).

When ABCB5β was reported to have a role in progenitor cell fusion, the protein was proposed to localise to the plasma membrane, due to flow cytometry analysis of antibody binding (Frank et al., 2003). This same paper, however, also showed clear intracellular staining using the same antibody when permeablised cells are examined by immunofluorescence microscopy, which suggested that the vast majority, if not all, of the protein is actually retained intracellularly (Frank et al., 2003). Intracellular

localisation of ABCB5β has also been observed by others (Linley et al., 2012, Mathieu et al., 2014).

3.1.1 Aims

The overall hypothesis for the work detailed within this chapter was that ABCB5fl and ABCB5β are plasma membrane proteins that can be expressed effectively in a variety of cell types, conferring resistance to a variety of toxic xenobiotic compounds. The hypothesis of this project was studied by transiently expressing the two largest isoforms of ABCB5, ABCB5fl and ABCB5β, in a naive cell type, and to using this platform to further characterise the proteins. Specifically, the aims were to:

- Express EGFP- or His-tagged ABCB5fl and ABCB5β in a mammalian cell line, and confirm protein expression by western blotting and confocal microscopy;
- Evaluate the sub-cellular localisation of ABCB5fl and ABCB5β using EGFP-tagged proteins;
- Create point mutations to prevent ATP catalysis by ABCB5fl and ABCB5β, and investigate the effect on expression, localisation and transport function;
- Generate TaqMan primer/probe sets against *ABCB5fl* and *ABCB5β* to distinguish between the two isoforms at the mRNA level; and
- Utilise RT-qPCR and western blotting to characterise endogenous *ABCB5fl* and *ABCB5β* expression at the mRNA and protein level in cell lines for further study.

3.2 Results

3.2.1 ABCB5fl and ABCB5β protein expression in HEK293T cells

In order to study ABCB5fl and ABCB5β protein expression effectively, a transient expression system in HEK293T cells was chosen, which allowed for changes in the protein to be easily made via point mutation of the plasmid. A similar approach has been used previously to study other ABCB family transporters with great success (Zolnerciks et al., 2007, Groen et al., 2011).

Plasmids encoding ABCB5fl or ABCB5β with either a C-terminal V5 and 6-histidine (V5-6His) tag or a C-terminal enhanced green fluorescent protein (EGFP) tag were obtained. These plasmids encoding ABCB5fl (pcDNA3.1-ABCB5fl-wt_V5-6His, pcDNA3.1-ABCB5fl-wt_EGFP), and ABCB5β (pcDNA3.1-ABCB5β-wt_V5-6His, pcDNA3.1-ABCB5β-wt_EGFP), were kindly provided by Prof. Michael Gottesman (NIH, Maryland, MD, USA; Table 2-2).

The plasmids were transfected into HEK293T cells in 6-well plates using PEI conditions previously optimised for expression of ABCB1 (Zolnerciks et al., 2007), and successfully used with a variety genes such as *ABCB1*, *ABCB4*, *CDC50*, *ATP8B1*, *CD36* and *FATP4* (see Section 2.10), along with the appropriate control plasmid, which lacked any inserted gene (pcDNA3.1-EGFP or pcDNA3.1-V5-6His).

3.2.1.1 Immunoblot analysis of ABCB5fl and ABCB5β transiently expressed in HEK293T cells

In order to assess the transfection efficiency of the HEK293T cells, and the expression of the two ABCB5 isoforms, three commercially available antibodies were purchased, each reported to recognise both ABCB5fl and ABCB5β (Table 2-21). Whole cell lysates were prepared from HEK293Ts 48 h after transfection and 0.5 μg of total protein from each sample was separated by electrophoresis through a 7.5% SDS-PAGE gel. The samples were transferred onto a nitrocellulose membrane and blocked before incubation with the appropriate antibodies.

The anti ABCB5 antibody purchased from Atlas Antibodies AB (Atlas) was found to recognise specific proteins migrating as 140 kDa and 90 kDa species in samples prepared from HEK293T cells transfected with plasmids encoding ABCB5fl and ABCB5β proteins, respectively (Figure 3-1 panel A). These bands correspond accurately to the predicted molecular weights of ABCB5fl (138 kDa) and ABCB5β (89 kDa). In addition to the proteins at the predicted molecular weights, further smaller molecular weight species were observed on the western blot. As the Atlas antibody detected no protein in either of the control samples (untransfected HEK293T cells, or cells transfected with an empty vector), it was hypothesised that these are degradation products of ABCB5fl and ABCB5β that retain the Atlas antibody epitope, and were not due to non-specific binding. This result also demonstrated that there was no (or undetectable levels of) ABCB5fl or ABCB5β protein expressed endogenously in HEK239T cells.

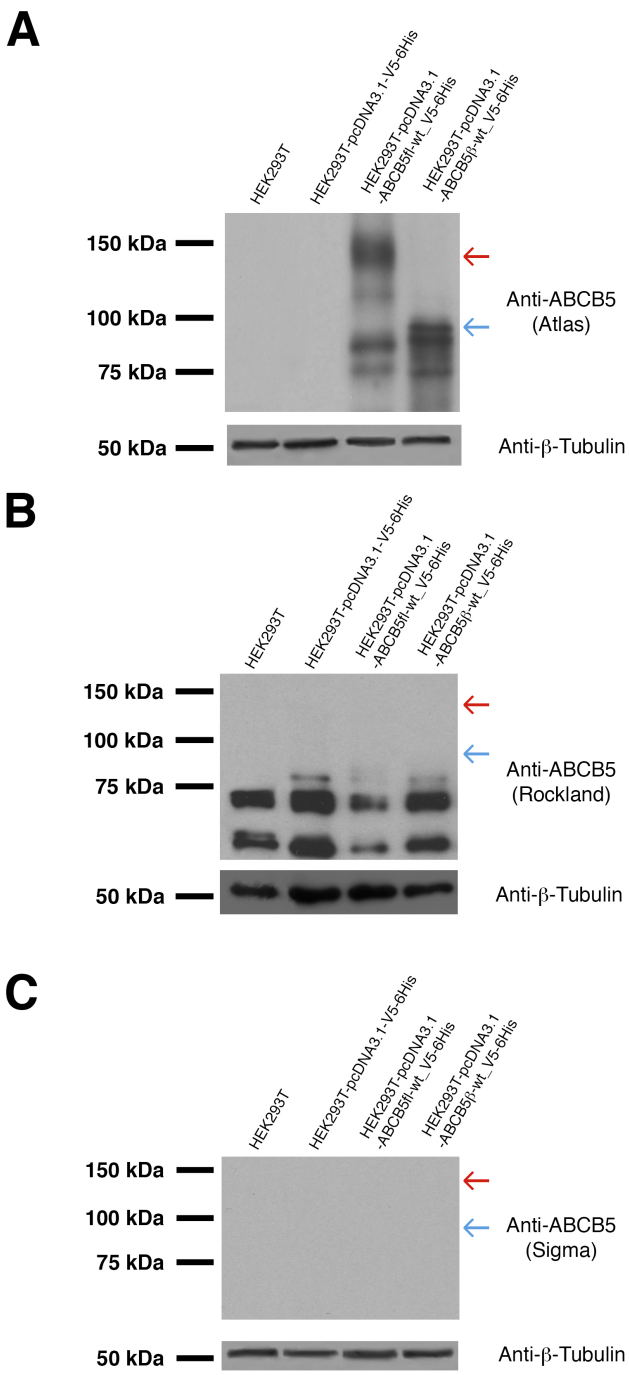

Figure 3-1. Western blot analysis of ABCB5 expression in transfected HEK293T cells using three commercially available antibodies.

Lysates prepared from untransfected HEK293T cells, and HEK293T cells transfected with empty vector (pcDNA3.1-V5-6His), a plasmid encoding ABCB5fl (pcDNA3.1-ABCB5fl-wt_V5-6His), or a plasmid encoding ABCB5β (pcDNA3.1-ABCB5β-wt_V5-6His) were probed using three commercially available antibodies. A. Anti-ABCB5 (Atlas) detected proteins at the expected molecular weights for ABCB5fl (140 kDa) and ABCB5β (90 kDa) in the appropriate samples. B. Anti-ABCB5 (Rockland) detected multiple proteins migrating with apparent molecular weights of less than ABCB5fl and ABCB5β. C. Anti-ABCB5 (Sigma) failed to detect any protein. Protein loading was controlled in all western blots using an anti-β-tubulin antibody at different exposures, to ensure a strong signal. Arrows show the predicted molecular weights of ABCB5fl (red) and ABCB5β (blue). n = 2 biological repeats.

In addition to the Atlas antibody, two others that have previously been used in published studies were purchased from Sigma Aldrich Ltd (Sigma) (Linley et al., 2012, Grimm et al., 2012), and Rockland Inc. (Rockland) (Wilson et al., 2011, Ramgolam et al., 2011). When these two antibodies were used to probe blots generated from transfected HEK293T cell lysates, no bands corresponding to the predicted molecular weights of ABCB5fl or ABCB5β were detected (Figure 3-1 panels B and C).

]The Rockland antibody recognised proteins in all samples prepared from transfected HEK293T cells, including the negative controls. Two proteins were detected in each sample, of approximately 70 kDa and 55 kDa. A larger protein was also present in each of the samples prepared from transfected HEK293T cells, which migrated with an apparent molecular weight of approximately 75 kDa. None of the observed protein species correlated with the predicted size of either ABCB5fl or ABCB5β, suggesting that the antibody does not detect either isoform under the conditions tested. The three proteins detected are most likely due to non-specific antibody binding to cellular unrelated to either ABCB5fl or ABCB5β.

The Sigma antibody failed to detect any proteins by western blotting in any of the samples tested, also suggesting that in the conditions utilised, this antibody is ineffective at detecting either ABCB5fl or ABCB5β protein.

These western blots show that the Atlas antibody for ABCB5 is the most suitable for further use in this study. It is curious that the other two antibodies tested could not detect ABCB5fl or ABCB5β as both of these have previously been used in published studies to report ABCB5fl and ABCB5β expression.

3.2.1.2 Expression of EGFP-tagged ABCB5fl and ABCB5β

In addition to the analysis of transient ABCB5fl and ABCB5β expression in HEK239T cells by western blot, both expression and localisation were studied by confocal microscopy of HEK293T cells transfected with plasmids encoding EGFP-tagged ABCB5fl or ABCB5β. As ABCB5β has previously been reported to be present at the plasma membrane of melanoma cells (Frank et al., 2003), this was the expected subcellular location of both ABCB5fl and ABCB5β.

Confocal analysis of transfected HEK293T cells showed a high transfection efficiency, with around 80% of cells exhibiting green fluorescence when transfected with the CD36_Venus positive control plasmid pcDNA3.1-CD36_Venus (Figure 3-2). Low transfection efficiency was observed with both the ABCB5fl and ABCB5β expressing plasmids, with approximately 5% of cells found to express either protein isoform. Of the cells expressing either ABCB5fl or ABCB5β, the majority of cells express the proteins at low levels, but small numbers of cells display very high levels of expression. None of the ABCB5 expressing cells were found to have fluorescently tagged ABCB5 protein at the plasma membrane, with all observed fluorescence seen intracellularly, as opposed to the plasma membrane localisation observed with CD36_Venus expression.

As the protein was not found to localise to the plasma membrane, the opportunity to carry out informative functional studies of ABCB5fl and ABCB5β is greatly reduced. It should be noted that although ABCB5β was proposed to be present at the plasma membrane, the reporting paper clearly showed intracellular staining of ABCB5β in

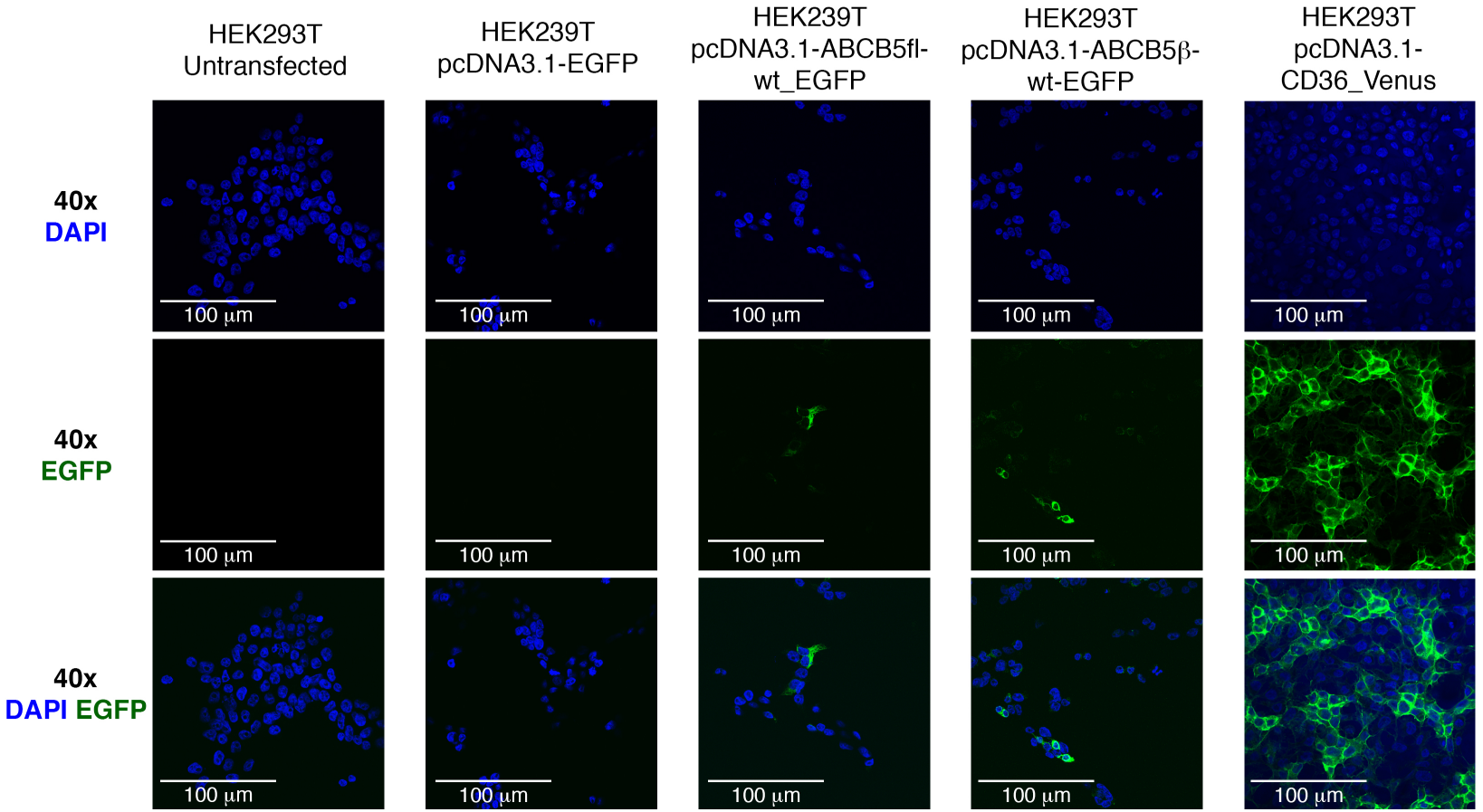
HEK293T
Untransfected
HEK239T
pcDNA3.1-EGFP
HEK239T
pcDNA3.1-ABCB5fl-
wt_EGFP
HEK293T
pcDNA3.1-ABCB5β-
wt-EGFP
HEK293T
pcDNA3.1-
CD36_Venus
40x
DAPI
40x
EGFP
40x
DAPI EGFP
100 μm

melanoma cells with a non-commercially available antibody (Frank et al., 2003). This localisation was also published in both Linley et al., (2012) and Mathieu et al., (2014) supporting the findings reported here (see Section 3.3.2).

3.2.1.3 ABCB5fl-EGFP and ABCB5β-EGFP localise to the endoplasmic reticulum in HEK293T cells

To further study the localisation of ABCB5fl-EGFP and ABCB5β–EGFP in HEK293T cells, the cells were fixed, permeablised and co-stained with an antibody against the carboxy-terminal ER retention sequence KDEL, and an appropriate secondary antibody (Figure 3-3 panel A).

In cells expressing either ABCB5fl-EGFP or ABCB5β-EGFP, co-localisation[1] of the EGFP tag and the ER KDEL marker is apparent, strongly suggesting that the EGFP-tagged ABCB5 isoforms do not traffic beyond the ER. In order to confirm co-localisation, line scans were performed on the images (Figure 3-3 panel B). These revealed that the vast majority of green fluorescence from EGFP tagged ABCB5fl (93.3%) or ABCB5β (94.8%) was found within regions of high red fluorescence, supporting the hypothesis that both ABCB5fl and ABCB5β are retained intracellularly.

No fluorescence was visualised in the plasma membrane of any cells expressing the proteins, disputing earlier claims that this is the primary location of ABCB5β

[1] Due to the limitations of the objectives of confocal microscope being used, the maximum resolution that can be achieved is 240 nm. Therefore, co-localisation is defined in this study as being when two fluorophores are within 240 nm of each other.

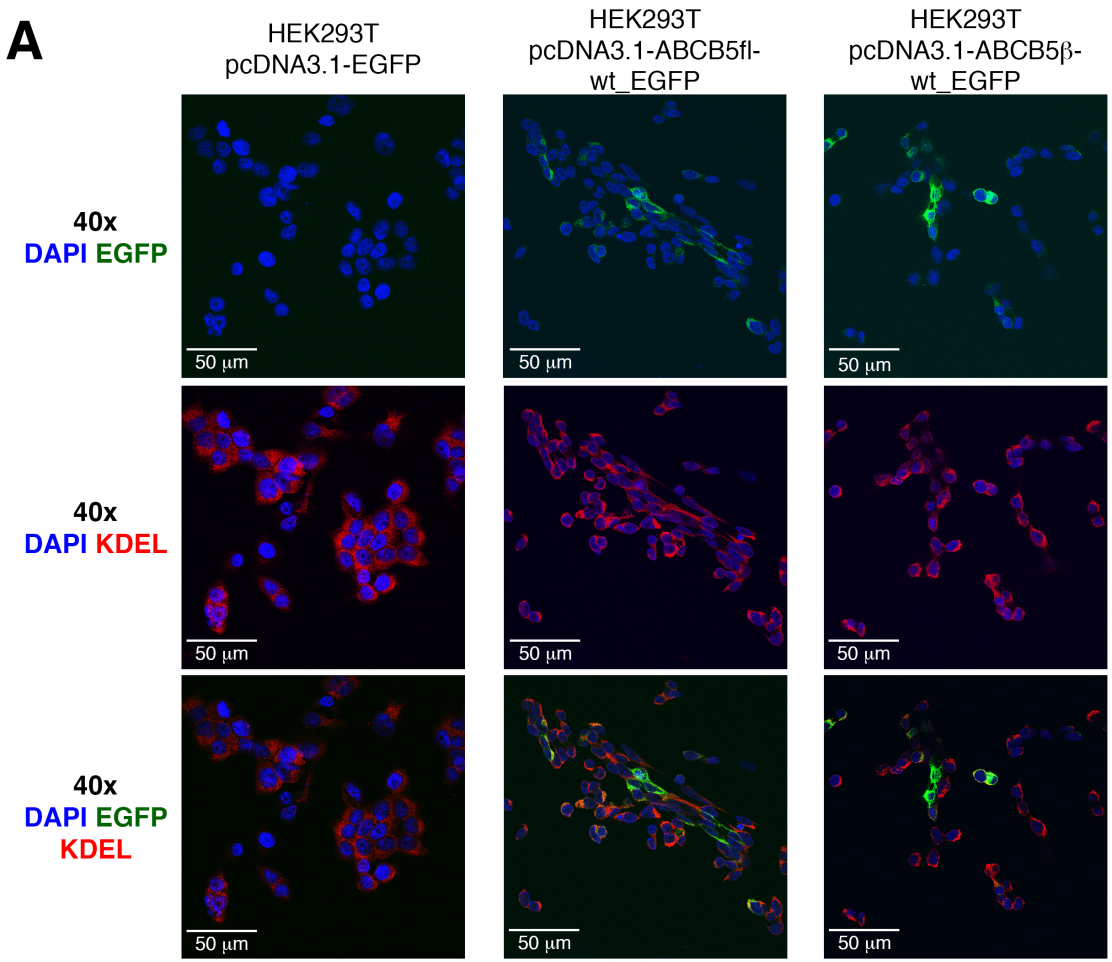

Figure 3-3. Subcellular localisation of ABCB5fl and ABCB5β in HEK293T cells.

A. Representative images show untransfected HEK293T cells, or cells transfected with pcDNA3.1-EGFP, pcDNA3.1-ABCB5fl-wt_EGFP, or pcDNA3.1ABCB5β-wt_EGFP. Fluorescently tagged ABCB5fl and ABCB5β protein (green), fluorescently labelled KDEL (red), and DAPI staining of nuclei (blue) were observed 48 h post transfection at 40x magnification. n = 4 biological repeats.

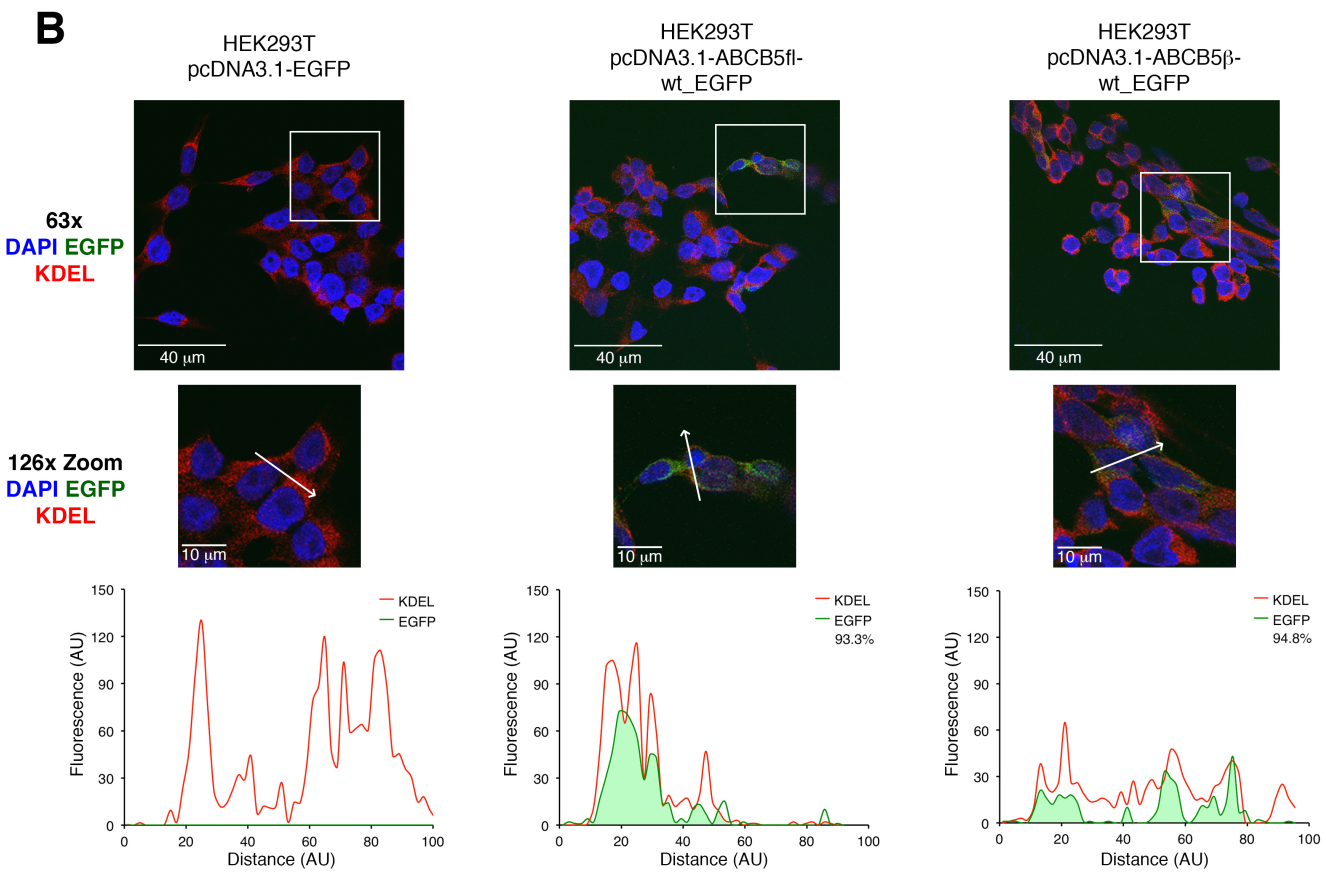

Figure 3-3. (continued) Subcellular localisation of ABCB5fl and ABCB5β in HEK293T cells.

B. Representative images show untransfected HEK293T cells, or cells transfected with pcDNA3.1-EGFP, pcDNA3.1-ABCB5fl-wt_EGFP, or pcDNA3.1ABCB5β-wt_EGFP. Fluorescently tagged ABCB5fl and ABCB5β protein (green), fluorescently labelled KDEL (red), and DAPI staining of nuclei (blue) were observed 48 h post transfection at 63x magnification. White boxes represent magnified area in the subsequent image. Line graphs show KDEL (red) and EGFP (green) fluorescence along the white arrow in each magnified image. Areas of the EGFP fluorescence within areas of KDEL fluorescence are filled in green. This area is represented as a percentage of total EGFP fluorescence in each figure legend. n = 4 biological repeats.

(Frank et al., 2003), and supporting visual evidence of an intracellular localisation of ABCB5β (Linley et al., 2012, Mathieu et al., 2014).

3.2.2 Cytotoxicity and mutation of ABCB5fl and ABCB5β

In a previous study, the closely related ABC transporter, ABCB4, was found to have a cytotoxic effect when over-expressed in HEK293T cells (Groen et al., 2011). It was therefore hypothesised that the low expression of ABCB5fl and ABCB5β observed may be due to a similar cytotoxic effect in these transfected cells. In order to test this hypothesis, two approaches were used: an LDH assay to measure the release of a cytosolic enzyme, and the generation of 'inactive' ABCB5 isoforms to examine whether these are better tolerated.

3.2.2.1 ABCB5fl and ABCB5β are not cytotoxic in HEK293T cells

The LDH assay measures the activity of the stable cytosolic LDH enzyme in the culture supernate, where higher activity denotes more LDH release due to cell lysis, and therefore higher levels of cytotoxicity. The level of LDH release from untransfected cells was compared to that of cells transfected with an empty vector, or transfected with a vector expressing ABCB5fl or ABCB5β.

The previously published study (Groen et al., 2011), found that expression of ABCB4 in HEK293T cells caused a 3-fold increase in LDH release from cells compared to a vector only control (Figure 3-4 panel A). In contrast to this, no significant changes in LDH release were observed upon transfection of plasmids containing ABCB5fl or ABCB5β into HEK293T cells (Figure 3-4 panel B), when compared to the empty control plasmids. These results suggested that neither ABCB5fl nor ABCB5β were cytotoxic to HEK293T cells.

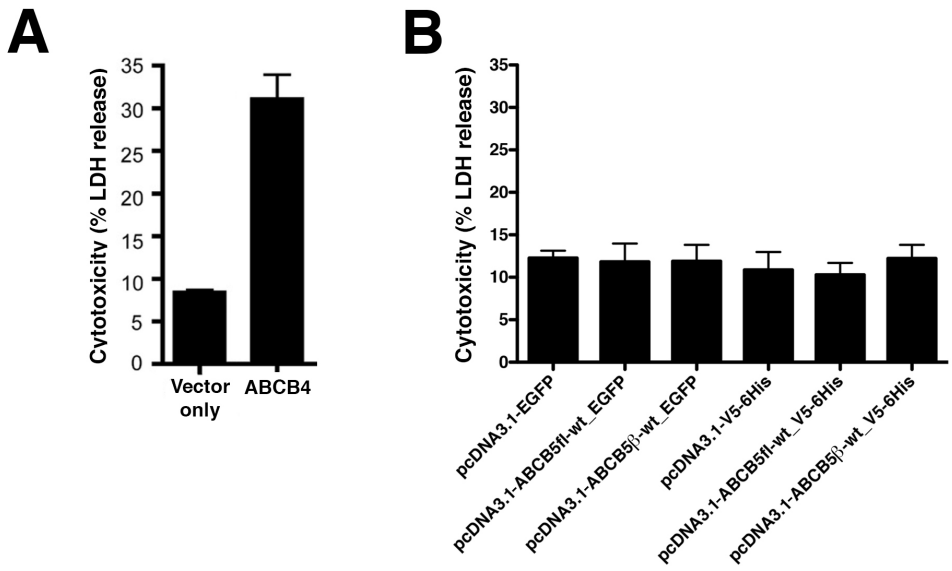

Figure 3-4. ABCB5fl and ABCB5β expression in HEK293T cells do not cause cell death.

A. Expression of ABCB4 in HEK239T cells causes cytotoxicity as measured by increased LDH release (Groen et al., 2011)[1]. B. Introduction of vectors encoding ABCB5fl or ABCB5β into HEK293T cells caused no significant change in cell cytotoxicity compared to the introduction of empty vectors, as measured by percentage LDH release 48 h post transfection. Error bars represent 1 SD, n = 3 biological repeats.

3.2.2.2 Generation of 'non-functional' ABCB5fl and ABCB5β mutants

To confirm that ABCB5fl and ABCB5β are not cytotoxic to cells, and to rule out that the primary active function of the isoforms was not responsible for the low level of expression, mutations were made in the Walker B motifs of ABCB5fl and ABCB5β to prevent ATP hydrolysis. The consensus sequence of the Walker B motif is hhhhDE (where h is any hydrophobic amino acid), with the glutamate residue being essential for ATP hydrolysis (Hanson and Whiteheart, 2005). This glutamate residue was therefore mutated to encode a glutamine, by site-directed mutagenesis of the two Walker B motifs in NBD1 and NBD2 of ABCB5fl (E550 in NBD1 and E1181 NBD2), and the single

[1] Reproduced and adapted from: Groen et al., (2011) Complementary Functions of the Flippase ATP8B1 and the Floppase ABCB4 in Maintaining Canalicular Membrane Integrity, Figure 1 panel D; with permission of the publisher (Gastroenterology). License number 3371380502686.

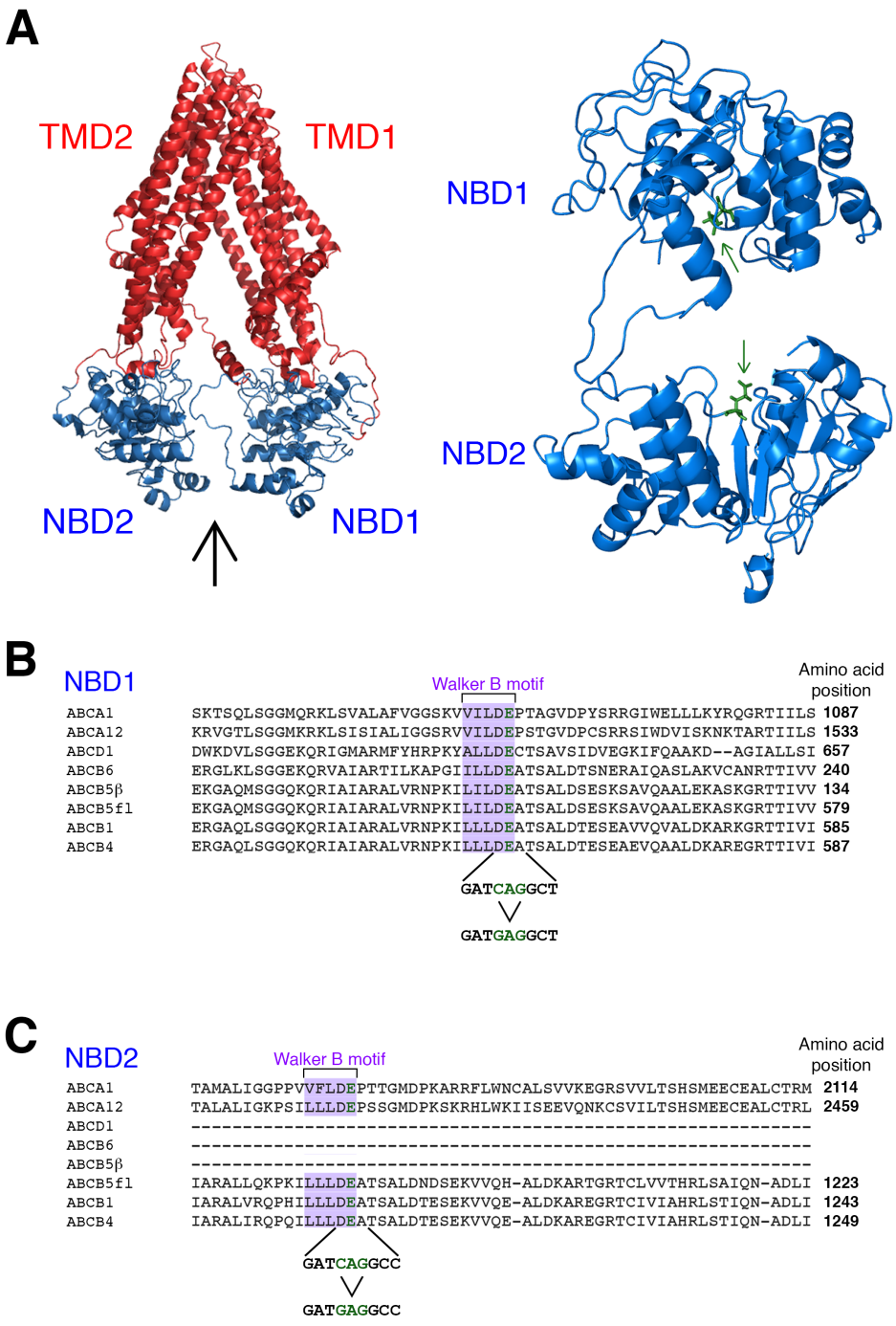

Figure 3-5. Mutation of the conserved Walker B glutamate residues in ABCB5fl and ABCB5β.

A. The predicted structure of ABCB5fl as generated by the I-TASSER prediction server, based on the mouse Abcb1 structure (see Section 1.5.1). NBDs are shown in blue and TMDs are shown in red. The black arrow on the left image signifies the viewpoint of the right hand image, in which the TMD sequences are also removed for clarity. Conserved glutamate residues (green) are shown at the NBD:NBD interface. B. The Walker B motif (purple) in the NBD1 is conserved across multiple ABC transporters. The essential glutamate residue (green) was mutated to a glutamine with a CAG > GAG codon mutation. C. The Walker B motif (purple) in the NBD2 is conserved across multiple full ABC transporters; ABCD1 and ABCB6 are both half transporters and lack NBD2. The essential glutamate residue (green) was mutated to a glutamine with a CAG > GAG codon mutation.

Walker B motif in ABCB5β (E736 in NBD2, equivalent to E1181 in ABCB5fl; Figure 3-5 panel A).

NBD1 of ABCB5fl was mutated by site-directed mutagenesis using the mutagenic primers described in Table 2-3, to make an 1885G>C alteration in the cDNA sequence (Figure 3-5 panel B). NBD2 of both ABCB5fl and ABCB5β were mutated to 3778G>C and 2752G>C, respectively (Figure 3-5 panel C). As a result of the mutation experiments, plasmids encoding EGFP- and V5-6His- tagged mutants of ABCB5fl and ABCB5β were generated at follows: ABCB5fl NBD1 mutant (pcDNA3.1-ABCB5fl-E550Q_EGFP or _V5-6His); ABCB5fl NBD2 mutant (pcDNA3.1-ABCB5-E1181Q_EGFP or _V5-6His); ABCB5fl NBD1 and NBD2 double mutant (pcDNA3.1-ABCB5fl-E550/1181Q_EGFP or _V5-6His); and ABCB5β NBD2 mutant (pcDNA3.1-ABCB5β-E736Q_EGFP or _V5-6His).

3.2.2.3 Expression of ABCB5fl and ABCB5β Walker B mutants in HEK293T cells

The predicted non-functional mutants of ABCB5fl and ABCB5β were transfected into HEK293Ts as before so that any effect on expression and localisation could be evaluated.

Western blotting of the ABCB5fl mutant showed small variations in the amount of total protein, and relative sizes of each band for each individual mutation (Figure 3-6 panel A). Fluctuations in total protein were observed with expression of both the single Walker B mutants (NBD1 mutant – pcDNA3.1-ABCB5fl-E550Q_V5-6His; NBD2

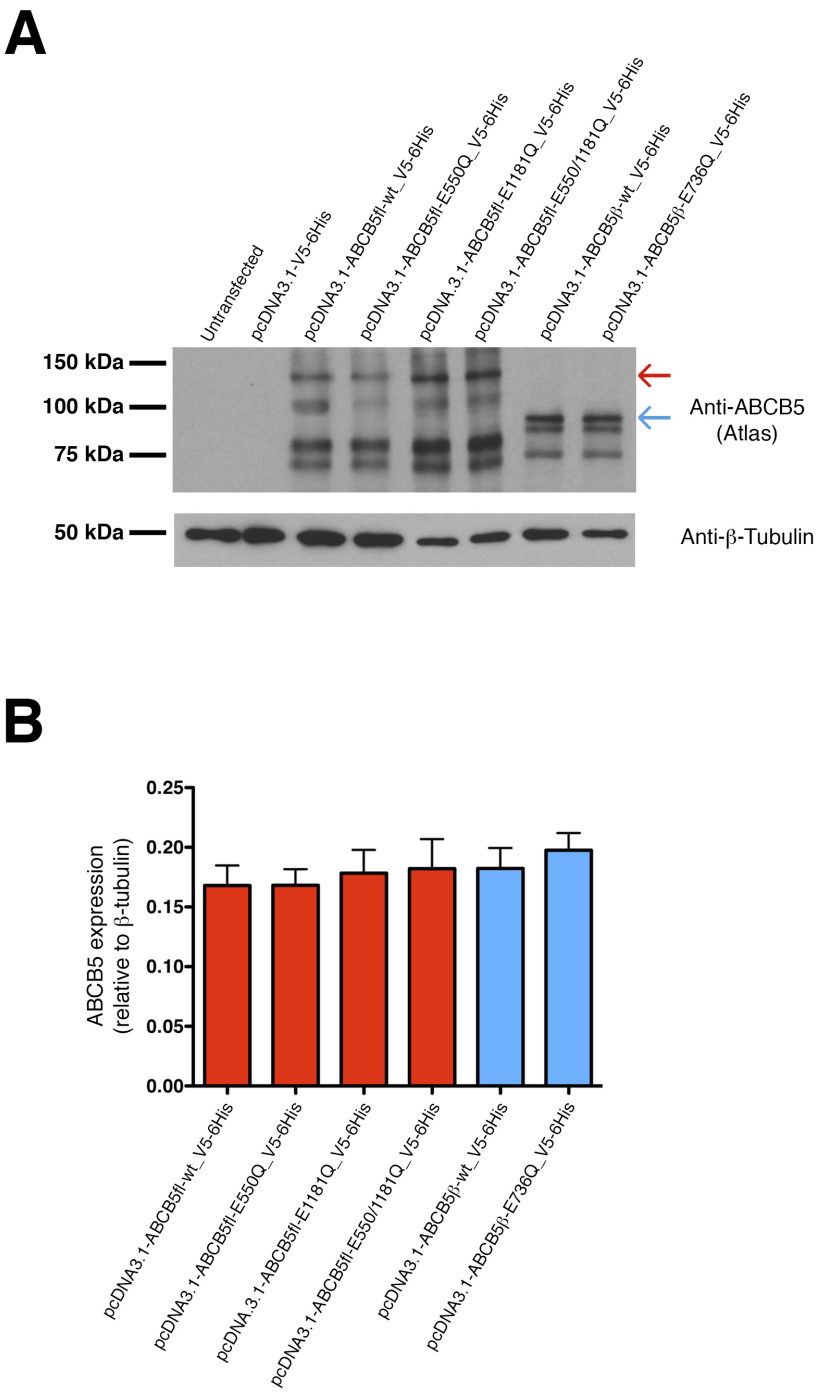

Figure 3-6. Expression of ABCB5 Walker B mutants in HEK293T cells.

A. Western blotting of whole cell lysates from HEK293Ts transfected with wild type and mutant ABCB5fl or ABCB5β show small variations in expression. Arrows show the predicted molecular weights of ABCB5fl (red) and ABCB5β (blue). B. Quantitation of western blotting by densitometry, normalised to β-tubulin expression, shows no significant changes in protein expression between wild type and mutant forms of ABCB5fl and ABCB5β. n = 3 biological repeats.

mutant – pcDNA3.1-ABCB5fl-E1181Q_V5-6His), and the double mutant of ABCB5fl (pcDNA3.1-ABCB5fl-E550/1181Q_V5-6His). Small changes in the protein level of the ABCB5β mutant (pcDNA3.1-ABCB5β-E736Q_V5-6His) were also observed when compared to the β-tubulin loading control. Densitometric analysis of the western blotting results showed no significant changes in expression, of the highest molecular weight species, between the ABCB5fl and ABCB5β mutant and wild type proteins, when compared to β-tubulin (Figure 3-6 panel B). The lower molecular weight proteins detected on the western blot were not included in the densitometric analysis, as these most likely represent partially degraded protein species, and may not accurately represent the protein they are derived from.

This data suggests that the ability of ABCB5fl and ABCB5β to hydrolyse ATP is not related to the low level of expression observed for these proteins. It is possible that the protein does not require ATP to function, however, this is unlikely as ATP-independent function has not been previously been reported for any human ABC transporters.

In addition to western blot analysis of the mutants, -EGFP tagged ABCB5fl and ABCB5β mutants were expressed in HEK293T cells, fixed, and stained with DAPI and KDEL as previously described, in order to assess whether any changes in protein localisation had occurred in response to mutation.

Low expression levels of mutant ABCB5fl and ABCB5β protein were observed, resembling the levels previously seen for wild type protein (Figure 3-7 panel A). Co-localisation of fluorescently tagged mutant ABCB5fl and ABCB5β was seen with the

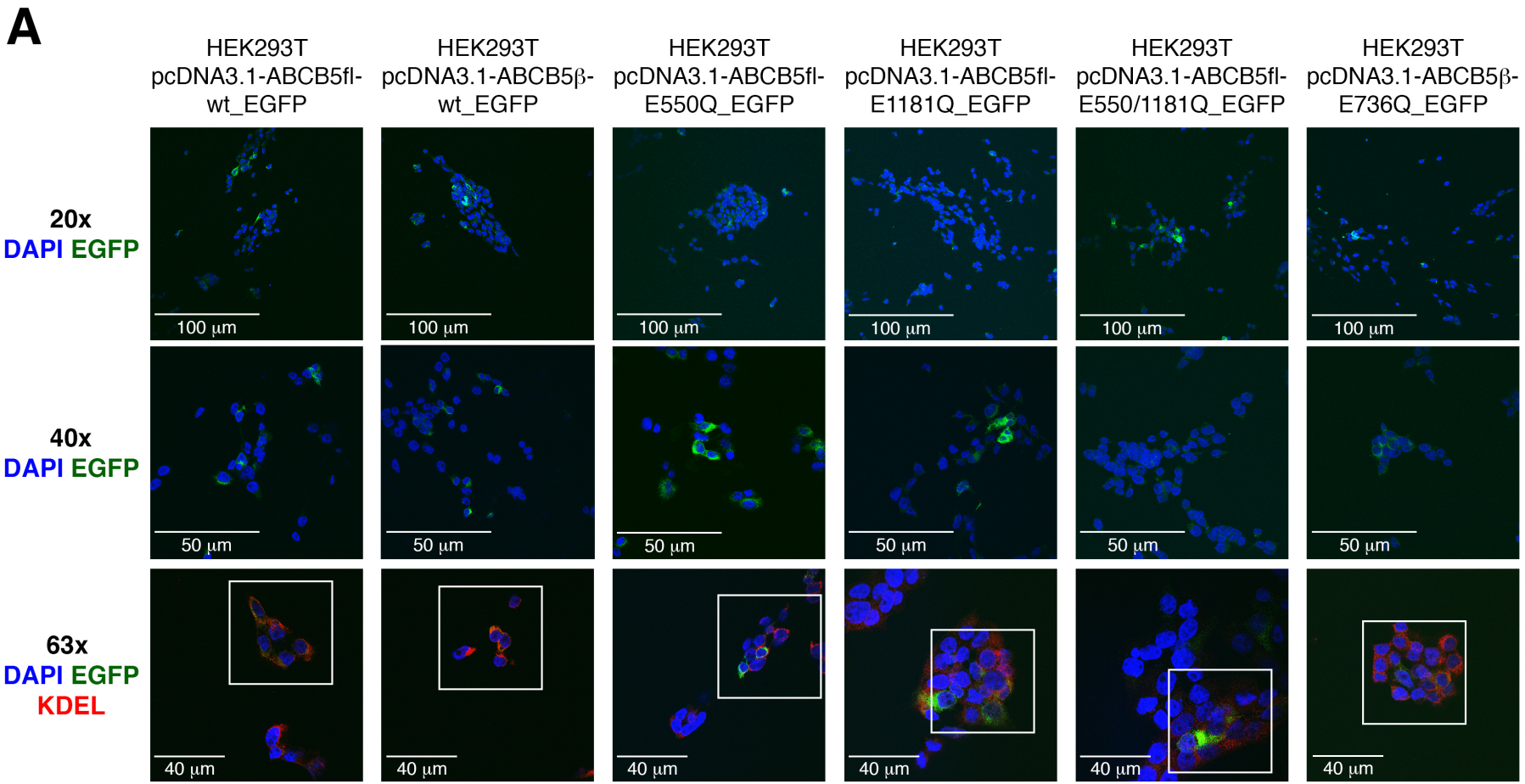

Figure 3-7. Subcellular localisation of ABCB5fl and ABCB5β Walker B mutants in HEK293T cells.

Representative images showing HEK293T cells transfected with wild type or mutant ABCB5fl or ABCB5β. Fluorescently tagged ABCB5fl and ABCB5β (green), fluorescently labelled KDEL (red), and DAPI staining of nuclei (blue) were observed 48 h post transfection at 40x and 63x magnification. White boxes represent magnified areas in the panels B and C. n = 4 biological repeats.

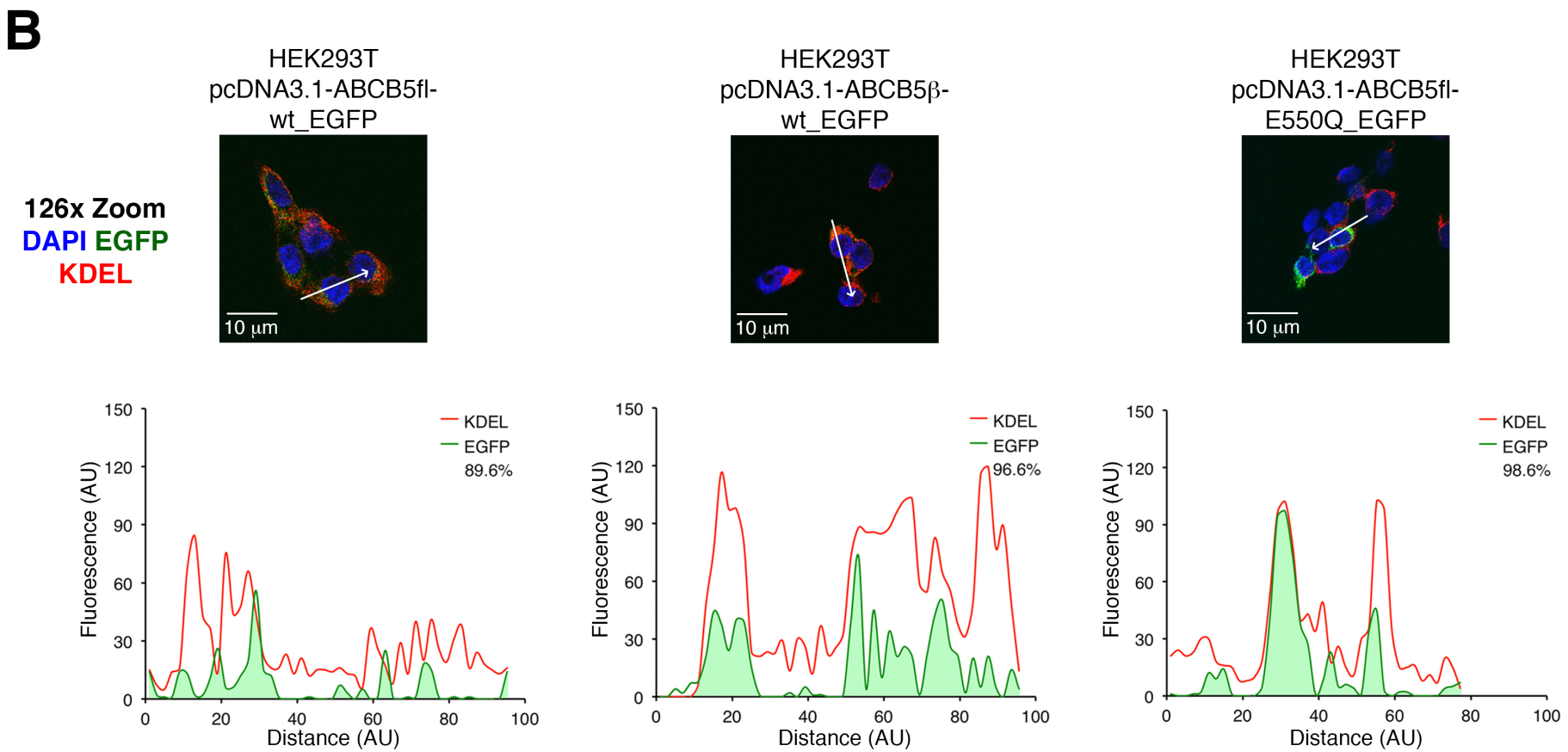

Figure 3-7. (Continued) Subcellular localisation of ABCB5fl and ABCB5β Walker B mutants in HEK293T cells.

Representative images showing HEK293T cells transfected with wild type or mutant ABCB5fl or ABCB5β. Fluorescently tagged ABCB5fl and ABCB5β (green), fluorescently labelled KDEL (red), and DAPI staining of nuclei (blue) were observed 48 h post transfection at 63x magnification (zoomed to 126x). Line graphs show KDEL (red) and EGFP (green) fluorescence along the white arrow in each magnified image. Areas of the EGFP fluorescence within areas of KDEL fluorescence are filled in green. This area is represented as a percentage of total EGFP fluorescence in each figure legend. n = 4 biological repeats.

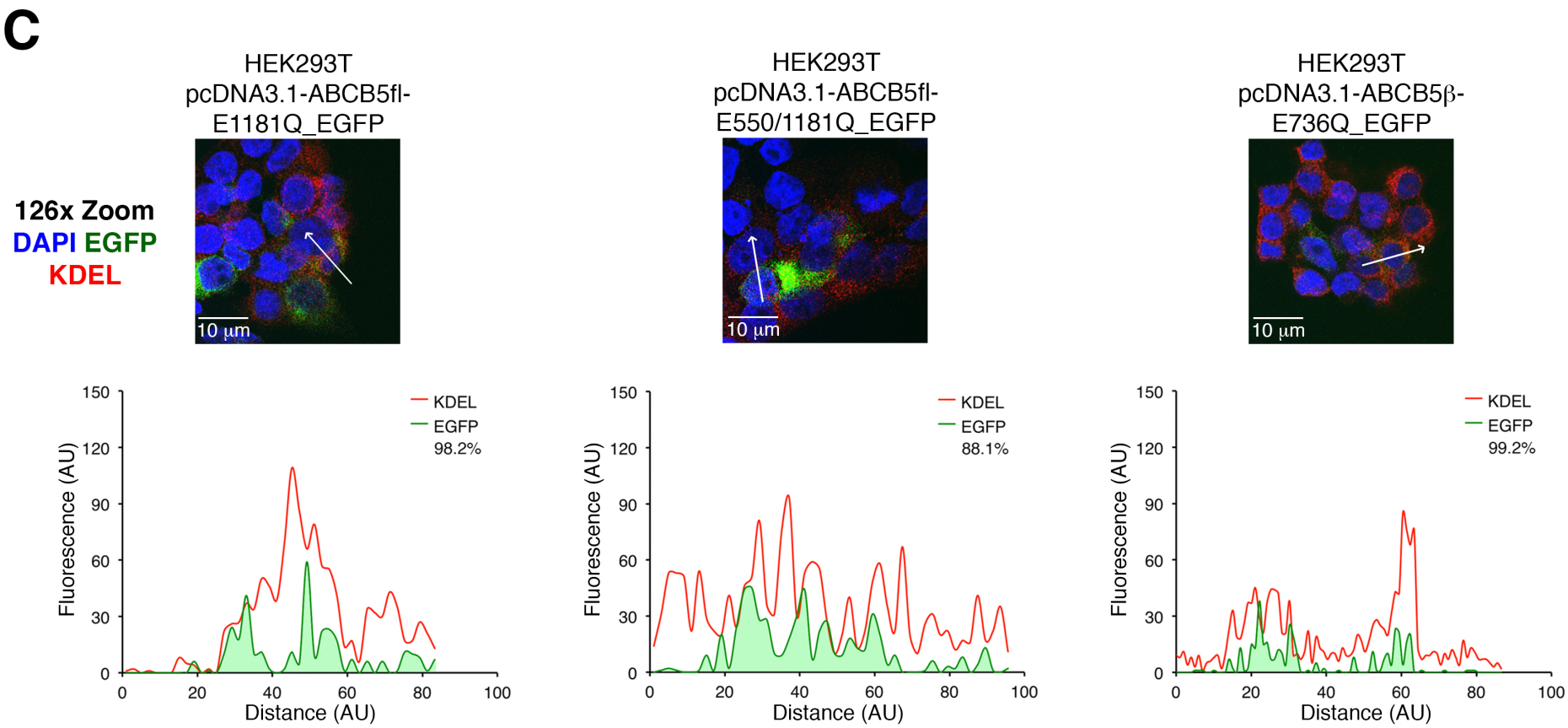

Figure 3-7. (Continued) Subcellular localisation of ABCB5fl and ABCB5β Walker B mutants in HEK293T cells.

Representative images showing HEK293T cells transfected with wild type or mutant ABCB5fl or ABCB5β. Fluorescently tagged ABCB5fl and ABCB5β (green), fluorescently labelled KDEL (red), and DAPI staining of nuclei (blue) were observed 48 h post transfection at 63x magnification (zoomed to 126x). Line graphs show KDEL (red) and EGFP (green) fluorescence along the white arrow in each magnified image. Areas of the EGFP fluorescence within areas of KDEL fluorescence are filled in green. This area is represented as a percentage of total EGFP fluorescence in each figure legend. n = 4 biological repeats.

ER marker KDEL, mirroring earlier results (Figure 3-7 panels B and C). Line scans of cells exhibiting co-localisation of EGFP and KDEL confirmed these findings, with the majority of green fluorescence marking ABCB5fl and ABCB5β locations found within areas of red fluorescence marking the ER.

Together, these data show that the single and double Walker B mutations of ABCB5fl and ABCB5β did not have any effect on their expression and localisation. Although there is a possibility that the hydrolysis of ATP is not required for protein function, it is more probable that the activity of the proteins has no bearing on their localisation within the cell. In fact, as earlier suggested, the localisation seen in these experiments could be correct, as all previous studies claiming a plasma membrane localisation have been carried out using antibodies, and not tagged protein.

3.2.3 Primers for ABCB5 isoforms

3.2.3.1 TaqMan primer/probe generation

The success of the transient transfection experiments allowed conditions for RT-qPCR to be optimised for both *ABCB5fl* and *ABCB5β* using mRNA extracted from untransfected and transfected HEK293T cells.

TaqMan primer/probe sets were purchased to amplify *ABCB5fl* and *ABCB5β* cDNA (Table 2-4). A pre-designed primer/probe set (tmABCB5) was purchased from Life Technologies Ltd (UK), to amplify a sequence common to both *ABCB5fl* and *ABCB5β* (Figure 3-8). Two additional primer/probe sets were designed, and purchased, to distinguish between *ABCB5fl* (tmABCB5flonly; using the 5' mRNA sequence unique

to this isoform), and *ABCB5β* (tmABCB5βonly using the, 197 nucleotide, retained intronic sequence in the 5'-UTR; Appendix I).

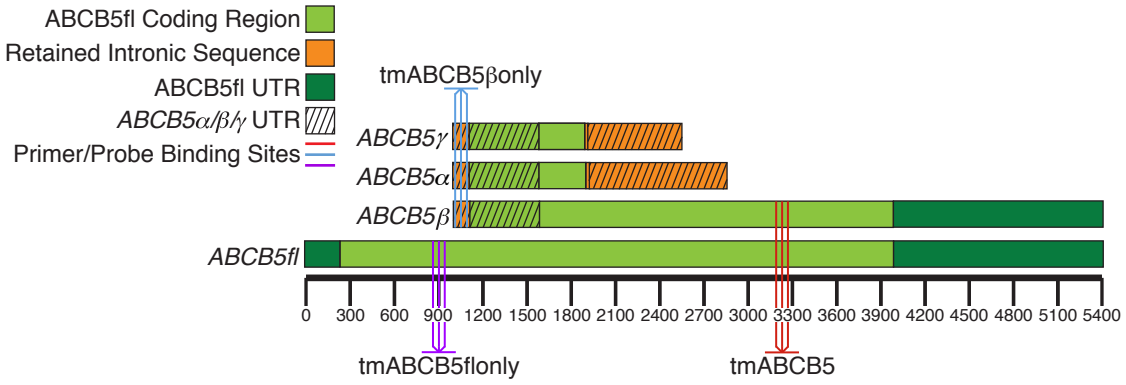

Figure 3-8. TaqMan target sites within the *ABCB5* cDNA sequence.

Cartoon illustrating the positions of the qPCR primer and probe binding sites within the mature mRNAs of *ABCB5β* and *ABCB5fl*. Binding sites of the primer/probe sets tmABCB5, tmABCB5flonly and tmABCB5βonly and are shown in red, purple and blue respectively.

Although primer/pair tmABCB5βonly has the possibility of targeting *ABCB5α* and *ABCB5γ* in addition to *ABCB5β*, this is the only region of the gene that can be targeted to distinguish between *ABCB5fl* and *ABCB5β*.

3.2.3.2 Primer/probe validation using transiently-transfected HEK239T

The generated primer/probe sets were validated using cDNA generated from HEK293T cells transfected with the ABCB5fl and ABCB5β encoding plasmids pcDNA3.1-ABCB5fl-wt_EGFP and pcDNA3.1-ABCB5β-wt_EGFP, and the control plasmid pcDNA3.1-EGFP. The data were normalised against the expression of *GAPDH* (primer/probe set tmGAPDH) for each of the samples (Figure 3-9 panels A and B).

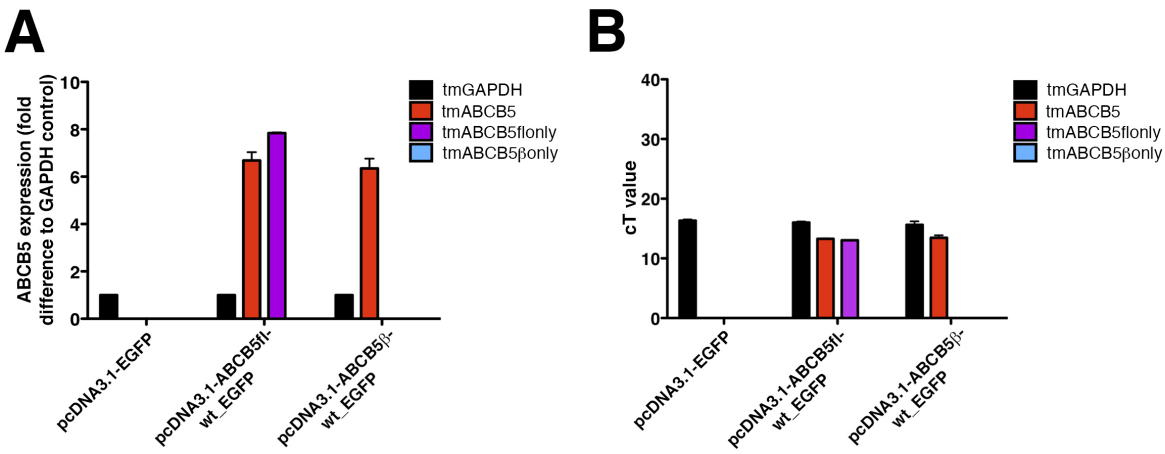

Figure 3-9. TaqMan primer/probe validation in transfected HEK293T cells.

Validation of TaqMan primer/probe sets for *ABCB5fl* (tmABCB5 (red) and tmABCB5flonly (purple)) and *ABCB5β* (tmABCB5 and tmABCB5βonly (blue)) was performed on cDNA derived from HEK293T cells transiently transfected with pcDNA3.1-EGFP, pcDNA3.1-ABCB5fl-wt_EGFP or pcDNA3.1-ABCB5β-wt_EGFP. A. The presence of *ABCB5fl* was detected by both tmABCB5 and tmABCB5flonly. The presence of *ABCB5β* was only detected by tmABCB5 B. qPCR cT values show that in conditions where no expression was observed, the signal was completely undetected. Error bars represent 1 SD from the triplicate mean. n = 3 biological repeats.

No endogenous expression of *ABCB5fl* or *ABCB5β* was detected in HEK293Ts at the mRNA level, making them an ideal cell line to validate the specificity of the TaqMan primer/probe sets. Primer/probe set tmABCB5 detected expression in cells transfected with the plasmids encoding either ABCB5fl or ABCB5β, but not in cells transfected with the empty vector, showing that this primer/probe set can amplify both *ABCB5fl* and *ABCB5β* specifically. tmABCB5flonly was specific for *ABCB5fl*, as product was only detected in cDNA prepared from cells transfected with pcDNA3.1-ABCB5fl-wt_EGFP. Primer/probe set tmABCB5βonly did not amplify cDNA produced from any of the transfected cells, including the cells transfected with the pcDNA3.1-ABCB5β-wt_EGFP plasmid, indicating that this primer/probe set is not effective at detecting expression of ABCB5β.

For all subsequent qPCR experiments, the tmABCB5 and tmABCB5flonly primer/probe sets were used. The combined data from these allowed the expression of

both *ABCB5fl* and *ABCB5β* to be estimated even in the absence of a primer/probe set to specifically amplify *ABCB5β*. For example, in a sample where a high level of expression is observed with tmABCB5, but a low level of expression is seen with tmABCB5flonly, it can be deduced that the product amplified is from *ABCB5β*.

3.2.4 Measuring the endogenous expression levels of *ABCB5fl* and *ABCB5β* mRNA and protein in cell lines

In order to discover cell lines with endogenous expression of ABCB5fl or ABCB5β, which could potentially be utilised for future study of the proteins, both RT-qPCR and western blotting were used to examine mRNA and whole cell lysate from six cell lines. The chronic myelogenous leukaemia (CML) cell line, K562, and the squamous cell carcinoma (SCC) cell line, A431, were used as positive controls, as endogenous expression of ABCB5β had previously been reported in both (Lehne et al., 2009). The melanoma cell lines A375M, WM1158, Mel224 and Mel505 were tested for expression of ABCB5fl and ABCB5β, as high expression ABCB5β is frequently reported in this type of cancer.

Expression of *ABCB5fl* and *ABCB5β* was studied relative to the expression of the housekeeping gene *GAPDH* in each of the cell lines. Expression of *ABCB5fl* mRNA was only detected in the K562 ($2.89 \times 10^{-3}\% \pm 0.56 \times 10^{-3}\%$) and A431 ($1.44 \times 10^{-3}\% \pm 0.36 \times 10^{-3}\%$) cell lines (Figure 3-10 panel A). Expression of *ABCB5β* mRNA was observed in cDNA generated from both of the control cell lines K562 (0.115% ± 0.010%) and A431 (0.060% ± 0.005%), as well as the melanoma cell lines Mel224 (0.027% ± 0.002%) and Mel505 (0.012% ± 0.003%). In total *ABCB5fl* mRNA

expression was found at much lower levels compared to *ABCB5β* (40 fold lower in K562, and 42 fold lower in A431) in expressing cells.

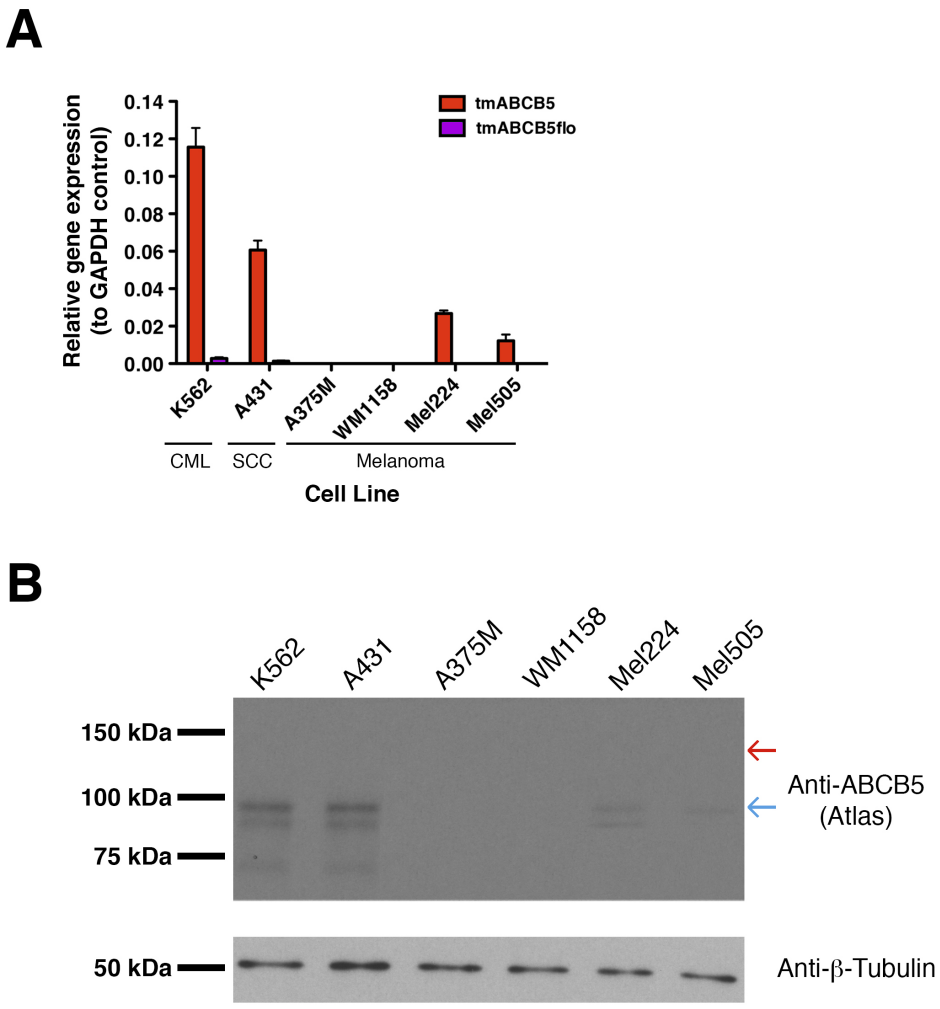

Figure 3-10. Endogenous expression of *ABCB5* in multiple cancer cell lines.

A. qPCR was carried out on cDNA derived from a CML (K562), SCC (A431) and four melanoma (A375M, WM1158, Mel224 and Mel505) cell lines. *ABCB5* expression (red) was detected in four (K562, A431, Mel224 and Mel505) of the six cell lines. *ABCB5fl* expression (purple) was detected at low levels in two (K562 and A431) of the cell lines. B. Low levels of ABCB5β protein were detected by western blotting of whole cell lysates in four (K562, A431, Mel224 and Mel505) of the six evaluated cell lines. Arrows show the predicted molecular weights of ABCB5fl (red) and ABCB5β (blue).

Western blotting of whole cell lysates using the Atlas antibody for ABCB5 showed low-level expression of ABCB5β (89 kDa) in K562, A431, Mel224, and Mel505 cells (Figure 3-10 panel B). Although *ABCB5fl* mRNA was detected in both the K562 and

A431 cell lines, ABCB5fl (138 kDa) protein was not detected in either of these, or any of the other cell lines tested.

Together, these data suggest that the K562, A431, Mel224 and Mel505 cell lines could be used to investigate the endogenous expression and function of ABCB5β, with the K562 line being the prime candidate, as it was found to have the highest protein expression level of the four.

3.3 Discussion

3.3.1 Summary of the findings

A HEK293T-based transient expression system was chosen in which to study ABCB5fl and ABCB5β, as the same approach had already been used to study other ABCB family transporters with success (Zolnerciks et al., 2007, Groen et al., 2011). PEI transfection of HEK293T cells was carried out using plasmids encoding ABCB5fl or ABCB5β, each with either a V5-6His or EGFP tag, and were analysed by western blotting or fluorescence microscopy, respectively.

Western blotting was carried out using three commercially available antibodies, two of which have previously been included in published studies using endogenously expressed protein (Ramgolam et al., 2011, Wilson et al., 2011, Grimm et al., 2012, Linley et al., 2012). Western blot analysis carried out on cell lysates from untransfected HEK293Ts, and HEK293Ts transfected with either the empty V5-6His plasmid, or the plasmid encoding ABCB5fl or ABCB5β, showed that only one of the three antibodies

tested (Atlas) could specifically recognise both ABCB5fl and ABCB5β, where as the other two (previously published) antibodies (Rockland and Sigma) could not.

Confocal analysis of HEK293Ts transfected with EGFP-tagged ABCB5fl and ABCB5β revealed poor transfection efficiency and low level expression compared to the positive control plasmid encoding Venus tagged CD36. The fluorescently labelled ABCB5fl and ABCB5β did not traffic to the plasma membrane as previously reported (Frank et al., 2003), as all green fluorescence was observed in an intracellular localisation. Co-localisation of both ABCB5fl and ABCB5β was observed with the ER marker KDEL, confirming the intracellular localisation of the proteins.

The hypothesis that ABCB5fl and ABCB5β may be detrimental to HEK293Ts, thereby preventing proper expression and localisation, was investigated by an LDH activity assay and protein mutation. The LDH activity assay showed that no cytotoxicity was associated with transfection of plasmids containing ABCB5fl or ABCB5β compared to empty control plasmids. Predicted non-functional mutants of both ABCB5fl and ABCB5β were produced to investigate whether functional activity had any impact on expression and localisation. No significant changes in expression or localisation were observed upon transfection of any mutant protein into HEK293T cells, when compared to the wild type proteins.

TaqMan primer/probe sets were generated in order to study *ABCB5fl* and *ABCB5β* mRNA levels. Primer/probe sets targeting either *ABCB5fl* or *ABCB5β*, and one targeting both were tested for specificity. The tmABCB5βonly was found to be

ineffective at detecting either transcript, and thus was not used any further. tmABCB5 was able to detect both *ABCB5fl* and *ABCB5β*, and tmABCB5flonly was found to only detect *ABCB5fl*. A combination of the primer/probe sets tmABCB5 and tmABCB5flonly were used for all future RT-qPCR experiments so that the expression of *ABCB5fl* and *ABCB5β* could be delineated.

Finally, the expression levels of endogenous *ABCB5fl* and *ABCB5β* mRNA and protein were tested in six cell lines. Expression of *ABCB5β* was detected in four of the cell lines at both the mRNA and protein level (K562, A431, Mel224, Mel505). *ABCB5fl* mRNA was only detected in two of the cell lines (K562, A431), with the protein undetectable in all samples.

3.3.2 Discussion

Antibodies against ABCB5β have previously been used in multiple published studies to identify endogenously expressing cells, and more commonly MMICs (Ma et al., 2010, Schatton et al., 2010, Frank et al., 2011, Ramgolam et al., 2011, Wilson et al., 2011, Linley et al., 2012, Aldaz et al., 2013, Mathieu et al., 2014). This investigation found that two of the commercially available antibodies used in previous studies for targeting ABCB5β are ineffective.

The three antibodies evaluated in this study (Atlas, Rockland and Sigma) were used to target HEK293T cells that were untransfected, transfected with an empty vector, or transfected with a vector encoding either ABCB5fl or ABCB5β. The only antibody found to produce bands of the expected molecular weight for both ABCB5fl and ABCB5β (Atlas), only did so in protein samples taken from HEK293Ts transfected with

the relevant transcript, and not in either of the negative control samples. This signified that the Atlas antibody against ABCB5 is specific, and could be used for the further study of cells with endogenous ABCB5fl and ABCB5β expression. Multiple bands with lower molecular weights than those of ABCB5fl and ABCB5β were also observed with the antibody in each of the relevant samples. The most likely possibility is that these bands are seen due to ABCB5fl or ABCB5β protein degradation, resulting in smaller protein fragments containing the antibody binding epitope migrating down the gel along with the full size protein. It should also be noted that the pattern of bands in the ABCB5β expression HEK293T cells was very similar to that of the endogenously expressing K562, A431, Mel224 and Mel505 cell lines also tested for protein expression. This may suggest that the protein degradation which results in this banding pattern may have occured during or after the cell lysis step of protein recovery, although protease inhibitors were used, and at twice the manufacturer's recommended concentration.

Two antibodies used in previously published studies (Rockland and Sigma) were also tested (Ramgolam et al., 2011, Wilson et al., 2011, Linley et al., 2012, Grimm et al., 2012), but were not found to produce any bands at the expected molecular weights in the same samples used to test the Atlas antibody. The Rockland antibody produced bands in all samples tested, including the sample taken from untransfected HEK293Ts, which do not endogenously express ABCB5fl or ABCB5β as suggested by the results obtained the Atlas antibody, and confirmed by RT-qPCR. The bands produced by the Rockland antibody were all below the expected molecular weight of ABCB5β (89 kDa), with two major bands present in all samples, and three bands present in the cells transfected with the empty vector, or the vector encoding ABCB5fl or ABCB5β. These

bands are unlikely to be due to unspecific antibody binding, due to the stringent washes used during the western blotting protocol, but are probably due to a contamination of the polyclonal antibody with antibodies which are not specific to ABCB5 and are in fact targeted to a different epitope than the one desired. The Sigma antibody failed to detect ABCB5fl or ABCB5β, or indeed any other protein in any of the samples tested, suggesting that is ineffective at detecting either of these isoforms of ABCB5.

Overall expression of both ABCB5fl and ABCB5β was found to be relatively low when compared to cells transfected with the CD36 encoding control plasmid. This issue was not rectified by the mutation of the proteins, which was previously found to resolve this issue for ABCB4 (Groen et al., 2011). High expression of both *ABCB5fl* and *ABCB5β* mRNA was detected by RT-qPCR, suggesting that the low levels of protein observed are likely to be due to either inefficient translation or high turnover of the isoforms. Indeed, the band pattern observed on the western blots of transfected HEK293T lysates may be indicative of a high protein turnover due to ubiquitin mediated degradation by the 26S proteasome.

One possible reason for a low translation efficiency is that the mRNA may contain one or more rare codons in its sequence, leading to longer than normal pauses within the translation mechanism as rare tRNAs (transfer RNAs) are needed to continue extending the peptide sequence. These longer than normal pauses in translation have been linked to both changes in protein stability (Tsai et al., 2008, Fung et al., 2014), and substrate specificity in ABCB1 (Fung et al., 2014, Kimchi-Sarfaty et al., 2007). It is, therefore, possible that the inclusion or rare codons within the *ABCB5fl* and *ABCB5β* mRNA may

cause a pause in translation which either stops translation altogether, or causes the protein to misfold, resulting in a protein which is targeted by the cell for degradation.

Although ABCB5β has been described as having a plasma membrane localisation (Frank et al., 2003), papers have consistently included images which show ABCB5β as having an intracellular localisation (Figure 3-11) (Frank et al., 2003, Mathieu et al., 2014, Linley et al., 2012). Although it should be noted that these papers only show ABCB5 targeted antibody binding and not tagged protein, this localisation is consistent with the results seen within this study where EGFP-tagged ABCB5fl and ABCB5β failed to reach the plasma membrane in all cells where it was overexpressed. In addition, the predicted non-functional mutants of ABCB5fl and ABCB5β were also found in the same intracellular localisation as their wild type counterparts, suggesting that the function of these proteins has no effect on their localisation within the cell. It should also be noted that both ABCB2 (TAP1) and ABCB3 (TAP2) are localised within the ER (Kleijmeer et al., 1992), and ABCB6 is localised to the outer mitochondrial membrane (Krishnamurthy et al., 2006b), and as such, the intracellular localisation of ABCB family proteins is not without precedent.

One of the supporting arguments that ABCB5β is present at the plasma membrane is that expression of the protein is reported to extrude doxorubicin from endogenously expressing cells (Frank et al., 2005). This data may be inaccurate, however, as ABCB5β expression was confirmed via antibody staining, which as previously stated here, may not be able to accurately determine the presence of ABCB5β. Additionally, the presence

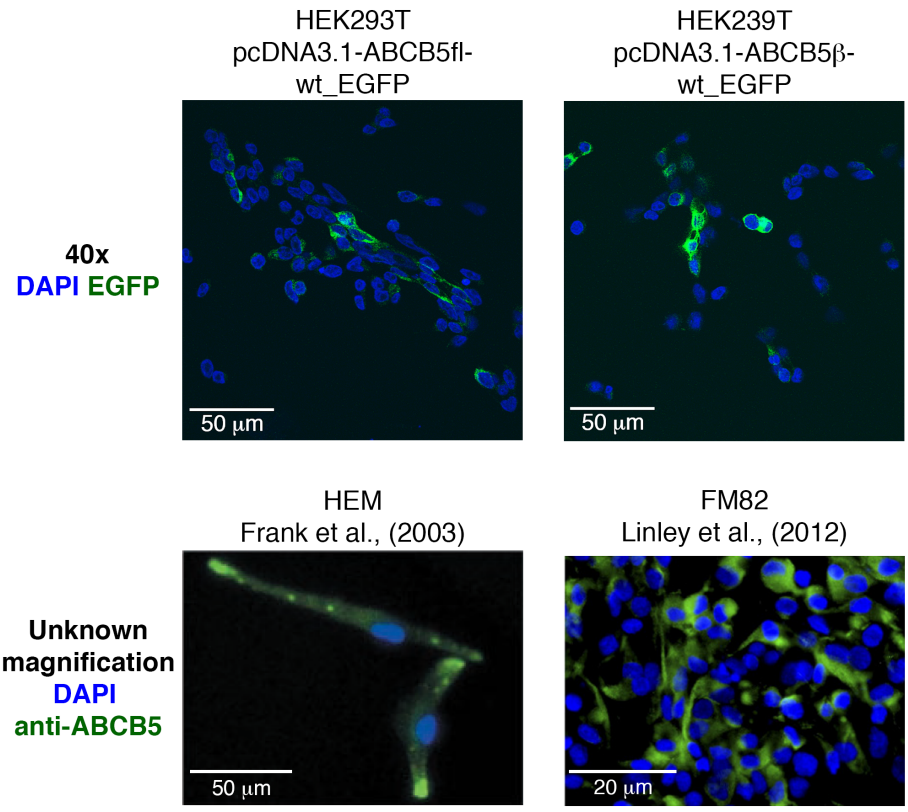

Figure 3-11. Subcellular localisation of ABCB5 in previous studies.

HEK293T were cells transfected with pcDNA3.1-ABCB5fl-wt_EGFP or pcDNA3.1ABCB5β-wt_EGFP. Fluorescently tagged ABCB5fl and ABCB5β (green) and DAPI staining of nuclei (blue). Immunofluorescent staining of ABCB5β (green) and DAPI staining on nuclei (blue) in HEM (human epidermal melanocytes) and FM82 (human melanoma) cells was previously published[I] by Frank et al., (2003), and Linley et al., (2012).

of other ABC transporters, such as ABCC1 and ABCG2, which are known to extrude doxorubicin (Calcagno et al., 2008, Jungsuwadee et al., 2012), was not properly ruled out. Therefore, it is likely these or other ABC proteins are responsible for the removal of doxorubicin from the cells as it is doubtful that ABCB5β is a functional protein.

[I] Reproduced and adapted from: Frank et al., (2003) Regulation of Progenitor Cell Fusion by ABCB5 P-glycoprotein, a Novel Human ATP-binding Cassette Transporter, Figure 3 panel C; and Linley et al., (2012) The Helicase HAGE Expressed by Malignant Melanoma-Initiating Cells Is Required for Tumor Cell Proliferation *in vivo*, Figure 5 panel B; with permission of the publisher (The Journal of Biological Chemistry).

Expression of ABCB5fl has been linked to drug resistance in another study using exogenously expressed protein (Kawanobe et al., 2012), although the cellular localisation of the protein was not reported. It is possible that ABCB5fl could have both a drug resistance role and an intracellular localisation, as it has previously been shown that ABCB1 can confer drug resistance to expressing cells by actively transporting doxorubicin into lysosomes (Yamagishi et al., 2013). A similar mechanism for ABCB5fl would allow the previous observations of drug resistance properties, and the subcellular localisation seen previously, and within this study, to be reconciled.

3.3.3 Future work

This study has been concerned with exogenously expressing both ABCB5fl and ABCB5β protein. Through the use of confocal microscopy, and fluorescently tagged protein, the localisation of both isoforms has been called into question with respect to previously published data. In order to accurately determine which subcellular organelle the two isoforms localise to, differential centrifugation should be performed on HEK293T cells transfected with vectors encoding both wild type and mutant ABCB5fl and ABCB5β. The centrifugation should be carried out in such a way that the internal organelles (ER, Golgi apparatus, mitochondria lysosomes etc.) are separated, as these are the likely areas of ABCB5fl and ABCB5β localisation, with the ER identified in this study as site of strong ABCB5-related fluorescence. This technique, and the subsequent western blotting of the separated samples for both ABCB5 and additional proteins – used to mark organelles – would allow for the precise intracellular location of both the wild type and mutant forms of each isoform to be determined. This technique could subsequently be carried out to determine whether the localisation of ABCB5fl and ABCB5β is any different in cells with endogenous expression, such as the A431 and K562 cell lines identified in this study.

There is a possibility that within these experiments the presence of an EGFP tag upon the C-terminus of ABCB5fl and ABCB5β may have adversely effected proteins localisation, has EGFP tagging of proteins has previously been shown to alter localisation in some cases (Palmer and Freeman, 2004, Zhu et al., 2013a). This is unlikely however, as the images taken agree with ones previously published, but if it were the case, the localisation data presented here could be erroneous. This possibility could be eliminated however by carrying out the previously described differential centrifugation with protein extracted from HEK239T cells transfected with both -EGFP, or -V5-6His tagged ABCB5fl/ABCB5β. If the -EGFP tagged protein was found to reside within the same organelles as the -V5-6His tagged protein, the ABCB5fl and ABCB5β protein localisation findings reported in this study could be confirmed as accurate.

Glycosylation of the proteins may also have an effect on their localisation, as previously reported for a wide array of membrane proteins (Graf et al., 2004, Hoosdally et al., 2009, Haga et al., 2011, Moharir et al., 2013). Both ABCB5fl and ABCB5β contain potential glycosylation sites, although only ABCB5fl has sites that are predicted to be in a region where glycosylation could take place (see Section 1.5.1.2). In order to examine whether glycosylation can effect localisation in these proteins, lysates taken from HEK293T cells transfected with ABCB5fl and ABCB5β should be subjected to PNGase F treatment in order to remove any bound glycans. Western blotting of these samples could then be used to visualise any changes in the motility of the ABCB5 species during SDS-PAGE as a result of deglycosylation. If changes in motility are seen with either ABCB5fl or ABCB5β point mutations could then be made in the protein coding

sequence, in order to remove the glycan binding sites. Expression of these mutants in HEK293T cells would then allow any change in subcellular localisation due to the prevention of glycan formation to be studied.

In order to enhance the expression of ABCB5fl and ABCB5β, multiple small molecules previously shown to enhance the expression of other ABC transporters could be tested for efficacy. Although not strictly enhancing expression, the proteasome inhibitor MG132 has previously been shown to increase ABC protein abundance due to a reduction in degradation (Fukuda et al., 2011). The histone deacetylase (HDAC) inhibitors sodium butyrate and 4-phenyl butyrate could also be tested, as they are both reported to increase expression of a wide array of genes, some involved in transcription and translation, by preventing the tight wrapping of DNA around deacetylated histones (Gorman et al., 1983). In addition to these, it has been shown in other ABC transporters that treatment of cells with their substrates allows better ABC transporter expression, presumably due to the stabilisation of protein folding in an environment where the transporter can fold around its substrate (Loo and Clarke, 1997).

The possibility of rare codons being present within the ABCB5fl and ABCB5β mRNA coding sequences should also be addressed. In order to investigate this, the coding sequences of both isoforms should be checked against a list of the most and least common codons in human cells. Two avenues of approach could then be taken; the first involving the identification of particularly rare codons, and the mutation of them into more common ones; the second approach would be to codon optimise the entirety of both ABCB5fl and ABCB5β, and to have them synthesised. Both of these methods would provide a coding sequence with a reduced chance of translation termination or

misfolding. If either of these issues were a problem for the cell in the expression of ABCB5fl and ABCB5β, an increased level of protein, and possibly an alternative subcellular localisation, would be expected in subsequent experiments.

In this study, multiple Walker B mutants of ABCB5fl and ABCB5β were generated, which were predicted to be non-functional. A recent study of SNPs within the ABCB5 gene identified one causing a non-synonymous mutation of K115E in ABCB5β (K560E in ABCB5fl; 10 amino acids away from the first Walker B mutation made in this study – E550Q) (Lin et al., 2013). K115 is an amino acid residue found between the D-loop and H-loop of NBD1, and the lysine to glutamate change was reported to be associated with decreased melanoma risk and reduced transport activity. The same mutation could be carried out in both the ABCB5fl and ABCB5β vectors described previously, and transfected into HEK293T cells to allow any changes in either the expression or localisation to be visualised when compared to the wild type proteins.

An informative avenue of future study would be to create stably expressing cell lines with the wild type or mutant ABCB5fl and ABCB5β as previously carried out by Kawanobe et al., (2012), who used their cell lines to study transport activity, and measure the related kinetics. The stable expression of the proteins will allow for the cell clones with the highest expression of ABCB5fl or ABCB5β to be selected for further study. The resulting cell lines could subsequently be utilised, together with the endogenously expressing cell lines identified in this study, for more in depth studies using flow cytometry to study both transport activity, and the destination of the transport substrates – such as anthracyclines or taxanes – within the cell.

Together, the experiments proposed here would provide a further insight into the function and activities of ABCB5fl and ABCB5β and corroborate or call into question large amounts of the previously published literature on these proteins.

Chapter Four

4 Investigating the relationship between ABCB5 and the tumour suppressor p16

4.1 Introduction

p16, encoded by *CDKN2A*, is an important regulator of the normal cell cycle, controlling the cell's passage through the r-point of the cell cycle – the main checkpoint of the G_1/S phase transition – via its interaction with CDK4/6 (Serrano et al., 1993, Gil and Peters, 2006). p16 expression increases with age *in vivo*, causing cells to lose their proliferative capability and enter senescence. This, and the linkage of the *INK4A/ARF* locus by GWAS to many age-related diseases (Krishnamurthy et al., 2006a, McPherson et al., 2007, Matheu et al., 2009), makes p16 an attractive target for modulation in relation to treating these diseases. Either reducing the expression of p16 or clearing p16-expressing senescent cells from the body could potentially relieve the symptoms of age-related disease. This idea is given more weight by a recent study which showed that in the transgenic INK-ATTAC mice selective clearance of the marked p16-positive senescent cells by drug-induced caspase activity could either delay the onset of age-related disorders (with lifelong drug treatment), or attenuate the progression of already established disorders (with drug treatment in later life) (Baker et al., 2011). Any therapy involving modulation of p16 in humans, however, would have to be carefully monitored due to the strong link between lack of p16 expression and cancer in humans (Kamb et al., 1994), although this is normally due to promoter methylation or mutation.

Expression of p16 is commonly reduced in human tumours, where the *INK4A/ARF* locus may be deleted, mutated or epigenetically down regulated (Esteller et al., 2001, Forbes et al., 2006). p16 was initially discovered in melanoma (Serrano et al., 1993), where expression of *ABCB5β* and *ABCB5α* are reported to be frequently up-regulated (Chen et al., 2005a, Frank et al., 2005, Fukunaga-Kalabis et al., 2010, Gazzaniga et al., 2010).

The *ABCB5* gene is predicted to encode an integral, dodecaspan membrane protein of the ABC superfamily of transport proteins. Members of the B family of these transporters have been found to efflux a wide variety of substrates from the cell, ranging from chemotherapeutic agents (ABCB1), to lipids such as phosphatidylcholine (ABCB4; (Szakács et al., 2006). Four isoforms of ABCB5 have been described (ABCB5fl, ABCB5α, ABCB5β and ABCB5γ), and the two longest isoforms ABCB5fl and ABCB5β have been reported to be encode active efflux transporters, which are capable of extruding chemotherapeutic drugs – specifically doxorubicin – from melanoma cells (Frank et al., 2005, Kawanobe et al., 2012). Not long after it was first described, ABCB5β was proposed to also have a role in progenitor cell fusion, and more recently it has been suggested that it is highly expressed in a sub-population of melanoma cells, namely the cancer stem cell-like MMICs (Frank et al., 2003, Schatton et al., 2008).

Recently, a genome-wide siRNA screen identified novel modulators of p16 in normal HMECs (Bishop et al., 2010), which have a finite lifespan with well-documented p16-mediated senescence resulting from normal serial passage (Garbe et al., 2009). This screen suggested that siRNA-mediated knockdown of *ABCB5* expression caused a concomitant reduction in the level of p16 protein, combined with an increase in cellular proliferation and decrease in cell and nuclear size (Bishop et al., 2010). Both ABCB5fl and ABCB5β are predicted and reported to be plasma membrane proteins, and as such, are potentially accessible targets via which to modulate p16.

4.1.1 High-content-fluorescent microscopy

Fluorescence microscopy is a powerful tool to study biological processes. The fluorescent labelling of proteins (by antibody staining or conjugation to a fluorescent protein, such as EGFP) and nucleic acids (by using fluorescent molecules which intercalate into DNA or RNA) has made the labelling of virtually any structure in the cell possible, even in live cells (Giepmans et al., 2006, Conrad and Gerlich, 2010). With a wide variety of fluorescent biosensors and imaging modalities available it has become possible to detect post-translational modifications, protein-protein interactions, small molecules and measure steady state protein dynamics (Lippincott-Schwartz et al., 2003, Giepmans et al., 2006). Early difficulties in systematic and quantitative analyses limited imaging-based assays to manual, low-throughput experiments, capable of studying just a few candidate genes. However, due to developments in the automation of microscope control and image analysis, it is now possible to evaluate large numbers of candidate genes in a single study (Conrad et al., 2004, Pepperkok and Ellenberg, 2006).

The main readout used in this study is also one of the most basic that high-content microscope systems can perform, fluorescence intensity. This readout is often used to score protein abundance (Müller et al., 2005, Loo et al., 2007), but can also be used for many other types of study, including: cellular DNA content (Kittler et al., 2007); lipoprotein uptake (Bartz et al., 2009); mitochondrial Ca^{2+} transport (Jiang et al., 2009); or the entry of viruses into cells (Brass et al., 2008).

It is also possible to study the morphology of cells by staining the cytoskeleton, chromatin and nucleic acids enabling the measurement of different aspects of cell morphology including nuclear area (by staining DNA) and whole cell area (by staining

all nucleic acids (Bishop et al., 2010)). Utilising these measurements, analysis software can be 'taught' to identify individual cells, allowing cell number to be calculated, and information to be collected on a well-by-well and cell-by-cell basis.

4.1.2 Aims

The hypothesis for the work carried out in this chapter was that cellular levels of ABCB5 and are linked to p16 expression, and that understanding the pathway by which this occurs may provide reveal potential therapeutic targets for age-related disorders associated with p16 expression. The aim of this project was to understand and characterise the relationship between the ATP-binding cassette transporter family member ABCB5 and the tumour suppressor p16. Specifically, to:

- Confirm the results reported by Bishop *et al*. (2010), in which siRNAs targeting *ABCB5* mRNA caused morphological and proliferative changes, with a concomitant reduction of p16 in HMEC;
- Validate the knockdown phenotype at the mRNA level by RT-qPCR and protein level by western blotting of ABCB5;
- Identify the relevant isoform of *ABCB5* involved in p16 reduction by:
    - RT-qPCR to determine which isoforms of *ABCB5* are expressed in HMECs, and
    - The use of siRNAs to target specific *ABCB5* isoforms and determine the effect on p16 expression;
- Investigate ABCB5 expression at the mRNA and protein levels in early to late passage HMECs and evaluate its relationship to p16 expression.

4.2 Results

4.2.1 Optimisation of HMEC transfection

4.2.1.1 HMEC characteristics

HMECs undergo p16-mediated senescence in cell culture (Brenner et al., 1998, Garbe et al., 2009), making them a suitable model to study the effects of modulating senescence and p16 expression using siRNA-mediated gene knockdown. With serial passaging, the

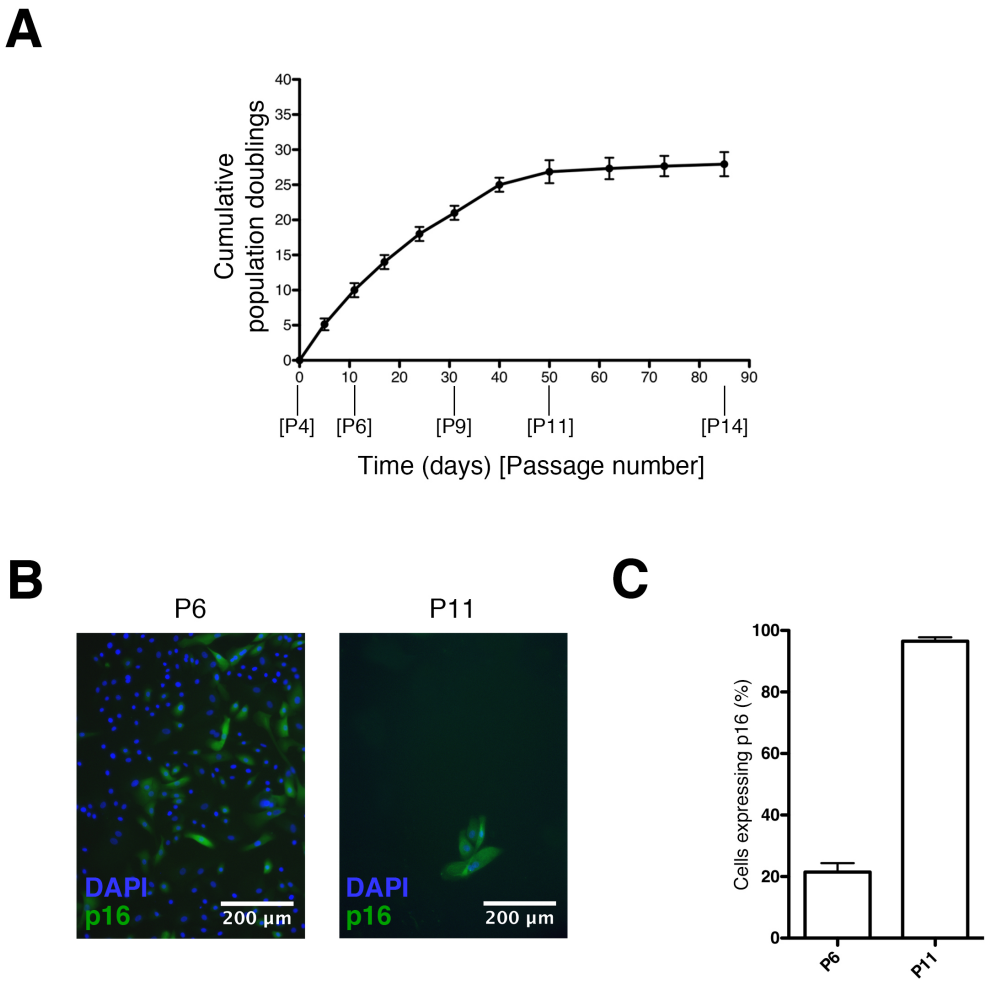

Figure 4-1. Population doublings and p16 expression in serially passaged HMECs.

A. Population doublings of HMECs in culture from passage 4 (P4) to passage 14 (P4). B. Immunofluorescence images of HMEC fixed at P6 and P11 showing DAPI staining of nuclei (blue) and antibody staining of p16 (green). C. The percentage of p16 expressing cells at P6 (21.5 ± 1.4) and P11 (96.5 ± 0.6), quantified using the Developer Toolbox 1.7 (GE Healthcare, UK). Error bars represent one SD. n = 3 biological repeats.

expression of p16 gradually increases throughout the population, triggering senescence and reducing the overall proliferative capacity of the culture (Figure 4-1 panel A). The expression of p16 in cells was visualised by antibody staining at passage 6 (P6) and passage 11 (P11; Figure 4-1 panel B; see Section 2.28). When p16 staining was quantified, 21.5% (± 1.4%) of cells were found to express p16 at P6, where as at P11, 96.5% (± 0.6%) were found to express the protein (Figure 4-1 panel C; see Section 2.28).

4.2.2 siRNA knockdown of *ABCB5*

4.2.2.1 Controlling for phenotypic changes

Three siRNAs targeting *Cyclophilin B, CBX7* and *p16* were used alongside the *ABCB5*-targeting siRNAs to be examined in order to control for both induction and reduction in cellular p16 levels. siRNA targeting *Cyclophilin B* (*siGLO;* Dharmacon, DE), conjugated to a fluorescent tag (Pierce NuLight™ DY-547), was used to track cellular uptake of siRNA-transfection reagent complexes. *siGLO* also functions as a negative siRNA control, as knockdown of this gene causes no phenotypic changes in p16 expression or senescence (Bishop et al., 2010). siRNA targeting the polycomb group (PcG) protein, *CBX7,* was used as a positive control (see Section 1.14.3). Loss of CBX7 induces senescence by removing the epigenetic repression of *p16*, thereby reducing cell proliferation and increasing cell area. The opposite effect is observed for the control siRNA targeting *p16*, which knocks down expression of the protein product and therefore increases cell proliferation and decreases cell area.

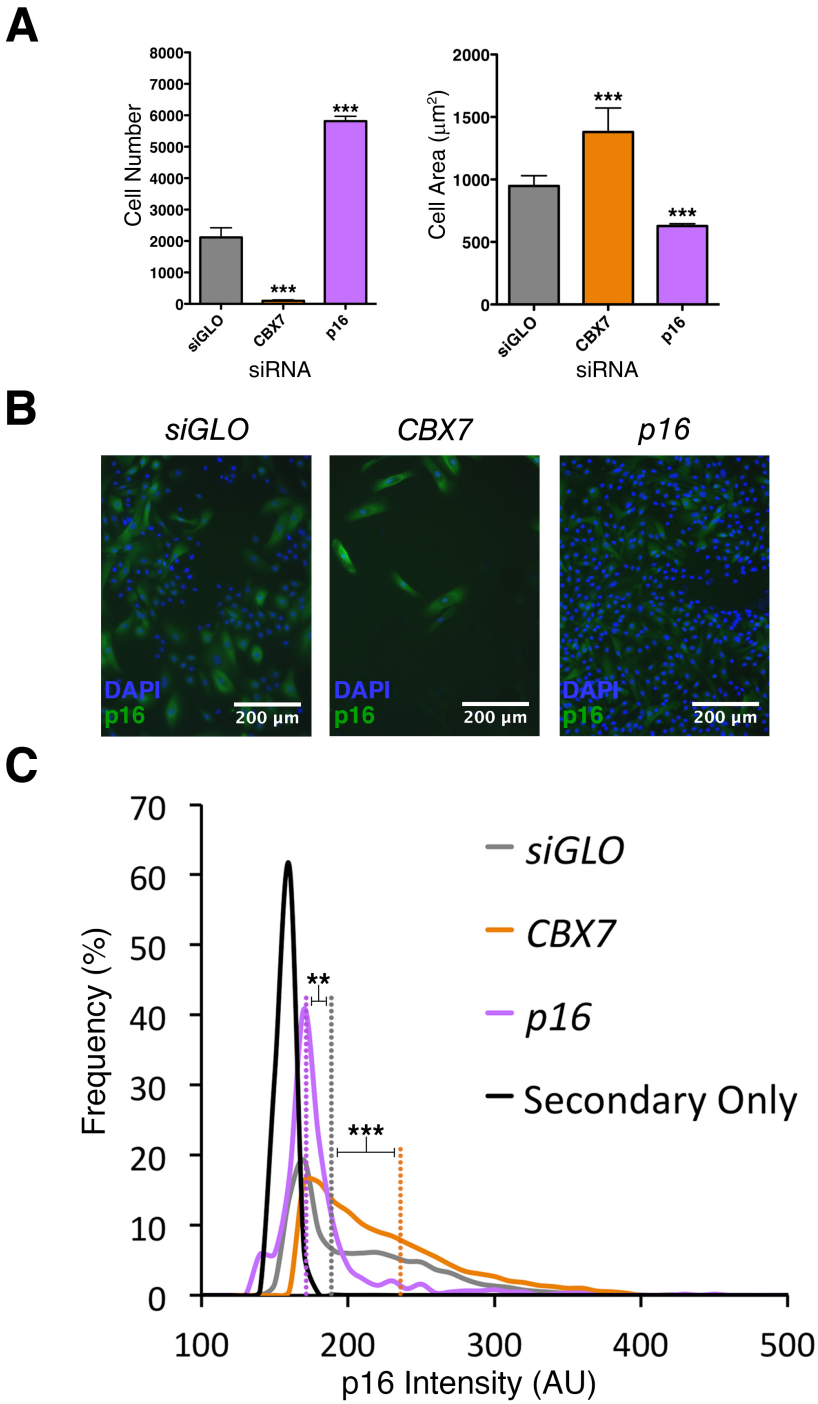

Figure 4-2. The effect of *p16* and *CBX7* targeting siRNAs on proliferation, cell area and p16 levels.

A. Quantitated cell number and cell area. Significant changes in both cell number and cell area were observed ($p < 0.001$ for all) when cells were transfected with siRNA targeting *CBX7* (orange) or *p16* (purple) compared to the *siGLO* negative control (grey). B. Immunofluorescence images of HMECs 120 h post transfection with 30 nM *siGLO*, *CBX7* or *p16* siRNAs. Antibody staining of p16 is shown in green and DAPI staining of nuclei is shown in blue. C. Control siRNAs targeting *CBX7* (orange) or *p16* (purple) show a respective increase and reduction in p16 intensity (AU), relative to the *siGLO* negative control (grey). Median p16 intensity values (AU) are shown by the dotted lines. The solid black line represents fluorescence intensity from control staining with the secondary antibody alone. All error bars represent one SD, ** $p < 0.01$, *** $p < 0.001$, n = 4 biological repeats.

To confirm that the positive control siRNAs targeting *CBX7* and *p16* affected cell number and cell morphology via modulation of p16 protein level, HMECs were transfected with siRNA targeting *p16, CBX7* and the negative control siRNA (*siGLO*) at the previously optimised conditions (see Appendix II) and analysed for p16 protein intensity. High content analysis using the IN Cell system was performed 120 h post transfection as described (see Section 0) to quantify changes in cell number, cell area and p16 intensity (Figure 4-2). This multi-parameter analysis allowed the cellular phenotypes caused by positive control siRNAs targeting *CBX7* (induction of senescence) or *p16* (increased proliferation) to be distinguished accurately and in an unbiased manner.

Targeting of *CBX7* caused a significant decrease in cell number ($p < 0.001$), together with significant increases in cell area ($p < 0.001$) and p16 intensity ($p = 0.0005$), establishing *CBX7* knockdown as an effective positive control for *p16* activation and cellular senescence (Figure 4-2). By contrast, targeting of *p16* directly caused a significant increase in cell number ($p < 0.001$) and significant decreases in cell area ($p < 0.001$) and p16 intensity ($p = 0.0325$), confirming that the measures effectively quantitate the phenotype resulting from a reduction in cellular p16. As both the siRNAs targeting *CBX7* and *p16* showed strong phenotypic changes compared to *siGLO*, in line with what was predicted, they were used as positive controls for all subsequent transfections in HMECs.

4.2.2.2 Ambion siRNAs

Following transfection optimisation of HMECs, the first aim of the project was to confirm the data generated previously (Bishop et al., 2010), in which siRNAs targeting of *ABCB5* reduced the level of p16.

In order to validate the findings of Bishop et al. (2010), the three siRNAs targeting *ABCB5* (Table 2-5) used in the study were purchased from Ambion (Ambion-1, Ambion-2 and Ambion-3). The pool of these three siRNAs (Ambion-P) had previously been shown to significantly reduce the expression of p16, causing an increase in cell number and decrease in cell area. The region of the *ABCB5* mRNA targeted by the each of these three siRNAs is shown in Figure 4-3.

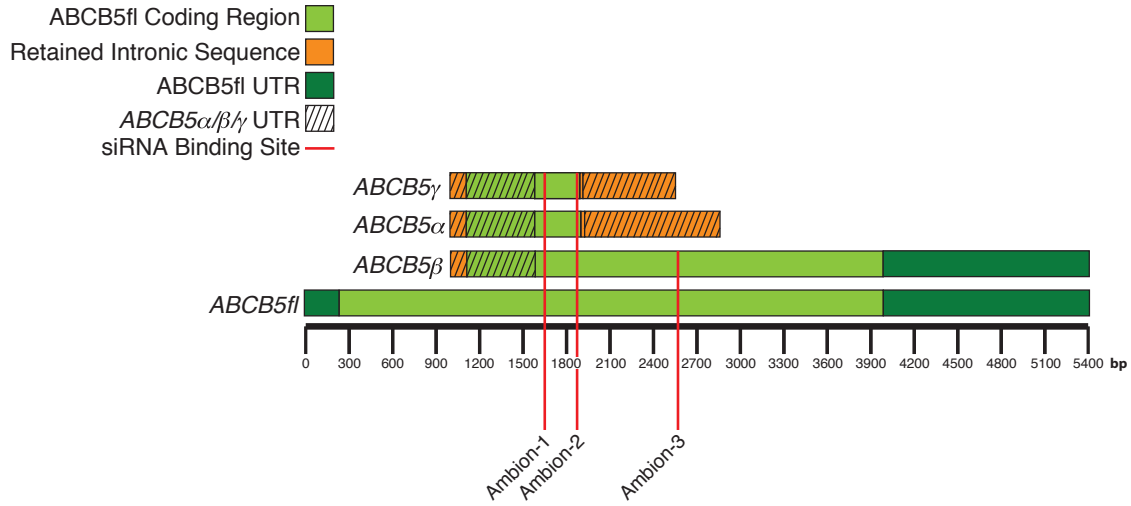

Figure 4-3. Ambion siRNA target sites within the mRNA sequence of the four ABCB5 isoforms.

Cartoon illustrating the positions of the three Ambion siRNAs within the mature mRNA of the *ABCB5* isoforms. Red lines represent siRNA binding sites.

The optimised protocol for transfecting HMECs in 384-well plates (see Section 4.2.1) was used to introduce the three siRNAs targeting *ABCB5* into the cells, both individually and as a pool (by addition of equal amounts of each individual siRNA to give a final, total concentration of 30 nM per well). A decrease in p16 intensity was observed for all three Ambion siRNAs and the pool, similar to cells which have undergone *p16* knockdown (Figure 4-4 panels A and B). Transfection with two siRNAs

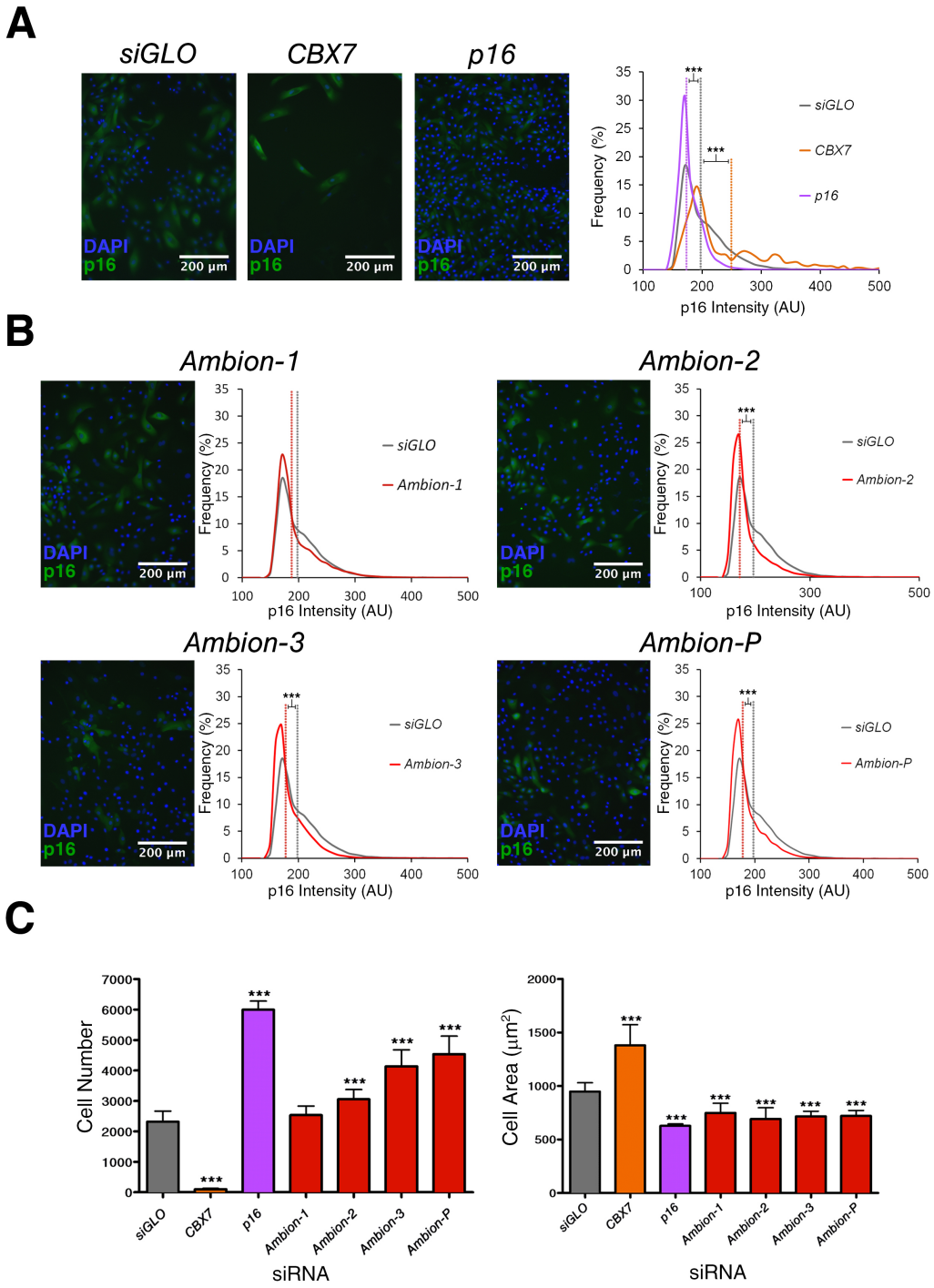

Figure 4-4. Ambion siRNAs targeting *ABCB5* reduce p16 and induce a proliferative phenotype in HMECs.

A. Control siRNAs targeting *CBX7* (orange) or *p16* (purple) increased and decreased p16 intensity (AU) respectively compared to the *siGLO* control (grey). Median p16 intensity values are shown by the dotted lines. B. Transfection with individual Ambion siRNAs (red) and the pool of all three siRNAs targeting *ABCB5* (red) reduced p16 intensity relative to the *siGLO* control. Representative images show antibody staining of p16 (green) and DAPI staining of nuclei (blue) 120 h post transfection. Median p16 intensity values (AU) are shown by the dotted lines C. An increase in cell number and decrease in cell area were observed upon transfection of all Ambion siRNAs and the pool of all three compared to the *siGLO* control. All error bars represent one SD. *** $p < 0.001$. n = 4 biological repeats.

(Ambion-2, Ambion-3) and the pool were found to cause a decrease that was statistically significant ($p < 0.001$). These siRNAs were also found to cause a significant increase in cell number ($p < 0.001$), suggesting that siRNA-mediated loss of *ABCB5* caused an increase in proliferation (Figure 4-4 panel C). Each Ambion siRNA and the pool were also found to cause a significant reduction in cellular area ($p < 0.001$).

Together, these data strongly suggest that transfection of the HMECs with siRNA targeting *ABCB5* causes reduction in cellular p16, and therefore an increase in proliferation, mirroring the findings previously reported by Bishop *et al.,* (2010). The efficacy of Ambion-3 implies that transcripts *ABCB5α* and *ABCB5γ* are irrelevant in the regulation of senescence, and that the phenotype is dependent on either the *ABCB5fl* or the *ABCB5β* transcript.

4.2.3 ABCB5 isoform expression in HMEC

To validate knockdown of *ABCB5* mRNA by the Ambion siRNAs TaqMan RT-qPCR was used (described in Section 3.2.3). First, the primer/probe sets tmABCB5 and tmABCB5flonly (Table 2-4) were used to elucidate which isoforms of *ABCB5* were expressed in the HMECs (Figure 4-5 panel A). As discussed previously, tmABCB5 will detect both ABCB5fl and ABCB5β, where as tmABCB5flonly will detect only ABCB5fl (see Section 3.2.3).

In order to test the efficacy of these primer/probe sets with very low levels of cDNA, qPCR was carried out using tmABCB5flonly and tmABCB5 on serially diluted plasmid DNA containing the cDNA sequence of ABCB5fl (pcDNA3.1-ABCB5fl-wt_EGFP; Figure 4-5 panel B) and ABCB5β (pcDNA3.1-ABCB5β-wt_EGFP; Figure 4-5 panel C). 500 ng plasmid DNA was serially diluted from 10 fold to 100,000 fold. This

experiment showed that both primer/probe sets were able to detect very low levels of DNA (cT values of 38.58 for tmABCB5flonly, and 38.11 for tmABCB5), whilst still being in the linear range.

mRNA extracted from HMECs at P6 and analysed by RT-qPCR using primer/probe set tmABCB5flonly consistently failed to detect expression of *ABCB5fl*, suggesting that HMECs do not express this isoform (Figure 4-5 panels D and E). qPCR was subsequently carried out on the same cDNA using primer/probe set tmABCB5 which can amplify both *ABCB5fl* and *ABCB5β*. qPCR using tmABCB5 demonstrated expression of ABCB5β, although at very low levels (cT = 36.92 ± 0.07) compared to GAPDH (cT = 19.13 ± 0.10).

To determine whether there is a total absence of *ABCB5fl* mRNA in the HMECs, a high cycle end point RT-PCR technique was used. cDNA generated from HMEC P6 mRNA was amplified by PCR using primer set ABCB5-EP (Table 2-3; Figure 4-5 panel A) over 50 cycles in an effort to detect low level expression. cDNA generated from HEK239T cells transfected with the pcDNA3.1-ABCB5fl-wt_EGFP vector (Table 2-2; see Section 2.10.1) acted as a positive control (Figure 4-5 panel F). PCR product was detected in cDNA prepared from the transfected HEK293T mRNA, but no *ABCB5fl* was detected in cDNA prepared from HMECs. It was therefore concluded that HMECs do not express *ABCB5fl*. However, as primer/probe set tmABCB5 successfully detected expression, it was concluded that HMECs do express *ABCB5β*.

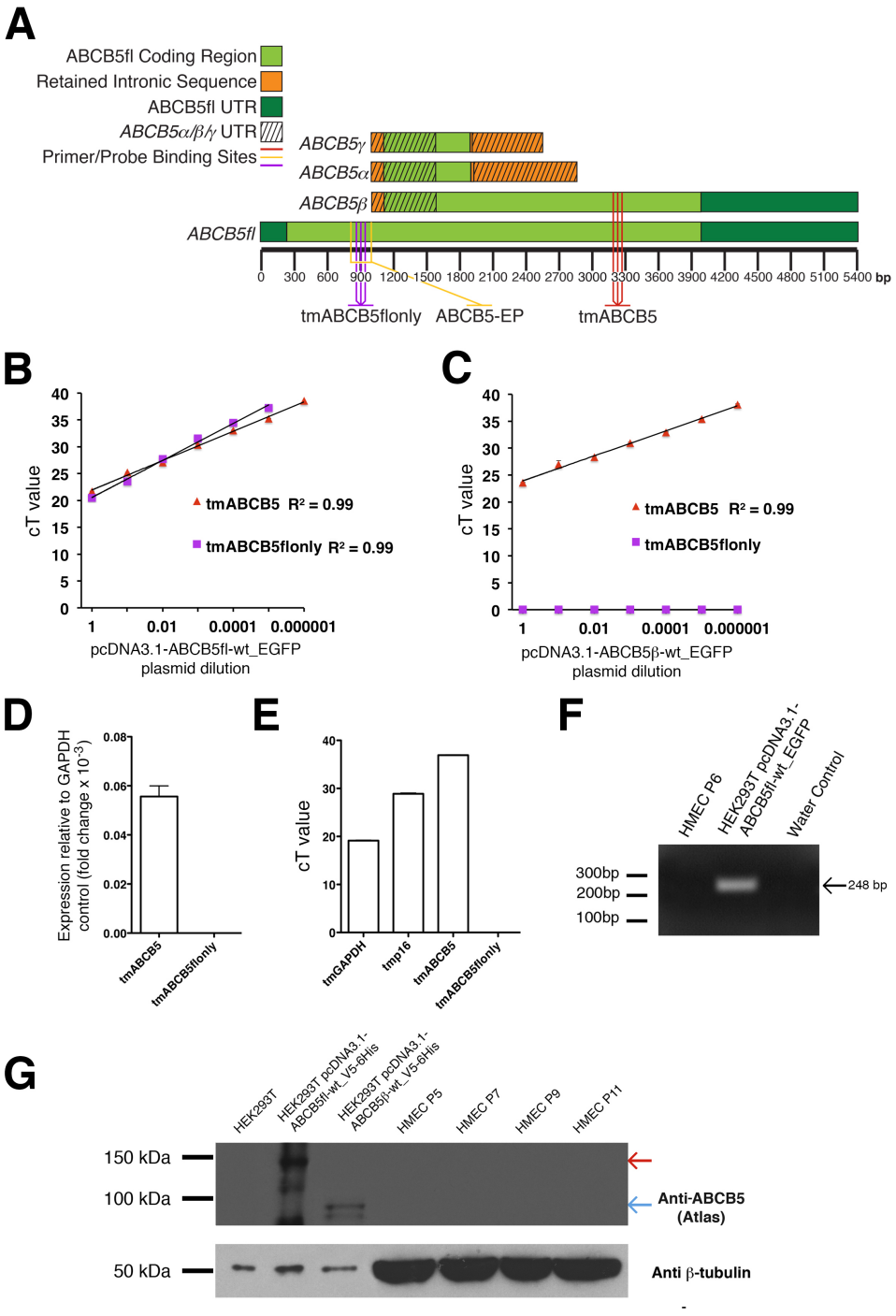

Figure 4-5. HMECs at P6 express *ABCB5β* but lack *ABCB5fl* mRNA and ABCB5 protein at all passages.

A. Cartoon illustrating the positions of the PCR primer and probe binding sites within the mature mRNAs of the ABCB5 isoforms. Binding sites of the primer set ABCB5-EP, and the primer/probe sets tmABCB5flonly and tmABCB5 are shown in yellow, purple and red, respectively. B and C. qPCR of serially diluted plasmids (500 ng plasmid DNA diluted 10 to 100,000 fold) encoding ABCB5fl (pcDNA3.1-ABCB5fl-wt_EGFP) and ABCB5β (pcDNA3.1-ABCB5β-wt_EGFP) using primer/probe sets tmABCB5 (red) and tmABCB5flonly (purple) shows detection of the appropriate sequences even at high cT values. D. qPCR of HMEC derived cDNA shows low level expression of either *ABCB5fl* or *ABCB5β*, primers specifically targeting *ABCB5fl* could not detect any expression. E. cT values from qPCR of HMEC derived cDNA show low-level expression of either *ABCB5fl*

or *ABCB5β* relative to GAPDH and p16 using tmABCB5. tmABCB5flonly specifically targeting *ABCB5fl* failed to detect any expression. F. No expression of *ABCB5fl* mRNA was observed in the HMECs but a product of the predicted size (248 bp) was amplified from the transiently transfected HEK293T positive control. G. Western blotting of lysates prepared from HMECs at P5 to P11 failed to detect either ABCB5β or ABCB5fl protein. Arrows show the predicted molecular weights of ABCB5fl (red) and ABCB5β (purple). Error bars represent one SD. n = 3 biological repeats.

In order to study ABCB5 protein levels, HMEC lysates were generated from cells at P5 to P11 (see Section 2.23). Protein levels were determined as described in Section 2.24; from each passage number, 30 μg of protein was electrophoresed on an SDS-PAGE gel, alongside 1 μg of protein taken from HEK293T cells transfected with either pcDNA3.1-ABCB5fl-wt_V5-6His or pcDNA3.1-ABCB5β-wt_V5-6His to act as positive controls, and subjected to western blotting for ABCB5 (see Section 2.25). Figure 4-5 panel G shows neither ABCB5fl nor ABCB5β protein was detected at any passage number tested, even with the high amount of protein loaded. As a result, it must be presumed that any observed effect of *ABCB5β* knockdown on p16 levels is as a result of a reduction in *ABCB5β* mRNA and not as a reduction in ABCB5β protein.

4.2.4 Validation of siRNA knockdown of *ABCB5* by RT-qPCR

It is important to validate the knockdown of *ABCB5* mRNA by the Ambion siRNAs to ensure that the proliferative phenotype is due to knockdown of *ABCB5* and not the result of off-target effects. The TaqMan primer/probe set tmABCB5 (see Section 3.2.3; Table 2-4; Figure 4-5 panel A) was therefore used for RT-qPCR analysis of siRNA transfected HMECs. The expression of *ABCB5fl* could not be detected in the HMECs used for the siRNA knockdown experiments, therefore any amplified product will reflect the abundance of the *ABCB5β* transcript.

RT-qPCR was carried out on mRNA prepared from HMECs transfected with siRNAs targeting *ABCB5, siGLO, CBX7* and *p16* in 6-well format (see Section 2.11.1.2) and normalised to GAPDH expression, as assessed using tmGAPDH. All Ambion siRNAs against *ABCB5* were found to give a significant knockdown of *ABCB5β* mRNA relative to the *siGLO* negative control ($p < 0.001$; Figure 4-6 panel A). Ambion-3 and Ambion-P gave the largest knockdown in mRNA with a respective 82% (± 3.7%) and 79% (± 1.8%) reduction. Ambion-2 produced a 52% (± 5.5%) reduction in *ABCB5β* mRNA, and Ambion-1 showed a 21% (± 6.0%) reduction.

RT-qPCR of the same mRNA using the TaqMan primer/probe set tmp16 (Table 2-4) targeting *p16* showed an 85% (± 7.5%) increase in *p16* expression following transfection with the *CBX7* siRNA ($p < 0.001$), and a 75% (± 8.3%) decrease in *p16* mRNA levels upon transfection with siRNA targeting *p16* directly ($p < 0.001$), as compared to the *siGLO* negative control (Figure 4-6 panel B). Importantly, decreases in *p16* mRNA levels were detected with transfection of Ambion-1 (8% ± 7.6% decrease), Ambion-2 (19% ± 4.6% decrease), Ambion-3 (39% ± 7.2% decrease) and Ambion-P (37% ± 3.9% decrease), with Ambion-2, Ambion-3 and Ambion-P all giving significant decrease ($p < 0.001$), suggesting that the effect of *ABCB5β* knockdown is upstream of *p16* mRNA generation.

When both the phenotypic analysis and validation results of the *ABCB5* knockdown are taken together, they show that the *ABCB5* targeting siRNAs, which cause a significant knockdown of *ABCB5* mRNA ($p < 0.001$), also cause a significant decrease in p16 intensity, *p16* mRNA levels and cell area, and a significant increase in cell number.

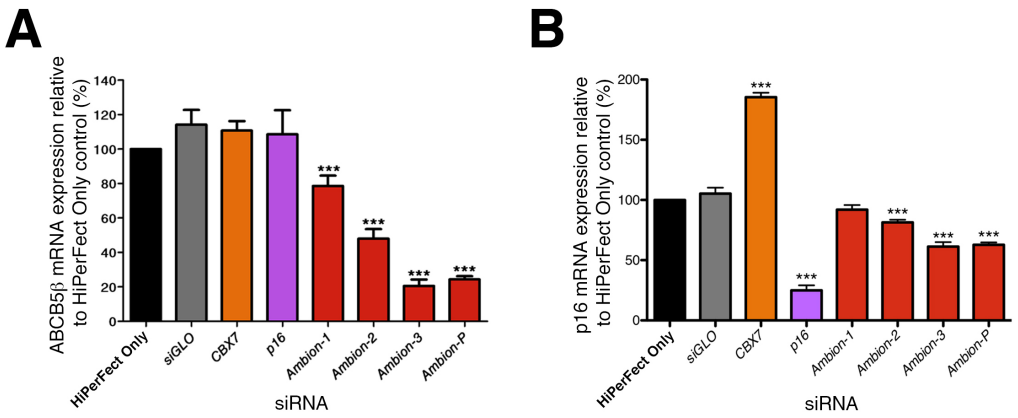

Figure 4-6. Knockdown of *ABCB5β* mRNA by Ambion siRNAs in HMECs.

A. qPCR carried out using the tmABCB5 primer pair on cDNA generated from HMEC mRNA isolated 48 h post transfection shows all Ambion siRNAs (red) generated a significant reduction in *ABCB5β* message following transfection. Error bars represent one SD. *** $p < 0.001$. B. qPCR carried out using tmp16 shows a significant reduction in *p16* mRNA following transfection with Ambion-2, Ambion-3 and Ambion-P. n = 3 biological repeats.

With qPCR and PCR data suggesting that HMECs do not express the full-length isoform of *ABCB5*, and with only siRNA Ambion-1 targeting the alpha and gamma isoforms, knockdown of *ABCB5β* is likely responsible for the p16 reduction phenotype. If either the alpha or gamma isoforms were responsible, only siRNA Ambion-1 would be predicted to produce a p16 reduction phenotype in the HMECs.

With the knockdown of *ABCB5β* by multiple, different siRNAs mirroring the level of phenotypic changes observed in the cells, it is highly likely that the phenotype is due to *ABCB5β* knockdown, and not due to off-target effects of the siRNA transfection. Additionally, as no change was seen in the levels of *ABCB5β* mRNA upon transfection with siRNAs targeting either *CBX7* or *p16*, a reciprocal effect of p16 acting on *ABCB5β* is unlikely, indicating that the effect on p16 and cell cycle control is downstream of *ABCB5β*.

4.2.5 Targeting the *ABCB5β* mRNA with specific siRNA

4.2.5.1 Generating siRNAs that target the *ABCB5β* isoform but not *ABCB5fl*

One of the aims of this investigation was to determine which isoform of *ABCB5* was responsible for the effect on p16. The siRNAs and RT-qPCR experiments above implicate *ABCB5β* as the relevant transcript. In an attempt to confirm this, siRNAs that specifically target *ABCB5β* but not ABCB5fl were designed.

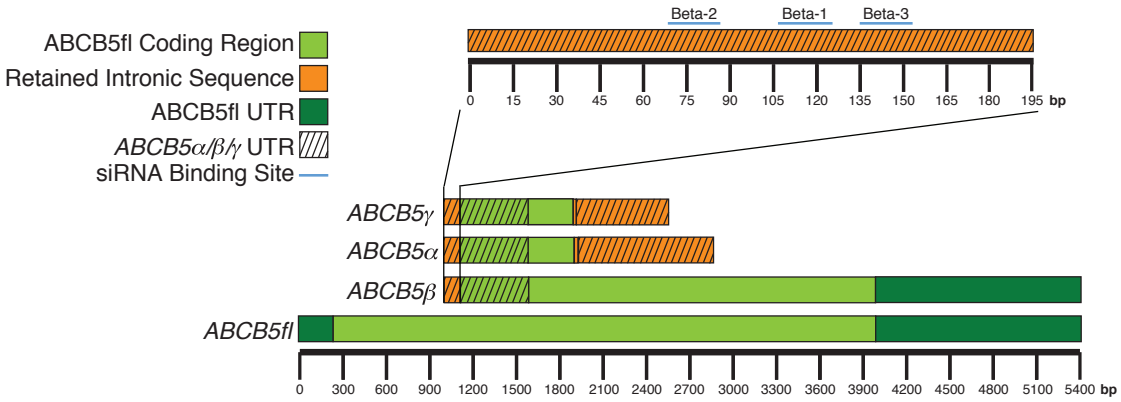

Figure 4-7. *ABCB5β*-specific siRNA target sites within the *ABCB5* mRNA sequence.

A cartoon illustrating the positions of the siRNAs targeting *ABCB5β* within the mature mRNA of the ABCB5 isoforms. Blue lines represent siRNA binding sites for Beta-1, Beta-2 and Beta-3.

ABCB5β is reported to include a short but unique 5'-UTR that is absent from the full-length transcript. siRNAs targeting the 5'-UTR of *ABCB5β* were custom made by submitting the 5'-UTR sequence to the GeneAssist™ Custom siRNA Builder[I] (Life Technologies, UK; Table 2-2). The siRNAs (Beta-1, Beta-2 and Beta-3) – designated set one – were designed to target a 197-nucleotide retained-intronic section of the

[I] Available at http://www5.invitrogen.com/custom-genomic-products/tools/sirna/

ABCB5β mRNA 5'-UTR (Appendix I; Figure 4-7). These siRNAs should target *ABCB5β* without targeting *ABCB5fl*. The siRNAs would also target both the *ABCB5α* and *ABCB5γ* isoforms, but these have previously been shown to be irrelevant to the p16 phenotype (see Section 4.2.2).

4.2.5.2 Transfection of HMECs with *ABCB5β* siRNA set one

In an attempt to knockdown *ABCB5β* specifically, the set one siRNAs designed to target the isoform were transfected into HMECs (see Section 4.2.5.1). Beta-1, Beta-2 and Beta-3 and a pool of all three siRNAs (Beta-P1) were transfected into HMECs at P6 alongside the three control siRNAs, as described previously.

CBX7 and *p16* control siRNAs significantly changed p16 intensity following transfection into the HMECs, compared to the siGLO control, as described previously ($p < 0.001$; Figure 4-8 panel A). Very slight variations in p16 intensity were observed in cells transfected with Beta-1, Beta-2, Beta-3 and the Beta-pool, however, none of these were found to be significant (Figure 4-8 panel B). Furthermore, no significant phenotypic changes in cell number or cell area were apparent after transfection with any of the *ABCB5β* siRNAs targeting the 5'-UTR (Figure 4-8 panel C). Together, the data report no significant changes in cell phenotype when the cells are transfected with any of the set one siRNAs designed to specifically target *ABCB5β*.

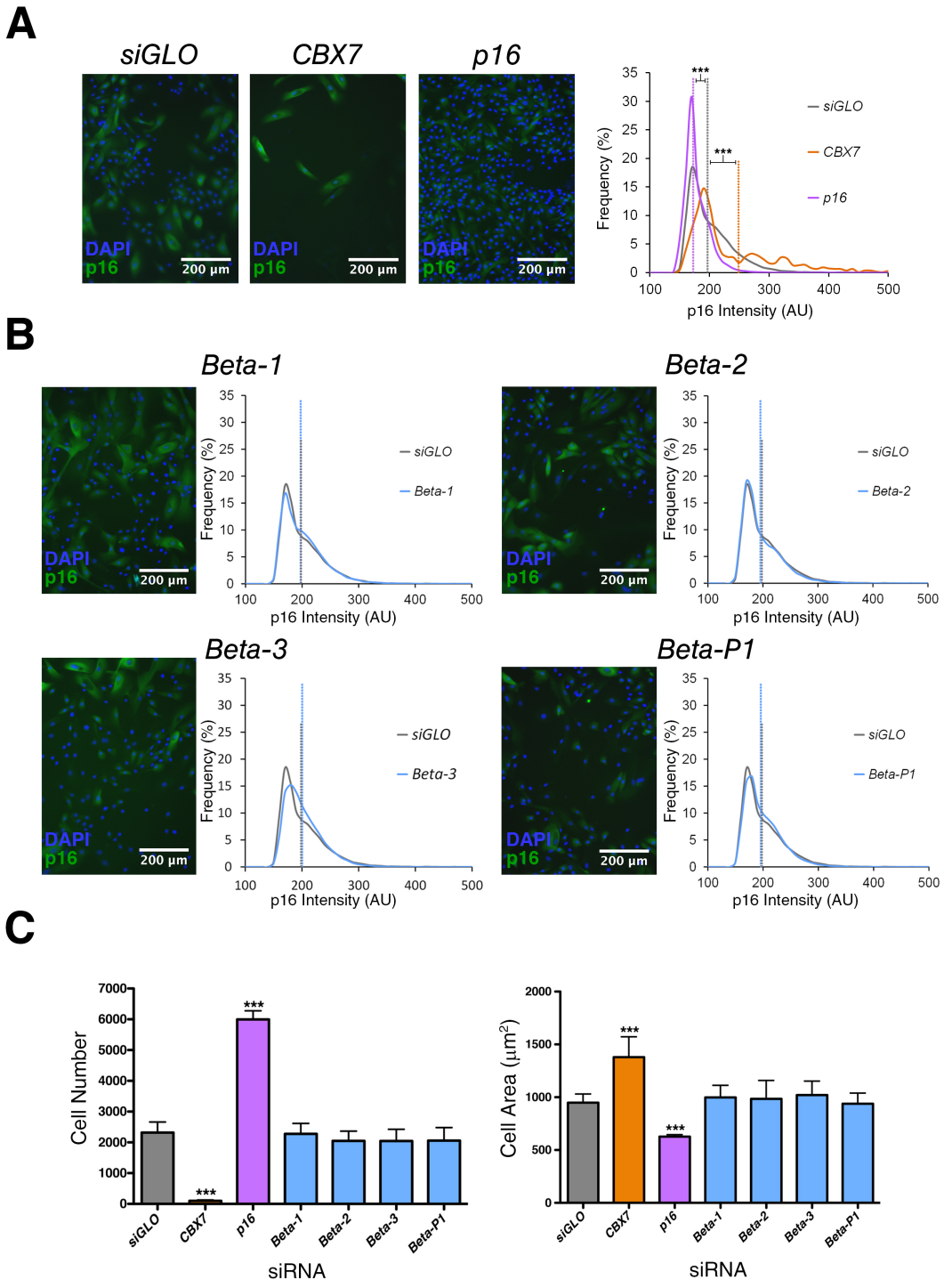

Figure 4-8. *ABCB5β*-targeted siRNAs show no p16 reduction phenotype in HMECs.

A. Control siRNAs targeting *CBX7* (orange) or *p16* (purple) show an increase in p16 intensity and a reduction in p16 intensity, respectively when compared to the *siGLO* control (grey). Median p16 intensity values (AU) are shown by the dotted lines. B. Transfection with set one siRNAs targeting the 5'-UTR of *ABCB5β* (blue) showed no significant change in p16 intensity compared to *siGLO* control (grey). Representative images show antibody staining of p16 (green) and DAPI staining of nuclei (blue) 120 h post transfection. C. No change in cell number or cell area was observed in cells transfected with siRNAs targeting the 5'-UTR of *ABCB5β* at 120 h time point. All error bars represent one SD. *** $p < 0.001$. n = 4 biological repeats.

4.2.5.3 RT-qPCR quantitation of *ABCB5β* knockdown by Beta-1, Beta-2 and Beta-3

To assess whether the beta isoform-specific siRNAs knocked down *ABCB5β* mRNA, cDNA generated from the transfected HMECs was analysed by qPCR as before (Figure 4-9 panel A), by normalising *ABCB5β* levels to GAPDH. None of the three siRNAs, or the Beta pool, caused a significant knockdown of the *ABCB5β* mRNA, consistent with the lack of phenotypic change in cell proliferation, cell morphology and p16 abundance.

When the expression of p16 was evaluated in the same samples by qPCR, the control siRNAs targeting *CBX7* and *p16* caused a significant increase and decrease in levels of mRNA, respectively ($p < 0.001$; Figure 4-9 panel B). None of the siRNAs targeting *ABCB5β* caused any significant change in the levels of p16 expression, as predicted given the lack of efficacy in their ability to knockdown *ABCB5β*.

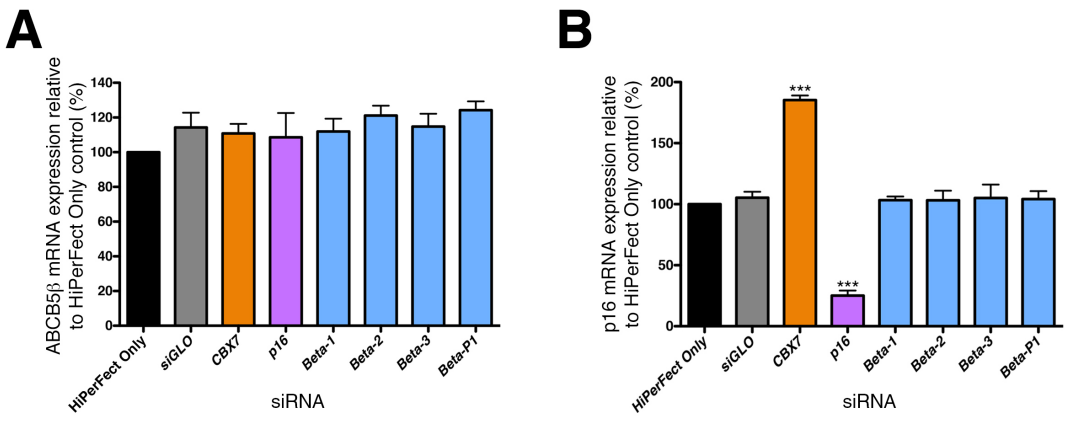

Figure 4-9. Knockdown of *ABCB5β* by siRNAs in HMECs.

A. qPCR carried out using tmABCB5 on cDNA generated from HMEC mRNA isolated 48 h post transfection showed no significant change with any control siRNAs; *siGLO* (grey), *CBX7* (orange) and *p16* (purple). All three siRNAs targeted to *ABCB5β* (blue), and the pool, also showed no significant reduction in *ABCB5β* message. B. qPCR carried out using tmp16 also shows no significant change in levels of p16 mRNA following transfection with any siRNAs targeting *ABCB5β*. Error bars represent one SD. *** $p < 0.001$. n = 3 biological repeats.

4.2.5.4 Transfection of HMEC with ABCB5β 5'-UTR-specific siRNAs Beta-4, Beta-5 and Beta-6

Due to the lack of efficacy of the first three ABCB5β 5'-UTR-specific siRNAs, a further set targeting *ABCB5β* were generated (Beta-4, Beta-5, Beta-6 and the pool of all three, Beta-P2; designated set two; Figure 4-10). These siRNAs, targeting different sequences within the short 5'-UTR of the *ABCB5β* transcript, were transfected into the HMECs, but again no significant changes were seen for p16 intensity or cell area (Figure 4-11). Unexpectedly, siRNA Beta-5 did, however, cause a small but significant reduction in cell number ($p < 0.01$). This siRNA only affected cell number and not cell area or p16 intensity, and as a consequence, the effect on cell number is most likely due to an off-target effect, causing cell death and not cellular senescence.

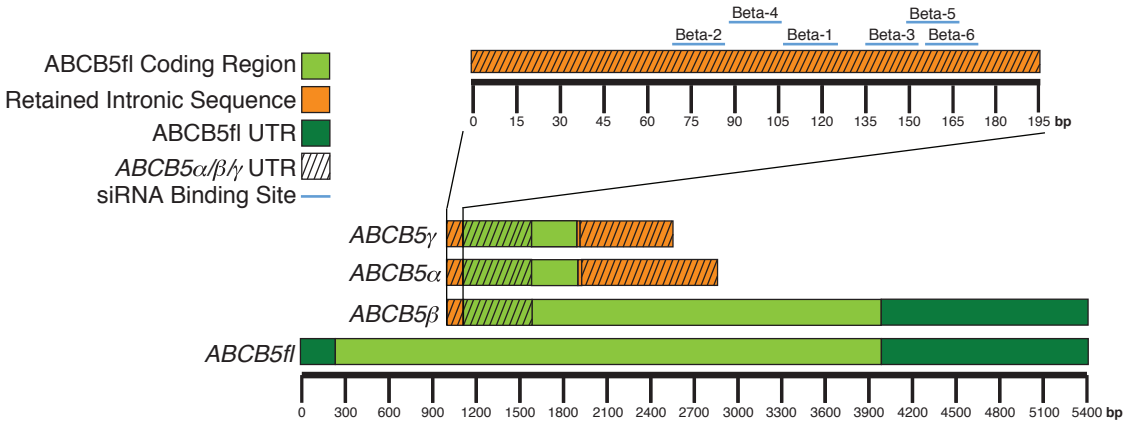

Figure 4-10. Additional *ABCB5β* specific siRNA target sites within the *ABCB5* mRNA sequence.

A cartoon illustrating the positions of the siRNAs targeting *ABCB5β* within the mature mRNA of the *ABCB5* isoforms. Blue lines represent siRNA binding sites.

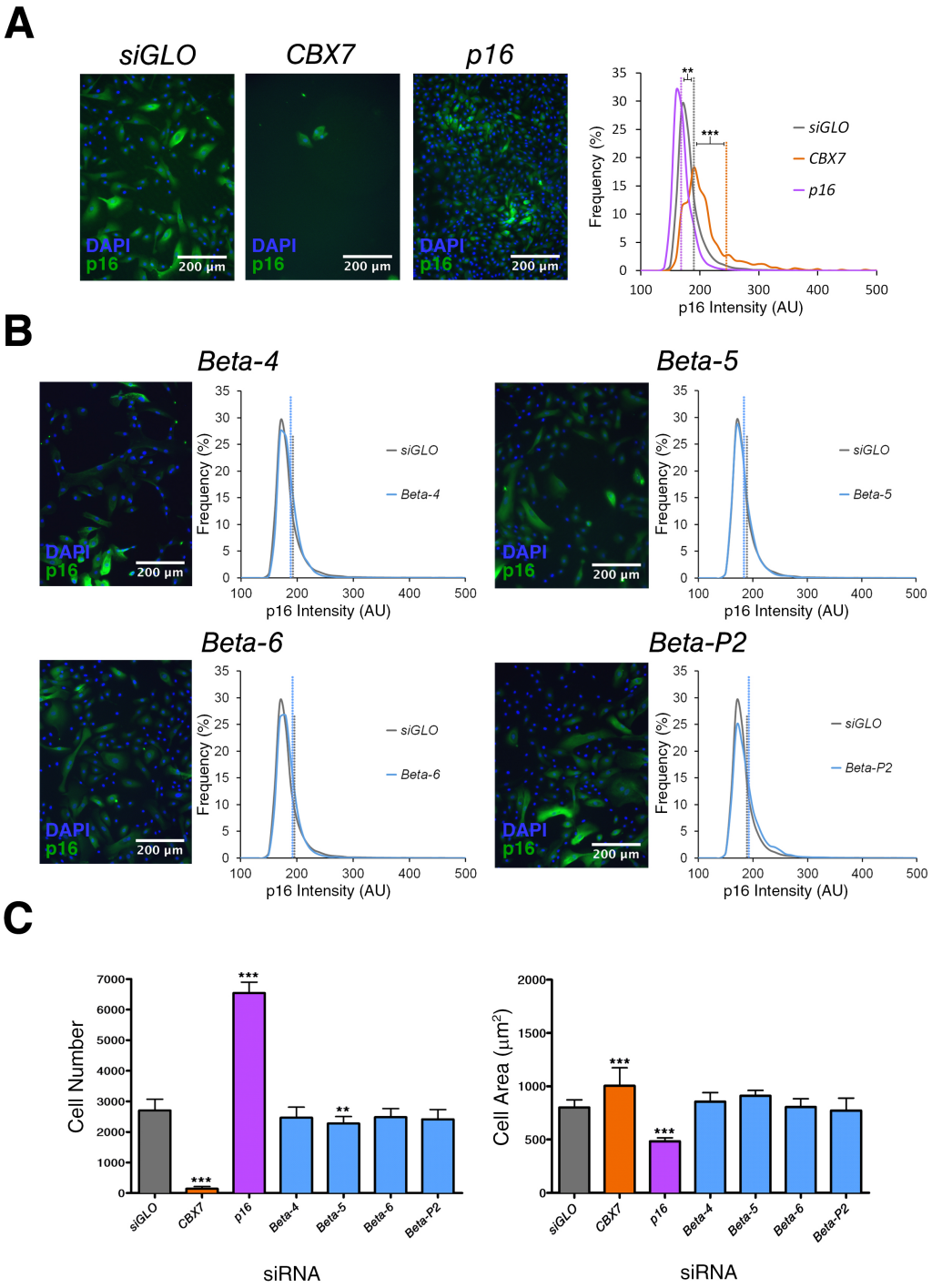

Figure 4-11. siRNAs Beta-4, 5, 6 or Beta-P2 targeting *ABCB5β* show no p16 reduction phenotype in HMEC.

A. Control siRNAs targeting *CBX7* (orange) or *p16* (purple) show an increase in p16 intensity and a reduction in p16 intensity, respectively when compared to the *siGLO* control (grey). Median p16 intensity values (AU) are shown by the dotted lines. B. Transfection with siRNAs targeting the *ABCB5β* 5'-UTR (blue) showed no significant change in p16 intensity with compared to the siGLO control (grey). Representative images show antibody staining of p16 (green) and DAPI staining of nuclei (blue) 120 h post transfection. C. No significant change in cell number or cell area was observed in cells transfected with siRNAs targeting *ABCB5β*, apart from a small but statistically significant reduction in cell number with *Beta-5*. All error bars represent one SD. * $p < 0.05$, ** $p < 0.01$, *** $p < 0.001$. n = 3 biological repeats.

4.2.5.5 Test of ABCB5β 5'-UTR-specific siRNAs Beta-4, Beta-5 and Beta-6 efficacy by RT-qPCR

The failure of siRNAs Beta-4, Beta-5, Beta-6 or Beta-P2 to induce a p16-reduction phenotype in the cells prompted experiments to validate knockdown of *ABCB5β* at the mRNA level. qPCR was performed using the tmABCB5 primers on cDNA prepared

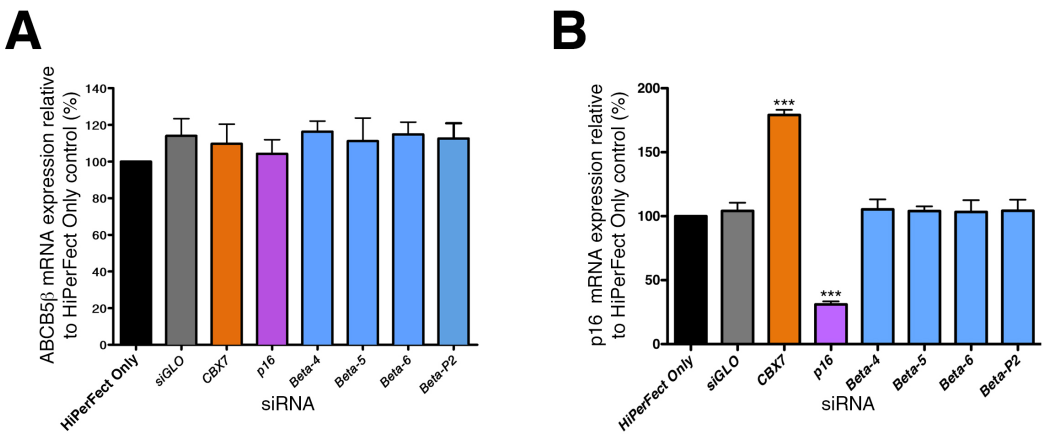

Figure 4-12. Further knockdown of *ABCB5β* by siRNAs in HMECs.

A. qPCR carried out using tmABCB5 on cDNA generated from HMECs transfected with the control siRNAs *siGLO* (grey), *CBX7* (orange) and *p16* (purple) showed no significant change in *ABCB5β* mRNA levels. siRNAs Beta-4, Beta-5 and Beta-6 targeting the *ABCB5β* 5'-UTR (blue), and the pooled siRNA Beta-P2, also caused no significant reduction in *ABCB5β* mRNA. Error bars represent one SD. B. qPCR carried out using tmp16 showed no significant change in p16 mRNA following transfection with any siRNAs targeting *ABCB5β*. *** $p < 0.001$. n = 3 biological repeats.

from HMECs as described previously (Figure 4-12 panel A), and normalised to GAPDH expression levels. The results show that these further siRNAs had no effect on the endogenous *ABCB5β* mRNA, explaining the lack of proliferative phenotype observed after transfection. Additionally, levels of *p16* mRNA assessed by RT-qPCR using the tmp16 primer/probe set also showed no significant change upon transfection with any of the siRNAs targeting the 5'-UTR of *ABCB5β* (Figure 4-12 panel B).

4.2.6 Sequencing the *ABCB5β* 5'-UTR endogenous to HMECs

Due to the lack of efficacy of all six siRNAs targeting the *ABCB5β* 5'-UTR, it was hypothesised that the NCBI consensus sequence (NM_178559.5), used to design the siRNAs, could be different to the sequence found in HMECs. To investigate this, the 5'-UTR of *ABCB5β* in HMECs was sequenced from cDNA amplified using a 5' Rapid Amplification of cDNA Ends (RACE) PCR (Figure 4-13; see Section 2.18).

RACE PCR is a technique employed to amplify a nucleic acid sequence from a mRNA template between a defined internal site and an unknown sequence at either the 3' or the 5'-end of the mRNA (Frohman et al., 1988). Normally, PCR amplification requires two sequence-specific primers that flank the region to be amplified; not knowing the sequence of one end of the region provides a severe limitation (Loh et al., 1989). 3' and 5' RACE approaches can solve this problem.

5' RACE allows the isolation and characterisation of 5'-ends from low-copy messages and was carried out as follows. First strand cDNA synthesis was primed using a gene-specific antisense oligonucleotide (GSP1), which allowed the conversion of a specific mRNA to cDNA, and maximised potential for complete extension to the 5'-end of the message. After the cDNA was synthesised, the product was purified from unincorporated dNTPs and GSP1, and treated with terminal deoxynucleotidyl transferase (TdT), which added a homopolymeric tail to the 3'-ends of the cDNA.

Amplification of the target sequence was then carried out using a nested gene-specific primer (GSP2), which anneals 3' to GSP1, and a complementary homopolymer-

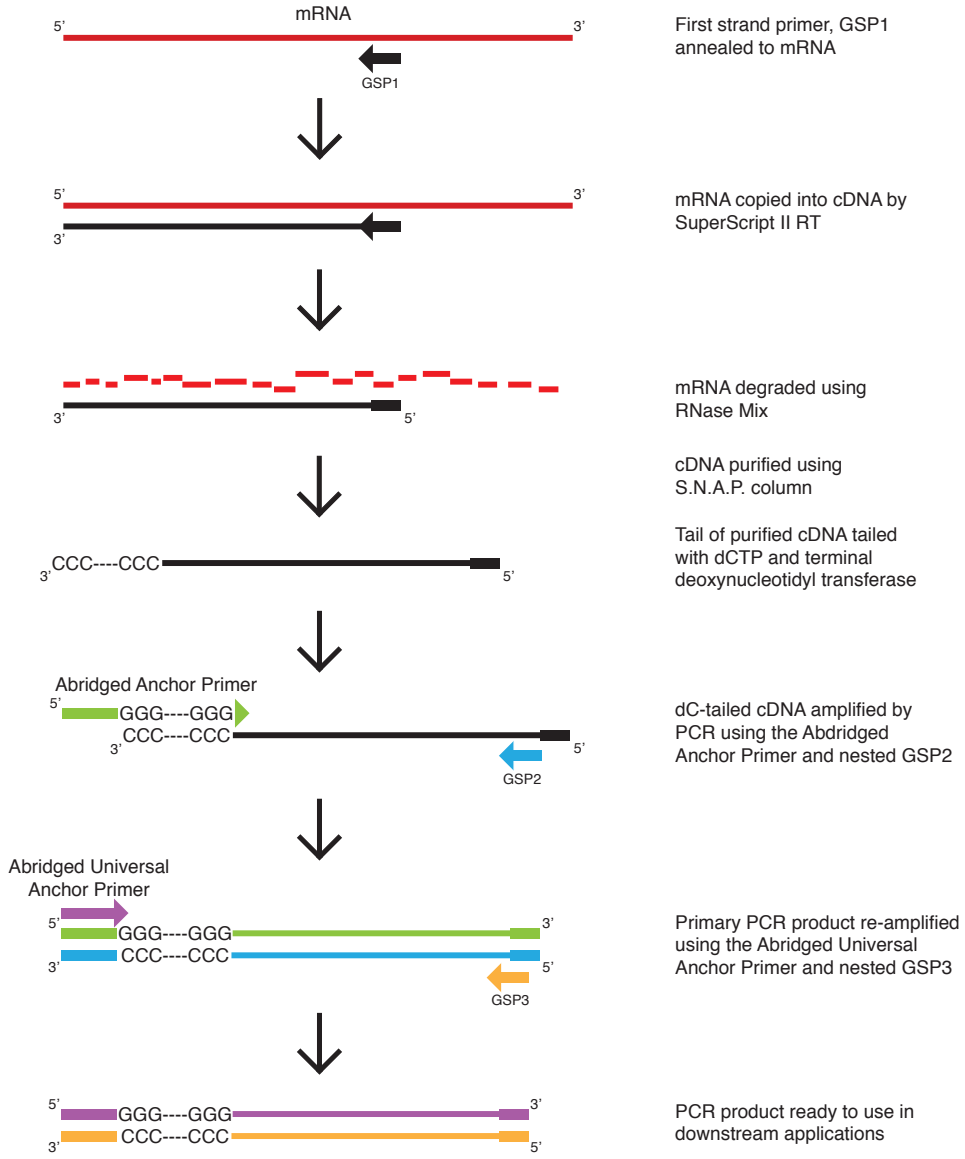

Figure 4-13. Overview of 5' RACE procedure.

mRNA isolated from cells is reverse-transcribed to cDNA using a gene-specific primer (GSP1) and SuperScript II. The mRNA is degraded using RNase and the remaining cDNA is purified using a S.N.A.P. column. Purified cDNA is tailed with dCTP by the activity of terminal deoxynucleotidyl transferase. The resulting dC-tailed cDNA is amplified by PCR using the Abridged Anchor Primer (AAP) – which binds to the dC-tail – and another gene specific primer (GSP2), nested from the location of GSP1. The PCR product is then re-amplified using the Abridged Universal Anchor Primer – which binds to the anchor site created by the AAP – and another nested gene-specific primer (GSP3).

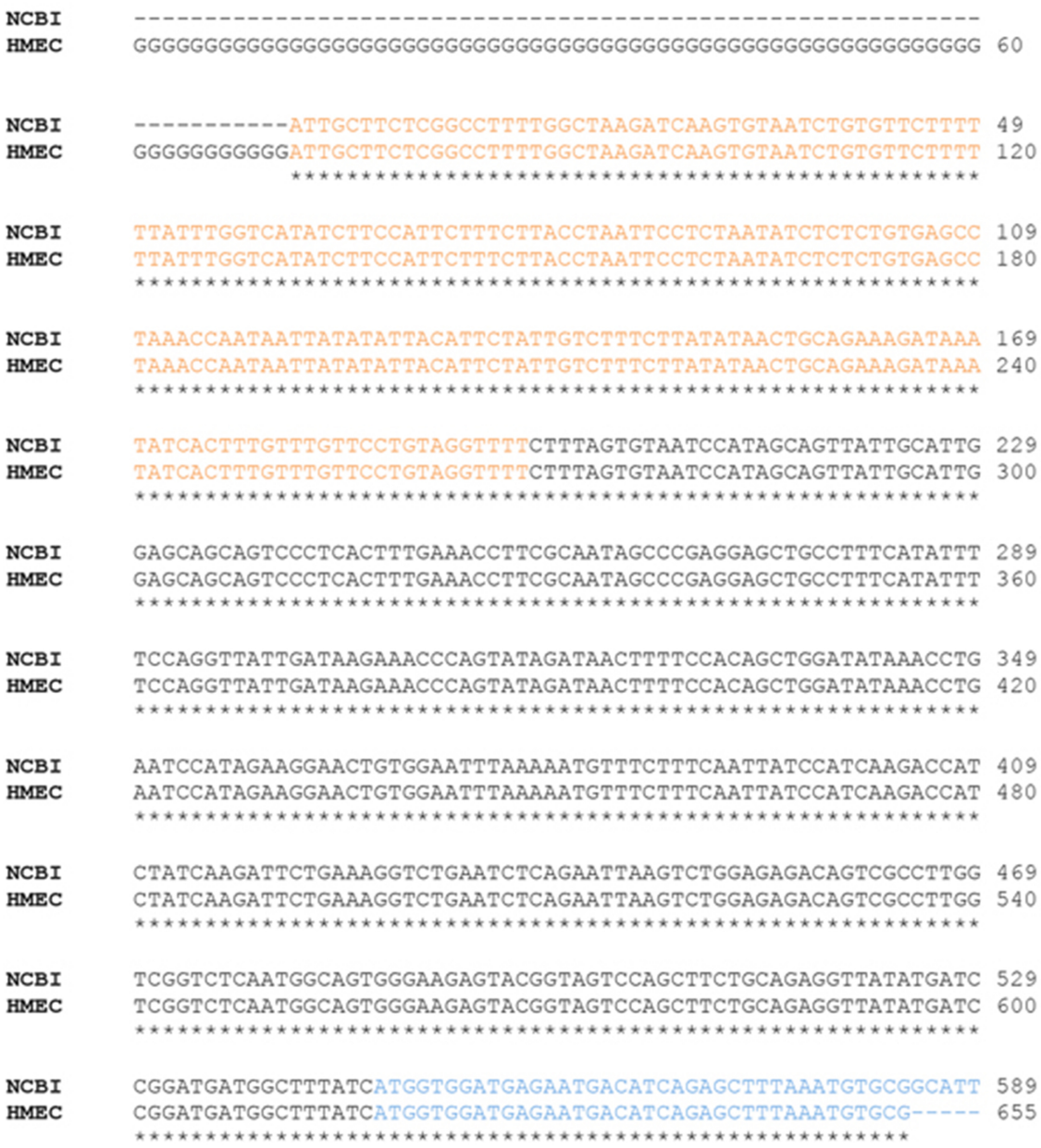
NCBI ----------
HMEC GGGG

containing anchor primer, which allowed amplification of the homopolymeric cDNA tail. This permitted amplification of the unknown sequence between the GSP2 and the 5'-end of the mRNA. After an additional nested PCR, the product was sequenced directly (Innis et al., 1990).

The sequenced 5'-UTR of *ABCB5β* was aligned against the NCBI consensus sequence using ClustalW2 (Figure 4-14). No differences between the two sequences were found, confirming the expression of the *ABCB5β* isoform in HMECs and the veracity of the published sequence. The lack of knockdown by the specific *ABCB5β*-targeting siRNAs was, therefore, not due to incorrect sequence targeting, but possibly due to steric hindrance at the target site due to mRNA secondary structure or bound proteins.

4.2.7 Prediction of *ABCB5β* 5'-UTR secondary structure

Sequencing of the *ABCB5β* 5'-UTR did not show any differences between the NCBI consensus sequence and the endogenous message in HMECs, therefore it was hypothesised that the binding sites for the six *ABCB5β* targeting siRNAs may be inaccessible in stable RNA secondary structures. This could prevent the binding of siRISC and the subsequent degradation of target mRNA (Luo and Chang, 2004, Overhoff et al., 2005, Schubert et al., 2005).

In an attempt to test this hypothesis the secondary structure of the 5' end of the *ABCB5β* message was modelled using the mfold web server[I] (Zuker, 2003). The mRNA sequence was submitted to the web server in 500-nucleotide sections covering the

[I] The mfold web server can be found at: http://mfold.rna.albany.edu/?q=mfold/rna-folding-form

binding sites of siRNAs Beta-1 to Beta-6 (Bases 1 – 500), Ambion-1 and Ambion-2 (1601 – 2100), and Ambion-3 (2501 – 3000; see Appendix III). The binding sites for the Ambion siRNAs (which knocked down the mRNA) were included as a comparison for the Beta siRNAs (which failed to knockdown the message).

The mRNA folding software predicted that the 5'-UTR containing the binding sites for siRNAs Beta-1 to Beta-6 contains a highly structured mix of stem, hairpin and loop sections (Figure 4-15 panel A). The binding sites for siRNAs Beta-1 to 6 are mostly in energetically stable stem and hairpin structures, although Beta-2 targets a relatively open conformation. mRNA secondary structure has previously been reported to hinder siRISC binding, however, the secondary structure predicted for the target sequences of Ambion-1, Ambion-2 and Ambion-3 are not dissimilar (Figure 4-15 panels B, C and D).

The similarities between the secondary structure in these regions, but the differences in the knockdown produced by the siRNAs targeting them, suggests that either the predicted conformations are not physiologically relevant, or that they have little effect on siRNA binding. If the predicted secondary structures generated here are accurate and did predict siRNA-binding efficiency, it would be probable that the Ambion siRNAs would also have failed to knockdown *ABCB5β* mRNA in the cells.

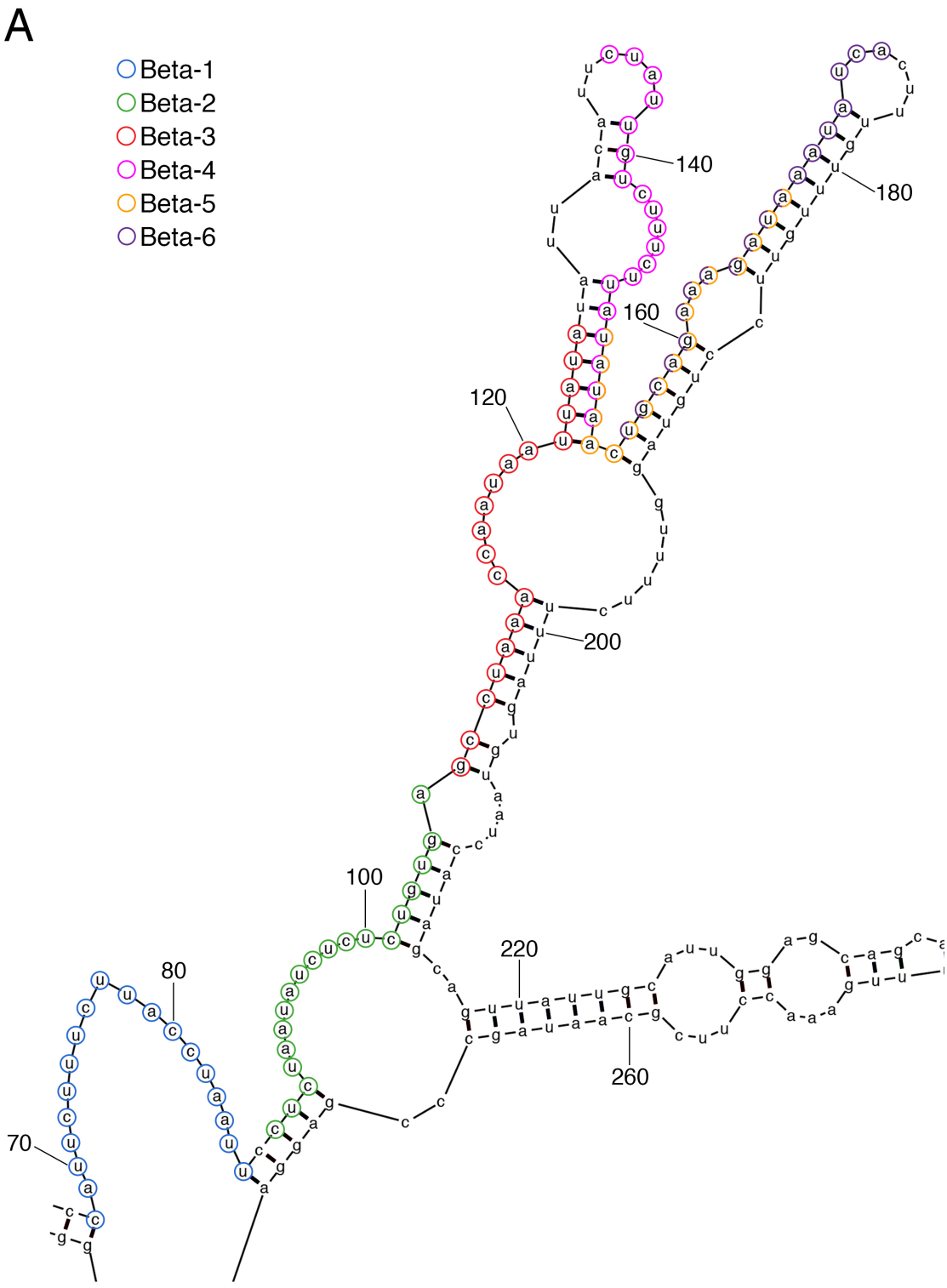

Figure 4-15. Predicted mRNA secondary structure in regions targeted by the siRNAs used in the investigation.

mRNA secondary structure was predicted by uploading 500 nt sections of the *ABCB5β* mRNA to the mfold web server (Zuker, 2003). siRNA binding sites are represented by coloured dots. Numbers indicate every 20 nucleotides. A. The binding sites of siRNAs Beta-1 to Beta-6. Circles with half colours represent bases targeted by two different siRNAs.

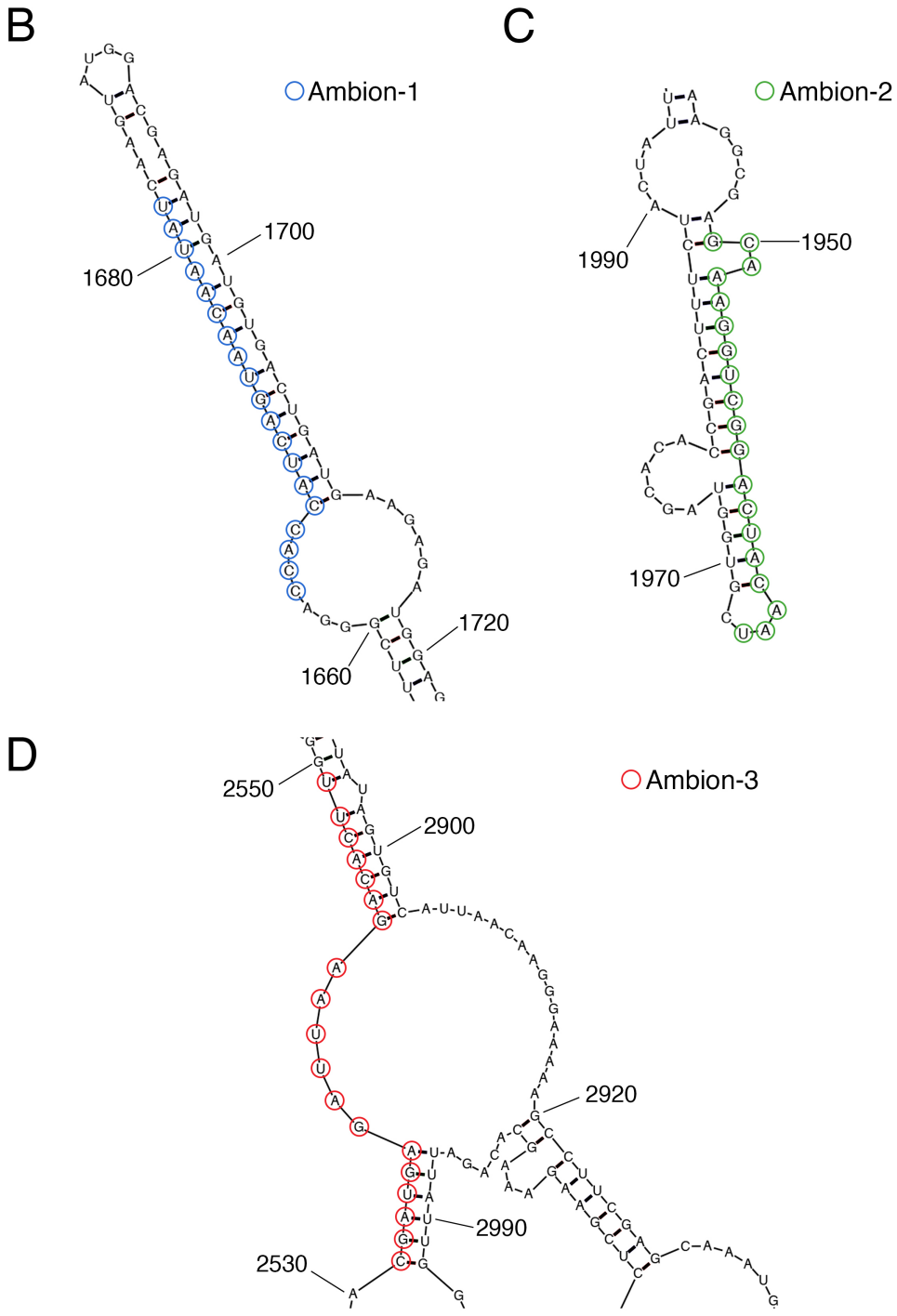

Figure 4-17. (Continued) Predicted mRNA secondary structure in regions targeted by siRNAs used in the investigation.

mRNA secondary structure was predicted by uploading 500 nt sections of the *ABCB5β* mRNA to the mfold web server (Zuker, 2003). siRNA binding sites are represented by coloured dots. Numbers indicate every 20 nucleotides. B-D. The binding sites of siRNAs Ambion-1 (B), Ambion-2 (C) and Ambion-3 (D).

4.2.8 *ABCB5β* and *p16* expression in HMEC with increasing passage

To further investigate the relationship between the expression of *p16* and *ABCB5β* in HMECs, the relative abundance of each of the transcripts was assessed by RT-qPCR of mRNA isolated from early (P5) to late (P10) passage cells (Figure 4-16).

Data for the expression of both *p16* (using primer/probe set tmp16; Table 2-4) and *ABCB5β* (tmABCB5) show a step-wise increase in mRNA expression with increasing passage number. The expression of *ABCB5β* is significantly increased at P8 ($p < 0.05$) compared to P5, and its expression at P10 is 2.1 (± 0.2; $p < 0.001$) fold higher than P5. The expression of *p16* increases with passage in HMECs as has been previously reported (Garbe et al., 2009), with the increase in expression becoming significant at P7 ($p < 0.001$). At P10 the expression of *p16* is 1.7 (± 0.1; $p < 0.001$) fold higher than at

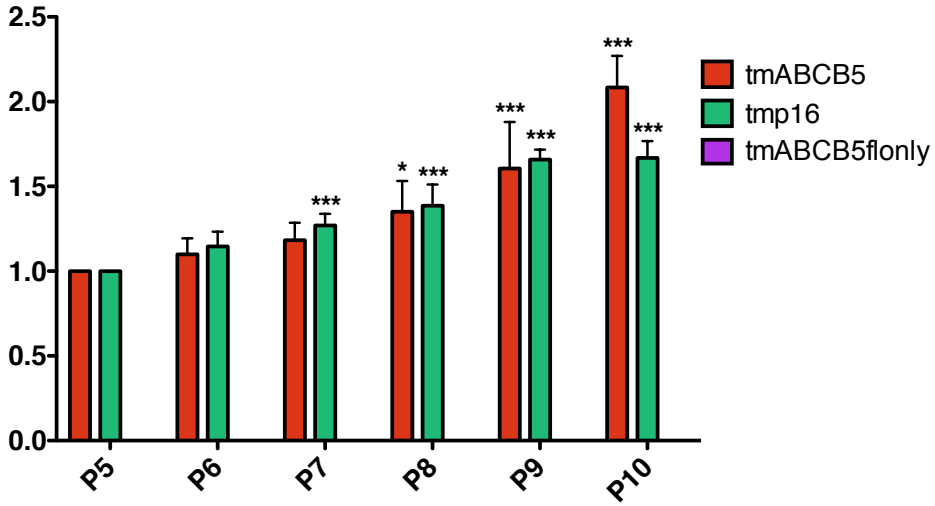

Figure 4-16. RT-qPCR analysis of *p16* and *ABCB5* expression in HMECs with passage.

mRNA was subjected to RT-qPCR analysis and normalised to a GAPDH housekeeping control. Results show significant increases in both the expression of *p16* (using primer/probe set tmp16) and *ABCB5* (using primer probe set tmABCB5) with increasing passage number compared to their expression at passage 5 (P5). ABCB5fl expression could not be detected using primer/probe set tmABCB5flonly at any passage number. Error bars represent one SD. * $p < 0.05$; ** $p < 0.01$; *** $p < 0.001$. n = 3 biological repeats.

P5. As previously noted in this study (see Section 4.2.3), the expression of *ABCB5fl* could not be detected at any passage number tested.

All data concerning expression of *ABCB5β* and *p16* show that both increase with passage. It is possible that this is due to an effect of one on the other, and in light of the data discussed here it could be due to a downstream effect of *ABCB5β* mRNA on *p16*.

4.3 Discussion

4.3.1 Summary of the findings

HMECs were chosen as the model cell type in which to study the effect ABCB5 knockdown on p16, as they undergo a well characterised p16-mediated senescence response in cell culture (Brenner et al., 1998, Garbe et al., 2009), making them an ideal system to study p16 and senescence *in vitro* (see Section 4.2.1.1). The cells were optimised for transfection with 30 nM siRNA, by finding both the optimum seeding density (10,000 cm^{-2}; see Appendix II) and optimum volume of transfection reagent per well (0.25 μL $well^{-1}$), to provide the greatest target gene knockdown, with the lowest toxicity possible.

Control siRNAs targeting *CBX7* and *p16* were tested as positive controls for modulation of senescence. siRNA targeting *CBX7* was found to cause a significant increase in p16 intensity and cell area, with a significant decrease in cell number making *CBX7* siRNA a robust positive control for increase in *p16* expression and cellular senescence. The *p16* targeting siRNA was found to cause significant decreases in p16 intensity and cell area,

and a significant increase in cell number establishing direct knockdown of *p16* as an effective positive control for a reduction in cellular p16.

Three siRNAs (Ambion-1, Ambion-2 and Ambion-3) and their pool (Ambion-P) that target *ABCB5* were then used to determine the effect of loss of ABCB5 in HMECs (see Section 4.2.2.2). All three siRNAs and the pool decreased p16 intensity and caused a statistically significant reduction in cell area. Ambion-2, Ambion-3 and Ambion-P caused a significant, concomitant increase in cell number.

RT-qPCR using two TaqMan primer/probe sets, one targeting *ABCB5fl* only (tmABCB5flonly), and the other targeting both *ABCB5fl* and *ABCB5β* (tmABCB5; see Section 4.2.3), and high-cycle endpoint RT-PCR using the primer set ABCB5-EP established that HMECs lack detectable levels of *ABCB5fl* expression but must express *ABCB5β*. siRNA knockdown was validated using the tmABCB5 primer/probe set to amplify *ABCB5β* in all subsequent experiments (see Section 4.2.4). All three Ambion siRNAs targeting *ABCB5* significantly knocked down *ABCB5β* mRNA, compared to the negative control. Ambion-3 and Ambion-P gave the largest knockdown of the target mRNA. No changes in the levels of *ABCB5β* were observed upon transfection of the cells with siRNAs targeting *CBX7* or *p16*. The *p16* mRNA level was reduced following transfection with all Ambion siRNAs and the pool, with Ambion-2, Ambion-3 and Ambion-P generating a statistically significant decrease. Together these data strongly suggest that knockdown of *ABCB5β* is causative in the reduction of p16 observed in transfected HMECs.

Western blotting showed that neither ABCB5fl (as expected) nor ABCB5β were detectable at the mid to late passages numbers tested even with heavily overloaded samples. While it is impossible to rule out a role for ABCB5 protein, expression that is below the detectable threshold suggests that it is unlikely ABCB5 acts at the protein level to influence proliferative phenotype and regulation of p16.

These experiments implicate *ABCB5β* as the relevant transcript in the regulation of p16. siRNAs were therefore designed to specifically target *ABCB5β,* utilising the 5'-UTR of the transcript that is not present in *ABCB5fl* (see Section 4.2.5.1). None of the six *ABCB5β*-specific siRNAs, or their respective pools caused significant changes in p16 intensity, cell size or cell number. Neither was there any significant change in the level of *ABCB5β* mRNA, strongly suggesting that these siRNAs did not knockdown their intended target. The 5'-UTR of *ABCB5β* in HMECs was therefore amplified by 5' RACE PCR, and sequenced. The sequence was identical to the NCBI consensus sequence, ruling out the possibility that the published sequence used to design the *ABCB5β* specific siRNAs was incorrect. These data also provided direct evidence that *ABCB5β* was expressed in HMECs.

Finally, the expression of *p16* and *ABCB5β* in HMECs was measured by RT-qPCR in early (P5) to late (P10) passage cells (see Section 4.2.8). The expression of both *p16* and *ABCB5β* was found to increase step-wise and in parallel with increasing passage number.

4.3.2 Discussion

Multiple individual siRNAs targeting *ABCB5* were found to reduce p16, HMEC cell size, and cause an increase in cell number, suggesting, that loss of *ABCB5* drives the culture into a more proliferative state, away from the p16-positive senescent phenotype associated with ageing. Through a process of elimination, *ABCB5β* was established as the relevant isoform.

Western blotting failed to show detectable ABCB5β protein in samples taken from P5 to P11. Given that expression of *ABCB5β* mRNA was confirmed by RT-qPCR in both young and old cells, this is a curious result. It is possible that the low levels of *ABCB5β* mRNA observed give rise to a protein level that is too low to detect with the Atlas antibody, despite significant protein loading. It is also possible that either the cells rapidly degrade the small amount of protein being produced, or that the mRNA is inefficiently translated as suggested previously for expression in HEK293T cells (see Section 3.2). However, it may be possible that the p16-reduction phenotype observed following *ABCB5β* knockdown is a direct consequence of a reduction in *ABCB5β* mRNA, and not reduction in ABCB5β protein.

Concomitant reduction in both *p16* mRNA and protein was observed upon *ABCB5β* knockdown, therefore it is hypothesised that transfection with the *ABCB5β* targeting siRNAs leads to a reduction in the transcription of *p16*, or causes an increase in *p16* mRNA degradation. Direct reduction or increase in the levels of p16 by either transfection with siRNA targeting *p16* or *CBX7*, respectively, did not cause an increase in *ABCB5β* mRNA, making it likely that the reduction of *p16* is a downstream result of *ABCB5β* knockdown. The lack of a reciprocal change in *ABCB5β* mRNA levels

following transfection with siRNA targeting *p16* or *CBX7* rules out the possibility of a feedback loop in which the modulation of *p16* levels affects the level of *ABCB5β*.

None of the six siRNAs designed to specifically target *ABCB5β* caused any reduction in the mRNA upon transfection. It seems likely that the siRISC complex if formed in the cell with these siRNAs might not degrade the mRNA for one of several reasons. It is possible that the siRISC complex does not recognise the heteroduplex due to steric hindrance, from either stable RNA secondary structure formed within the region (Luo and Chang, 2004, Overhoff et al., 2005, Schubert et al., 2005), or because other proteins are already bound to the message. Computer modelling of the *ABCB5β* mRNA secondary structure found no obvious differences between binding sites of siRNA with high and low knockdown efficacies, but *in silico* modelling of RNA structure may not be particularly reliable, and would require direct investigation to confirm. The possibility of RNA-binding proteins (RBPs) occluding the RISC binding sites should also be investigated.

A further possibility is that the 197 base region of mRNA is simply not a 'good' region for siRNAs to be designed against. Although siRNAs have been in use for nearly 15 years, the algorithms used for their design are imperfect and knockdown of the intended target in never ensured (Liu et al., 2014). It is possible that this inexact method of siRNA sequence prediction, coupled with the small size of the submitted sequence (submitted sequences are usually at least 1000 bases in length), may provide the prediction software with too little information to produce a reliable siRNA sequence.

The most pressing question arising from these results is how the knockdown of *ABCB5β* mRNA causes a reduction in p16 mRNA and protein within the HMECs. If the ABCB5β protein product was translated, theoretically it would be possible that it could secrete a molecule that promotes p16-induced senescence from the cytosol. This seems unlikely, however, as the ABCB5β protein was undetectable in the HMECs, and, in any case, the truncated protein encoded by the transcript would be unlikely to function as an ABC transporter (Chen et al., 2009).

A remaining possibility is that *ABCB5β* mRNA acts as an lncRNA (see Section 1.20). lncRNAs are functional RNA molecules, not just intermediates, and as such are more likely to be found in complexes than mRNA, often bound to proteins or other nucleic acids (Geisler and Coller, 2013). If *ABCB5β* acted as an lncRNA, it may help to explain some of the more perplexing results reported here. If the RNA was bound to other proteins (not involved in translation), it may explain both why the ABCB5β protein is poorly translated, and why some of the siRNAs failed to knockdown the transcribed product. There is no precedent for an RNA transcript to have a duel role as both mRNA and lncRNA, however it is theoretically possible for *ABCB5β*, given the results here described.

At present, no direct link between *ABCB5β* and cellular senescence or the cell cycle has been described in the literature. The only connection between ABCB5β and the cell cycle currently reported is the observation that in ABCB5β^{+} MMICs the DEAD box polypeptide 43 (HAGE) is up-regulated, leading to down-regulation of promyelocytic leukaemia protein (PML) isoforms II and III (PML-II/III; Linely et al., 2012). The cause

of the increased expression of HAGE in these cells was not identified, although it could result from ABCB5β expression. Increased expression of HAGE is known to induce suppressor of cytokine signalling 1 (SOCS1), which ubiquitinates janus kinase 2 (JAK2) and targets it for degradation (Mathieu et al., 2014). Degradation of JAK2 blocks signal transduction and the downstream expression of PML in these cells. PML has previously been shown to bind hypophosphorylated pRB, preventing its phosphorylation, and subsequent release of the E2F transcription factors (Figure 4-17 section 2; (Alcalay et al., 1998). This lead Linley *et al*. to conclude that the proliferation of ABCB5^{+} MMICs resulted from reduced PML expression, due to increased HAGE expression (Linley et al., 2012, Mathieu et al., 2014).

The increase in HAGE expression removes an anti-proliferative signal by reducing pRB phosphorylation inhibition, therefore, it is possible that this event constitutes cellular stress that results in increased p16 expression. Accordingly, it is therefore possible that *ABCB5β* knockdown reduces expression of HAGE, causing up-regulation of PML-II/III to restore the repression of pRB phosphorylation. As this layer of cell-cycle control is restored it may relieve cell stress, leading to a reduction in p16 expression. Intriguingly, expression of another isoform of PML, PML-IV, has previously been linked to premature senescence in fibroblasts, through the phosphorylation and acetylation of p53 (Pearson and Pelicci, 2001).

Another possible explanation linking the knockdown of *ABCB5β* to down-regulation of p16, is that *ABCB5β* mRNA may cause a cell stress phenotype in response to yet unknown mechanism (Figure 4-17 section 3). As previously discussed, lncRNAs have a

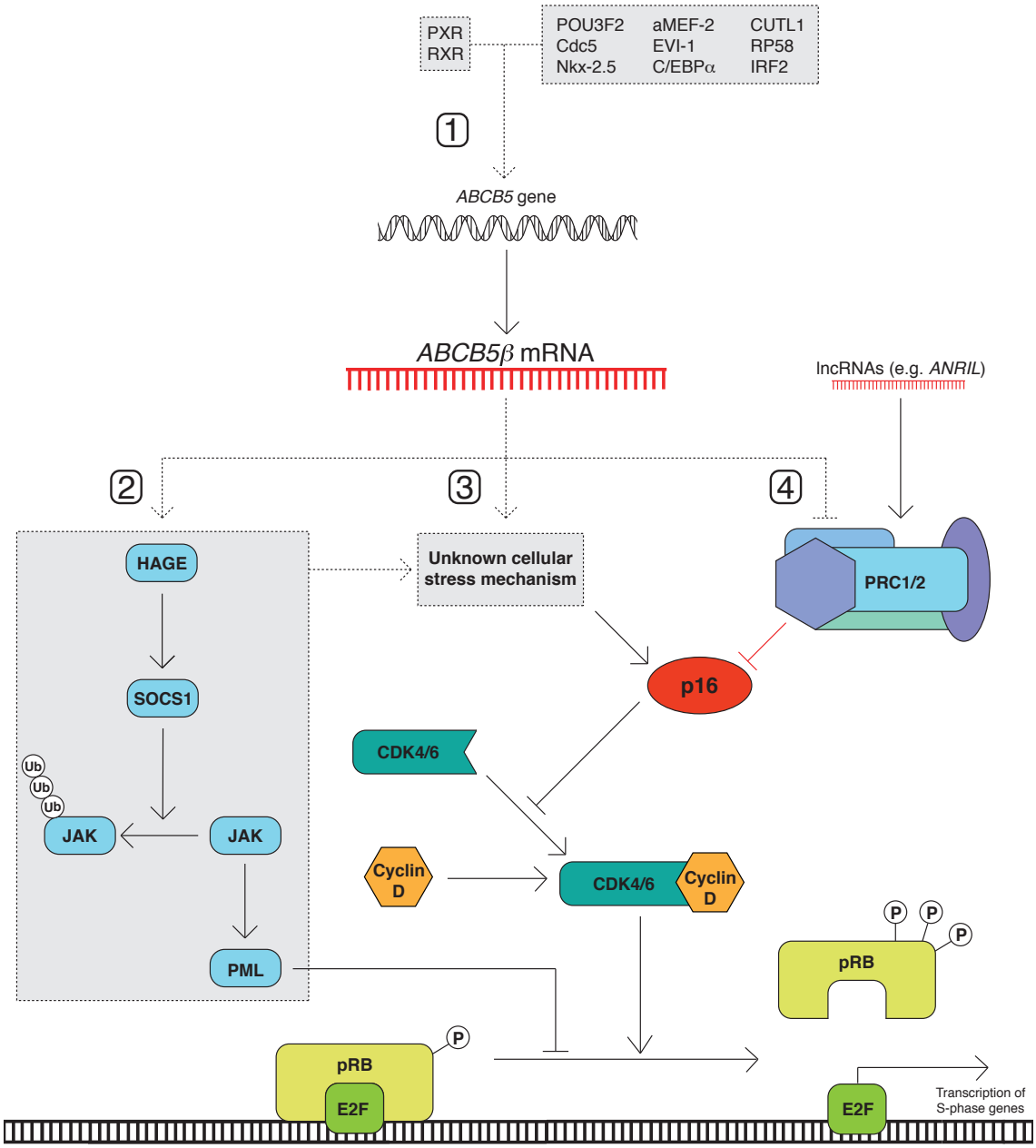

Figure 4-17. Possible mechanisms describing the relationship of *ABCB5β* and p16.

1. *ABCB5β* transcription may be controlled by a number of transcription factors with binding sites within the *ABCB5* promoter region, or due to PXR and RXR, which are known to activate transcription of other ABC family transporters in the presence of cytotoxic drugs (see Section 6.1). 2. ABCB5β$^+$ MMICs are reported to have increased HAGE expression, leading to hyperphosphorylation of pRB due to a reduction in PML expression. This growth signal could be viewed as 'cellular stress', leading to induction of p16 expression. 3. *ABCB5β* may act through another, currently unknown, route to produce cellular stress leading to induction of p16 expression. 4. *ABCB5β* may act as a repressor of PRC1/2, or reduce expression of essential complex components. Solid lines signify reported interactions, where as dotted lines signify proposed interactions. Red lines represent epigenetic silencing.

wide array of possible actions, and therefore *ABCB5β* could effect the expression of multiple genes and proteins in many different ways. It is possible that *ABCB5β* RNA may be involved in the up-regulation, or activation, of a gene or protein that increases the level of cellular stress in HMECs. Knockdown of *ABCB5β* may therefore lead to a reduction of p16 expression as the stress on the cell is relieved.

It is also hypothesised that *ABCB5β* may act by reducing the expression of certain PcG proteins which are known to be involved in the negative regulation of p16 expression (Figure 4-17 section 4) (Bracken et al., 2007). If this were the case, knockdown of *ABCB5β* may lead to increased repression of the INK/ARF locus, and so decreased p16 expression. Alternatively, *ABCB5β* may be directly involved in the regulation of PRC1/2 by association with proteins that form the complex. ANRIL, the lncRNA encoded by the antisense strand of the INK/ARF locus, is already known to associate with both PRC1 and PRC2, acting as a scaffold for complex formation (Yap et al., 2010). Although ANRIL positively regulates the actions of PRC1/2, it sets a precedent for the binding of lncRNA to the component proteins.

4.3.3 Future Work

Although the link between *ABCB5β* knockdown and p16 reduction in HMECs has been established, many questions remain unanswered. For example, the consequence of overexpression of *ABCB5β* in HMECs has not been studied. Elevated levels of both *ABCB5β* and p16 were seen with increasing passage number, associating them with cellular senescence. The transfection of HMECs with a plasmid encoding *ABCB5β*, such as the one used in this study (see Chapter 3), could be an avenue of future investigation. Overexpression of *ABCB5β* may cause an increase in p16 expression and

induce premature senescence in HMECs, if this is the case, it would strengthen the hypothesis that *ABCB5β* causes an increase in p16 via a stress-induced senescence manner. If the addition of *ABCB5β* was not found to cause an increase in p16-mediated senescence, it would suggest either that the low levels of mRNA expressed within the HMECs are sufficient to fully effect p16 expression, or that increased levels of *ABCB5β* do not drive an increase in p16 expression. Additionally, the transfection of HMECs with plasmids encoding *ABCB5fl*, could be carried out within this experiments, to assess whether this isoform can produce the same effects observed upon introduction of *ABCB5β*.

The long-term effects of *ABCB5β* knockdown are also currently unknown. To investigate this, lentiviral particles carrying short hairpin RNA (shRNA) targeted to *ABCB5β* could be introduced into the HMECs, resulting in a consistent, stable knockdown of the mRNA. Culturing HMECs with a stable *ABCB5β* knockdown would generate more information about the relationship between *ABCB5β* and p16. One intriguing question is whether a long-term knockdown of *ABCB5β* would either delay, or indeed stop the onset of the p16 induced senescence phenotype observed in these cells. If p16 induced senescence is bypassed, cell growth may be subsequently arrested by telomere shortening, as previously reported in p16$^-$ HMECs (Yaswen and Stampfer, 2002). If this is not the case, the reason for this should be investigated, primarily by studying the expression of hTERT within the stably transduced HMECs. Within these experiments, a double stable knockdown of *ABCB5β* and *p16* should be performed, so that any differences between the double and single knockdowns can be assessed. These

experiments may give rise to data either confirming or rejecting the hypothesis that *ABCB5β* expression is an important factor in the p16-mediated senescence of HMECs.

The hypothesis that *ABCB5β* may function as an lncRNA should also be explored in detail. As lncRNAs have a wide array of functions within the cells, with over 15 different modes of action currently known (Geisler and Coller, 2013), elucidating the function of a particular lncRNA can be a challenge. Most commonly, lncRNAs perform their functions whilst bound to RBPs. In order to test this possibility, endogenous *ABCB5β* from HMECs could be analysed for bound RBPs using a modified RBP immunoprecipitation (RIP) technique. RIP can be viewed as the RNA equivalent of the well-known chromatin immunoprecipitation (ChIP) technique. Where ChIP identifies proteins bound to DNA, RIP can be used to identify specific RNA molecules bound to RBPs. RIP is performed by immunoprecipitation of endogenous RBP complexes, and the co-isolation of RNAs associated with the precipitated complex. Once performed, RNA probes could be used to pull out the *ABCB5β* transcript and any associated RBPs, which can then be used for further investigations into the function of *ABCB5β*.

An important avenue of future study should be the investigation of how the level of *ABCB5β* mRNA is linked to p16 expression. At present, the link between HAGE and *ABCB5β* is restricted to the increased expression of HAGE in ABCB5β$^+$ MMICs. In order to expand the knowledge around this possible interaction, the expression of HAGE in HMECs subjected to *ABCB5β* knockdown should be investigated; in particular, the relative levels of *HAGE*, *SOCS1* and *PML* expression should be studied, as these genes were previously identified as having altered expression in ABCB5β$^+$ MMICs (Linley et al., 2012, Mathieu et al., 2014). Changes in the relative expression

levels of these genes in response to *ABCB5β* knockdown would bolster the hypothesis that HAGE is up regulated in response to an increase in *ABCB5β* expression. Additionally, the relative expression of these genes should be studied in HMECs of increasing passage number. Increased levels of HAGE in samples taken from cells with a higher passage number may be further indication of *ABCB5β* playing an important role in the induction of p16-mediated senescence in HMECs, and strengthen the hypothesis that *ABCB5β* acts on p16 via HAGE, SOCS1 and PML.

It was hypothesised within Section 4.3.2 that *ABCB5β* may act to negatively regulate PRC1/2, either through a direct interaction, or via down regulation of constituent components of the complexes. To investigate this further, RT-qPCR should be performed on mRNA extracted from both control cells, and cells transfected with siRNA targeting *ABCB5β*, in order to analyse any changes in the expression levels of PcG proteins essential for *p16* repression, such as *CBX7*, *CBX8*, *EZH2*, *BMI1* and *SUZ12* (Bracken et al., 2007). If any of these genes are found to exhibit altered expression patterns in cells transfected with *ABCB5β* targeting siRNA, any array of additional PcG proteins, and their regulators, could also be studied to gain a further insight. Another approach to this possible mechanism would be to investigate whether any changes occur in both the PcG proteins, and histone modifications found at the *INK/ARF* locus, after transfection of HMECs with *ABCB5β* targeting siRNAs. Both the PcG proteins and histone modifications could be assessed using a ChIP assay, with kits for the assessment of these features commercially available. Evaluating changes in either the expression of the PcG proteins, or their presence across the *INK/ARF* locus could provide valuable understanding of the mechanism by which *ABCB5β* knockdown leads to decreased p16 expression.

In addition to the continuation of the study of *ABCB5β* knockdown HMECs described above, the effects of *ABCB5β* in other endogenously expressing cell lines could be evaluated, for example, the A431 and K562 cell lines described in Chapter 3. Knockdown of *ABCB5β* in these cells will allow the comparison of knockdown in cells expressing both mRNA and protein (A431 and K562) and cells expressing only mRNA (HMEC). Similar experiments could be carried out upon the two cell lines to the ones described for HMECs in this study, such as changes in proliferation and changes in expression of p16 (depending on the p16 status of the cell lines). If similar changes are apparent in the cell lines upon knockdown of *ABCB5β*, a system would be provided wherein the cellular changes resulting from *ABCB5β* knockdown can be studied in a more 'cancer like' environment, in comparison to the 'normal cells' used within this investigation.

Further to the techniques described above, RNA sequencing (RNA-seq) could be utilised to further understand the cellular response to *ABCB5β* knockdown. RNA-seq on total RNA extracted from HMECs transfected with siRNAs targeting *ABCB5β* would allow the changes in gene expression, miRNAs and other ncRNAs (non-coding RNAs) to be studied in detail. Although each siRNA targeting *ABCB5β* will have its own array of off target effects, these can be corrected for by the use of the multiple siRNAs, each of which has a different target sequence, for example Ambion-2 and Ambion-3, which were used in this study. By eliminating the changes seen in mRNA, miRNA and ncRNA levels that are not shared by all *ABCB5β* targeting siRNAs, only the changes due to the downstream effects of *ABCB5β* mRNA reduction will remain. These results

can in turn be compared to data collected from HMECs which have had p16 expression reduced (siRNA targeting *p16*) or increased (siRNA targeting *CBX7*), allowing the cellular changes which occur following *ABCB5β* knockdown to be accurately compared to the changes observed when p16 itself is directly modulated. Bioinformatic analysis of the resulting list of genes, and their changes in expression, for example by Ingenuity Pathway Analysis (IPA; see Section 5.2.3.2) could be used to identify potential links between the *ABCB5β* and *p16*, and inform changes, or conformations in the possible mechanisms outlined in Section 4.3.2.

Another possible avenue for the use of RNA-seq is to assess the changes that happen in young vs. old (early passage to late passage) HMECs. As increasing expression of *ABCB5β* over time has previously been demonstrated, a more in-depth analysis of these changes may provide valuable insights into the changes occurring. Any data could then be compared to the previous results, for example: how similar are the older HMECs compared to HMECs which have has the expression of p16 induced via *CBX7* knockdown.

Any putative intermediates of the *ABCB5β* – p16 relationship found by RNA-seq, or any other technique, should subsequently be investigated in HMECs via both knockdown and overexpression experiments, so that their relationship, if any, to the proteins of interested can be properly established. Analysis of the pathway linking *ABCB5β* and p16 may provide potential targets for therapy, in which p16 expression could be modulated. Indeed, various components of the mechanism may already have known chemical modulators that could be quickly and efficiently tested for efficacy.

Chapter Five

5 Oncogenic miRNAs, p16 and basal-like breast cancer

5.1 Introduction

Basal-like breast cancers (BLBCs) account for around 15 – 20 % of all breast cancers, and commonly present at grade-3 with a clinically aggressive phenotype making them a priority for treatment (Fulford et al., 2006). The majority of BLBCs belong to the triple negative breast cancer (TNBC) subtype of breast tumours, which lack expression of oestrogen receptor (OR), progesterone receptor (PR) and human epidermal growth factor receptor (HER2) (Abd El-Rehim et al., 2004, Nielsen et al., 2004, Abd El-Rehim et al., 2005), although BLBCs are also defined by their expression of CK5/6 and 17, EGFR, VEGF and c-kit (Nielsen et al., 2004, Brenton et al., 2005, Linderholm et al., 2009). Unlike other types of breast cancer, BLBCs cannot be treated with targeted therapies such as trastuzumab, tamoxifen or aromatase inhibitors, because they lack OR and HER2 expression. This means that surgical resection of the tumour, generic chemotherapy and radiotherapy are often the only treatments available.

As described in Chapter 1, p16 is an important regulator of the normal cell cycle, controlling passage through the R-point of the cell cycle – the main checkpoint of the G_1/S phase transition – via its interaction with CDK4/6 (Serrano et al., 1993, Gil and Peters, 2006). p16 expression increases with age *in vivo*, causing cells to lose their proliferative capability and enter senescence. p16 can also trigger oncogene-induced senescence (OIS), in which the presence of an oncogenic signal causes up-regulation of p16 expression, and thus cellular senescence (Serrano et al., 1997, Lin et al., 1998).

Expression of p16 is often altered in human tumours, where it can be deleted, mutated, or epigenetically down-regulated (Esteller et al., 2001, Forbes et al., 2006). Inactivation of p16 is commonly thought to be an important step in tumour development (Kamb et

al., 1994, Ruas and Peters, 1998). In BLBC, overexpression of wild-type p16 has consistently been found to correlate with a poor prognosis (Hui et al., 2000, Milde-Langosch et al., 2001), with higher expression also suggested to confer a more homogeneous subgroup of BLBC (Abou-Bakr and Eldweny, 2013). Although the link between p16 expression in BLBC and poor prognosis has been demonstrated multiple times, the underlying mechanism behind this, and its relevance to the aggressiveness of the disease, are unknown.

Recently, a genome-wide miRNA screen identified novel miRNAs involved in p16 regulation and senescence in P6 human mammary epithelial cells (HMECs) (Overhoff et al., 2014). HMECs have a finite lifespan with well-documented p16-mediated senescence associated with stress resulting from normal serial passage *in vitro* (Garbe et al., 2009). This study identified 12 miRNAs (hsa-miR-24, hsa-miR-140-3p, hsa-miR-212, hsa-miR-221, hsa-miR-451, hsa-miR-512-5p, hsa-miR-520h, hsa-miR-574-5p, hsa-miR-770-5p, hsa-miR-992, hsa-miR-1207-3p and hsa-miR-1297), which when transfected into HMECs, increased the expression of p16 and cellular proliferation. These potentially oncogenic – because they caused an increase in also cellular proliferation, independent of cellular stimuli – miRNAs (oncomiRs) were noted to change the HMECs into a more proliferative, although p16-positive, phenotype, similar to that of BLBCs.

The expression of these 12 miRNAs were examined in 1,302 breast cancer tissue samples (Figure 5-1; Dr. Cleo Bishop, Barts and The London School of Medicine and Dentistry, personal communication) (Curtis et al., 2012). The five putative oncomiRs found to have the greatest dysregulation in breast cancer samples, when compared to

normal breast tissue samples, were selected for further study here: hsa-miR-24 (*miR-24*), hsa-miR-140-3p (*miR-140-3p*), hsa-miR-221 (*miR-221*), hsa-miR-451 (*miR-451*) and hsa-miR-574-5p (*miR-574*).

By investigating their mechanism of action it is hoped that important insights into the biology of BLBC will be revealed, which may provide clues for the development of future targeted-therapies.

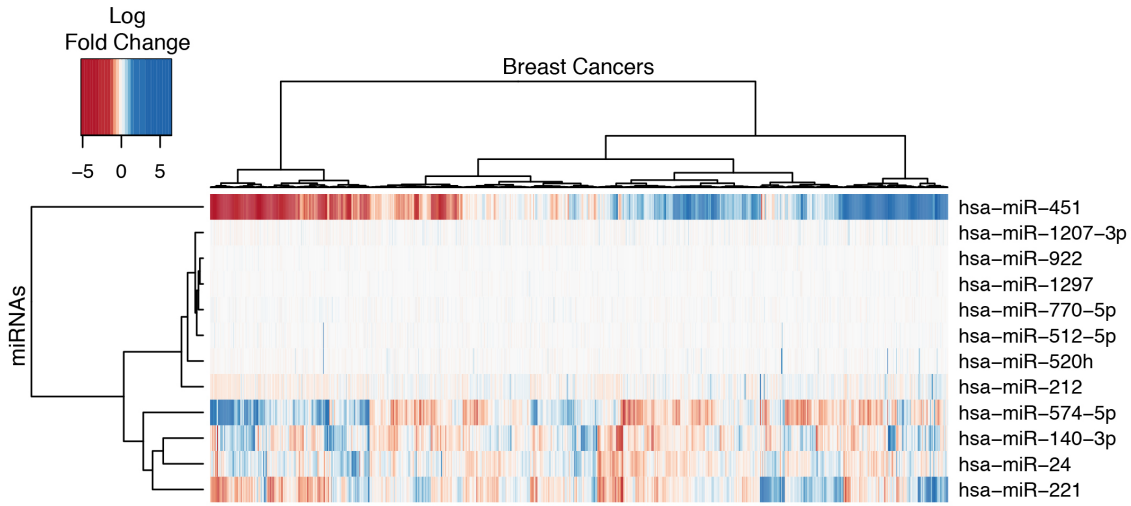

Figure 5-1. Expression profiles of twelve putative oncomiRs in breast cancer.

Heat map of up-regulation (blue) and down-regulation (red) of putative oncomiRs in breast cancer tumour samples, compared to normal breast samples, shown as log fold change. miRNAs were grouped by unsupervised hierarchical clustering to compare the dysregulation pattern of each miRNA. hsa-miR-24, hsa-miR-140-3p, hsa-miR-221, hsa-miR-451 and hsa-miR-574-5p were the most dysregulated miRNAs across the panel of breast tumours, with the dysregulation profile of hsa-miR-451 being the most dissimilar to that of any other miRNAs. Dr. Cleo Bishop, personal communication.

5.1.1 Putative oncomiRs

5.1.1.1 hsa-miR-24

Although *miR-24* has been widely reported to promote cancer cell proliferation and metastasis (Du et al., 2013, Giglio et al., 2013, Li et al., 2013a, Murata et al., 2013), it has contradictorily also been found to inhibit cell division in osteosarcoma through its

targeting of lysophosphatidic acid acyltransferase β (Song et al., 2013). Studies have also found that *miR-24* promotes cell proliferation by directly targeting the tumour suppressors *p16* and $p27^{Kip1}$ (Lal et al., 2008, Giglio et al., 2013), potentially playing a role in carcinogenesis. Additionally, miR-24 has been implicated in promoting erythropoiesis (Wang et al., 2014), regulating aldosterone and cortisol production (Robertson et al., 2013), and mediating pancreatic β-cell dysfunction (Zhu et al., 2013b).

5.1.1.2 hsa-miR-140-3p

Little is known currently of *miR-140-3p*, however, it has been identified as a potential blood-borne biomarker for cancer, type 2 diabetes mellitus and coronary artery disease (Taurino et al., 2010, Taguchi and Murakami, 2013, Collares et al., 2013). Other research has found that *miR-140-3p* is down-regulated in cutaneous squamous cell carcinoma, lung squamous cell carcinoma, basal cell carcinoma and ovarian cancer (Tan et al., 2011, Sand et al., 2012a, Sand et al., 2012b, Linley et al., 2012, Miles et al., 2012).

5.1.1.3 hsa-miR-221

miR-221 has previously been reported to have an oncogenic role in glioblastoma multiform-initiating cells, where high expression of this miRNA was reported and suggested to be one of the key regulators in cell transformation (Aldaz et al., 2013). This miRNA is found to be consistently up-regulated in replicatively senescent endothelial cells (Dellago et al., 2013), and its knockdown in differentiated cells is reported to reduce expression of differentiation markers, and increase expression of stem cell markers (Aldaz et al., 2013).

5.1.1.4 hsa-miR-451

At present there are multiple studies which have identified *miR-451* as being either up-regulated (osteosarcoma) (Dai et al., 2013), or down-regulated in various cancers (squamous cell lung carcinoma, bladder urothelial carcinoma) (Gao et al., 2011, Xie et al., 2012), with no role clearly identified.

5.1.1.5 hsa-miR-574-5p

miR-574 has been identified as significantly up-regulated in both non-small-cell lung cancer and oesophageal squamous cell carcinoma (Foss et al., 2011, Yang et al., 2013), and its presence in the blood has been suggested as a possible serum-based biomarker for the former (Foss et al., 2011).

5.1.2 Aims

The hypothesis for the investigations carried out in this chapter was that expression of the five putative oncomiRs previously identified may accurately model $p16^+$ BLBC, and that the identification of their target genes and modes of action would point towards potential therapies for $p16^+$ BLBC. To investigate the relationship between the tumour suppressor gene *p16* and the putative oncomiRs: *miR-24*, *miR-140-3p*, *miR-221*, *miR-451* and *miR-574*. Specifically, to:

- Recapitulate the effect of miRNAs detailed in Overhoff *et al*. (2014), in which their introduction into HMECs caused an increase in *p16* expression and proliferation;
- Introduce anti-miRNAs (antimiRs) targeting the miRNAs into HMECs to examine endogenous expression of the miRNAs and their phenotypic effects;
- Search for potential oncomiR gene targets that could link *p16* expression and cell proliferation using bioinformatics techniques and web-databases; and

- Investigate the effect of introducing miRNAs and antimiRs into the p16-positive BLBC cancer cell line MDA-MB-468, to model the affect of miRNAs in the disease.

5.2 Results

5.2.1 Effect of putative oncogenic miRNAs in HMECs

In order to confirm the findings originally reported by Overhoff *et al*., the five putative oncomiRs were transfected into HMECs using the conditions previously optimised for the study of *ABCB5* by siRNA knockdown (see Section 4.2.1). The miRNAs were transfected into the cells individually at 60 nM or 90 nM, alongside the negative control siRNA *siGLO*, and two positive control siRNAs targeting *CBX7* and *p16*. Also included as an additional positive control was the miRNA hsa-miR-181a (*miR-181a*), which has previously been found to induce senescence in both HMECs (Overhoff et al., 2014) and other cells (Shin et al., 2011), although not to the same extent as *CBX7* knockdown. The higher concentrations of RNA used in these experiments (60 nM and 90 nM compared to the previous concentration of 30 nM) are due to the lower potency of miRNA, with respect to the reduction in target gene translation, compared to that of siRNA.

Upon transfection of HMECs with the control siRNAs at 60 nM targeting *CBX7* and *p16*, significant increases ($p = 0.0004$) and decreases ($p = 0.0013$) in p16 intensity were observed compared to the *siGLO* control (Figure 5-2 panel A). In addition to these siRNAs, the positive control miRNA, *miR-181a*, was also found to significantly increase the p16 intensity of transfected cells ($p = 0.0260$). Transfection of all putative oncomiRs into HMECs at 60 nM produced a significant increase in p16 intensity

(Figure 5-2 panel B). In addition to the miRNAs, their pool (*miR*-P) was also examined and caused the most significant change ($p = 0.0019$).

Transfection of the HMECs with control siRNAs at 90 nM caused a significant increase in p16 intensity upon transfection with *CBX7* targeting siRNA ($p = 0.0001$), and a significant decrease in p16 intensity upon transfection of siRNA targeting *p16* ($p = 0.0053$; Figure 5-2 panel C). The control miRNA *miR-181a* was again found to cause a significant increase in p16 intensity ($p = 0.0016$), as was observed at 60 nM. Transfection of all putative oncomiRs into HMECs at 90 nM again produced a significant increase in p16 intensity (Figure 5-2 panel D). With the higher concentration of miRNA, *miR-24* was found to cause the most significant change in p16 intensity of all the putative oncomiRs.

In addition to the measurement of p16 intensity, the cell number, cell area and nuclear area of the transfected HMECs were evaluated (Figure 5-3). Significant decreases in cell number were observed upon transfection of siRNA targeting *CBX7* or *miR-181a* into HMECs at 60 nM and 90 nM (all $p < 0.001$[1]; Figure 5-3 panel A). A significant increase in cell number was also observed upon transfection of *p16* targeting siRNA into HMECs at both concentrations (both $p < 0.001$). When the putative oncomiRs were transfected into the HMECs, significant increases (all $p < 0.001$) in cell number were observed upon introduction of all miRNAs and their pool, at both 60 nM and 90 nM.

[1] Accurate p-values cannot be calculated when using a one-way ANOVA due to limitations in the software being used (Prism v5.0d; GraphPad Software Inc, CA). See Section 2.29.2.

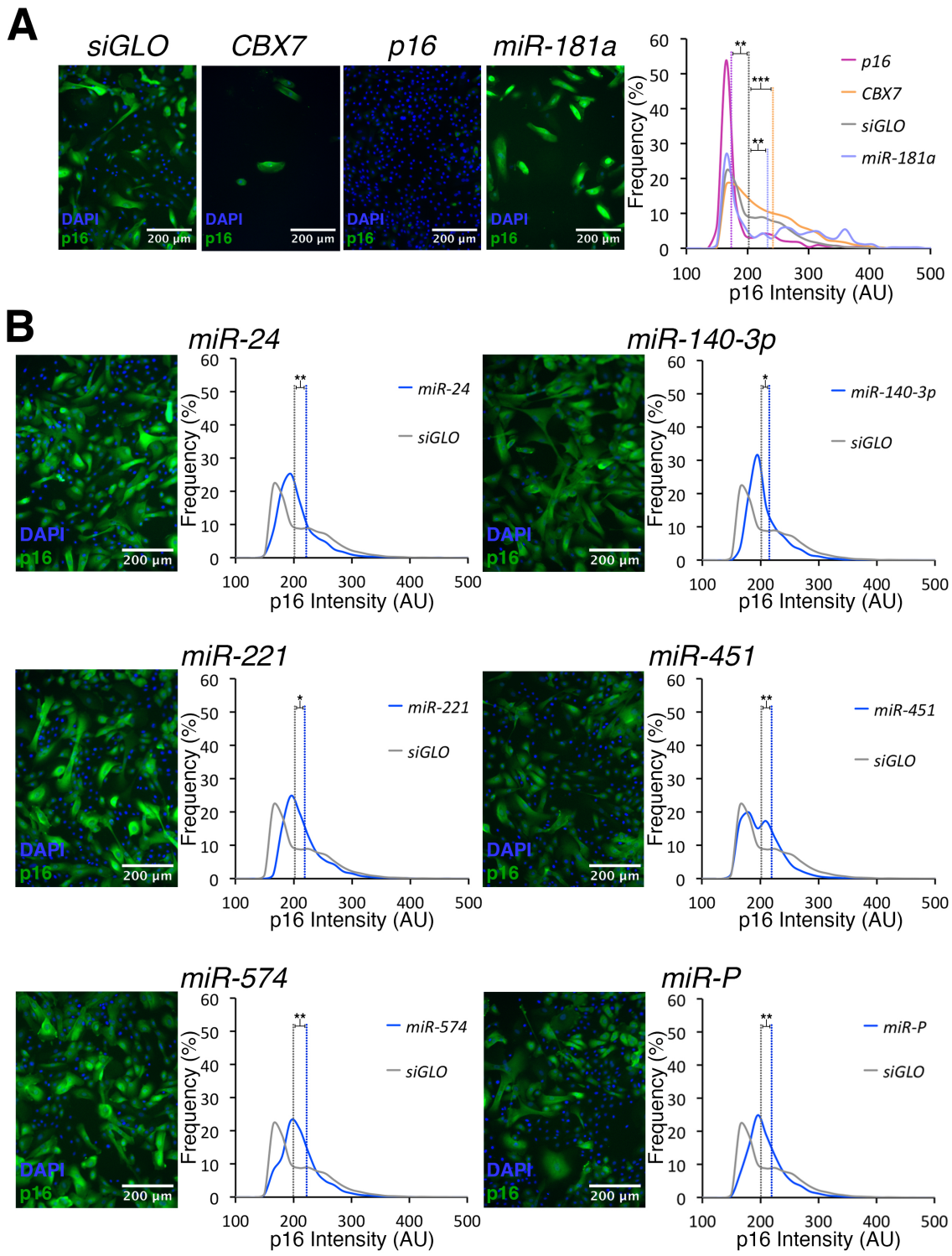

Figure 5-2. Putative oncomiRs increase p16 levels in HMECs.

A. HMECs transfected with 60 nM of the control siRNAs targeting *CBX7* (orange) or *p16* (purple) increased and decreased p16 intensity, respectively when compared to the *siGLO* control (grey). Introduction of 60 nM control miRNA *miR-181a* (mauve) also caused an increase in p16 intensity. Median p16 intensity values (AU) are shown by the dotted lines. B. Transfection with all putative oncomiRs (blue) and their pool (*miR-P*) at 60 nM caused significant increases in p16 intensity compared to *siGLO* control (grey). Representative images show antibody staining of p16 (green) and DAPI staining of nuclei (blue) 120 h post transfection. * $p < 0.05$; ** $p < 0.01$; *** $p < 0.001$. n = 3 biological repeats.

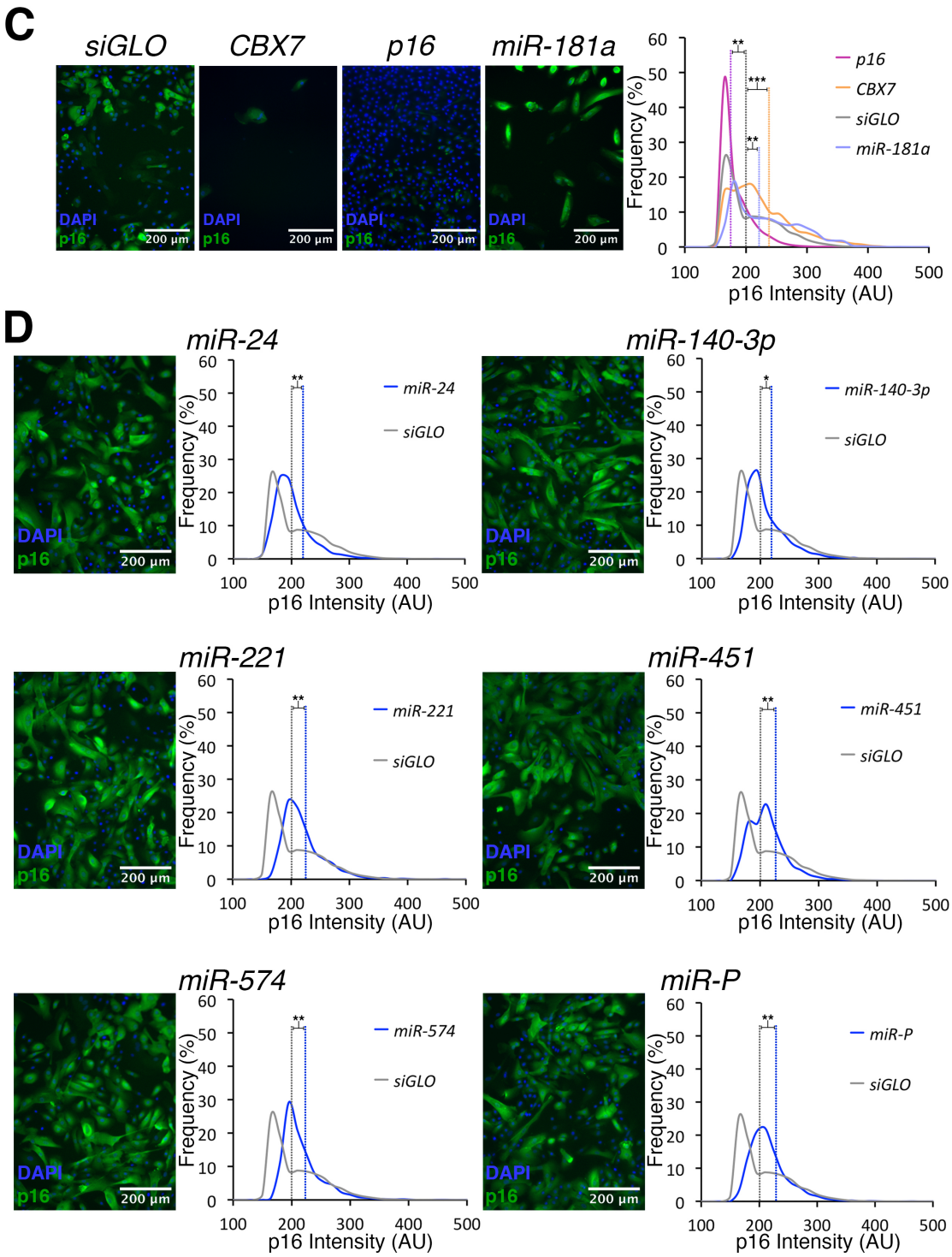

Figure 5-2. (continued) Putative oncomiRs increase p16 levels in HMECs.

C. HMECs transfected with 90 nM of the control siRNAs targeting *CBX7* (orange) or *p16* (purple) increased and decreased p16 intensity, respectively when compared to the *siGLO* control (grey). Introduction of 90 nM control miRNA *miR-181a* (mauve) also caused an increase in p16 intensity. Median p16 intensity values (AU) are shown by the dotted lines. D. Transfection with all putative oncomiRs (blue) and their pool (*miR-P*) at 90 nM caused significant increases in p16 intensity compared to *siGLO* control (grey). Representative images show antibody staining of p16 (green) and DAPI staining of nuclei (blue) 120 h post transfection. * $p < 0.05$; ** $p < 0.01$; *** $p < 0.001$. n = 3 biological repeats.

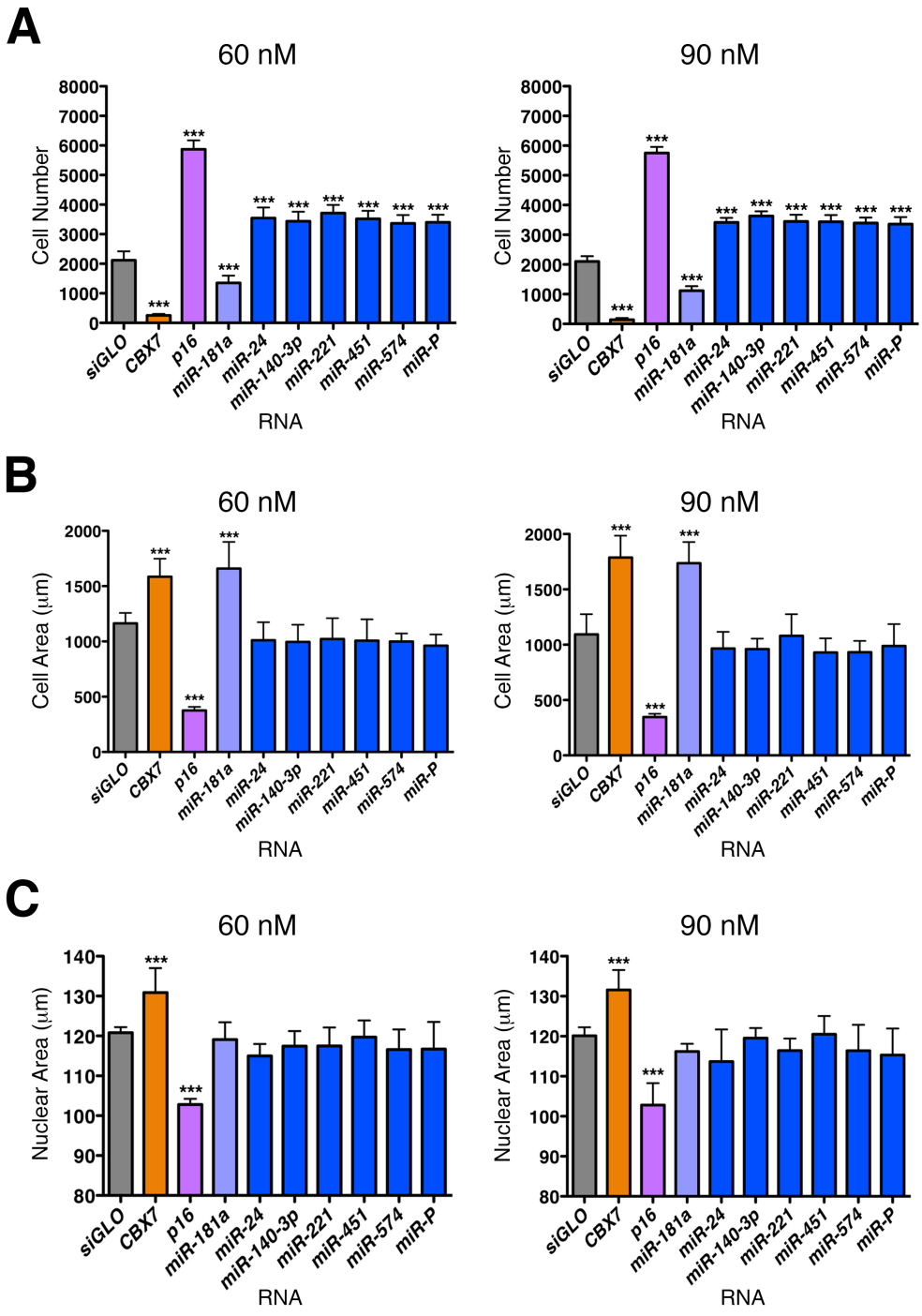

Figure 5-3. Cell number, cell area and nuclear area of HMECs transfected with putative oncomiRs.

A. Significant increases in cell number were observed upon transfection of all putative oncomiRs and their pool (*miR-P*) into HMECs at both 60 nM and 90 nM. B. No significant changes in cell area were observed upon transfection of any miRNAs into the HMECs at either 60 nM or 90 nM. C. Fluctuations in nuclear area were observed in cells transfected with the putative oncomiRs, although none of the changes were found to be significant at 60 nM or 90 nM. All error bars represent one SD. *** $p < 0.001$. n = 3 biological repeats.

Transfection of the positive control siRNAs targeting *CBX7* and *p16* into the cells caused respective increases, and decreases, in cell and nuclear area (Figure 5-3 panels B and C), in line with previous experiments in HMECs. Introduction of *miR-181a* into the HMECs produced a significant increase in cell area at both 60 mM and 90 nM (both $p < 0.001$), similar to *CBX7* knockdown, although this did not cause a significant increase in nuclear area. No significant changes in cell or nuclear area were seen upon introduction of any of the putative oncomiRs into the HMECs at either 60 nM or 90 nM.

Introduction of the miRNAs into HMECs appears to induce a more proliferative phenotype, whilst increasing expression of p16. These two phenotypes are at first sight contradictory, as there is a well documented pathway linking p16 expression to reduced proliferation and senescence in HMECs (see Section 5.1), and also in most other primary cell types (see Section 1.15). The fact that the other two hallmarks of senescence (increase in cell area and nuclear area) in these cells are not present further compounds the issue, and points towards an uncoupling of the p16 – cell cycle arrest pathway. Hypothetically, this might be explained by the increase in proliferation, inducing an increase in p16 via a protective positive feedback loop, which then cannot cause subsequent cellular senescence, supporting the putative oncomiR role for these miRNAs.

5.2.2 Transfection of anti-miRNAs into HMECs

AntimiRs targeting the five miRNAs were also transfected in to the cells in separate experiments. This was carried out in order to examine whether any endogenous expression of the oncomiRs was present within the HMECs. If any of the five miRNAs are expressed endogenously, their depletion would be postulated to cause the opposite

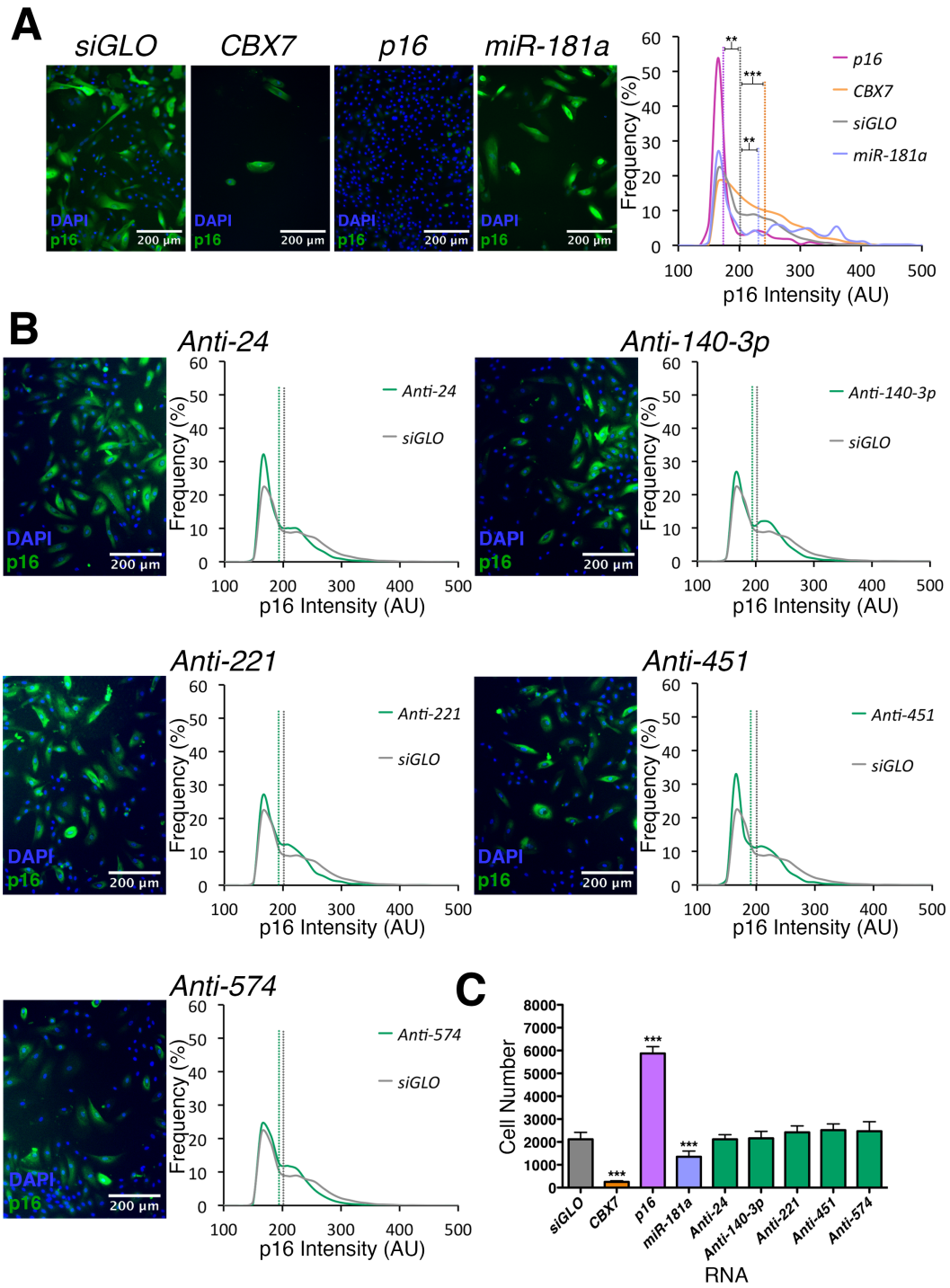

Figure 5-4. antimiRs targeting putative oncomiRs have no effect on HMECs.

A. Control siRNAs targeting *CBX7* (orange) or *p16* (purple) cause an increase in p16 intensity and a reduction in p16 intensity, respectively when compared to the *siGLO* control (grey) at 60 nM. Introduction of 60 nM control miRNA *miR-181a* (mauve) also caused an increase in p16 intensity. Median p16 intensity values (AU) are shown by the dotted lines. B. Transfection with antimiRs targeting putative oncomiRs (green) at 60 nM showed no significant change in p16 intensity compared to *siGLO* control (grey). Representative images show antibody staining of p16 (green) and DAPI staining of nuclei (blue) 120 h post transfection. C. No significant changes in cell number were observed in cells transfected with antimiRs at 60 nM, when counted at the 120 h time point. All error bars represent one SD. ** $p < 0.01$; *** $p < 0.001$. n = 3 biological repeats.

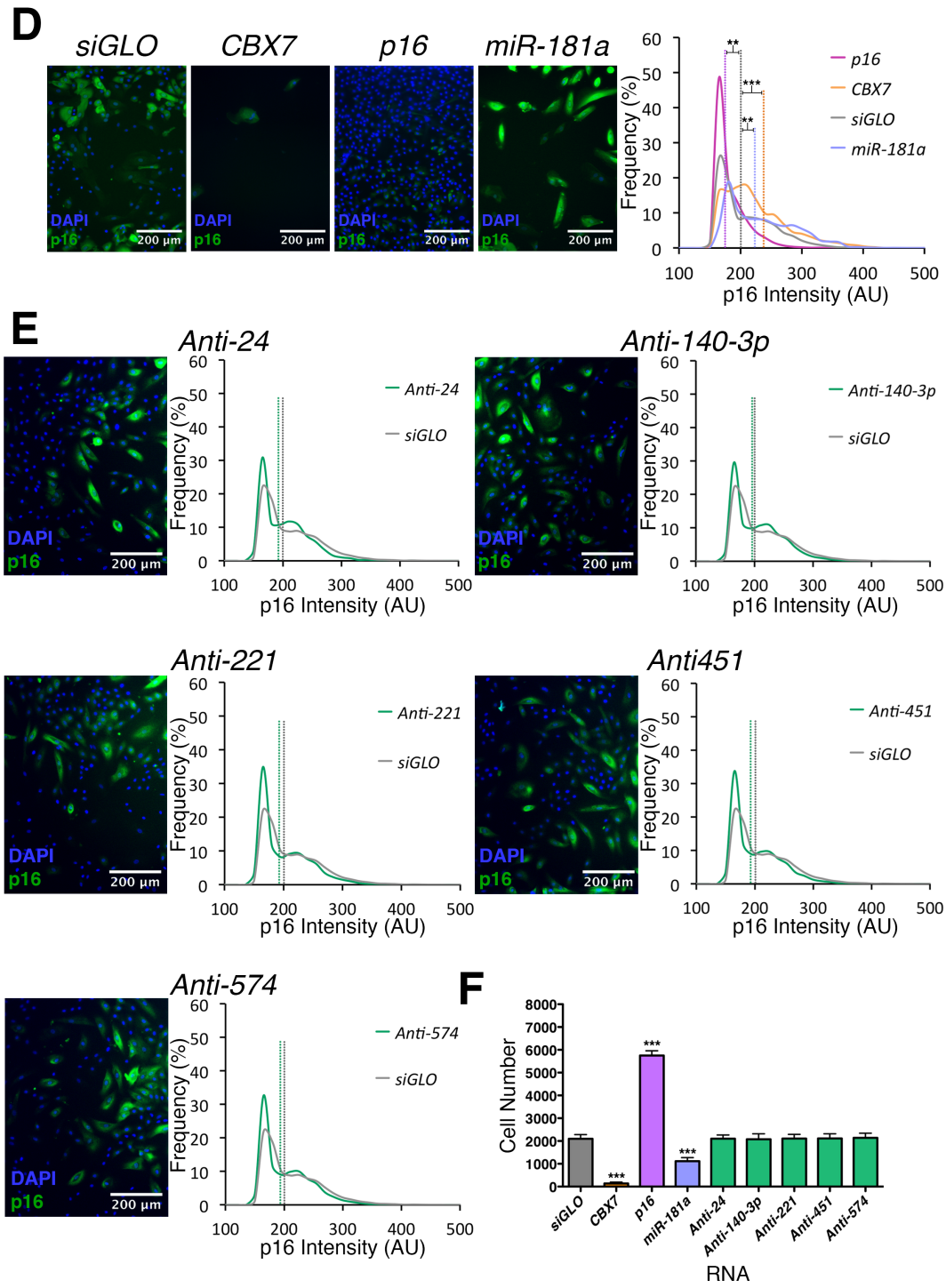

Figure 5-4. (continued) antimiRs targeting putative oncomiRs have no effect on HMECs

D. Control siRNAs targeting *CBX7* (orange) or *p16* (purple) cause an increase in p16 intensity and a reduction in p16 intensity, respectively, when compared to the *siGLO* control (grey) at 90 nM. Introduction of 90 nM control miRNA *miR-181a* (mauve) also caused an increase in p16 intensity. Median p16 intensity values (AU) are shown by the dotted lines. E. Transfection with antimiRs targeting putative oncomiRs (green) at 90 nM showed no significant change in p16 intensity compared to *siGLO* control (grey). Representative images show antibody staining of p16 (green) and DAPI staining of nuclei (blue) 120 h post transfection. F. No significant changes in cell number were observed in cells transfected with antimiRs at 90 nM, when counted at the 120 h time point. All error bars represent one SD. ** $p < 0.01$; *** $p < 0.001$. n = 3 biological repeats.

phenotype of introducing the oncomiR, specifically: a decrease in cell proliferation, and a decrease in p16 intensity. These experiments were carried out at the same time as the ones previously described (see Section 5.2.1), therefore all of the controls are identical (Figure 5-4 panels A and D).

Transfection of the antimiRs targeting the five putative oncomiRs had no significant effect on p16 intensity at 60 nM in the HMECs (Figure 5-4 panel B). The transfection of antimiRs into the cells did not cause any significant change in cell number (Figure 5-4 panel C), whereas introduction of the control siRNAs and miRNA were all found to cause significant (all $p < 0.001$) increases, and decreases in cell number.

When transfected into HMECs at 90 nM, the antimiRs again had no effect on p16 intensity (Figure 5-4 panel E). There was also no significant change in the cell number (Figure 5-4 panel F).

These results, taken together with those described in Section 5.2.1, suggest that the HMECs are sensitive to the expression of the five putative oncomiRs examined here: miR-24, miR-140-3p, miR-221, miR-451, and miR-574. The data also suggest that the HMECs do not express the miRNAs endogenously at P6, as the opposite phenotype would be expected upon transfection of the antimiRs into the cells.

5.2.3 Identifying potential miRNA target genes

5.2.3.1 Mining potential target genes from prediction programs

To further investigate the effect of the putative oncomiRs on the expression of *p16* and cellular proliferation, potential target genes of the five miRNAs were searched for.

These genes were mined from the online miRNA binding prediction comparison program miRWalk[I] (Dweep et al., 2011).

The database was interrogated by searching for the targets of each miRNA individually in the 3'-UTR of human genes, with a comparative analysis across five prediction programs: miRanda, miRDB, miRWalk, miR22 and TargetScan. The predicted gene targets from the five programs were compared, with genes common to all prediction programs analysed further. The list of target genes provided a p value for each candidate representing the probability at which they are targeted by the miRNAs[II] (Appendix III). A total of 991 unique genes were taken forward for further analysis, each with a p value of less than 0.05 (400 for *miR-24*; 277 for *miR-140-3p*; 219 for *miR-221*; 48 for *miR-451*; and 193 for *miR-574*).

5.2.3.2 Evaluating miRNA potential targets

Ingenuity Pathway Analysis[III] (IPA; Ingenuity® Systems) is a large database of up-to-date biological scientific findings coupled with complex analysis tools capable of finding links between genes on the basis of expression in diseases, cellular function and functional pathways. A vast database of information at the analysis tool's disposal makes IPA a powerful program for studying large sets of genes generated from a variety of sources such as RNA-seq, siRNA screens, and as in the case presented here, miRNA target prediction.

[I] The miRWalk miRNA predicted target search can be found at http://www.umm.uni-heidelberg.de/apps/zmf/mirwalk/micrornapredictedtarget.html (accessed June 2013).
[II] The probability of an miRNA sequence targeting a given mRNA sequence, calculated using the Poisson distribution. More information can be found at http://www.umm.uni-heidelberg.de/apps/zmf/mirwalk/documentation.html#pv (Accessed June 2013).
[III] Ingenuity Pathway Analysis can be found at http://www.ingenuity.com/products/ipa#/?tab (accessed August 2013).

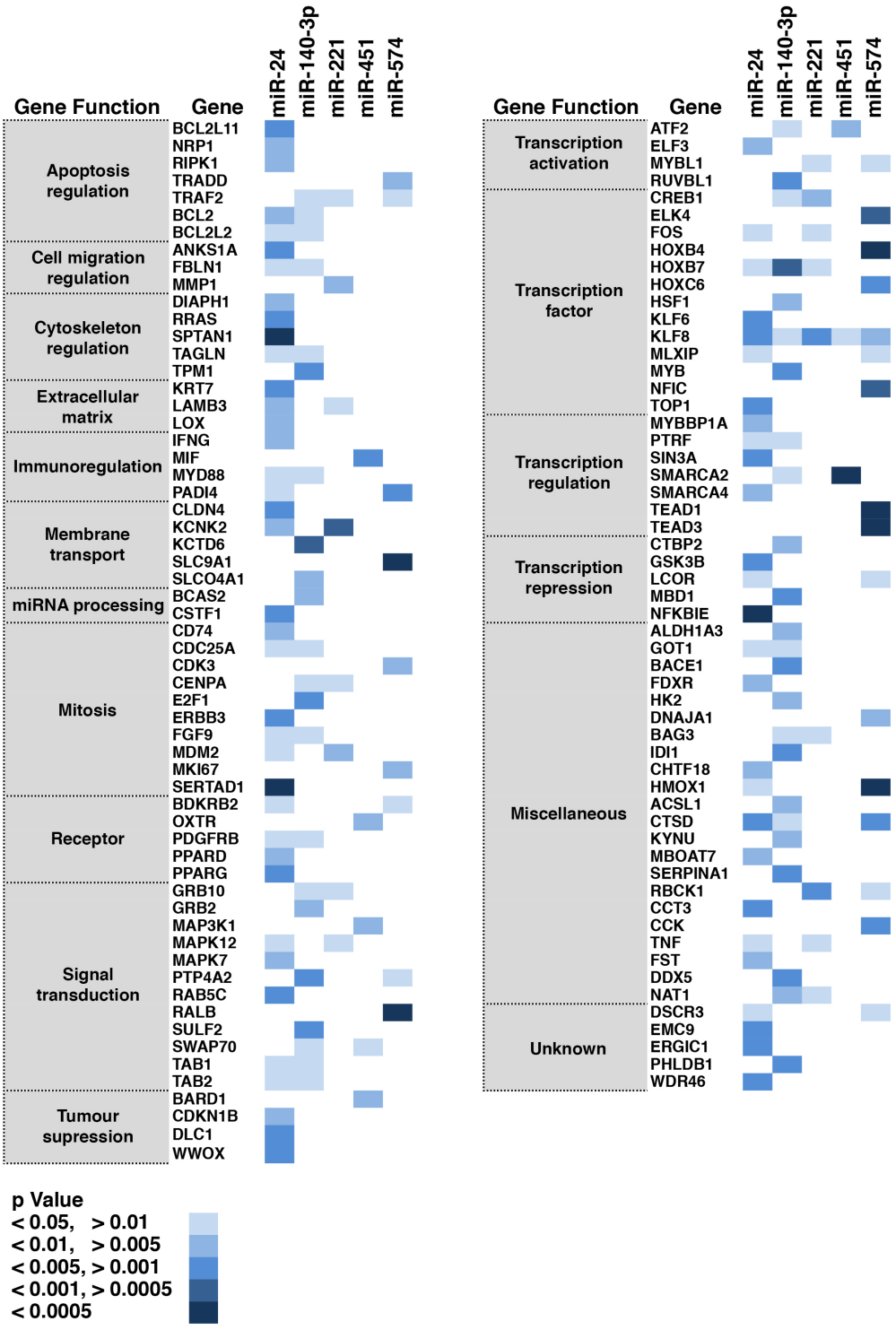

Figure 5-5. Heat map showing predicted targeting of candidate genes by putative oncomiRs.

The top 116 candidate genes grouped by gene function. The majority of the genes are targeted by two or more miRNAs, with *KLF8* the only gene targeted by all five.

Further analysis of the 991 putative target genes was carried out using IPA, in an attempt to identify genes involved in the regulation of p16 expression and cellular proliferation. The potential target genes for each miRNA were uploaded to IPA and used in a Core Analysis search for experimentally observed, direct and indirect links between the genes in the data set, in both mice and humans.

In total, 294 genes linked to *p16* expression and cellular proliferation were found by the Core Analysis performed on the 991 predicted target genes of the five miRNAs (Appendix). This shortlist of genes was ranked by scoring both the p value and the number of miRNAs targeting each gene. Higher scores were given to genes with lower p values that were targeted by more of the miRNAs. The top ranked genes (116) were then selected as candidates for further analysis in future experiments (see 5.3.3), and grouped by cellular function (Figure 5-5).

5.2.4 Effect of putative oncogenic miRNAs on MDA-MB-468 cells

To further test the effect of the putative oncomiRs on p16 expression and cellular proliferation, the BLBC cell line MDA-MB-468 was chosen (see Section 2.1.2.9). This cell line was chosen to model the effects of the oncomiRs in BLBCs, as these cancers frequently are found to have both a highly proliferative, aggressive phenotype, and a high expression of *p16* (see Section 1.18.1). Any results alluding to a miRNA-related mechanism could be exploited to aid in the management of these aggressive tumours.

To test this hypothesis, the miRNAs were transfected into the MDA-MB-468 cell line using the conditions optimised in Appendix IV. Each miRNA was transfected into the cells at 60 nM and 90 nM, alongside the negative control siRNA *siGLO*, and the two

positive control siRNAs targeting *p16* and *KIF11* (an essential molecular motor protein required for mitosis, the knockdown of which causes apoptosis).

Upon transfection of the control siRNAs at 60 nM, no change in p16 intensity was observed with siRNA *KIF11*, whereas p16 intensity significantly reduced with the *p16* targeting siRNA, as predicted (Figure 5-6 panel A; $p = 0.0053$). A significant increase and decrease in cell number were observed upon transfection of siRNAs targeting *p16* and *KIF11*, respectively (Figure 5-6 panel C; $p < 0.001$). Upon transfection of putative oncomiRs at 60 nM, no significant variation was observed in either p16 intensity (Figure 5-6 panel B), or cell number (Figure 5-6 panel C).

Transfection of MDA-MB-468 with control siRNAs at 90 nM displayed a significant increase in p16 intensity upon transfection of *KIF11* siRNA ($p = 0.0221$), and a significant decrease in p16 intensity upon transfection of siRNA targeting *p16* (Figure 5-6 panel D; $p = 0.0424$). The increase in p16 intensity upon transfection of the siRNA targeting *KIF11* at 90 nM is most likely indicative of a cellular response to cytotoxicity due to the higher concentration of siRNA used. Significant decreases in cell number were seen with siRNAs targeting *p16* and *KIF11* when transfected at 90 nM (Figure 5-6; $p < 0.001$). The reduced cell number upon transfection with siRNA targeting *p16* at

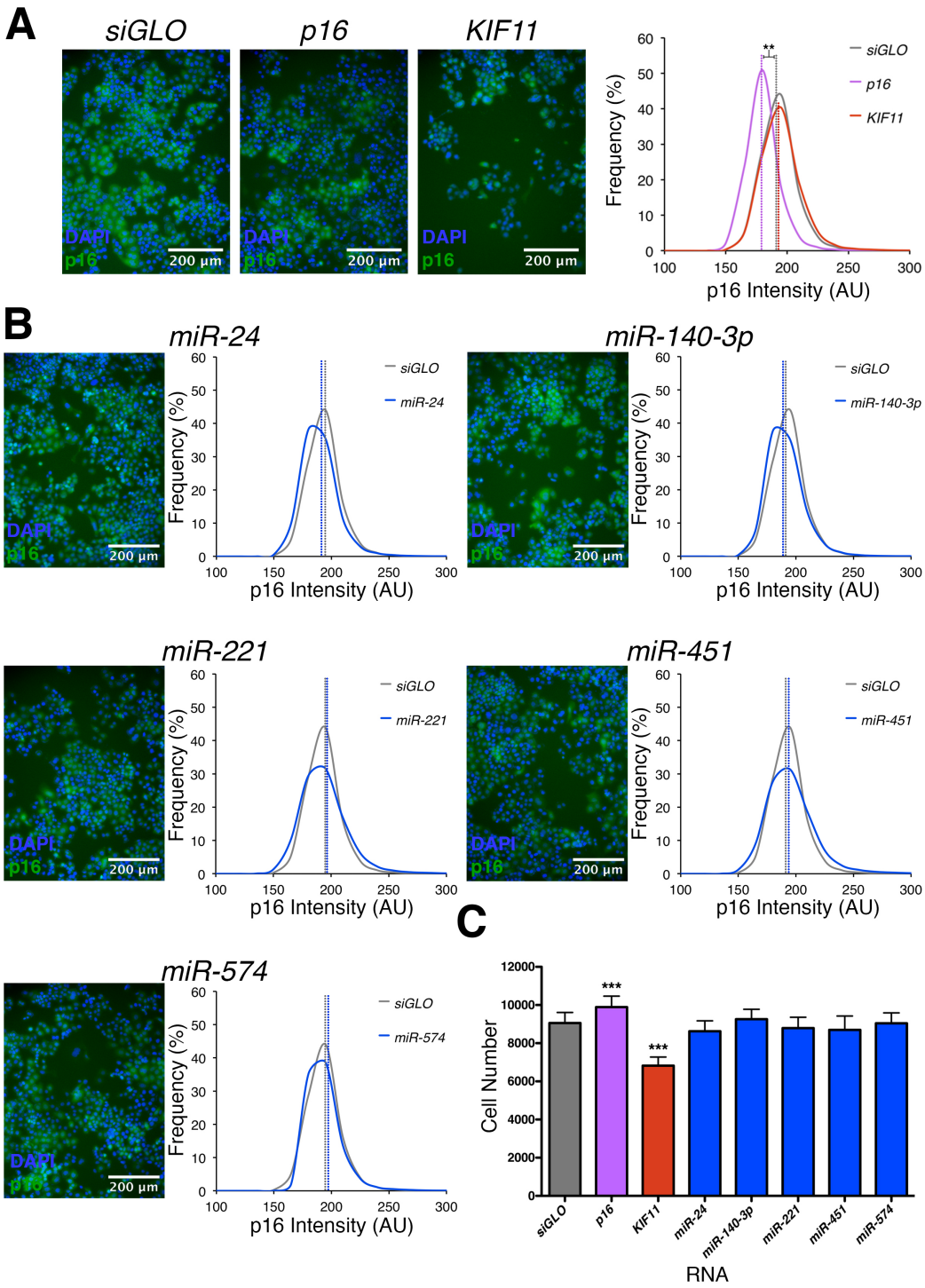

Figure 5-6. Putative oncomiRs have no effect on MDA-MB-468 cells.

A. The positive control siRNA targeting *p16* (purple) reduced p16 intensity at 60 nM compared to the *siGLO* control (grey). The killer control siRNA targeting *KIF11* (red) was found to have significant effect on p16 intensity compared to *siGLO* at 60 nM. Median intensity values (AU) are shown by the dotted lines. B. Transfection with putative oncomiRs (blue) at 60 nM showed no significant change in p16 intensity compared to *siGLO* control (grey). Representative images show antibody staining of p16 (green) and DAPI staining of nuclei (blue) 120 h post transfection. C. No significant change in cell number was observed in cells transfected with putative oncomiRs at 60 nM when counted at the 120 h time point. All error bars represent one SD. ** $p < 0.01$; *** $p < 0.001$. n = 3 biological repeats.

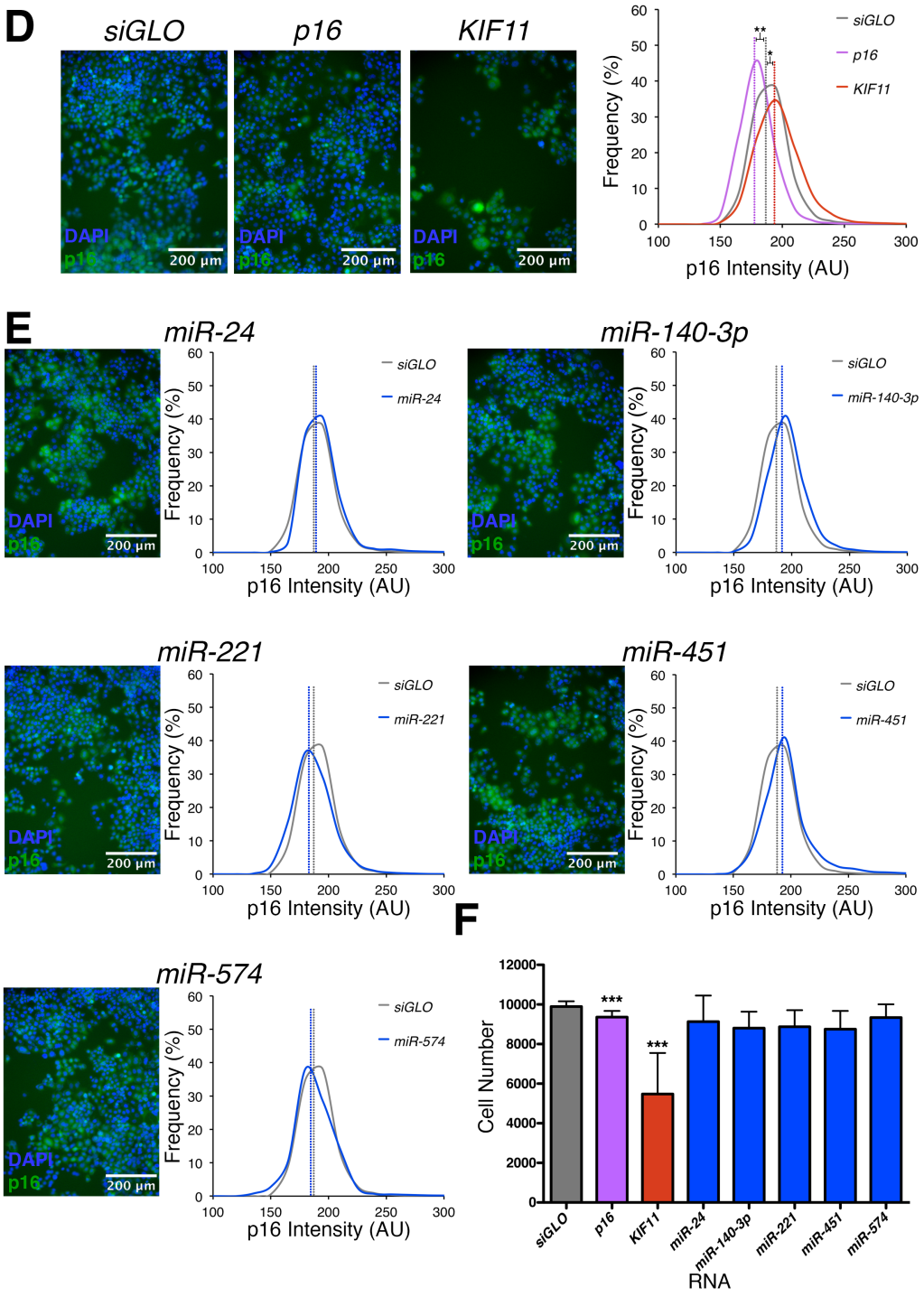

Figure 5-8. (continued) Putative oncomiRs transfected at 90 nM have no effect on MDA-MB-468 cells.

D. The positive control siRNAs targeting *p16* (purple) and *KIF11* (red) reduce p16 intensity and increase p16 intensity, respectively, at 90 nM compared to the *siGLO* control (grey). Median intensity values (AU) are shown by the dotted lines. E. Transfection with putative oncomiRs (blue) at 90 nM showed no significant change in p16 intensity compared to *siGLO* control (grey). Representative images show antibody staining of p16 (green) and DAPI staining of nuclei (blue) 120 h post transfection. F. No significant change in cell number was observed in cells transfected with putative oncomiRs at 90 nM when counted at the 120 h time point. All error bars represent one SD. * $p < 0.05$; ** $p < 0.01$; *** $p < 0.001$. n = 3 biological repeats.

90 nM, compared to an increase upon transfection at 60 nM, is again probably due to an increased level of toxicity with the higher dose of siRNA. When the putative oncomiRs were introduced into the MDA-MB-468s at 90 nM, again no significant changes in either p16 intensity (Figure 5-6 panel E), or cell number were observed (Figure 5-6 panel F).

The introduction of exogenous miRNAs may not cause any observable change in cell morphology and behaviour, if they are already highly expressed within the cell. This hypothesis may explain the lack of effect described following transfection of the MDA-MB-468s, although this will need to be confirmed by RT-qPCR to demonstrate endogenous miRNA expression.

5.2.5 Effect of anti-miRNAs on MDA-MB-468 cells

To investigate the role of the putative oncomiRs in the MDA-MB-468 cells, antimiRs were used to downregulate endogenous expression. If the oncomiRs induce the p16 positive, proliferative phenotype of the MDA-MB-468 cells, it was postulated that transfection of the antimiRs into the cells may reduce p16 intensity and reduce proliferation. When the antimiRs targeting the putative oncomiRs were introduced into the cells at either 60 nM or 90 nM, no significant changes in either p16 intensity (Figure 5-7 panels B and E), or cell number were observed (Figure 5-7 panels C and F).

Although the endogenous expression level of each of the five putative oncomiRs in MDA-MB-468s is currently unknown, this data suggests that they are not linked to p16

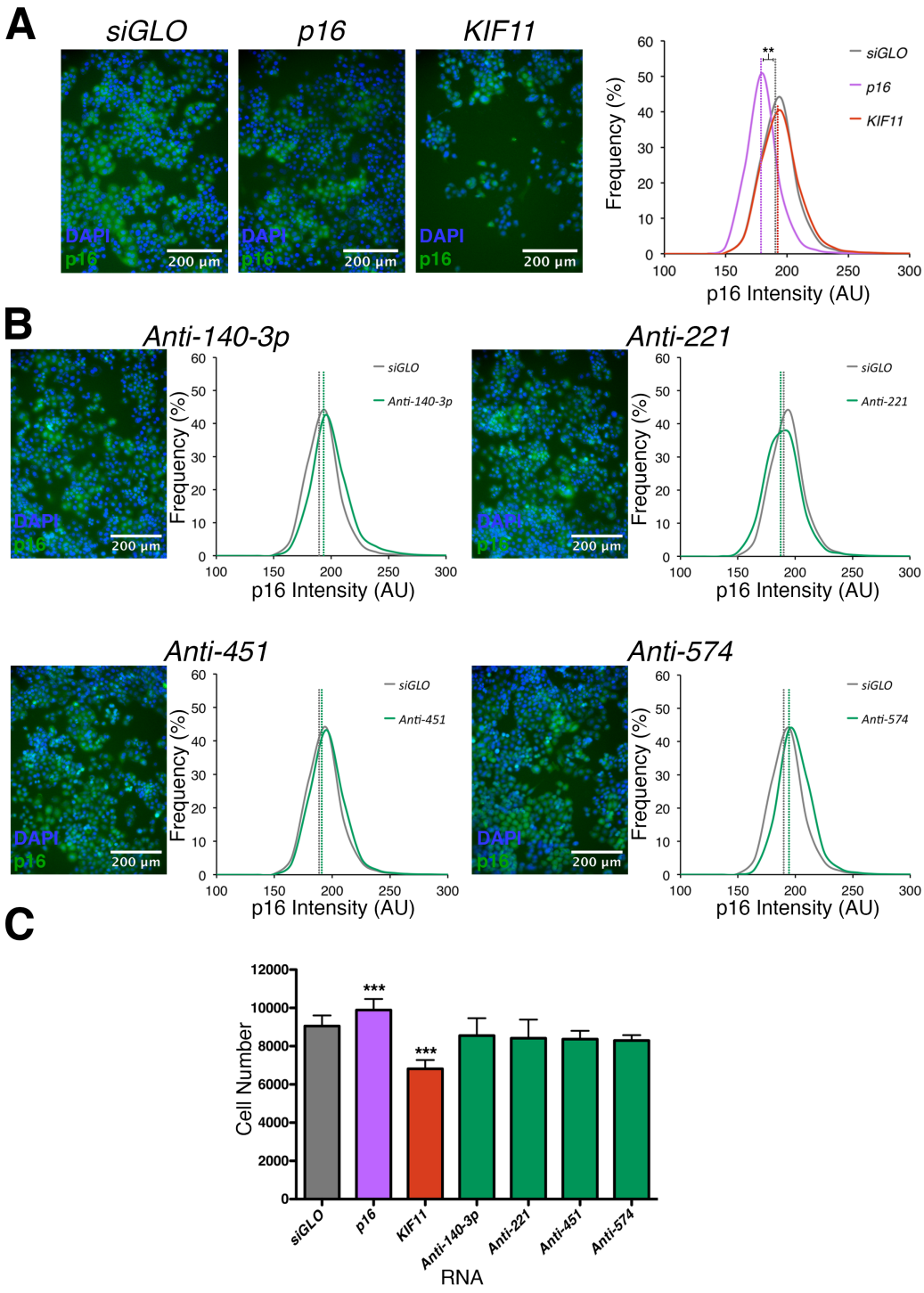

Figure 5-7. AntimiRs targeting putative oncomiRs have no effect on MDA-MB-468 cells.

A. The positive control siRNA targeting *p16* (purple) reduced p16 intensity at 60 nM compared to the *siGLO* control (grey). The killer control siRNA targeting *KIF11* (red) was not found to have significant effect on p16 intensity at 60 nM. Median intensity values (AU) are shown by the dotted lines. B. Transfection with antimiRs targeting putative oncomiRs (green) at 60 nM showed no significant change in p16 intensity compared to *siGLO* control (grey). Representative images show antibody staining of p16 (green) and DAPI staining of nuclei (blue) 120 h post transfection. C. No significant change in cell number was observed in cells transfected with antimiRs targeting putative oncomiRs at 60 nM when counted at the 120 h time point. All error bars represent one SD. ** $p < 0.01$; *** $p < 0.001$. n = 3 biological repeats.

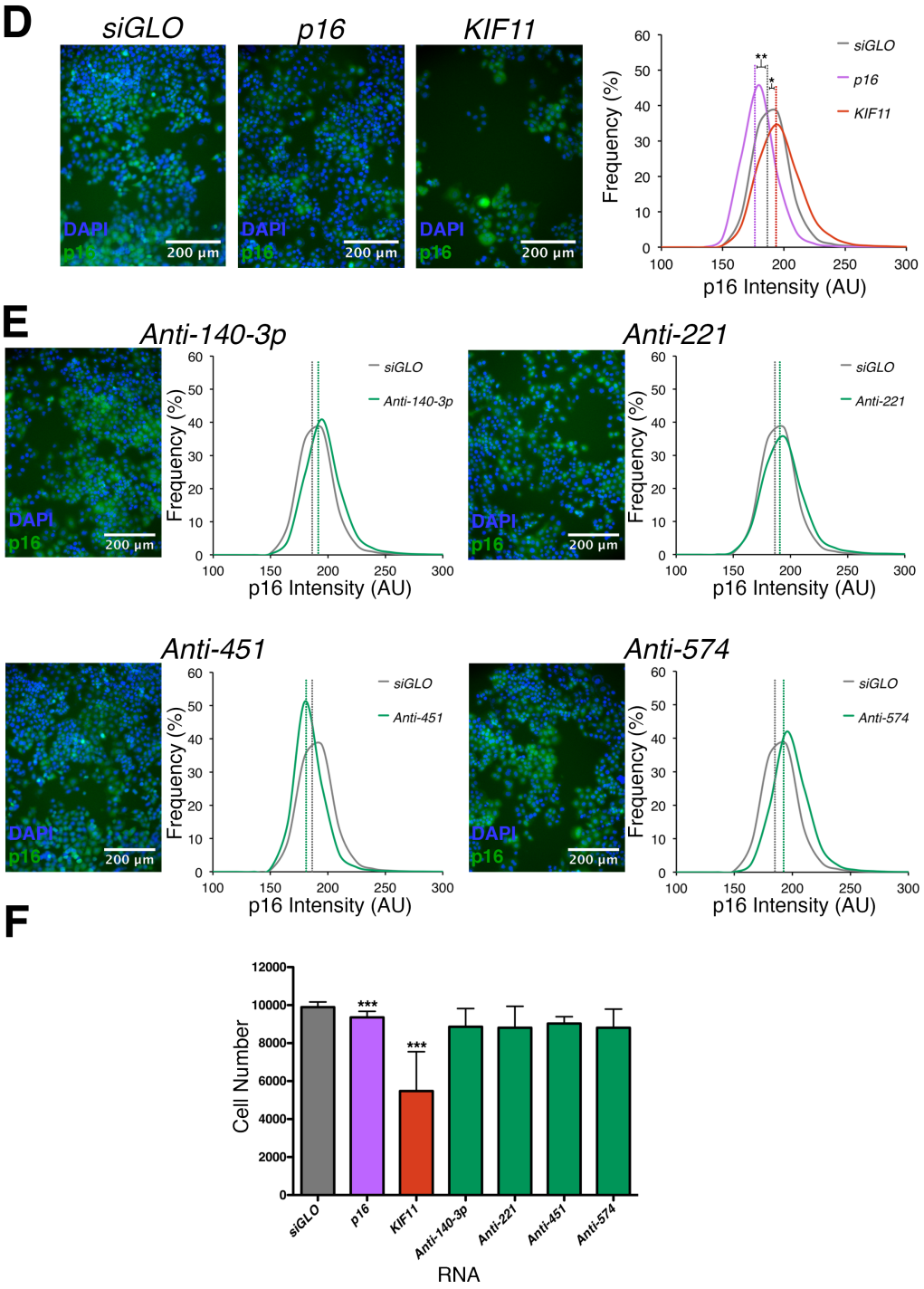

Figure 5-9. (continued) AntimiRs targeting putative oncomiRs have no effect on MDA-MB-468 cells.

D. The positive control siRNAs targeting *p16* (purple) and *KIF11* (red) reduced p16 intensity and increased p16 intensity respectively at 90 nM compared to the *siGLO* control (grey). Median intensity values (AU) are shown by the dotted lines. E. Transfection with antimiRs targeting putative oncomiRs (green) at 90 nM showed no significant change in p16 intensity compared to *siGLO* control (grey). Representative images show antibody staining of p16 (green) and DAPI staining of nuclei (blue) 120 h post transfection. F. No significant change in cell number was observed in cells transfected with antimiRs targeting putative oncomiRs at 90 nM when counted at the 120 h time point. All error bars represent one SD. * $p < 0.05$; ** $p < 0.01$; *** $p < 0.001$. n = 3 biological repeats.

expression and cellular proliferation in these cells, given that neither addition nor depletion of these miRNAs from the cells had a measurable effect on p16 expression, or cell proliferation.

5.3 Discussion

5.3.1 Summary of the findings

In previously published work, transfection of five miRNAs into HMECs caused an increase in both cellular proliferation and p16 expression (Overhoff et al., 2014). In order to confirm and build upon these findings, HMECs were transfected with each the miRNAs and also their corresponding antimiRs. The HMECs were transfected with 60 nM or 90 nM miRNA or antimiR, or with control siRNAs or control miRNA.

The control siRNAs targeting *p16* and *CBX7*, and the control miRNA *miR-181a* were used as positive controls for modulation of p16 in senescence by siRNA, and miRNA, respectively. The siRNA targeting *CBX7* and *p16* were used as controls for expression and depletion of p16, respectively, as before (see Section 4.2.2.1). Introduction of the control miRNA *miR-181a* caused significant increase in both p16 intensity and cell area, and a significant decrease in cell number, demonstrating that introduction of *miR-181a* is a positive control for miRNA modulation of p16 expression (see Section 5.2.1).

Introduction of all five putative oncomiRs, and their pool, into the HMECs caused significant increase in p16 intensity compared to the *siGLO* negative control, at both 60 nM and 90 nM concentrations. The most significant changes were observed with *miR-P* and *miR-24* at 60 nM and 90 nM, respectively. Introduction of all miRNAs and their

pool also caused significant increase in cell number, although no significant changes were recorded for cell or nuclear area.

These results confirm the original findings, and show that the HMECs become surprisingly more proliferative while expressing p16 upon transfection of these miRNAs. Transfection of the antimiRs targeting the five miRNAs into HMECs, however, did not produce any phenotypic changes at either 60 nM or 90 nM, suggesting that the miRNAs are not expressed endogenously (see Section 5.2.2).

In order to understand the mechanism of action leading to proliferation despite p16 expression in HMECs, bioinformatic investigation of potential gene targets of the miRNAs was carried out (see Section 5.2.3). The miRWalk prediction comparison program initially identified potential targets, and significant hits were taken forward for further analysis by IPA. A total of 991 genes were analysed by IPA Core Analysis, with genes linked to cellular proliferation and *p16* expression selected for more in-depth analysis. Potential target genes identified by IPA were ranked by miRNA targeting probability and the number of miRNAs targeting each gene. This stratified the candidates and the top 116 were designated for future study.

p16 expression alongside cellular proliferation is a hallmark of BLBC. The miRNAs were therefore transfected into the $p16^{+}$ MDA-MB-468 cell line, as a model of the disease. siRNAs targeting *p16* and *KIF11* were used as positive controls under optimised transfection conditions. Transfection of the positive control siRNA targeting *p16* at 60 nM into MDA-MB-468 cells caused a significant decrease in p16 intensity, and increase in cell number, again establishing introduction of this siRNA as a control

for p16 removal in the cells. At 90 nM, however, this siRNA caused a significant decrease in cell number in addition to p16 intensity, most likely due to an increase in cytotoxicity with the higher dose of siRNA. The introduction of siRNA targeting *KIF11* significantly reduced cell number at both 60 nM and 90 nM, and increased p16 intensity at 90 nM, showing it to be a robust control for cell death, and transfection efficiency.

The introduction of all five putative oncomiRs and their corresponding antimiRs into the MDA-MB-468s at both 60 nM and 90 nM failed to cause any significant changes in either p16 intensity or cell number. This result suggested that whether the five miRNAs are endogenously expressed in the cells or not, they are not likely to be as biologically relevant to the cellular phenotype in the MDA-MB-468s as they are in the HMECs.

5.3.2 Discussion

Introduction of the five putative oncomiRs into HMECs were found to cause increases in both p16 levels and cellular proliferation, despite these two processes being generally recognised as contradictory. As the transfection of antimiRs targeting the five miRNAs into HMECs did not induce any phenotypic changes, it is likely that they are either not expressed, or expressed at such low levels that their removal does not cause a discernable change. Performing an RT-qPCR assay to determine the presence or absence of these miRNAs in HMECs should be a priority for any future work.

Although transfection of the five miRNAs into HMECs caused an increase in p16 expression and cell number, neither the cell area nor nuclear area of the cells were significantly altered. Usually in HMECs, cells that proliferate at a higher rate also tend to be smaller, and contain smaller nuclei than slower cycling cells, as observed in the results of Chapter 4. The results from the introduction of the miRNAs therefore suggest

that the transfected cells are either proliferating at the same rate as the control cells, or that the change in the rate of proliferation is too small to cause a significant change on the size of the cell and its nucleus. If there was no change in the rate of proliferation following transfection, the higher cell number observed may be due to a lack of senescence in response to p16 expression; meaning that cells which would have normally ceased to divide will continue to divide in the transfected population.

As the introduction of the miRNAs caused an increase in both cell number and p16 levels in HMECs, the molecular pathway linking p16 activity to cell cycle arrest must be decoupled. p16 acts by preventing the association of CDK4/6 and cyclin D, thus preventing the kinase activity of D-CDK4/6 phosphorylating pRB (see Section 1.13) (Serrano et al., 1993, Gil and Peters, 2006). One mechanism by which the cell could divide in the presence of p16, would be by loss of pRB activity, either through an inactivating mutation, or repression of the coding *RB1* gene (Figure 5-8 section 1). Loss of the *RB1* gene was first observed in patients with familial retinoblastoma (Murphree and Benedict, 1984), and since then its inactivation has been repeatedly described in a variety of cancers (Stefansson et al., 2011, Anwar et al., 2014, McEvoy et al., 2014).

One of the hallmarks of BLBC is the expression of p16 in the proliferating cells as previously described (see Section 1.18.2) (Hui et al., 2000). Research has shown that the loss of *RB1* appears to be a common event in *BRCA1*-negative BLBC (Herschkowitz et al., 2008, Jönsson et al., 2012), whereas this is not the case in *BRCA2* deficient breast cancers. The high levels of p16 expression in these proliferating tumours cells could be explained by an OIS-like feedback loop caused by loss of pRB and the subsequent induction of *p16* expression as a result of unrestricted cell division

(Figure 5-8 sections 2 and 3). Loss of pRB has previously been found to correlate with high p16 expression in mammary carcinoma and BLBC (Dublin et al., 1998, Herschkowitz et al., 2008).

Among the top 116 predicted target genes related to cellular proliferation and the control of p16 expression were 17 whose gene products are signalling proteins, and 29 proteins involved in gene transcription (see Section 5.2.3.2). Many of these proteins are likely to be involved in induction of downstream pathways, and together may regulate a large number of genes within the cell.

Multiple transcription factor binding sites have been predicted within the promoter region of *RB1* by SABiosciences' (QIAGEN, NL) proprietary DECODE (Decipherment Of DNA Elements) database[I], with four of the transcription factors appearing within the top 116 predicted target genes from IPA (PPARG, targeted by miR-24; ATF2, targeted by miR-140-3p and miR-451; E2F1, targeted by miR-140-3p; CREB1, targeted by miR-140-3p and miR-221). Thus, four of the five putative oncomiRs were identified as having predicted transcription factor targets that are involved in *RB1* expression. Further interrogation of the IPA analysis identified another transcriptional regulator of *RB1,* CREBBP that is targeted by miR-574 (Appendix IV). This gene was previously excluded during the final ranking phase as it was given a low score.

[I] The SABiosciences DECODE database entry for p16 can be found at: http://www.sabiosciences.com/chipqpcrsearch.php?factor=Over+200+TF&species_id=0&ninfo=n&ngene=n&nfactor=y&gene=RB1 (accessed June 2014).

The fact that all five miRNAs are predicted to target transcriptional factors of *RB1* strongly suggests that pRB depletion is a possible cause of the higher cell number and elevated p16 observed in transfected HMECs (Figure 5-8 section 4). These results mirror the phenotype seen in BLBCs and suggest that the loss of pRB causes a common phenotype in both cell types. Current research into the knockout of *RB1* in BLBC shows that it commonly occurs as a result of intragenic breaks (Jönsson et al., 2012), which is not the case in the transfected HMECs. It is therefore hypothesised that although the HMECs take on an extreme BLBC-like phenotype when transfected with the oncomiRs, the root cause of this change is not the same as in BLBCs.

The MDA-MB-468 cell line was chosen as a model of BLBC in which to carry out further investigation into the activity of the five oncomiRs. This breast cancer cell line was selected on the basis of its proliferation in the presence of p16 (Hui et al., 2000), so that the effect of adding or removing the miRNAs could be assessed in a different system to the HMECs. These experiments proved to be wholly unsuccessful, as neither the transfection of the five miRNAs into the cells, nor the introduction of their corresponding antimiRs caused any significant changes in phenotype. In light of the bioinformatic analysis and the reported disruption of pRB in BLBCs, the status of pRB expression in the MDA-MB-468s was investigated. The MDA-MB-468 cell line was previously been found to lack pRB expression due to a deletion mutation, and its absence was confirmed by western blotting (Mizuarai et al., 2011, Robinson et al., 2013).

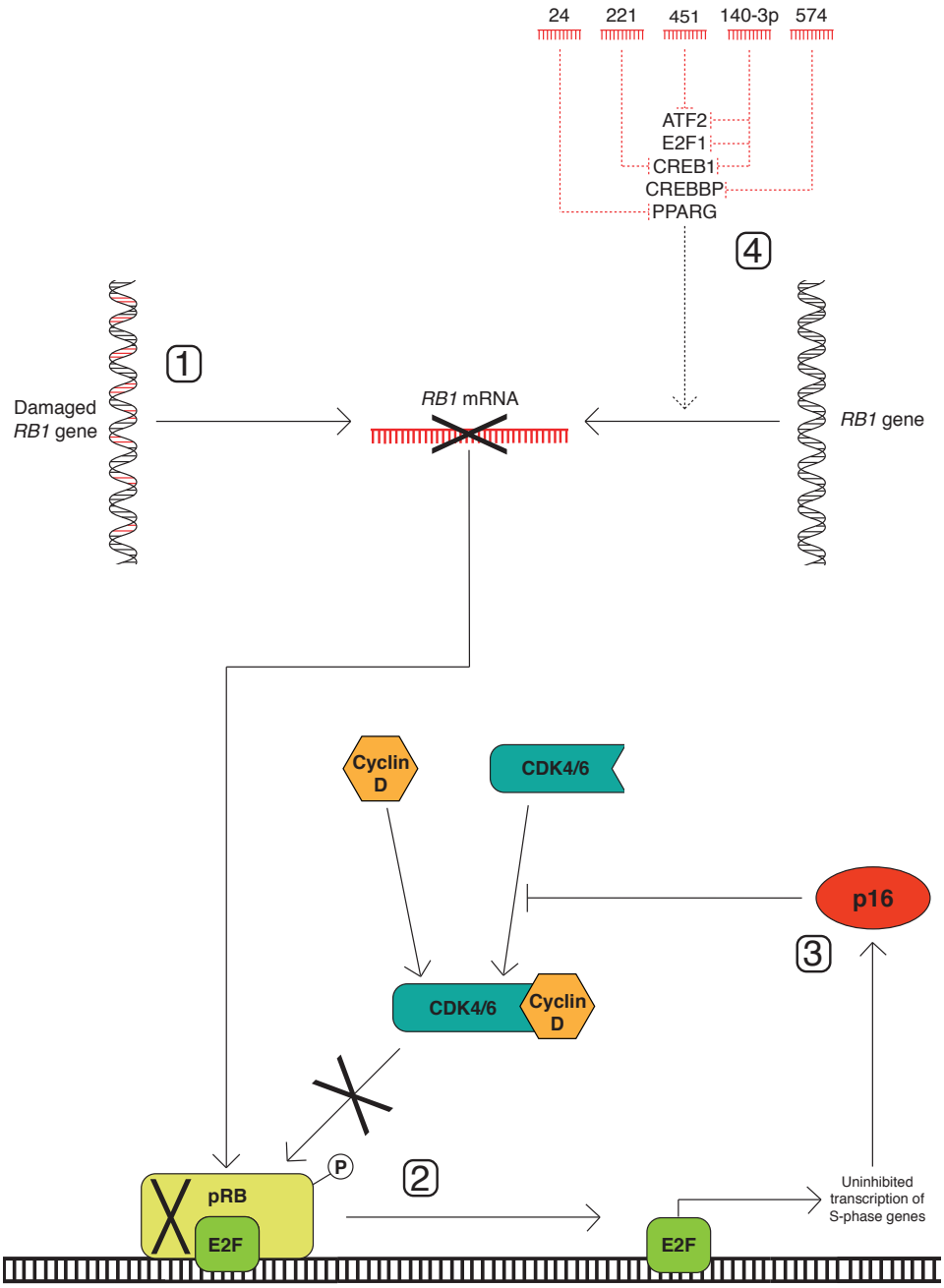

Figure 5-8. Possible mechanism describing the relationship between cell proliferation and p16 expression in BLBC and HMECs transfected with oncomiRs.

1. In BLBC and MDA-MB-468 cells the *RB1* gene is lost or mutated, and therefore cannot be transcribed. 2. Loss of pRB as a result of transcriptional inhibition or mutation of *RB1* results in the constitutive activation of the E2F transcription factors that drive cellular proliferation. As the E2F transcription factors no longer need to be released by pRB, the process is independent of D-CDK4/6 activity. 3. Uninhibited transcription of S-phase genes induces the expression of p16. p16 Activity blocks the association of CDK4/6 and cyclin D but has no effect on the rate of proliferation, as D-CDK4/6 activity is irrelevant due to the absence of pRB. 4. The five oncomiRs miR-24 (24), miR-140-3p (140-3p), miR-221 (221), miR-451 (451) and miR-574 (574) are predicted to target transcriptional factors of *RB1*. Knockdown or translational repression of the transcription factors prevents transcription of the *RB1* gene. Solid lines signify reported interactions, where as dotted lines signify proposed interactions. Black crosses mark miRNA, protein and functions not present is these cells.

The lack of pRB expression in the MDA-MB-468 cells, whilst unfortunate from an experimental standpoint, reinforces the hypothesis that the five oncomiRs act independently to increase cellular proliferation via reduction in pRB expression, leading to a positive feedback loop that induces p16 expression. If this were not the case, it is likely that the introduction or removal of the five oncomiRs would have caused a phenotypic change in the MDA-MB-468 cells. As a result of this complication, an alternative cell line in which to model BLBC should be found. In fact, the HMECs may prove an ideal cell type in which to study this process, as gene expression analysis has previously shown HMECs to resemble some BLBCs (see Section 6.2).

Another recent study has shown that loss of *DUSP4* in BLBC can lead to activation of the MAPK pathway and promote a CSC-like phenotype in the cells (Balko et al., 2013). Constitutive activation of the MAPK pathway is a well-known cause of p16 expression in cells (Lin et al., 1998), and therefore the effect of this pathway may exacerbate the observed up-regulation of p16 in BLBC. The predicted target genes contain three components of the MAPK pathway (*MAP3K1*, *MAPK7* and *MAPK12*), however these have not been found to have any association with p16 or proliferation, and are concerned with embryogenesis (*MAPK12*) (Jin et al., 2013), cardiovascular development (*MAPK7*) (Hayashi and Lee, 2004), and myoblast differentiation (MAPK12) (Lechner et al., 1996).

5.3.3 Future work

Although a strong link has been hypothesised within this chapter regarding the expression of p16 in BLBC, and in HMECs following transfection with the oncogenic miRNAs, many opportunities for future experiments based upon these findings present themselves. One of the first experiments to be carried out should be assess whether the

HMECs endogenously express any of the five oncomiRs. While the transfection of the antimiRs into the cells suggested that they were not present, carrying out a RT-qPCR assay to confirm this would allow for a clearer interpretation of the results.

Another informative experiment that could be carried out in the HMECs, is to study the effects of long term miRNA expression, in terms of cellular growth over time and p16 expression. The miRNA genes could be introduced into the cells using a lentiviral miRNA vector, allowing for constant expression to be studied. Assays could be performed on these cells to investigate whether other cell cycle checkpoints can halt cell growth in the absence of p16-mediated senescence. Long-term rates of proliferation could also be measured, and compared to wild type cells to determine whether the transfected HMECs divide at an accelerated, or equivalent rate relative to low passage HMECs.

During the course of these experiments, the antimiRs could also be transfected into the HMECs to perform rescue experiments. These experiments would investigate whether removal of the oncomiRs restores the cell to its original phenotype of being highly sensitive to p16 expression. If these antimiRs experiments were successful, older cells stably expressing the oncomiRs, could also be tested, to see whether any changes in cell behaviour occur in response to long-term dysregulation of pRB. The experiments described here may provide an insight into whether the reactivation of pRB could be used as a potential therapy for BLBC.

In addition to the experiments previously suggested, the hypothesis that both BLBCs and the oncomiRs act by dysregulation of pRB should be investigated in more detail.

An important first experiment would be to quantify the expression of the key genes identified in Section 5.3.2, namely: *RB1, ATF2*, *E2F1*, *CREB1*, *CREBBP* and *PPARG*; either by western blot or RT-qPCR. If these genes were down-regulated in HMECs after transfection with the appropriate miRNA, it would provide further evidence for the hypothesis. Additionally, as miRNAs do not always cause target mRNA degradation, 3'UTR luciferase assays, together with target site mutagenesis for the genes should be carried out to ensure the miRNAs can repress these predicted target genes.

If possible, the levels of the other predicted genes from the top 116 hits should be evaluated using luciferase assays, to discover which of these are physiologically relevant in the HMECs. The genes found to be affected by the miRNAs could then be studied in the cells, by observing their expression levels in a variety of situations; such as the differences between low and high passage cells, and transfected and untransfected cells. In addition to these genes, the expression of *BRCA1* should also be evaluated, as it was previously found to coincide with pRB disruption in BLBC (Stefansson et al., 2011).

For more in-depth analysis of the molecular changes undergone by HMECs in response to transfection with the five oncomiRs, RNA-seq could be employed to examine changes in gene expression, miRNAs, and other ncRNAs. The technique could be carried out to look at the differences between untransfected HMECs and HMECs transfected with each of, and combinations of, the five miRNAs. The technique would allow recognition the molecular mechanisms at play in each condition, identify common pathways, and inform further study with respect to each miRNA and the downstream cascade of cellular changes each induces. In addition to these samples, extra RNA-seq

studies could be carried out in HMECs by looking for changes in the expression of relevant genes between young cells, old cells, and cells which have escaped cellular senescence. These experiments might provide insight into any similarities and differences in the transcriptome of cells that have escaped senescence 'naturally', compared to cells that have bypassed senescence as a result of oncomiR activity.

Any extra genes or ncRNAs identified by RNA-seq should be subsequently investigated further by overexpression or knockdown experiments in HMECs, depending on their expression profiles. Detailed and careful mapping of each of the possible interacting genes in these pathways will allow for the mechanisms behind the enhanced cellular proliferation in the presence of p16 observed in transfected HMECs, and possibly the similar phenotype seen in BLBC, to be properly understood.

The list of predicted target genes generated in this study could also be used in future bioinformatic studies of patient data. The expression levels of both the miRNAs and the predicted targets genes could be studied in patient-sample data set in order to search for correlations between gene and miRNA expression, and survival. In depth analysis of this type of data may provide novel genetic markers for disease progression, and therefore inform future therapy choices for patients.

Chapter Six

6 General Discussion

6.1 ABCB5 and p16

In Chapter 3, wild type and mutant forms of ABCB5fl and ABCB5β were transiently expressed in HEK293T cells in order to characterise these proteins. The proteins were poorly expressed and found to localise to the endoplasmic reticulum, as apparent from previous studies (Frank et al., 2003, Linley et al., 2012, Mathieu et al., 2014), although not highlighted by authors in the published data (see Section 3.3.2). In Chapter 4, siRNA knockdown of *ABCB5β* in HMECs was shown to cause a concomitant reduction in *p16* expression. RT-qPCR and 5' RACE PCR confirmed that *ABCB5β* mRNA was present in these primary cells, but neither ABCB5fl nor ABCB5β protein were detectable, leading to the hypothesis that the *ABCB5β* mRNA may act as a lncRNA in HMECs.

6.1.1 Antibodies targeting ABCB5

The ability to engineer expression of ABCB5fl and ABCB5β in a naïve host allowed the three commercially available antibodies, designated Atlas, Rockland and Sigma, to be validated. Only the Atlas antibody was found to accurately identify ABCB5fl and ABCB5β (see Section 3.2.1). Some of the prior investigations used the Rockland (Kawanobe et al., 2012) and Sigma (Linley et al., 2012, Mathieu et al., 2014) antibodies found to lack efficacy in the current study, necessitating re-evaluation of the data. Several of the other studies of these proteins have used antibodies generated in-house (Frank et al., 2003, Frank et al., 2005, Schatton et al., 2008, Ksander et al., 2014). These in-house generated antibodies were not available to test herein, therefore their veracity has not been examined alongside those that are commercially available. This poses an issue because most of the previous work on ABCB5fl and ABCB5β is based largely

upon antibody use, and the assumption that they are highly effective markers of ABCB5 protein expression.

Some studies, using polyclonal antibodies have used blocking peptides as negative controls (Wilson et al., 2011, Ramgolam et al., 2011). However, these do not always provide a true negative control. If an antibody is polyclonal, the preparation may contain antibodies against other proteins in addition to the immunogen (Saper and Sawchenko, 2003). These non-specific antibodies are likely to bind proteins other than the intended target. Presumably, this is the case with the Rockland polyclonal antibody against ABCB5, in which the number of antibodies targeting other proteins appear to greatly outnumber those that target ABCB5.

It is also understood that no two animals will produce an identical immune response to the same immunogen, as each animal has its own distinct immune system, and thus will have a different immune response to the immunogen (Ritter, 2000, Saper and Sawchenko, 2003). All the antibodies tested in this work were polyclonal; it is therefore theoretically possible that some of the differences in specificity observed between this study and those in the literature are due to differences in antibody composition between batches. It is more likely, however, that some of the earlier observations are erroneous due to the lack of specificity of the commercially available antibodies.

6.1.2 Re-evaluation of published anti-ABCB5 antibody data

As two of the three commercially available antibodies were not found to target ABCB5fl or ABCB5β, the conclusions of some previously published papers, which

used these (Kawanobe et al., 2012, Linley et al., 2012, Mathieu et al., 2014), need to be re-examined for accuracy.

6.1.2.1 Does ABCB5 confer drug resistance to expressing cells?

The 2012 study published by Kawanobe et al. used the Rockland anti-ABCB5 antibody to detect expression of ABCB5fl protein in stably expressing naive HEK293 cells (Kawanobe et al., 2012). When evaluated by western blot in Chapter 3, the Rockland antibody failed to detect any protein of the expected molecular weight in whole cell lysates of cells expressing ABCB5fl or ABCB5β, but bound to many other proteins of lower molecular weights in both transfected and untransfected control HEK239T cells. The figure reportedly showing antibody binding to ABCB5fl in the paper is heavily cropped, with multiple proteins are detected in each lane, no indicators of molecular weight, and protein detected in the untransfected control cells with lack endogenous ABCB5 (Kawanobe et al., 2012).

However, ABCB5fl protein expression is corroborated by the use of a Myc-tagged ABCB5fl construct, detected by an anti-Myc antibody (Kawanobe et al., 2012). These data are more convincing showing a similar pattern of staining to that observed for the Atlas anti-ABCB5 antibody used herein. The use of the Rockland antibody in the published study formed a pattern of staining, although different from the pattern observed with the anti-Myc antibody, and resembling the lower pattern of lower molecular weight bands recorded for the Rockland antibody in Chapter 3. Without the molecular weight marker visible in the figure, however, it is impossible to determine the migration of the presented bands (Kawanobe et al., 2012). Similar to my findings, ABCB5fl expressed poorly following transient transfection, but Kawanobe *et al*. were

able to clone stably transfected cell lines, which provided more robust expression. The intracellular localisation of the expressed protein was not determined.

The study aimed to evaluate whether ABCB5fl expressed in HEK293s could confer resistance to doxorubicin, paclitaxel and docetaxel; three chemotherapeutic agents which are thought to be substrates of ABCC1 and ABCC2 (Cui et al., 1999, Borst et al., 2000, Huisman et al., 2005), two ABC transporters which are endogenously expressed within this cell line (Borel et al., 2011). The difference in resistance between the expressing and control cells is relatively small (two fold, whereas ABCB1 often confers a three fold or higher change resistance to expressing cells (Shen et al., 1986)) and could be accounted for by experimental variation, or changes in the cell line as a result of serial selection of the ABCB5fl expressing clones.

Studies using cells endogenously expressing ABCB5β have previously reported the ability of the protein to efflux doxorubicin, with drug accumulation found to be half that of non-expressing cells (Frank et al., 2005). The cells (G3361 melanoma cells) were sorted for ABCB5β expression by fluorescence-activated cell sorting using an in-house generated monoclonal antibody. The efficacy of this antibody is unknown as it was not available for testing herein, and the study did not use a cell line that was known to lack ABCB5β expression as a negative control. Given these caveats, I remain to be convinced that either recombinant ABCB5fl or endogenous ABCB5β can effectively confer drug resistance to naïve cells.

6.1.2.2 Is ABCB5 important in malignant melanoma?

In both their 2012 and 2014 papers, the Regad group used the Sigma anti-ABCB5 antibody to assess the expression of ABCB5 in MMICs (Linley et al., 2012, Mathieu et al., 2014). In these studies, the antibody was used for both immunofluorescence and immunoblot assays to identify ABCB5 expression, and its correlation to HAGE (an RNA helicase linked to malignancy in melanoma) expression across the cells. The immunoblots using the antibody in this study identified a single protein species migrating at around 90 kDa, equating to ABCB5β, although as the blots were cropped at 75 kDa, any bands at lower molecular weights are not visible. In Chapter 3, this antibody was unable to detect any ABCB5fl or ABCB5β protein by western blotting under conditions in which the Rockland antibody clearly and cleanly detects both.

In these papers, the Sigma anti-ABCB5 antibody is used as a marker of ABCB5β and clear differences are observed when normal tissue and malignant melanoma samples are compared (Mathieu et al., 2014, Linley et al., 2012). From my data, the Sigma antibody does not appear to detect ABCB5β, which leaves me to conclude that either: I was provided with bad batches of antibody from Sigma (two separate batches were tested in total); or while the antibody may be able to mark a population of MMICs, it is not ABCB5β or a protein that is expressed in HEK293T cells.

ABCB5β expression was first identified as a possible marker for MMICs by the Frank group (Schatton et al., 2008), although no immunoblots were performed in this study. Consequently, the results of this study and the Kawanobe study cannot be directly compared. All detection of ABCB5β in the Frank study was performed by flow cytometry and immunohistochemistry with a monoclonal antibody that was generated

in-house. No negative controls for the accuracy of antibody staining were used, so it is difficult to know how specific the detection of ABCB5β in this study was (Schatton et al., 2008). It is possible that the antibody may be raised against a similar peptide sequence to the Sigma antibody allowing the same, although incorrect, protein to be identified as marking MMICs in both studies.

6.1.3 *ABCB5β* and *p16* expression in ageing HMECs

The parallel rise in expression of the *ABCB5β* and *p16* transcripts with HMEC culture age remains to be explained. At present, there is no published information on which transcription factors or cellular signals act to induce the expression of *ABCB5β,* or indeed any of the isoforms of *ABCB5*.

Although it is questionable at present, if expression of ABCB5fl does actually confer drug resistance to expressing cells (Frank et al., 2005, Kawanobe et al., 2012), it is possible that the nuclear receptors pregnane X receptor (PXR), and retinoid X receptor (RXR), could induce expression of the ABCB5 isoforms in response to xenobiotic compounds (Kliewer et al., 2002), as these receptors are known to do for the drug efflux pumps ABCB1 and ABCG2 (Geick et al., 2001, Synold et al., 2001, Lemmen et al., 2013).

Multiple, though not experimentally confirmed, transcription factor binding sites have been identified in the 3' region of the *ABCB5* gene by SABiosciences' (QIAGEN, NL)

proprietary DECODE (Decipherment Of DNA Elements) database[I] (Figure 4-17 section 1). None of the predicted transcription factor binding sites for *ABCB5* are shared with *p16,* suggesting that the coordinate expression is not simply due to both genes being regulated by the same transcription factor. This could have possibly accounted for their tandem increase in expression in ageing cells, but would not have accounted for the concomitant decrease in p16 observed upon knockdown of *ABCB5β.*

6.1.4 ABCB5β in stem cell maintenance

A very recent study has suggested that ABCB5β protein is essential for corneal development and repair, via the maintenance of the limbal stem cell (LSC) population in the eye (Ksander et al., 2014). This paper contains the first reported description of an *Abcb5*$^{-/-}$ knockout mouse, which was engineered to lack expression of both *ABCB5fl* and *ABCB5β*. These mice are reported to be physically indistinguishable from the wild type animals (Ksander et al., 2014).

This work was carried out by the Frank group, who have extensively used in-house generated monoclonal antibodies, which were not available for testing, to assess ABCB5β and ABCB5fl protein expression in multiple tumours and cell types (Schatton et al., 2008, Frank and Frank, 2009, Volpicelli et al., 2014). The antibodies were used for western blotting and immunofluorescence, alongside RT-PCR, to demonstrate the knockout of *ABCB5β*. It should be noted that the immunofluorescence data published in

[I] The SABiosciences DECODE database entry for ABCB5 can be found at: http://www.sabiosciences.com /chipqpcrsearch.php?species_id=0&nfactor=n&ninfo=n&ngene=n&B2=Search&src=genecard&factor=Over+200+TF&gene=ABCB5 (accessed January 2014).

this paper appears to be intracellular, as with their previous work (see Section 3.3.2) (Ksander et al., 2014).

Histological examination of the knockout animals' eyes revealed various developmental abnormalities, such as reduced epithelial cell numbers, defects in epithelial tight junctions, a disorganised basal cell layer, and increased cornea fragility. These observations, and subsequent experiments, identified an important role for the *Abcb5* gene in maintaining the LSC population. Additionally, the grafting of human or murine LSCs with endogenous *ABCB5*$^{+}$ (or *Abcb5*$^{+}$) expression to LSC-deficient mice was able to fully restore the cornea. Only *ABCB5*$^{+}$ (or *Abcb5*$^{+}$) LSCs had this restorative effect, as apposed to LSCs which lacked endogenous expression of the protein.

Knockout of *Abcb5β* in LSCs was found to cause enhanced proliferation and apoptosis, leading to a reduction in the number of quiescent LSCs available for corneal differentiation and wound healing (Ksander et al., 2014). Knockout of *Abcb5β* in LSCs increased cellular proliferation, similar to the phenotype following the knockdown of *ABCB5β* in HMECs. It would be interesting to explore whether these observations in different cell types are related. This could be achieved by RNA-seq methodology outlined in Section 4.3.3, where changes in both HMEC and LSC RNA expression patterns after *ABCB5β* knockdown could be compared.

Studies have previously identified senescence to be important in wound healing (Jun and Lau, 2010) and embryonic development (via p21 as apposed to p16) (Muñoz-Espín et al., 2013). The finding that Abcb5β is essential for the development and healing of murine eyes by LSCs could be an indication of a more ubiquitous role for expression of

ABCB5β in mechanisms of senescence. Future experiments could investigate a possible role for ABCB5β in these processes of senescence by studying differences in wound healing between wild type and *ABCB5β*-null cells.

It should be noted, however, that some of the changes in LSC phenotype were also seen upon blockade of Abcb5β by antibodies (although not antibodies tested herein), suggesting an active role for the Abcb5β protein within the cells (Ksander et al., 2014). This result could suggest that the ABCB5β protein is relevant in HMECs, although present at undetectable levels. If this were the case, it would suggest that ABCB5β is an extremely potent effector of the cell cycle, if such small changes in protein level were found to cause such a drastic change in cellular phenotype.

6.2 Oncogenic miRNAs and BLBC

In Chapter 6, the effect of five putative oncomiRs on p16 expression and cellular proliferation in HMECs and a model of BLBC were examined. The five putative oncomiRs were found to cause an increase in cellular proliferation, and subsequent response of *p16* expression, confirming their oncogenic status. Bioinformatic analysis suggested that the oncomiRs act by disrupting expression of the pRB gene *RB1*, allowing unrestricted cellular proliferation, even in the presence of the potent tumour suppressor p16.

6.2.1 HMECs as a model for BLBC

As discussed in Section 5.3, one of the aims of this project was to identify an alternative cell type to the HMECs in which to model BLBC. The MBA-MB-468 cell line was chosen, as it both expresses *p16* and continues to divide, in a similar manner to the

cancer subtype. The experiments that introduced the five oncomiRs and their respective antimiRs into these cells, found no changes in cellular phenotype or proliferative rate. This is likely to be due to the lack of pRB expression in this cell line. Other research indicates that HMECs may in fact be an excellent cell type in which to construct a model of BLBC, as the cells share many of the same expression characteristics (Perou et al., 1999, Perou et al., 2000).

These studies from the Botstein lab showed that both HMECs and BLBCs highly express a cluster of IFN-regulated genes, including *STAT1* and *LOX*, which are known to increase proliferation in expressing cells (Perou et al., 1999, Sun et al., 2007, Wang et al., 2013). The induction of these genes in HMECs coincides with growth arrest as a result of premature senescence, suggesting that this gene cluster may be involved in the activation of OIS, thereby laying the groundwork for cellular transformation (Perou et al., 1999). Indeed, a high level of *STAT1* expression was detected in many of the breast cancer samples used in the study, as a result of the IFN-regulated cluster previously mentioned (Perou et al., 1999). STAT1 has been suggested to play a role in the carcinogenic process which breast cells undergo to become tumourous, although the exact mechanism is currently unknown (Perou et al., 1999).

Overall, these data point to HMECs as an ideal cell type in which the stepwise transformation of normal breast cells to breast cancer cells could be modelled and studied to gain an understanding into the cellular mechanisms at play in the process. Additional work to identify a cell line that can be used as a model of established disease may be prudent for future study of the oncomiRs, although for the time being the

HMECs may actually provide a wealth of information about the action of the oncomiRs, and about the transformation of breast cells in general.

6.2.2 OncomiRs in p16-associated disease

In addition to the possible mechanisms of oncomiR and p16 interaction proposed in Section 5.3, which were hypothesised as a result of the predicted target genes, the five oncomiRs have all previously been linked to age-related disorders which are either known to, or thought to, involve p16.

All five oncomiRs have been reported to be disregulated in cancers, although this could be due to the large number of changes in gene expression commonly observed in transformed cells. *miR-24*, *miR-221*, *miR-451* and *miR-574* are, however, all up-regulated in various cancers (Foss et al., 2011, Du et al., 2013, Aldaz et al., 2013, Dai et al., 2013), with *miR-221* suggested to hold an actively oncogenic role, especially in glioblastoma multiform (Aldaz et al., 2013). The altered expression of the oncomiRs observed in a variety of cancers suggests strong links to cellular proliferation.

In addition to their dysregulation in cancer, the oncomiRs have been associated with other age-related diseases linked to the up regulation of *p16* expression such as type 1 diabetes mellitus (*miR-24*) (Zhu et al., 2013b), type 2 diabetes mellitus (*miR-140-3p*) (Collares et al., 2013) and coronary heart disease (*miR-140-3p*) (Taurino et al., 2010). These studies are consistent with a role for these oncomiRs in the induction of cellular senescence via expression of p16.

The oncomiRs can clearly act by different mechanisms in different cell types to produce disparate effects, such as *miR-24* being able to promote (Giglio et al., 2013), or inhibit

(Song et al., 2013), cancer cell proliferation, in keratinocytes and osteosarcoma, respectively. A important point for future study should be to identify the genes, which are responsible for driving the cellular phenotypes observed upon oncomiR expression. This could be carried out by transfecting a panel of cancer cells from a range of relevant tissues with the oncomiRs, and examining the changes in gene expression and the corresponding cellular phenotype which occur compared to untransfected control cells. The cross-referencing of this dataset could reveal which genes are key for driving the proliferative phenotypes. The aim of this experimental plan would be to provide possible candidate genes for further investigation, and potentially identify new therapeutic targets.

6.3 Concluding remarks

The experiments described in this thesis have provided important insights into mechanisms of p16 regulation, which will inform future work around this topic.

Finding a cell line in which ABCB5fl and ABCB5β can be efficiently expressed transiently would provide an avenue for further research into the intriguing isoforms of this protein. The experiments here described were not able to establish the HEK293T cell line as an effective host for the expression of these proteins, although they did raise questions about, and provide useful insights into, the interpretation of data previously published from other laboratories. The efficacies of previously described antibodies are clearly questionable, and the practice of solely relying on antibody binding to mark ABCB5β expression for expansive studies is improvident. Antibodies are biological molecules and are not infallible in the assessment of protein expression.

The knockdown of *ABCB5β* mRNA by siRNA has been demonstrated to cause a concomitant reduction in *p16* expression. This result has added to the growing body of evidence suggesting that products of the *ABCB5* gene have a variety of downstream implications in addition to the possible transport of substrates across membranes by protein products of the gene. The observation that the ABCB5β protein does not appear to be present within the HMECs was surprising, especially as previous studies examining the role of ABCB5β in cells have suggested that the effects of expression are mediated at the protein level, with changes in cellular phenotype observed upon blockade with an ABCB5β-targeting monoclonal antibody. The simplest interpretation of the data reported herein is that the *ABCB5β* mRNA can act as a lncRNA. Future studies to confirm the exact nature of the relationship between *ABCB5β* and *p16* expression will be critical to understanding the mechanism of action.

Providing further insights into the mechanism of *p16* expression and cellular proliferation in cancer, five oncomiRs have been identified which contradictorily increase both of these factors in HMECs. The recognition that these oncomiRs can cause the cell to enter an OIS-like feedback-loop as a result of their expression has provided an exciting opportunity to use these cells as a model of breast cell transformation. The bioinformatic identification of predicted gene targets for each of the oncomiRs has provided a basis on which future studies can be systematically carried out, to gain a real insight into the processes that go into the formation and progression of these aggressive breast tumours.

Bibliography

ABD EL-REHIM, D. M., BALL, G., PINDER, S. E., RAKHA, E., PAISH, C., ROBERTSON, J. F., MACMILLAN, D., BLAMEY, R. W. & ELLIS, I. O. 2005. High-throughput protein expression analysis using tissue microarray technology of a large well-characterised series identifies biologically distinct classes of breast cancer confirming recent cDNA expression analyses. *Int J Cancer,* 116**,** 340-50.

ABD EL-REHIM, D. M., PINDER, S. E., PAISH, C. E., BELL, J., BLAMEY, R. W., ROBERTSON, J. F., NICHOLSON, R. I. & ELLIS, I. O. 2004. Expression of luminal and basal cytokeratins in human breast carcinoma. *J Pathol,* 203**,** 661-71.

ABOU-BAKR, A. A. & ELDWENY, H. I. 2013. p16 expression correlates with basal-like triple-negative breast carcinoma. *Ecancermedicalscience,* 7**,** 317.

ACOSTA, J. C., BANITO, A., WUESTEFELD, T., GEORGILIS, A., JANICH, P., MORTON, J. P., ATHINEOS, D., KANG, T. W., LASITSCHKA, F., ANDRULIS, M., PASCUAL, G., MORRIS, K. J., KHAN, S., JIN, H., DHARMALINGAM, G., SNIJDERS, A. P., CARROLL, T., CAPPER, D., PRITCHARD, C., INMAN, G. J., LONGERICH, T., SANSOM, O. J., BENITAH, S. A., ZENDER, L. & GIL, J. 2013. A complex secretory program orchestrated by the inflammasome controls paracrine senescence. *Nat Cell Biol,* 15**,** 978-90.

ALCALAY, M., TOMASSONI, L., COLOMBO, E., STOLDT, S., GRIGNANI, F., FAGIOLI, M., SZEKELY, L., HELIN, K. & PELICCI, P. G. 1998. The promyelocytic leukemia gene product (PML) forms stable complexes with the retinoblastoma protein. *Mol Cell Biol,* 18**,** 1084-93.

ALDAZ, B., SAGARDOY, A., NOGUEIRA, L., GURUCEAGA, E., GRANDE, L., HUSE, J. T., AZNAR, M. A., DÍEZ-VALLE, R., TEJADA-SOLÍS, S., ALONSO, M. M., FERNANDEZ-LUNA, J. L., MARTINEZ-CLIMENT, J. A. & MALUMBRES, R. 2013. Involvement of miRNAs in the differentiation of human glioblastoma multiforme stem-like cells. *PLoS One,* 8**,** e77098.

AMBUDKAR, S. V., DEY, S., HRYCYNA, C. A., RAMACHANDRA, M., PASTAN, I. & GOTTESMAN, M. M. 1999. Biochemical, cellular, and pharmacological aspects of the multidrug transporter. *Annu Rev Pharmacol Toxicol,* 39**,** 361-98.

ANDERSON, E. M., BIRMINGHAM, A., BASKERVILLE, S., REYNOLDS, A., MAKSIMOVA, E., LEAKE, D., FEDOROV, Y., KARPILOW, J. & KHVOROVA, A. 2008. Experimental validation of the importance of seed complement frequency to siRNA specificity. *RNA,* 14**,** 853-61.

ANDERSON, W. F., CHU, K. C., CHATTERJEE, N., BRAWLEY, O. & BRINTON, L. A. 2001. Tumor variants by hormone receptor expression in white patients with node-negative breast cancer from the surveillance, epidemiology, and end results database. *J Clin Oncol,* 19**,** 18-27.

ANWAR, S. L., KRECH, T., HASEMEIER, B., SCHIPPER, E., SCHWEITZER, N., VOGEL, A., KREIPE, H. & LEHMANN, U. 2014. Deregulation of RB1 expression by loss of imprinting in human hepatocellular carcinoma. *J Pathol*. 223, 392-401.

BAEK, D., VILLÉN, J., SHIN, C., CAMARGO, F. D., GYGI, S. P. & BARTEL, D. P. 2008. The impact of microRNAs on protein output. *Nature,* 455**,** 64-71.

BAGGA, S., BRACHT, J., HUNTER, S., MASSIRER, K., HOLTZ, J., EACHUS, R. & PASQUINELLI, A. E. 2005. Regulation by let-7 and lin-4 miRNAs results in target mRNA degradation. *Cell,* 122**,** 553-63.

BAGULEY, B. C. 2010. Multiple drug resistance mechanisms in cancer. *Mol Biotechnol,* 46**,** 308-16.

BAKER, D. J., WIJSHAKE, T., TCHKONIA, T., LEBRASSEUR, N. K., CHILDS, B. G., VAN DE SLUIS, B., KIRKLAND, J. L. & VAN DEURSEN, J. M. 2011. Clearance of p16Ink4a-positive senescent cells delays ageing-associated disorders. *Nature,* 479**,** 232-6.

BALKO, J. M., SCHWARZ, L. J., BHOLA, N. E., KURUPI, R., OWENS, P., MILLER, T. W., GÓMEZ, H., COOK, R. S. & ARTEAGA, C. L. 2013. Activation of MAPK pathways due to DUSP4 loss promotes cancer stem cell-like phenotypes in basal-like breast cancer. *Cancer Res,* 73**,** 6346-58.

BARTEL, D. P. 2004. MicroRNAs: genomics, biogenesis, mechanism, and function. *Cell,* 116**,** 281-97.

BARTZ, F., KERN, L., ERZ, D., ZHU, M., GILBERT, D., MEINHOF, T., WIRKNER, U., ERFLE, H., MUCKENTHALER, M., PEPPERKOK, R. & RUNZ, H. 2009. Identification of cholesterol-regulating genes by targeted RNAi screening. *Cell Metab,* 10**,** 63-75.

BAVIK, C., COLEMAN, I., DEAN, J. P., KNUDSEN, B., PLYMATE, S. & NELSON, P. S. 2006. The gene expression program of prostate fibroblast senescence modulates neoplastic epithelial cell proliferation through paracrine mechanisms. *Cancer Res,* 66**,** 794-802.

BEERS, M. F., ZHAO, M., TOMER, Y., RUSSO, S. J., ZHANG, P., GONZALES, L. W., GUTTENTAG, S. H. & MULUGETA, S. 2013. Disruption of N-linked glycosylation promotes proteasomal degradation of the human ATP-binding cassette transporter ABCA3. *Am J Physiol Lung Cell Mol Physiol,* 305**,** L970-80.

BELINSKY, M. G., CHEN, Z. S., SHCHAVELEVA, I., ZENG, H. & KRUH, G. D. 2002. Characterization of the drug resistance and transport properties of multidrug resistance protein 6 (MRP6, ABCC6). *Cancer Res,* 62**,** 6172-7.

BERNSTEIN, B. E., BIRNEY, E., DUNHAM, I., GREEN, E. D., GUNTER, C., SNYDER, M. & CONSORTIUM, E. P. 2012. An integrated encyclopedia of DNA elements in the human genome. *Nature,* 489**,** 57-74.

BERTOLI, C., SKOTHEIM, J. M. & DE BRUIN, R. A. 2013. Control of cell cycle transcription during G1 and S phases. *Nat Rev Mol Cell Biol,* 14**,** 518-28.

BISHOP, C. L., BERGIN, A. M., FESSART, D., BORGDORFF, V., HATZIMASOURA, E., GARBE, J. C., STAMPFER, M. R., KOH, J. & BEACH, D. H. 2010. Primary cilium-dependent and -independent Hedgehog signaling inhibits p16(INK4A). *Mol Cell,* 40**,** 533-47.

BLAGOSKLONNY, M. V. 2003. Cell senescence and hypermitogenic arrest. *EMBO Rep,* 4**,** 358-62.

BOBADILLA, J. L., MACEK, M., FINE, J. P. & FARRELL, P. M. 2002. Cystic fibrosis: a worldwide analysis of CFTR mutations--correlation with incidence data and application to screening. *Hum Mutat,* 19**,** 575-606.

BOONSTRA, R., TIMMER-BOSSCHA, H., VAN ECHTEN-ARENDS, J., VAN DER KOLK, D. M., VAN DEN BERG, A., DE JONG, B., TEW, K. D., POPPEMA, S. & DE VRIES, E. G. 2004. Mitoxantrone resistance in a small cell lung cancer cell line is associated with ABCA2 upregulation. *Br J Cancer,* 90**,** 2411-7.

BOREL, F., VAN LOGTENSTEIN, R., KOORNNEEF, A., MACZUGA, P., RITSEMA, T., PETRY, H., VAN DEVENTER, S. J., JANSEN, P. L. & KONSTANTINOVA, P. 2011. In vivo knock-down of multidrug resistance transporters ABCC1 and ABCC2 by AAV-delivered shRNAs and by artificial miRNAs. *J RNAi Gene Silencing,* 7**,** 434-42.

BORST, P., EVERS, R., KOOL, M. & WIJNHOLDS, J. 2000. A family of drug transporters: the multidrug resistance-associated proteins. *J Natl Cancer Inst,* 92**,** 1295-302.

BRACKEN, A. P., KLEINE-KOHLBRECHER, D., DIETRICH, N., PASINI, D., GARGIULO, G., BEEKMAN, C., THEILGAARD-MÖNCH, K., MINUCCI, S., PORSE, B. T., MARINE, J. C., HANSEN, K. H. & HELIN, K. 2007. The Polycomb group proteins bind throughout the INK4A-ARF locus and are disassociated in senescent cells. *Genes Dev,* 21**,** 525-30.

BRADEN, W. A., LENIHAN, J. M., LAN, Z., LUCE, K. S., ZAGORSKI, W., BOSCO, E., REED, M. F., COOK, J. G. & KNUDSEN, E. S. 2006. Distinct action of the retinoblastoma pathway on the DNA replication machinery defines specific roles for cyclin-dependent kinase complexes in prereplication complex assembly and S-phase progression. *Mol Cell Biol,* 26**,** 7667-81.

BRASS, A. L., DYKXHOORN, D. M., BENITA, Y., YAN, N., ENGELMAN, A., XAVIER, R. J., LIEBERMAN, J. & ELLEDGE, S. J. 2008. Identification of host proteins required for HIV infection through a functional genomic screen. *Science,* 319**,** 921-6.

BREEDEN, L. & NASMYTH, K. 1987. Similarity between cell-cycle genes of budding yeast and fission yeast and the Notch gene of Drosophila. *Nature,* 329**,** 651-4.

BRENNER, A. J., STAMPFER, M. R. & ALDAZ, C. M. 1998. Increased p16 expression with first senescence arrest in human mammary epithelial cells and extended growth capacity with p16 inactivation. *Oncogene,* 17**,** 199-205.

BRENTON, J. D., CAREY, L. A., AHMED, A. A. & CALDAS, C. 2005. Molecular classification and molecular forecasting of breast cancer: ready for clinical application? *J Clin Oncol,* 23**,** 7350-60.

BURCHARD, J., JACKSON, A. L., MALKOV, V., NEEDHAM, R. H., TAN, Y., BARTZ, S. R., DAI, H., SACHS, A. B. & LINSLEY, P. S. 2009. MicroRNA-like off-target transcript regulation by siRNAs is species specific. *RNA,* 15**,** 308-15.

BURNETTE, W. N. 1981. "Western blotting": electrophoretic transfer of proteins from sodium dodecyl sulfate--polyacrylamide gels to unmodified nitrocellulose and radiographic detection with antibody and radioiodinated protein A. *Anal Biochem,* 112**,** 195-203.

BUSCHMAN, E., ARCECI, R. J., CROOP, J. M., CHE, M., ARIAS, I. M., HOUSMAN, D. E. & GROS, P. 1992. mdr2 encodes P-glycoprotein expressed in the bile canalicular membrane as determined by isoform-specific antibodies. *J Biol Chem,* 267**,** 18093-9.

BYEON, I. J., LI, J., ERICSON, K., SELBY, T. L., TEVELEV, A., KIM, H. J., O'MAILLE, P. & TSAI, M. D. 1998. Tumor suppressor p16INK4A: determination of solution structure and analyses of its interaction with cyclin-dependent kinase 4. *Mol Cell,* 1**,** 421-31.

BÄHLER, J. 2005. Cell-cycle control of gene expression in budding and fission yeast. *Annu Rev Genet,* 39**,** 69-94.

CAI, X., HAGEDORN, C. H. & CULLEN, B. R. 2004. Human microRNAs are processed from capped, polyadenylated transcripts that can also function as mRNAs. *RNA,* 10**,** 1957-66.

CAILLEAU, R., OLIVÉ, M. & CRUCIGER, Q. V. 1978. Long-term human breast carcinoma cell lines of metastatic origin: preliminary characterization. *In Vitro,* 14**,** 911-5.

CALCAGNO, A. M., FOSTEL, J. M., TO, K. K., SALCIDO, C. D., MARTIN, S. E., CHEWNING, K. J., WU, C. P., VARTICOVSKI, L., BATES, S. E., CAPLEN, N. J. & AMBUDKAR, S. V. 2008. Single-step doxorubicin-selected cancer cells overexpress the ABCG2 drug transporter through epigenetic changes. *Br J Cancer,* 98**,** 1515-24.

CAMPISI, J. 2013. Aging, cellular senescence, and cancer. *Annu Rev Physiol,* 75**,** 685-705.

CHANDLER, H. & PETERS, G. 2013. Stressing the cell cycle in senescence and aging. *Curr Opin Cell Biol,* 25**,** 765-71.

CHEN, H., GU, X., LIU, Y., WANG, J., WIRT, S. E., BOTTINO, R., SCHORLE, H., SAGE, J. & KIM, S. K. 2011. PDGF signalling controls age-dependent proliferation in pancreatic β -cells. *Nature,* 478**,** 349-55.

CHEN, K., SZAKÁCS, G., ANNEREAU, J., ROUZAUD, F., LIANG, X., VALENCIA, J., NAGINENI, C., HOOKS, J., HEARING, V. & GOTTESMAN, M. 2005a. Principal expression of two mRNA isoforms (ABCB 5alpha and ABCB 5beta) of the ATP-binding cassette transporter gene ABCB 5 in melanoma cells and melanocytes. *Pigment Cell Res,* 18**,** 102-12.

CHEN, K., VALENCIA, J., GILLET, J., HEARING, V. & GOTTESMAN, M. 2009. Involvement of ABC transporters in melanogenesis and the development of multidrug resistance of melanoma. *Pigment Cell Melanoma Res,* 22**,** 740-9.

CHEN, Z., TROTMAN, L. C., SHAFFER, D., LIN, H. K., DOTAN, Z. A., NIKI, M., KOUTCHER, J. A., SCHER, H. I., LUDWIG, T., GERALD, W., CORDON-CARDO, C. & PANDOLFI, P. P. 2005b. Crucial role of p53-dependent cellular senescence in suppression of Pten-deficient tumorigenesis. *Nature,* 436**,** 725-30.

CHEN, Z. S., LEE, K. & KRUH, G. D. 2001. Transport of cyclic nucleotides and estradiol 17-beta-D-glucuronide by multidrug resistance protein 4. Resistance to 6-mercaptopurine and 6-thioguanine. *J Biol Chem,* 276**,** 33747-54.

CHENDRIMADA, T. P., FINN, K. J., JI, X., BAILLAT, D., GREGORY, R. I., LIEBHABER, S. A., PASQUINELLI, A. E. & SHIEKHATTAR, R. 2007. MicroRNA silencing through RISC recruitment of eIF6. *Nature,* 447**,** 823-8.

CHENDRIMADA, T. P., GREGORY, R. I., KUMARASWAMY, E., NORMAN, J., COOCH, N., NISHIKURA, K. & SHIEKHATTAR, R. 2005. TRBP recruits the Dicer complex to Ago2 for microRNA processing and gene silencing. *Nature,* 436**,** 740-4.

CHILDS, S., YEH, R. L., HUI, D. & LING, V. 1998. Taxol resistance mediated by transfection of the liver-specific sister gene of P-glycoprotein. *Cancer Res,* 58**,** 4160-7.

CHKHOTUA, A. B., GABUSI, E., ALTIMARI, A., D'ERRICO, A., YAKUBOVICH, M., VIENKEN, J., STEFONI, S., CHIECO, P., YUSSIM, A. & GRIGIONI, W. F. 2003. Increased expression of p16(INK4a) and p27(Kip1) cyclin-dependent kinase inhibitor genes in aging human kidney and chronic allograft nephropathy. *Am J Kidney Dis,* 41**,** 1303-13.

CHONG, J. L., WENZEL, P. L., SÁENZ-ROBLES, M. T., NAIR, V., FERREY, A., HAGAN, J. P., GOMEZ, Y. M., SHARMA, N., CHEN, H. Z., OUSEPH, M., WANG, S. H., TRIKHA, P., CULP, B., MEZACHE, L., WINTON, D. J., SANSOM, O. J., CHEN, D., BREMNER, R., CANTALUPO, P. G., ROBINSON, M. L., PIPAS, J. M. & LEONE, G. 2009. E2f1-3 switch from activators in progenitor cells to repressors in differentiating cells. *Nature,* 462**,** 930-4.

CIGNA, E., GRADILONE, A., SORVILLO, V. & SCUDERI, N. 2011. ABCB5 in peripheral blood of a patient affected by multiple primary malignancies. *Ann Ital Chir,* 82**,** 49-53.

COBRINIK, D. 2005. Pocket proteins and cell cycle control. *Oncogene,* 24**,** 2796-809.

COLLARES, C. V., EVANGELISTA, A. F., XAVIER, D. J., RASSI, D. M., ARNS, T., FOSS-FREITAS, M. C., FOSS, M. C., PUTHIER, D., SAKAMOTO-HOJO, E. T., PASSOS, G. A. & DONADI, E. A. 2013. Identifying common and specific microRNAs expressed in peripheral blood mononuclear cell of type 1, type 2, and gestational diabetes mellitus patients. *BMC Res Notes,* 6**,** 491.

COLLINS, C. J. & SEDIVY, J. M. 2003. Involvement of the INK4a/Arf gene locus in senescence. *Aging Cell,* 2**,** 145-50.

CONRAD, C., ERFLE, H., WARNAT, P., DAIGLE, N., LÖRCH, T., ELLENBERG, J., PEPPERKOK, R. & EILS, R. 2004. Automatic identification of subcellular phenotypes on human cell arrays. *Genome Res,* 14**,** 1130-6.

CONRAD, C. & GERLICH, D. W. 2010. Automated microscopy for high-content RNAi screening. *J Cell Biol,* 188**,** 453-61.

COPPÉ, J. P., DESPREZ, P. Y., KRTOLICA, A. & CAMPISI, J. 2010. The senescence-associated secretory phenotype: the dark side of tumor suppression. *Annu Rev Pathol,* 5**,** 99-118.

COPPÉ, J. P., KAUSER, K., CAMPISI, J. & BEAUSÉJOUR, C. M. 2006. Secretion of vascular endothelial growth factor by primary human fibroblasts at senescence. *J Biol Chem,* 281**,** 29568-74.

CORBEIL, D., RÖPER, K., HELLWIG, A., TAVIAN, M., MIRAGLIA, S., WATT, S. M., SIMMONS, P. J., PEAULT, B., BUCK, D. W. & HUTTNER, W. B. 2000. The human AC133 hematopoietic stem cell antigen is also expressed in epithelial cells and targeted to plasma membrane protrusions. *J Biol Chem,* 275**,** 5512-20.

CUI, Y., KÖNIG, J., BUCHHOLZ, J. K., SPRING, H., LEIER, I. & KEPPLER, D. 1999. Drug resistance and ATP-dependent conjugate transport mediated by the apical multidrug resistance protein, MRP2, permanently expressed in human and canine cells. *Mol Pharmacol,* 55**,** 929-37.

CURTIS, C., SHAH, S. P., CHIN, S. F., TURASHVILI, G., RUEDA, O. M., DUNNING, M. J., SPEED, D., LYNCH, A. G., SAMARAJIWA, S., YUAN, Y., GRÄF, S., HA, G., HAFFARI, G., BASHASHATI, A., RUSSELL, R., MCKINNEY, S., LANGERØD, A., GREEN, A., PROVENZANO, E., WISHART, G., PINDER, S., WATSON, P., MARKOWETZ, F., MURPHY, L., ELLIS, I., PURUSHOTHAM, A., BØRRESEN-DALE, A. L., BRENTON, J. D., TAVARÉ, S., CALDAS, C., APARICIO, S. & GROUP, M. 2012. The genomic and transcriptomic architecture of 2,000 breast tumours reveals novel subgroups. *Nature,* 486**,** 346-52.

CUSHING, B., GILLER, R., ABLIN, A., COHEN, L., CULLEN, J., HAWKINS, E., HEIFETZ, S. A., KRAILO, M., LAUER, S. J., MARINA, N., RAO, P. V., RESCORLA, F., VINOCUR, C. D., WEETMAN, R. M. & CASTLEBERRY, R. P. 1999. Surgical resection alone is effective treatment for ovarian immature teratoma in children and adolescents: a report of the pediatric oncology group and the children's cancer group. *Am J Obstet Gynecol,* 181**,** 353-8.

DAI, N., ZHONG, Z. Y., CUN, Y. P., QING, Y., CHEN, C., JIANG, P., LI, M. X. & WANG, D. 2013. Alteration of the microRNA expression profile in human osteosarcoma cells transfected with APE1 siRNA. *Neoplasma,* 60**,** 384-94.

DALTON, W. S., CROWLEY, J. J., SALMON, S. S., GROGAN, T. M., LAUFMAN, L. R., WEISS, G. R. & BONNET, J. D. 1995. A phase III randomized study of oral verapamil as a chemosensitizer to reverse drug resistance in patients with refractory myeloma. A Southwest Oncology Group study. *Cancer,* 75**,** 815-20.

DANO, K. 1973. Active outward transport of daunomycin in resistant Ehrlich ascites tumor cells. *Biochim Biophys Acta,* 323**,** 466-83.

DAVIEL, M. & PARSONS, J. 1755. A Dissertation upon the Cancer of the Eye-Lids, Nose, Great Angle of the Eye, and Its Neighbouring Parts, Commonly Called the Noli-Me-Tangere, Deemed Hitherto Incureable by Both Antients and Moderns, but Now Shewn to be as Curable as Other Distempers. Translated from the French by James Parsons, M. D. and F. R. S. *Philosophical Transactions,* 49**,** 186-196

DAVIS, B. J. 1964. DISC ELECTROPHORESIS. II. METHOD AND APPLICATION TO HUMAN SERUM PROTEINS. *Ann N Y Acad Sci,* 121**,** 404-27.

DEAN, M. & ALLIKMETS, R. 2001. Complete characterization of the human ABC gene family. *J Bioenerg Biomembr,* 33**,** 475-9.

DEAN, M., HAMON, Y. & CHIMINI, G. 2001. The human ATP-binding cassette (ABC) transporter superfamily. *J Lipid Res,* 42**,** 1007-17.

DELLAGO, H., PRESCHITZ-KAMMERHOFER, B., TERLECKI-ZANIEWICZ, L., SCHREINER, C., FORTSCHEGGER, K., CHANG, M. W., HACKL, M., MONTEFORTE, R., KÜHNEL, H., SCHOSSERER, M., GRUBER, F., TSCHACHLER, E., SCHEIDELER, M., GRILLARI-VOGLAUER, R., GRILLARI, J. & WIESER, M. 2013. High levels of oncomiR-21 contribute to the senescence-induced growth arrest in normal human cells and its knock-down increases the replicative lifespan. *Aging Cell,* 12**,** 446-58.

DESROSIERS, D. C., BEARDEN, S. W., MIER, I., ABNEY, J., PAULLEY, J. T., FETHERSTON, J. D., SALAZAR, J. C., RADOLF, J. D. & PERRY, R. D. 2010. Znu is the predominant zinc importer in Yersinia pestis during in vitro growth but is not essential for virulence. *Infect Immun,* 78**,** 5163-77.

DIMRI, G. P., LEE, X., BASILE, G., ACOSTA, M., SCOTT, G., ROSKELLEY, C., MEDRANO, E. E., LINSKENS, M., RUBELJ, I. & PEREIRA-SMITH, O. 1995. A biomarker that identifies senescent human cells in culture and in aging skin in vivo. *Proc Natl Acad Sci U S A,* 92**,** 9363-7.

DOENCH, J. G., PETERSEN, C. P. & SHARP, P. A. 2003. siRNAs can function as miRNAs. *Genes Dev,* 17**,** 438-42.

DOYLE, L. & ROSS, D. D. 2003. Multidrug resistance mediated by the breast cancer resistance protein BCRP (ABCG2). *Oncogene,* 22**,** 7340-58.

DU, W. W., FANG, L., LI, M., YANG, X., LIANG, Y., PENG, C., QIAN, W., O'MALLEY, Y. Q., ASKELAND, R. W., SUGG, S. L., QIAN, J., LIN, J., JIANG, Z., YEE, A. J., SEFTON, M., DENG, Z., SHAN, S. W., WANG, C. H. & YANG, B. B. 2013. MicroRNA miR-24 enhances tumor invasion and metastasis by targeting PTPN9 and PTPRF to promote EGF signaling. *J Cell Sci,* 126**,** 1440-53.

DUBLIN, E. A., PATEL, N. K., GILLETT, C. E., SMITH, P., PETERS, G. & BARNES, D. M. 1998. Retinoblastoma and p16 proteins in mammary carcinoma: their relationship to cyclin D1 and histopathological parameters. *Int J Cancer,* 79**,** 71-5.

DUNNWALD, L. K., ROSSING, M. A. & LI, C. I. 2007. Hormone receptor status, tumor characteristics, and prognosis: a prospective cohort of breast cancer patients. *Breast Cancer Res,* 9**,** R6.

DWEEP, H., STICHT, C., PANDEY, P. & GRETZ, N. 2011. miRWalk--database: prediction of possible miRNA binding sites by "walking" the genes of three genomes. *J Biomed Inform,* 44**,** 839-47.

EBCTCG 1998. Tamoxifen for early breast cancer: an overview of the randomised trials. Early Breast Cancer Trialists' Collaborative Group. *Lancet,* 351**,** 1451-67.

ELLEDGE, S. J. 1996. Cell cycle checkpoints: preventing an identity crisis. *Science,* 274**,** 1664-72.

ESER, U., FALLEUR-FETTIG, M., JOHNSON, A. & SKOTHEIM, J. M. 2011. Commitment to a cellular transition precedes genome-wide transcriptional change. *Mol Cell,* 43**,** 515-27.

ESTELLER, M., CORN, P. G., BAYLIN, S. B. & HERMAN, J. G. 2001. A gene hypermethylation profile of human cancer. *Cancer Res,* 61**,** 3225-9.

EULALIO, A., HUNTZINGER, E. & IZAURRALDE, E. 2008. Getting to the root of miRNA-mediated gene silencing. *Cell,* 132**,** 9-14.

FARAWELA, H. M., KHORSHIED, M. M., KASSEM, N. M., KASSEM, H. A. & ZAWAM, H. M. 2014. The clinical relevance and prognostic significance of adenosine triphosphate ATP-binding cassette (ABCB5) and multidrug resistance (MDR1) genes expression in acute leukemia: an Egyptian study. *J Cancer Res Clin Oncol*. 140, 1323-30.

FIRE, A., XU, S., MONTGOMERY, M. K., KOSTAS, S. A., DRIVER, S. E. & MELLO, C. C. 1998. Potent and specific genetic interference by double-stranded RNA in Caenorhabditis elegans. *Nature,* 391**,** 806-11.

FISHER, B., REDMOND, C., FISHER, E. R. & CAPLAN, R. 1988. Relative worth of estrogen or progesterone receptor and pathologic characteristics of differentiation as indicators of prognosis in node negative breast cancer patients: findings from National Surgical Adjuvant Breast and Bowel Project Protocol B-06. *J Clin Oncol,* 6**,** 1076-87.

FORBES, S., CLEMENTS, J., DAWSON, E., BAMFORD, S., WEBB, T., DOGAN, A., FLANAGAN, A., TEAGUE, J., WOOSTER, R., FUTREAL, P. A. & STRATTON, M. R. 2006. COSMIC 2005. *Br J Cancer,* 94**,** 318-22.

FOSS, K. M., SIMA, C., UGOLINI, D., NERI, M., ALLEN, K. E. & WEISS, G. J. 2011. miR-1254 and miR-574-5p: serum-based microRNA biomarkers for early-stage non-small cell lung cancer. *J Thorac Oncol,* 6**,** 482-8.

FRANK, N. & FRANK, M. 2009. ABCB5 gene amplification in human leukemia cells. *Leuk Res,* 33**,** 1303-5.

FRANK, N., MARGARYAN, A., HUANG, Y., SCHATTON, T., WAAGA-GASSER, A., GASSER, M., SAYEGH, M., SADEE, W. & FRANK, M. 2005. ABCB5-mediated doxorubicin transport and chemoresistance in human malignant melanoma. *Cancer Res,* 65**,** 4320-33.

FRANK, N., PENDSE, S., LAPCHAK, P., MARGARYAN, A., SHLAIN, D., DOEING, C., SAYEGH, M. & FRANK, M. 2003. Regulation of progenitor cell fusion by ABCB5 P-glycoprotein, a novel human ATP-binding cassette transporter. *J Biol Chem,* 278**,** 47156-65.

FRANK, N. Y., SCHATTON, T., KIM, S., ZHAN, Q., WILSON, B. J., MA, J., SAAB, K. R., OSHEROV, V., WIDLUND, H. R., GASSER, M., WAAGA-GASSER, A. M., KUPPER, T. S., MURPHY, G. F. & FRANK, M. H. 2011. VEGFR-1 expressed by malignant melanoma initiating cells is required for tumor growth. *Cancer Res*. 71, 1474-85.

FREEMAN, J. B., GRAY, E. S., MILLWARD, M., PEARCE, R. & ZIMAN, M. 2012. Evaluation of a multi-marker immunomagnetic enrichment assay for the quantification of circulating melanoma cells. *J Transl Med,* 10**,** 192.

FROHMAN, M. A., DUSH, M. K. & MARTIN, G. R. 1988. Rapid production of full-length cDNAs from rare transcripts: amplification using a single gene-specific oligonucleotide primer. *Proc Natl Acad Sci U S A,* 85**,** 8998-9002.

FUKUDA, Y., AGUILAR-BRYAN, L., VAXILLAIRE, M., DECHAUME, A., WANG, Y., DEAN, M., MOITRA, K., BRYAN, J. & SCHUETZ, J. D. 2011. Conserved intramolecular disulfide bond is critical to trafficking and fate of ATP-binding cassette (ABC) transporters ABCB6 and sulfonylurea receptor 1 (SUR1)/ABCC8. *J Biol Chem,* 286**,** 8481-92.

FUKUNAGA-KALABIS, M., MARTINEZ, G., NGUYEN, T., KIM, D., SANTIAGO-WALKER, A., ROESCH, A. & HERLYN, M. 2010. Tenascin-C promotes melanoma progression by maintaining the ABCB5-positive side population. *Oncogene*. 29, 6115-24

FULFORD, L. G., EASTON, D. F., REIS-FILHO, J. S., SOFRONIS, A., GILLETT, C. E., LAKHANI, S. R. & HANBY, A. 2006. Specific morphological features predictive for the basal phenotype in grade 3 invasive ductal carcinoma of breast. *Histopathology,* 49**,** 22-34.

FUNG, K. L., PAN, J., OHNUMA, S., LUND, P. E., PIXLEY, J. N., KIMCHI-SARFATY, C., AMBUDKAR, S. V. & GOTTESMAN, M. M. 2014. MDR1 synonymous polymorphisms alter transporter specificity and protein stability in a stable epithelial monolayer. *Cancer Res,* 74**,** 598-608.

GAO, W., SHEN, H., LIU, L., XU, J. & SHU, Y. 2011. MiR-21 overexpression in human primary squamous cell lung carcinoma is associated with poor patient prognosis. *J Cancer Res Clin Oncol,* 137**,** 557-66.

GARBE, J. C., BHATTACHARYA, S., MERCHANT, B., BASSETT, E., SWISSHELM, K., FEILER, H. S., WYROBEK, A. J. & STAMPFER, M. R. 2009. Molecular distinctions between stasis and telomere attrition senescence barriers shown by long-term culture of normal human mammary epithelial cells. *Cancer Res,* 69**,** 7557-68.

GARBE, J. C., HOLST, C. R., BASSETT, E., TLSTY, T. & STAMPFER, M. R. 2007. Inactivation of p53 function in cultured human mammary epithelial cells turns the telomere-length dependent senescence barrier from agonescence into crisis. *Cell Cycle,* 6**,** 1927-36.

GAUTHIER, M. L., BERMAN, H. K., MILLER, C., KOZAKEIWICZ, K., CHEW, K., MOORE, D., RABBAN, J., CHEN, Y. Y., KERLIKOWSKE, K. & TLSTY, T. D. 2007. Abrogated response to cellular stress identifies DCIS associated with subsequent tumor events and defines basal-like breast tumors. *Cancer Cell,* 12**,** 479-91.

GAZZANIGA, P., CIGNA, E., PANASITI, V., DEVIRGILIIS, V., BOTTONI, U., VINCENZI, B., NICOLAZZO, C., PETRACCA, A. & GRADILONE, A. 2010. CD133 and ABCB5 as stem cell markers on sentinel lymph node from melanoma patients. *Eur J Surg Oncol*. 36, 1211-4.

GEICK, A., EICHELBAUM, M. & BURK, O. 2001. Nuclear receptor response elements mediate induction of intestinal MDR1 by rifampin. *J Biol Chem,* 276**,** 14581-7.

GEISLER, S. & COLLER, J. 2013. RNA in unexpected places: long non-coding RNA functions in diverse cellular contexts. *Nat Rev Mol Cell Biol,* 14**,** 699-712.

GERLOFF, T., STIEGER, B., HAGENBUCH, B., MADON, J., LANDMANN, L., ROTH, J., HOFMANN, A. F. & MEIER, P. J. 1998. The sister of P-glycoprotein represents the canalicular bile salt export pump of mammalian liver. *J Biol Chem,* 273**,** 10046-50.

GIARD, D. J., AARONSON, S. A., TODARO, G. J., ARNSTEIN, P., KERSEY, J. H., DOSIK, H. & PARKS, W. P. 1973. In vitro cultivation of human tumors: establishment of cell lines derived from a series of solid tumors. *J Natl Cancer Inst,* 51**,** 1417-23.

GIEPMANS, B. N., ADAMS, S. R., ELLISMAN, M. H. & TSIEN, R. Y. 2006. The fluorescent toolbox for assessing protein location and function. *Science,* 312**,** 217-24.

GIGLIO, S., CIROMBELLA, R., AMODEO, R., PORTARO, L., LAVRA, L. & VECCHIONE, A. 2013. MicroRNA miR-24 promotes cell proliferation by targeting the CDKs inhibitors p27Kip1 and p16INK4a. *J Cell Physiol,* 228**,** 2015-23.

GIL, J., BERNARD, D., MARTÍNEZ, D. & BEACH, D. 2004. Polycomb CBX7 has a unifying role in cellular lifespan. *Nat Cell Biol,* 6**,** 67-72.

GIL, J. & PETERS, G. 2006. Regulation of the INK4b-ARF-INK4a tumour suppressor locus: all for one or one for all. *Nat Rev Mol Cell Biol,* 7**,** 667-77.

GILLET, J. P., RUTLEDGE, R., WU, C.-P., ELISEEVA, T., CHEN, K., FITZGERALD, P. C., FALES, H. M., XIA, D., AMBUDKAR, S. V. & GOTTESMAN, M. M. Characterization of ABCB5, a poorly studied ABC transporter highly expressed in melanomas. Proceedings of the 100th

Annual Meeting of the American Association for Cancer Research, 2009 Denver, Colorado, USA.
GORMAN, C. M., HOWARD, B. H. & REEVES, R. 1983. Expression of recombinant plasmids in mammalian cells is enhanced by sodium butyrate. *Nucleic Acids Res,* 11**,** 7631-48.
GOTTESMAN, S. 2004. The small RNA regulators of Escherichia coli: roles and mechanisms*. *Annu Rev Microbiol,* 58**,** 303-28.
GRAF, G. A., COHEN, J. C. & HOBBS, H. H. 2004. Missense mutations in ABCG5 and ABCG8 disrupt heterodimerization and trafficking. *J Biol Chem,* 279**,** 24881-8.
GRAHAM, F. L., SMILEY, J., RUSSELL, W. C. & NAIRN, R. 1977. Characteristics of a human cell line transformed by DNA from human adenovirus type 5. *J Gen Virol,* 36**,** 59-74.
GRAÑA, X., GARRIGA, J. & MAYOL, X. 1998. Role of the retinoblastoma protein family, pRB, p107 and p130 in the negative control of cell growth. *Oncogene,* 17**,** 3365-83.
GREGORY, R. I., YAN, K. P., AMUTHAN, G., CHENDRIMADA, T., DORATOTAJ, B., COOCH, N. & SHIEKHATTAR, R. 2004. The Microprocessor complex mediates the genesis of microRNAs. *Nature,* 432**,** 235-40.
GRIMM, M., KRIMMEL, M., POLLIGKEIT, J., ALEXANDER, D., MUNZ, A., KLUBA, S., KEUTEL, C., HOFFMANN, J., REINERT, S. & HOEFERT, S. 2012. ABCB5 expression and cancer stem cell hypothesis in oral squamous cell carcinoma. *Eur J Cancer,* 48**,** 3186-97.
GROEN, A., ROMERO, M. R., KUNNE, C., HOOSDALLY, S. J., DIXON, P. H., WOODING, C., WILLIAMSON, C., SEPPEN, J., VAN DEN OEVER, K., MOK, K. S., PAULUSMA, C. C., LINTON, K. J. & OUDE ELFERINK, R. P. 2011. Complementary functions of the flippase ATP8B1 and the floppase ABCB4 in maintaining canalicular membrane integrity. *Gastroenterology,* 141**,** 1927-37.e1-4.
GUO, Y., KOTOVA, E., CHEN, Z. S., LEE, K., HOPPER-BORGE, E., BELINSKY, M. G. & KRUH, G. D. 2003. MRP8, ATP-binding cassette C11 (ABCC11), is a cyclic nucleotide efflux pump and a resistance factor for fluoropyrimidines 2',3'-dideoxycytidine and 9'-(2'-phosphonylmethoxyethyl)adenine. *J Biol Chem,* 278**,** 29509-14.
HAGA, Y., ISHII, K. & SUZUKI, T. 2011. N-glycosylation is critical for the stability and intracellular trafficking of glucose transporter GLUT4. *J Biol Chem,* 286**,** 31320-7.
HAN, J., LEE, Y., YEOM, K. H., NAM, J. W., HEO, I., RHEE, J. K., SOHN, S. Y., CHO, Y., ZHANG, B. T. & KIM, V. N. 2006. Molecular basis for the recognition of primary microRNAs by the Drosha-DGCR8 complex. *Cell,* 125**,** 887-901.
HANNA, W., KAHN, H. J. & TRUDEAU, M. 1999. Evaluation of HER-2/neu (erbB-2) status in breast cancer: from bench to bedside. *Mod Pathol,* 12**,** 827-34.
HANNON, G. J. & BEACH, D. 1994. p15INK4B is a potential effector of TGF-beta-induced cell cycle arrest. *Nature,* 371**,** 257-61.
HANSON, P. I. & WHITEHEART, S. W. 2005. AAA+ proteins: have engine, will work. *Nat Rev Mol Cell Biol,* 6**,** 519-29.
HARLEY, C. B., FUTCHER, A. B. & GREIDER, C. W. 1990. Telomeres shorten during ageing of human fibroblasts. *Nature,* 345**,** 458-60.
HAYASHI, M. & LEE, J. D. 2004. Role of the BMK1/ERK5 signaling pathway: lessons from knockout mice. *J Mol Med (Berl),* 82**,** 800-8.
HAYFLICK, L. & MOORHEAD, P. S. 1961. The serial cultivation of human diploid cell strains. *Exp Cell Res,* 25**,** 585-621.
HE, L., HE, X., LIM, L. P., DE STANCHINA, E., XUAN, Z., LIANG, Y., XUE, W., ZENDER, L., MAGNUS, J., RIDZON, D., JACKSON, A. L., LINSLEY, P. S., CHEN, C., LOWE, S. W., CLEARY, M. A. & HANNON, G. J. 2007. A microRNA component of the p53 tumour suppressor network. *Nature,* 447**,** 1130-4.
HELGADOTTIR, A., THORLEIFSSON, G., MAGNUSSON, K. P., GRÉTARSDOTTIR, S., STEINTHORSDOTTIR, V., MANOLESCU, A., JONES, G. T., RINKEL, G. J., BLANKENSTEIJN, J. D., RONKAINEN, A., JÄÄSKELÄINEN, J. E., KYO, Y., LENK, G. M., SAKALIHASAN, N., KOSTULAS, K., GOTTSÄTER, A., FLEX, A., STEFANSSON, H., HANSEN, T., ANDERSEN, G., WEINSHEIMER, S., BORCH-JOHNSEN, K., JORGENSEN, T., SHAH, S. H., QUYYUMI, A. A., GRANGER, C. B., REILLY, M. P., AUSTIN, H., LEVEY, A. I., VACCARINO, V., PALSDOTTIR, E., WALTERS, G. B., JONSDOTTIR, T., SNORRADOTTIR, S., MAGNUSDOTTIR, D., GUDMUNDSSON, G., FERRELL, R. E., SVEINBJORNSDOTTIR, S., HERNESNIEMI, J., NIEMELÄ, M., LIMET, R., ANDERSEN, K., SIGURDSSON, G., BENEDIKTSSON, R., VERHOEVEN, E. L., TEIJINK, J. A., GROBBEE, D. E., RADER, D. J., COLLIER, D. A., PEDERSEN, O., POLA, R., HILLERT, J., LINDBLAD, B., VALDIMARSSON, E. M., MAGNADOTTIR, H. B., WIJMENGA, C.,

TROMP, G., BAAS, A. F., RUIGROK, Y. M., VAN RIJ, A. M., KUIVANIEMI, H., POWELL, J. T., MATTHIASSON, S. E., GULCHER, J. R., THORGEIRSSON, G., KONG, A., THORSTEINSDOTTIR, U. & STEFANSSON, K. 2008. The same sequence variant on 9p21 associates with myocardial infarction, abdominal aortic aneurysm and intracranial aneurysm. *Nat Genet,* 40**,** 217-24.

HELIN, K., HARLOW, E. & FATTAEY, A. 1993. Inhibition of E2F-1 transactivation by direct binding of the retinoblastoma protein. *Mol Cell Biol,* 13**,** 6501-8.

HERSCHKOWITZ, J. I., HE, X., FAN, C. & PEROU, C. M. 2008. The functional loss of the retinoblastoma tumour suppressor is a common event in basal-like and luminal B breast carcinomas. *Breast Cancer Res,* 10**,** R75.

HIGGINS, C. F. 1992. ABC transporters: from microorganisms to man. *Annu Rev Cell Biol,* 8**,** 67-113.

HOOSDALLY, S. J., ANDRESS, E. J., WOODING, C., MARTIN, C. A. & LINTON, K. J. 2009. The Human Scavenger Receptor CD36: glycosylation status and its role in trafficking and function. *J Biol Chem,* 284**,** 16277-88.

HOPFNER, K. P., KARCHER, A., SHIN, D. S., CRAIG, L., ARTHUR, L. M., CARNEY, J. P. & TAINER, J. A. 2000. Structural biology of Rad50 ATPase: ATP-driven conformational control in DNA double-strand break repair and the ABC-ATPase superfamily. *Cell,* 101**,** 789-800.

HOPPER-BORGE, E., CHEN, Z. S., SHCHAVELEVA, I., BELINSKY, M. G. & KRUH, G. D. 2004. Analysis of the drug resistance profile of multidrug resistance protein 7 (ABCC10): resistance to docetaxel. *Cancer Res,* 64**,** 4927-30.

HORWITZ, K. B., KOSEKI, Y. & MCGUIRE, W. L. 1978. Estrogen control of progesterone receptor in human breast cancer: role of estradiol and antiestrogen. *Endocrinology,* 103**,** 1742-51.

HUANG, X., YUAN, T., TSCHANNEN, M., SUN, Z., JACOB, H., DU, M., LIANG, M., DITTMAR, R. L., LIU, Y., KOHLI, M., THIBODEAU, S. N., BOARDMAN, L. & WANG, L. 2013. Characterization of human plasma-derived exosomal RNAs by deep sequencing. *BMC Genomics,* 14**,** 319.

HUDIS, C. A. 2007. Trastuzumab--mechanism of action and use in clinical practice. *N Engl J Med,* 357**,** 39-51.

HUI, R., MACMILLAN, R. D., KENNY, F. S., MUSGROVE, E. A., BLAMEY, R. W., NICHOLSON, R. I., ROBERTSON, J. F. & SUTHERLAND, R. L. 2000. INK4a gene expression and methylation in primary breast cancer: overexpression of p16INK4a messenger RNA is a marker of poor prognosis. *Clin Cancer Res,* 6**,** 2777-87.

HUISMAN, M. T., CHHATTA, A. A., VAN TELLINGEN, O., BEIJNEN, J. H. & SCHINKEL, A. H. 2005. MRP2 (ABCC2) transports taxanes and confers paclitaxel resistance and both processes are stimulated by probenecid. *Int J Cancer,* 116**,** 824-9.

HUSCHTSCHA, L. I., NOBLE, J. R., NEUMANN, A. A., MOY, E. L., BARRY, P., MELKI, J. R., CLARK, S. J. & REDDEL, R. R. 1998. Loss of p16INK4 expression by methylation is associated with lifespan extension of human mammary epithelial cells. *Cancer Res,* 58**,** 3508-12.

HUSSUSSIAN, C., STRUEWING, J., GOLDSTEIN, A., HIGGINS, P., ALLY, D., SHEAHAN, M., CLARK, W. J., TUCKER, M. & DRACOPOLI, N. 1994. Germline p16 mutations in familial melanoma. *Nat Genet,* 8**,** 15-21.

HUTVÁGNER, G., MCLACHLAN, J., PASQUINELLI, A. E., BÁLINT, E., TUSCHL, T. & ZAMORE, P. D. 2001. A cellular function for the RNA-interference enzyme Dicer in the maturation of the let-7 small temporal RNA. *Science,* 293**,** 834-8.

INNIS, M. A., GELFAND, D. H., SNINSKY, J. J. & WHITE, T. J. 1990. *PCR Protocols: A Guide to Methods and Applications*, Science.

IRELAN, J. T., GUTIERREZ DEL ARROYO, A., GUTIERREZ, A., PETERS, G., QUON, K. C., MIRAGLIA, L. & CHANDA, S. K. 2009. A functional screen for regulators of CKDN2A reveals MEOX2 as a transcriptional activator of INK4a. *PLoS One,* 4**,** e5067.

ISHIDA, S., HUANG, E., ZUZAN, H., SPANG, R., LEONE, G., WEST, M. & NEVINS, J. R. 2001. Role for E2F in control of both DNA replication and mitotic functions as revealed from DNA microarray analysis. *Mol Cell Biol,* 21**,** 4684-99.

JACKSON, A. L., BARTZ, S. R., SCHELTER, J., KOBAYASHI, S. V., BURCHARD, J., MAO, M., LI, B., CAVET, G. & LINSLEY, P. S. 2003. Expression profiling reveals off-target gene regulation by RNAi. *Nat Biotechnol,* 21**,** 635-7.

JACKSON, A. L., BURCHARD, J., SCHELTER, J., CHAU, B. N., CLEARY, M., LIM, L. & LINSLEY, P. S. 2006. Widespread siRNA "off-target" transcript silencing mediated by seed region sequence complementarity. *RNA,* 12**,** 1179-87.

JACKSON, A. L. & LINSLEY, P. S. 2010. Recognizing and avoiding siRNA off-target effects for target identification and therapeutic application. *Nat Rev Drug Discov,* 9**,** 57-67.

JACOBS, J. J., KEBLUSEK, P., ROBANUS-MAANDAG, E., KRISTEL, P., LINGBEEK, M., NEDERLOF, P. M., VAN WELSEM, T., VAN DE VIJVER, M. J., KOH, E. Y., DALEY, G. Q. & VAN LOHUIZEN, M. 2000. Senescence bypass screen identifies TBX2, which represses Cdkn2a (p19(ARF)) and is amplified in a subset of human breast cancers. *Nat Genet,* 26**,** 291-9.

JACOBS, J. J., KIEBOOM, K., MARINO, S., DEPINHO, R. A. & VAN LOHUIZEN, M. 1999. The oncogene and Polycomb-group gene bmi-1 regulates cell proliferation and senescence through the ink4a locus. *Nature,* 397**,** 164-8.

JECK, W. R., SIEBOLD, A. P. & SHARPLESS, N. E. 2012. Review: a meta-analysis of GWAS and age-associated diseases. *Aging Cell,* 11**,** 727-31.

JEWETT, A., TSENG, H. C., ARASTEH, A., SAADAT, S., CHRISTENSEN, R. E. & CACALANO, N. A. 2012. Natural killer cells preferentially target cancer stem cells; role of monocytes in protection against NK cell mediated lysis of cancer stem cells. *Curr Drug Deliv,* 9**,** 5-16.

JIANG, D., ZHAO, L. & CLAPHAM, D. E. 2009. Genome-wide RNAi screen identifies Letm1 as a mitochondrial Ca2+/H+ antiporter. *Science,* 326**,** 144-7.

JIN, C., CHEN, J., MENG, Q., CARREIRA, V., TAM, N. N., GEH, E., KARYALA, S., HO, S. M., ZHOU, X., MEDVEDOVIC, M. & XIA, Y. 2013. Deciphering gene expression program of MAP3K1 in mouse eyelid morphogenesis. *Dev Biol,* 374**,** 96-107.

JOHNSON, A. & SKOTHEIM, J. M. 2013. Start and the restriction point. *Curr Opin Cell Biol,* 25**,** 717-23.

JULIANO, R. L. & LING, V. 1976. A surface glycoprotein modulating drug permeability in Chinese hamster ovary cell mutants. *Biochim Biophys Acta,* 455**,** 152-62.

JUN, J. I. & LAU, L. F. 2010. Cellular senescence controls fibrosis in wound healing. *Aging (Albany NY),* 2**,** 627-31.

JUNGSUWADEE, P., ZHAO, T., STOLARCZYK, E. I., PAUMI, C. M., BUTTERFIELD, D. A., ST CLAIR, D. K. & VORE, M. 2012. The G671V variant of MRP1/ABCC1 links doxorubicin-induced acute cardiac toxicity to disposition of the glutathione conjugate of 4-hydroxy-2-trans-nonenal. *Pharmacogenet Genomics,* 22**,** 273-84.

JÖNSSON, G., STAAF, J., VALLON-CHRISTERSSON, J., RINGNÉR, M., GRUVBERGER-SAAL, S. K., SAAL, L. H., HOLM, K., HEGARDT, C., ARASON, A., FAGERHOLM, R., PERSSON, C., GRABAU, D., JOHNSSON, E., LÖVGREN, K., MAGNUSSON, L., HEIKKILÄ, P., AGNARSSON, B. A., JOHANNSSON, O. T., MALMSTRÖM, P., FERNÖ, M., OLSSON, H., LOMAN, N., NEVANLINNA, H., BARKARDOTTIR, R. B. & BORG, Å. 2012. The retinoblastoma gene undergoes rearrangements in BRCA1-deficient basal-like breast cancer. *Cancer Res,* 72**,** 4028-36.

KAMB, A., GRUIS, N. A., WEAVER-FELDHAUS, J., LIU, Q., HARSHMAN, K., TAVTIGIAN, S. V., STOCKERT, E., DAY, R. S., JOHNSON, B. E. & SKOLNICK, M. H. 1994. A cell cycle regulator potentially involved in genesis of many tumor types. *Science,* 264**,** 436-40.

KANAVAROS, P., STEFANAKI, K., RONTOGIANNI, D., PAPALAZAROU, D., SGANTZOS, M., ARVANITIS, D., VAMVOUKA, C., GORGOULIS, V., SIATITSAS, I., AGNANTIS, N. J. & BAI, M. 2001. Immunohistochemical expression of p53, p21/waf1, rb, p16, cyclin D1, p27, Ki67, cyclin A, cyclin B1, bcl2, bax and bak proteins and apoptotic index in normal thymus. *Histol Histopathol,* 16**,** 1005-12.

KAWAHARA, Y., ZINSHTEYN, B., SETHUPATHY, P., IIZASA, H., HATZIGEORGIOU, A. G. & NISHIKURA, K. 2007. Redirection of silencing targets by adenosine-to-inosine editing of miRNAs. *Science,* 315**,** 1137-40.

KAWANOBE, T., KOGURE, S., NAKAMURA, S., SATO, M., KATAYAMA, K., MITSUHASHI, J., NOGUCHI, K. & SUGIMOTO, Y. 2012. Expression of human ABCB5 confers resistance to taxanes and anthracyclines. *Biochem Biophys Res Commun*. 418, 736-41.

KERR, I. D. 2002. Structure and association of ATP-binding cassette transporter nucleotide-binding domains. *Biochim Biophys Acta,* 1561**,** 47-64.

KHAN, A. A., BETEL, D., MILLER, M. L., SANDER, C., LESLIE, C. S. & MARKS, D. S. 2009. Transfection of small RNAs globally perturbs gene regulation by endogenous microRNAs. *Nat Biotechnol,* 27**,** 549-55.

KHVOROVA, A., REYNOLDS, A. & JAYASENA, S. D. 2003. Functional siRNAs and miRNAs exhibit strand bias. *Cell,* 115**,** 209-16.

KIMCHI-SARFATY, C., OH, J. M., KIM, I. W., SAUNA, Z. E., CALCAGNO, A. M., AMBUDKAR, S. V. & GOTTESMAN, M. M. 2007. A "silent" polymorphism in the MDR1 gene changes substrate specificity. *Science,* 315**,** 525-8.

KINO, T., HURT, D. E., ICHIJO, T., NADER, N. & CHROUSOS, G. P. 2010. Noncoding RNA gas5 is a growth arrest- and starvation-associated repressor of the glucocorticoid receptor. *Sci Signal,* 3**,** ra8.

KITTLER, R., PELLETIER, L., HENINGER, A. K., SLABICKI, M., THEIS, M., MIROSLAW, L., POSER, I., LAWO, S., GRABNER, H., KOZAK, K., WAGNER, J., SURENDRANATH, V., RICHTER, C., BOWEN, W., JACKSON, A. L., HABERMANN, B., HYMAN, A. A. & BUCHHOLZ, F. 2007. Genome-scale RNAi profiling of cell division in human tissue culture cells. *Nat Cell Biol,* 9**,** 1401-12.

KIYONO, T., FOSTER, S. A., KOOP, J. I., MCDOUGALL, J. K., GALLOWAY, D. A. & KLINGELHUTZ, A. J. 1998. Both Rb/p16INK4a inactivation and telomerase activity are required to immortalize human epithelial cells. *Nature,* 396**,** 84-8.

KLEIJMEER, M. J., KELLY, A., GEUZE, H. J., SLOT, J. W., TOWNSEND, A. & TROWSDALE, J. 1992. Location of MHC-encoded transporters in the endoplasmic reticulum and cis-Golgi. *Nature,* 357**,** 342-4.

KLIEWER, S. A., GOODWIN, B. & WILLSON, T. M. 2002. The nuclear pregnane X receptor: a key regulator of xenobiotic metabolism. *Endocr Rev,* 23**,** 687-702.

KOZLOWSKI, J. M., FIDLER, I. J., CAMPBELL, D., XU, Z. L., KAIGHN, M. E. & HART, I. R. 1984. Metastatic behavior of human tumor cell lines grown in the nude mouse. *Cancer Res,* 44**,** 3522-9.

KRIMPENFORT, P., QUON, K. C., MOOI, W. J., LOONSTRA, A. & BERNS, A. 2001. Loss of p16Ink4a confers susceptibility to metastatic melanoma in mice. *Nature,* 413**,** 83-6.

KRISHNAMURTHY, J., RAMSEY, M. R., LIGON, K. L., TORRICE, C., KOH, A., BONNER-WEIR, S. & SHARPLESS, N. E. 2006a. p16INK4a induces an age-dependent decline in islet regenerative potential. *Nature,* 443**,** 453-7.

KRISHNAMURTHY, P. C., DU, G., FUKUDA, Y., SUN, D., SAMPATH, J., MERCER, K. E., WANG, J., SOSA-PINEDA, B., MURTI, K. G. & SCHUETZ, J. D. 2006b. Identification of a mammalian mitochondrial porphyrin transporter. *Nature,* 443**,** 586-9.

KSANDER, B. R., KOLOVOU, P. E., WILSON, B. J., SAAB, K. R., GUO, Q., MA, J., MCGUIRE, S. P., GREGORY, M. S., VINCENT, W. J., PEREZ, V. L., CRUZ-GUILLOTY, F., KAO, W. W., CALL, M. K., TUCKER, B. A., ZHAN, Q., MURPHY, G. F., LATHROP, K. L., ALT, C., MORTENSEN, L. J., LIN, C. P., ZIESKE, J. D., FRANK, M. H. & FRANK, N. Y. 2014. ABCB5 is a limbal stem cell gene required for corneal development and repair. *Nature,* 511**,** 353-7.

KUMAR, M. S., LU, J., MERCER, K. L., GOLUB, T. R. & JACKS, T. 2007. Impaired microRNA processing enhances cellular transformation and tumorigenesis. *Nat Genet,* 39**,** 673-7.

KUO, C. L., MURPHY, A. J., SAYERS, S., LI, R., YVAN-CHARVET, L., DAVIS, J. Z., KRISHNAMURTHY, J., LIU, Y., PUIG, O., SHARPLESS, N. E., TALL, A. R. & WELCH, C. L. 2011. Cdkn2a is an atherosclerosis modifier locus that regulates monocyte/macrophage proliferation. *Arterioscler Thromb Vasc Biol,* 31**,** 2483-92.

LACROIX, M., ABI-SAID, D., FOURNEY, D. R., GOKASLAN, Z. L., SHI, W., DEMONTE, F., LANG, F. F., MCCUTCHEON, I. E., HASSENBUSCH, S. J., HOLLAND, E., HESS, K., MICHAEL, C., MILLER, D. & SAWAYA, R. 2001. A multivariate analysis of 416 patients with glioblastoma multiforme: prognosis, extent of resection, and survival. *J Neurosurg,* 95**,** 190-8.

LAEMMLI, U. K. 1970. Cleavage of structural proteins during the assembly of the head of bacteriophage T4. *Nature,* 227**,** 680-5.

LAL, A., KIM, H. H., ABDELMOHSEN, K., KUWANO, Y., PULLMANN, R., SRIKANTAN, S., SUBRAHMANYAM, R., MARTINDALE, J. L., YANG, X., AHMED, F., NAVARRO, F., DYKXHOORN, D., LIEBERMAN, J. & GOROSPE, M. 2008. p16(INK4a) translation suppressed by miR-24. *PLoS One,* 3**,** e1864.

LANKAT-BUTTGEREIT, B. & TAMPÉ, R. 2002. The transporter associated with antigen processing: function and implications in human diseases. *Physiol Rev,* 82**,** 187-204.

LARKIN, M. A., BLACKSHIELDS, G., BROWN, N. P., CHENNA, R., MCGETTIGAN, P. A., MCWILLIAM, H., VALENTIN, F., WALLACE, I. M., WILM, A., LOPEZ, R., THOMPSON, J. D., GIBSON, T. J. & HIGGINS, D. G. 2007. Clustal W and Clustal X version 2.0. *Bioinformatics,* 23**,** 2947-8.

LATOS, P. A., PAULER, F. M., KOERNER, M. V., ŞENERGIN, H. B., HUDSON, Q. J., STOCSITS, R. R., ALLHOFF, W., STRICKER, S. H., KLEMENT, R. M., WARCZOK, K. E., AUMAYR, K., PASIERBEK, P. & BARLOW, D. P. 2012. Airn transcriptional overlap, but not its lncRNA products, induces imprinted Igf2r silencing. *Science,* 338**,** 1469-72.

LECHNER, C., ZAHALKA, M. A., GIOT, J. F., MØLLER, N. P. & ULLRICH, A. 1996. ERK6, a mitogen-activated protein kinase involved in C2C12 myoblast differentiation. *Proc Natl Acad Sci U S A,* 93**,** 4355-9.

LEE, Y., AHN, C., HAN, J., CHOI, H., KIM, J., YIM, J., LEE, J., PROVOST, P., RÅDMARK, O., KIM, S. & KIM, V. N. 2003. The nuclear RNase III Drosha initiates microRNA processing. *Nature,* 425**,** 415-9.

LEE, Y., HUR, I., PARK, S. Y., KIM, Y. K., SUH, M. R. & KIM, V. N. 2006. The role of PACT in the RNA silencing pathway. *EMBO J,* 25**,** 522-32.

LEHNE, G., GRASMO-WENDLER, U., BERNER, J., MEZA-ZEPEDA, L., ADAMSEN, B., FLACK, A., REINER, A., CLAUSEN, O., HOVIG, E. & MYKLEBOST, O. 2009. Upregulation of stem cell genes in multidrug resistant K562 leukemia cells. *Leuk Res,* 33**,** 1379-85.

LEMMEN, J., TOZAKIDIS, I. E. & GALLA, H. J. 2013. Pregnane X receptor upregulates ABC-transporter Abcg2 and Abcb1 at the blood-brain barrier. *Brain Res,* 1491**,** 1-13.

LEWIS, B. P., SHIH, I. H., JONES-RHOADES, M. W., BARTEL, D. P. & BURGE, C. B. 2003. Prediction of mammalian microRNA targets. *Cell,* 115**,** 787-98.

LI, X., LIU, X., XU, W., ZHOU, P., GAO, P., JIANG, S., LOBIE, P. E. & ZHU, T. 2013a. c-MYC-regulated miR-23a/24-2/27a cluster promotes mammary carcinoma cell invasion and hepatic metastasis by targeting Sprouty2. *J Biol Chem,* 288**,** 18121-33.

LI, Y., HU, J., GUAN, F., SONG, L., FAN, R., ZHU, H., HU, X., SHEN, E. & YANG, B. 2013b. Copper induces cellular senescence in human glioblastoma multiforme cells through downregulation of Bmi-1. *Oncol Rep,* 29**,** 1805-10.

LIM, S. & KALDIS, P. 2013. Cdks, cyclins and CKIs: roles beyond cell cycle regulation. *Development,* 140**,** 3079-93.

LIN, A. W., BARRADAS, M., STONE, J. C., VAN AELST, L., SERRANO, M. & LOWE, S. W. 1998. Premature senescence involving p53 and p16 is activated in response to constitutive MEK/MAPK mitogenic signaling. *Genes Dev,* 12**,** 3008-19.

LIN, J. Y., ZHANG, M., SCHATTON, T., WILSON, B. J., ALLOO, A., MA, J., QURESHI, A. A., FRANK, N. Y., HAN, J. & FRANK, M. H. 2013. Genetically determined ABCB5 functionality correlates with pigmentation phenotype and melanoma risk. *Biochem Biophys Res Commun,* 436**,** 536-42.

LINDERHOLM, B. K., HELLBORG, H., JOHANSSON, U., ELMBERGER, G., SKOOG, L., LEHTIÖ, J. & LEWENSOHN, R. 2009. Significantly higher levels of vascular endothelial growth factor (VEGF) and shorter survival times for patients with primary operable triple-negative breast cancer. *Ann Oncol,* 20**,** 1639-46.

LINLEY, A. J., MATHIEU, M. G., MILES, A. K., REES, R. C., MCARDLE, S. E. & REGAD, T. 2012. The helicase HAGE expressed by malignant melanoma-initiating cells is required for tumor cell proliferation In Vivo. *J Biol Chem*. 287, 13633-43.

LINTON, K. J. & HOLLAND, I. B. 2011. *The ABC Transporters of Physiology and Disease: Genetics and Biochemistry of ATP Binding Cassette Transporters*, World Scientific Publishing Company Incorperated.

LIPPINCOTT-SCHWARTZ, J., ALTAN-BONNET, N. & PATTERSON, G. H. 2003. Photobleaching and photoactivation: following protein dynamics in living cells. *Nat Cell Biol,* Suppl**,** S7-14.

LIU, H., FERGUSSON, M. M., CASTILHO, R. M., LIU, J., CAO, L., CHEN, J., MALIDE, D., ROVIRA, I. I., SCHIMEL, D., KUO, C. J., GUTKIND, J. S., HWANG, P. M. & FINKEL, T. 2007. Augmented Wnt signaling in a mammalian model of accelerated aging. *Science,* 317**,** 803-6.

LIU, J. H., KÖNIG, S., MICHEL, M., ARNAUDEAU, S., FISCHER-LOUGHEED, J., BADER, C. R. & BERNHEIM, L. 2003. Acceleration of human myoblast fusion by depolarization: graded Ca2+ signals involved. *Development,* 130**,** 3437-46.

LIU, Q., ZHOU, H., ZHU, R., XU, Y. & CAO, Z. 2014. Reconsideration of in silico siRNA design from a perspective of heterogeneous data integration: problems and solutions. *Brief Bioinform,* 15**,** 292-305.

LIU, Y., SANOFF, H. K., CHO, H., BURD, C. E., TORRICE, C., MOHLKE, K. L., IBRAHIM, J. G., THOMAS, N. E. & SHARPLESS, N. E. 2009. INK4/ARF transcript expression is associated with chromosome 9p21 variants linked to atherosclerosis. *PLoS One,* 4**,** e5027.

LOH, E. Y., ELLIOTT, J. F., CWIRLA, S., LANIER, L. L. & DAVIS, M. M. 1989. Polymerase chain reaction with single-sided specificity: analysis of T cell receptor delta chain. *Science,* 243**,** 217-20.

LOO, L. H., WU, L. F. & ALTSCHULER, S. J. 2007. Image-based multivariate profiling of drug responses from single cells. *Nat Methods,* 4**,** 445-53.

LOO, T. W. & CLARKE, D. M. 1997. Correction of defective protein kinesis of human P-glycoprotein mutants by substrates and modulators. *J Biol Chem,* 272**,** 709-12.
LOWRY, O. H., ROSEBROUGH, N. J., FARR, A. L. & RANDALL, R. J. 1951. Protein measurement with the Folin phenol reagent. *J Biol Chem,* 193**,** 265-75.
LOZZIO, C. B. & LOZZIO, B. B. 1975. Human chronic myelogenous leukemia cell-line with positive Philadelphia chromosome. *Blood,* 45**,** 321-34.
LU, J., GETZ, G., MISKA, E. A., ALVAREZ-SAAVEDRA, E., LAMB, J., PECK, D., SWEET-CORDERO, A., EBERT, B. L., MAK, R. H., FERRANDO, A. A., DOWNING, J. R., JACKS, T., HORVITZ, H. R. & GOLUB, T. R. 2005. MicroRNA expression profiles classify human cancers. *Nature,* 435**,** 834-8.
LUKAS, J., PETERSEN, B. O., HOLM, K., BARTEK, J. & HELIN, K. 1996. Deregulated expression of E2F family members induces S-phase entry and overcomes p16INK4A-mediated growth suppression. *Mol Cell Biol,* 16**,** 1047-57.
LUND, E., GÜTTINGER, S., CALADO, A., DAHLBERG, J. E. & KUTAY, U. 2004. Nuclear export of microRNA precursors. *Science,* 303**,** 95-8.
LUO, K. Q. & CHANG, D. C. 2004. The gene-silencing efficiency of siRNA is strongly dependent on the local structure of mRNA at the targeted region. *Biochem Biophys Res Commun,* 318**,** 303-10.
LUX, S. E., JOHN, K. M. & BENNETT, V. 1990. Analysis of cDNA for human erythrocyte ankyrin indicates a repeated structure with homology to tissue-differentiation and cell-cycle control proteins. *Nature,* 344**,** 36-42.
MA, J., LIN, J. Y., ALLOO, A., WILSON, B. J., SCHATTON, T., ZHAN, Q., MURPHY, G. F., WAAGA-GASSER, A. M., GASSER, M., STEPHEN HODI, F., FRANK, N. Y. & FRANK, M. H. 2010. Isolation of tumorigenic circulating melanoma cells. *Biochem Biophys Res Commun*. 402, 711-7.
MACIEJCZYK, A., SZELACHOWSKA, J., EKIERT, M., MATKOWSKI, R., HAŁOŃ, A. & SUROWIAK, P. 2012. [Analysis of BCRP expression in breast cancer patients]. *Ginekol Pol,* 83**,** 681-7.
MACRAE, I. J., MA, E., ZHOU, M., ROBINSON, C. V. & DOUDNA, J. A. 2008. In vitro reconstitution of the human RISC-loading complex. *Proc Natl Acad Sci U S A,* 105**,** 512-7.
MASSAGUÉ, J. 2004. G1 cell-cycle control and cancer. *Nature,* 432**,** 298-306.
MASTERS, J. & PALSSON, B. 1999. Human Cell Culture. Great Britain: Kluwer Academic Publishers
MATHEU, A., MARAVER, A., COLLADO, M., GARCIA-CAO, I., CAÑAMERO, M., BORRAS, C., FLORES, J. M., KLATT, P., VIÑA, J. & SERRANO, M. 2009. Anti-aging activity of the Ink4/Arf locus. *Aging Cell,* 8**,** 152-61.
MATHIEU, M. G., MILES, A. K., AHMAD, M., BUCZEK, M. E., POCKLEY, A. G., REES, R. C. & REGAD, T. 2014. The helicase HAGE prevents interferon-α-induced PML expression in ABCB5+ malignant melanoma-initiating cells by promoting the expression of SOCS1. *Cell Death Dis,* 5**,** e1061.
MCEVOY, J., NAGAHAWATTE, P., FINKELSTEIN, D., RICHARDS-YUTZ, J., VALENTINE, M., MA, J., MULLIGHAN, C., SONG, G., CHEN, X., WILSON, M., BRENNAN, R., POUNDS, S., BECKSFORT, J., HUETHER, R., LU, C., FULTON, R. S., FULTON, L. L., HONG, X., DOOLING, D. J., OCHOA, K., MARDIS, E. R., WILSON, R. K., EASTON, J., ZHANG, J., DOWNING, J. R., GANGULY, A. & DYER, M. A. 2014. RB1 gene inactivation by chromothripsis in human retinoblastoma. *Oncotarget,* 5**,** 438-50.
MCPHERSON, R., PERTSEMLIDIS, A., KAVASLAR, N., STEWART, A., ROBERTS, R., COX, D. R., HINDS, D. A., PENNACCHIO, L. A., TYBJAERG-HANSEN, A., FOLSOM, A. R., BOERWINKLE, E., HOBBS, H. H. & COHEN, J. C. 2007. A common allele on chromosome 9 associated with coronary heart disease. *Science,* 316**,** 1488-91.
MELK, A., SCHMIDT, B. M., TAKEUCHI, O., SAWITZKI, B., RAYNER, D. C. & HALLORAN, P. F. 2004. Expression of p16INK4a and other cell cycle regulator and senescence associated genes in aging human kidney. *Kidney Int,* 65**,** 510-20.
MICHALOGLOU, C., VREDEVELD, L. C., SOENGAS, M. S., DENOYELLE, C., KUILMAN, T., VAN DER HORST, C. M., MAJOOR, D. M., SHAY, J. W., MOOI, W. J. & PEEPER, D. S. 2005. BRAFE600-associated senescence-like cell cycle arrest of human naevi. *Nature,* 436**,** 720-4.
MILDE-LANGOSCH, K., BAMBERGER, A. M., RIECK, G., KELP, B. & LÖNING, T. 2001. Overexpression of the p16 cell cycle inhibitor in breast cancer is associated with a more malignant phenotype. *Breast Cancer Res Treat,* 67**,** 61-70.
MILES, G. D., SEILER, M., RODRIGUEZ, L., RAJAGOPAL, G. & BHANOT, G. 2012. Identifying microRNA/mRNA dysregulations in ovarian cancer. *BMC Res Notes,* 5**,** 164.

MIZUARAI, S., MACHIDA, T., KOBAYASHI, T., KOMATANI, H., ITADANI, H. & KOTANI, H. 2011. Expression ratio of CCND1 to CDKN2A mRNA predicts RB1 status of cultured cancer cell lines and clinical tumor samples. *Mol Cancer,* 10**,** 31.

MOHARIR, A., PECK, S. H., BUDDEN, T. & LEE, S. Y. 2013. The role of N-glycosylation in folding, trafficking, and functionality of lysosomal protein CLN5. *PLoS One,* 8**,** e74299.

MOHR, S., BAKAL, C. & PERRIMON, N. 2010. Genomic screening with RNAi: results and challenges. *Annu Rev Biochem,* 79**,** 37-64.

MOITRA, K., SCALLY, M., MCGEE, K., LANCASTER, G., GOLD, B. & DEAN, M. 2011. Molecular Evolutionary Analysis of ABCB5: The Ancestral Gene Is a Full Transporter with Potentially Deleterious Single Nucleotide Polymorphisms. *PLoS One,* 6**,** e16318.

MOSAVI, L. K., CAMMETT, T. J., DESROSIERS, D. C. & PENG, Z. Y. 2004. The ankyrin repeat as molecular architecture for protein recognition. *Protein Sci,* 13**,** 1435-48.

MURATA, K., FURU, M., YOSHITOMI, H., ISHIKAWA, M., SHIBUYA, H., HASHIMOTO, M., IMURA, Y., FUJII, T., ITO, H., MIMORI, T. & MATSUDA, S. 2013. Comprehensive microRNA analysis identifies miR-24 and miR-125a-5p as plasma biomarkers for rheumatoid arthritis. *PLoS One,* 8**,** e69118.

MURPHREE, A. L. & BENEDICT, W. F. 1984. Retinoblastoma: clues to human oncogenesis. *Science,* 223**,** 1028-33.

MUÑOZ-ESPÍN, D., CAÑAMERO, M., MARAVER, A., GÓMEZ-LÓPEZ, G., CONTRERAS, J., MURILLO-CUESTA, S., RODRÍGUEZ-BAEZA, A., VARELA-NIETO, I., RUBERTE, J., COLLADO, M. & SERRANO, M. 2013. Programmed cell senescence during mammalian embryonic development. *Cell,* 155**,** 1104-18.

MÜLLER, H., BRACKEN, A. P., VERNELL, R., MORONI, M. C., CHRISTIANS, F., GRASSILLI, E., PROSPERINI, E., VIGO, E., OLINER, J. D. & HELIN, K. 2001. E2Fs regulate the expression of genes involved in differentiation, development, proliferation, and apoptosis. *Genes Dev,* 15**,** 267-85.

MÜLLER, P., KUTTENKEULER, D., GESELLCHEN, V., ZEIDLER, M. P. & BOUTROS, M. 2005. Identification of JAK/STAT signalling components by genome-wide RNA interference. *Nature,* 436**,** 871-5.

NIELSEN, G. P., STEMMER-RACHAMIMOV, A. O., SHAW, J., ROY, J. E., KOH, J. & LOUIS, D. N. 1999. Immunohistochemical survey of p16INK4A expression in normal human adult and infant tissues. *Lab Invest,* 79**,** 1137-43.

NIELSEN, T. O., HSU, F. D., JENSEN, K., CHEANG, M., KARACA, G., HU, Z., HERNANDEZ-BOUSSARD, T., LIVASY, C., COWAN, D., DRESSLER, L., AKSLEN, L. A., RAGAZ, J., GOWN, A. M., GILKS, C. B., VAN DE RIJN, M. & PEROU, C. M. 2004. Immunohistochemical and clinical characterization of the basal-like subtype of invasive breast carcinoma. *Clin Cancer Res,* 10**,** 5367-74.

NYHOLT, D. R., LOW, S. K., ANDERSON, C. A., PAINTER, J. N., UNO, S., MORRIS, A. P., MACGREGOR, S., GORDON, S. D., HENDERS, A. K., MARTIN, N. G., ATTIA, J., HOLLIDAY, E. G., MCEVOY, M., SCOTT, R. J., KENNEDY, S. H., TRELOAR, S. A., MISSMER, S. A., ADACHI, S., TANAKA, K., NAKAMURA, Y., ZONDERVAN, K. T., ZEMBUTSU, H. & MONTGOMERY, G. W. 2012. Genome-wide association meta-analysis identifies new endometriosis risk loci. *Nat Genet,* 44**,** 1355-9.

O'BRIEN, M. M., LACAYO, N. J., LUM, B. L., KSHIRSAGAR, S., BUCK, S., RAVINDRANATH, Y., BERNSTEIN, M., WEINSTEIN, H., CHANG, M. N., ARCECI, R. J., SIKIC, B. I. & DAHL, G. V. 2010. Phase I study of valspodar (PSC-833) with mitoxantrone and etoposide in refractory and relapsed pediatric acute leukemia: a report from the Children's Oncology Group. *Pediatr Blood Cancer,* 54**,** 694-702.

OGAWA, N., IMAI, Y., MORITA, H. & NAGAI, R. 2010. Genome-wide association study of coronary artery disease. *Int J Hypertens,* 2010**,** 790539.

ORNSTEIN, L. 1964. DISC ELECTROPHORESIS. I. BACKGROUND AND THEORY. *Ann N Y Acad Sci,* 121**,** 321-49.

OSBORNE, C. K. 1998. Steroid hormone receptors in breast cancer management. *Breast Cancer Res Treat,* 51**,** 227-38.

OSMAN, W., LOW, S. K., TAKAHASHI, A., KUBO, M. & NAKAMURA, Y. 2012. A genome-wide association study in the Japanese population confirms 9p21 and 14q23 as susceptibility loci for primary open angle glaucoma. *Hum Mol Genet,* 21**,** 2836-42.

OVERHOFF, M., ALKEN, M., FAR, R. K., LEMAITRE, M., LEBLEU, B., SCZAKIEL, G. & ROBBINS, I. 2005. Local RNA target structure influences siRNA efficacy: a systematic global analysis. *J Mol Biol,* 348**,** 871-81.

OVERHOFF, M. G., GARBE, J. C., KOH, J., STAMPFER, M. R., BEACH, D. H. & BISHOP, C. L. 2014. Cellular senescence mediated by p16INK4A-coupled miRNA pathways. *Nucleic Acids Res*. 42, 1606-18.

PALMER, E. & FREEMAN, T. 2004. Investigation into the use of C- and N-terminal GFP fusion proteins for subcellular localization studies using reverse transfection microarrays. *Comp Funct Genomics,* 5**,** 342-53.

PAPAVRAMIDOU, N., PAPAVRAMIDIS, T. & DEMETRIOU, T. 2010. Ancient Greek and Greco-Roman methods in modern surgical treatment of cancer. *Ann Surg Oncol,* 17**,** 665-7.

PASMANT, E., SABBAGH, A., VIDAUD, M. & BIÈCHE, I. 2011. ANRIL, a long, noncoding RNA, is an unexpected major hotspot in GWAS. *FASEB J,* 25**,** 444-8.

PAYNE, S. J., BOWEN, R. L., JONES, J. L. & WELLS, C. A. 2008. Predictive markers in breast cancer--the present. *Histopathology,* 52**,** 82-90.

PEARSON, M. & PELICCI, P. G. 2001. PML interaction with p53 and its role in apoptosis and replicative senescence. *Oncogene,* 20**,** 7250-6.

PEPPERKOK, R. & ELLENBERG, J. 2006. High-throughput fluorescence microscopy for systems biology. *Nat Rev Mol Cell Biol,* 7**,** 690-6.

PEROU, C. M., JEFFREY, S. S., VAN DE RIJN, M., REES, C. A., EISEN, M. B., ROSS, D. T., PERGAMENSCHIKOV, A., WILLIAMS, C. F., ZHU, S. X., LEE, J. C., LASHKARI, D., SHALON, D., BROWN, P. O. & BOTSTEIN, D. 1999. Distinctive gene expression patterns in human mammary epithelial cells and breast cancers. *Proc Natl Acad Sci U S A,* 96**,** 9212-7.

PEROU, C. M., SØRLIE, T., EISEN, M. B., VAN DE RIJN, M., JEFFREY, S. S., REES, C. A., POLLACK, J. R., ROSS, D. T., JOHNSEN, H., AKSLEN, L. A., FLUGE, O., PERGAMENSCHIKOV, A., WILLIAMS, C., ZHU, S. X., LØNNING, P. E., BØRRESEN-DALE, A. L., BROWN, P. O. & BOTSTEIN, D. 2000. Molecular portraits of human breast tumours. *Nature,* 406**,** 747-52.

PERSENGIEV, S. P., ZHU, X. & GREEN, M. R. 2004. Nonspecific, concentration-dependent stimulation and repression of mammalian gene expression by small interfering RNAs (siRNAs). *RNA,* 10**,** 12-8.

POLISENO, L., SALMENA, L., ZHANG, J., CARVER, B., HAVEMAN, W. J. & PANDOLFI, P. P. 2010. A coding-independent function of gene and pseudogene mRNAs regulates tumour biology. *Nature,* 465**,** 1033-8.

PONTING, C. P., OLIVER, P. L. & REIK, W. 2009. Evolution and functions of long noncoding RNAs. *Cell,* 136**,** 629-41.

RAMGOLAM, K., LAURIOL, J., LALOU, C., LAUDEN, L., MICHEL, L., DE LA GRANGE, P., KHATIB, A. M., AOUDJIT, F., CHARRON, D., ALCAIDE-LORIDAN, C. & AL-DACCAK, R. 2011. Melanoma spheroids grown under neural crest cell conditions are highly plastic migratory/invasive tumor cells endowed with immunomodulator function. *PLoS One,* 6**,** e18784.

RAND, T. A., PETERSEN, S., DU, F. & WANG, X. 2005. Argonaute2 cleaves the anti-guide strand of siRNA during RISC activation. *Cell,* 123**,** 621-9.

REID, A. L., MILLWARD, M., PEARCE, R., LEE, M., FRANK, M. H., IRELAND, A., MONSHIZADEH, L., RAI, T., HEENAN, P., MEDIC, S., KUMARASINGHE, P. & ZIMAN, M. 2013. Markers of circulating tumour cells in the peripheral blood of patients with melanoma correlate with disease recurrence and progression. *Br J Dermatol,* 168**,** 85-92.

RICHARD, V., SEBASTIAN, P., NAIR, M. G., NAIR, S. N., MALIECKAL, T. T., SANTHOSH KUMAR, T. R. & PILLAI, M. R. 2013. Multiple drug resistant, tumorigenic stem-like cells in oral cancer. *Cancer Lett,* 338**,** 300-16.

RIISING, E. M., COMET, I., LEBLANC, B., WU, X., JOHANSEN, J. V. & HELIN, K. 2014. Gene Silencing Triggers Polycomb Repressive Complex 2 Recruitment to CpG Islands Genome Wide. *Mol Cell*. 55, 347-60.

RITTER, M. A. 2000. *Diagnostic and Therapeutic Antibodies,* Totowa, NJ, USA., Humana Press.

ROBB, G. B. & RANA, T. M. 2007. RNA helicase A interacts with RISC in human cells and functions in RISC loading. *Mol Cell,* 26**,** 523-37.

ROBERTSON, S., MACKENZIE, S. M., ALVAREZ-MADRAZO, S., DIVER, L. A., LIN, J., STEWART, P. M., FRASER, R., CONNELL, J. M. & DAVIES, E. 2013. MicroRNA-24 is a novel regulator of aldosterone and cortisol production in the human adrenal cortex. *Hypertension,* 62**,** 572-8.

ROBINSON, T. J., LIU, J. C., VIZEACOUMAR, F., SUN, T., MACLEAN, N., EGAN, S. E., SCHIMMER, A. D., DATTI, A. & ZACKSENHAUS, E. 2013. RB1 status in triple negative breast cancer cells dictates response to radiation treatment and selective therapeutic drugs. *PLoS One,* 8**,** e78641.

ROMANOV, S. R., KOZAKIEWICZ, B. K., HOLST, C. R., STAMPFER, M. R., HAUPT, L. M. & TLSTY, T. D. 2001. Normal human mammary epithelial cells spontaneously escape senescence and acquire genomic changes. *Nature,* 409**,** 633-7.

ROY, A., KUCUKURAL, A. & ZHANG, Y. 2010. I-TASSER: a unified platform for automated protein structure and function prediction. *Nat Protoc,* 5**,** 725-38.

RUAS, M. & PETERS, G. 1998. The p16INK4a/CDKN2A tumor suppressor and its relatives. *Biochim Biophys Acta,* 1378**,** F115-77.

SAITO, Y., LIANG, G., EGGER, G., FRIEDMAN, J. M., CHUANG, J. C., COETZEE, G. A. & JONES, P. A. 2006. Specific activation of microRNA-127 with downregulation of the proto-oncogene BCL6 by chromatin-modifying drugs in human cancer cells. *Cancer Cell,* 9**,** 435-43.

SANAI, N., ALVAREZ-BUYLLA, A. & BERGER, M. S. 2005. Neural stem cells and the origin of gliomas. *N Engl J Med,* 353**,** 811-22.

SAND, M., SKRYGAN, M., GEORGAS, D., SAND, D., HAHN, S. A., GAMBICHLER, T., ALTMEYER, P. & BECHARA, F. G. 2012a. Microarray analysis of microRNA expression in cutaneous squamous cell carcinoma. *J Dermatol Sci,* 68**,** 119-26.

SAND, M., SKRYGAN, M., SAND, D., GEORGAS, D., HAHN, S. A., GAMBICHLER, T., ALTMEYER, P. & BECHARA, F. G. 2012b. Expression of microRNAs in basal cell carcinoma. *Br J Dermatol,* 167**,** 847-55.

SAPER, C. B. & SAWCHENKO, P. E. 2003. Magic peptides, magic antibodies: guidelines for appropriate controls for immunohistochemistry. *J Comp Neurol,* 465**,** 161-3.

SCHATTON, T. & FRANK, M. 2009. Antitumor immunity and cancer stem cells. *Ann N Y Acad Sci,* 1176**,** 154-69.

SCHATTON, T., MURPHY, G., FRANK, N., YAMAURA, K., WAAGA-GASSER, A., GASSER, M., ZHAN, Q., JORDAN, S., DUNCAN, L., WEISHAUPT, C., FUHLBRIGGE, R., KUPPER, T., SAYEGH, M. & FRANK, M. 2008. Identification of cells initiating human melanomas. *Nature,* 451**,** 345-9.

SCHATTON, T., SCHÜTTE, U., FRANK, N., ZHAN, Q., HOERNING, A., ROBLES, S., ZHOU, J., HODI, F., SPAGNOLI, G., MURPHY, G. & FRANK, M. 2010. Modulation of T-cell activation by malignant melanoma initiating cells. *Cancer Res,* 70**,** 697-708.

SCHERF, U., ROSS, D. T., WALTHAM, M., SMITH, L. H., LEE, J. K., TANABE, L., KOHN, K. W., REINHOLD, W. C., MYERS, T. G., ANDREWS, D. T., SCUDIERO, D. A., EISEN, M. B., SAUSVILLE, E. A., POMMIER, Y., BOTSTEIN, D., BROWN, P. O. & WEINSTEIN, J. N. 2000. A gene expression database for the molecular pharmacology of cancer. *Nat Genet,* 24**,** 236-44.

SCHNEIDER, C. A., RASBAND, W. S. & ELICEIRI, K. W. 2012. NIH Image to ImageJ: 25 years of image analysis. *Nat Methods,* 9**,** 671-5.

SCHUBERT, S., GRÜNWELLER, A., ERDMANN, V. A. & KURRECK, J. 2005. Local RNA target structure influences siRNA efficacy: systematic analysis of intentionally designed binding regions. *J Mol Biol,* 348**,** 883-93.

SCHWARZ, D. S., HUTVÁGNER, G., DU, T., XU, Z., ARONIN, N. & ZAMORE, P. D. 2003. Asymmetry in the assembly of the RNAi enzyme complex. *Cell,* 115**,** 199-208.

SERRANO, M., HANNON, G. & BEACH, D. 1993. A new regulatory motif in cell-cycle control causing specific inhibition of cyclin D/CDK4. *Nature,* 366**,** 704-7.

SERRANO, M., LIN, A. W., MCCURRACH, M. E., BEACH, D. & LOWE, S. W. 1997. Oncogenic ras provokes premature cell senescence associated with accumulation of p53 and p16INK4a. *Cell,* 88**,** 593-602.

SHARPLESS, N. E., BARDEESY, N., LEE, K. H., CARRASCO, D., CASTRILLON, D. H., AGUIRRE, A. J., WU, E. A., HORNER, J. W. & DEPINHO, R. A. 2001. Loss of p16Ink4a with retention of p19Arf predisposes mice to tumorigenesis. *Nature,* 413**,** 86-91.

SHARPLESS, N. E., RAMSEY, M. R., BALASUBRAMANIAN, P., CASTRILLON, D. H. & DEPINHO, R. A. 2004. The differential impact of p16(INK4a) or p19(ARF) deficiency on cell growth and tumorigenesis. *Oncogene,* 23**,** 379-85.

SHEN, D. W., CARDARELLI, C., HWANG, J., CORNWELL, M., RICHERT, N., ISHII, S., PASTAN, I. & GOTTESMAN, M. M. 1986. Multiple drug-resistant human KB carcinoma cells independently selected for high-level resistance to colchicine, adriamycin, or vinblastine show changes in expression of specific proteins. *J Biol Chem,* 261**,** 7762-70.

SHERR, C. J. & DEPINHO, R. A. 2000. Cellular senescence: mitotic clock or culture shock? *Cell,* 102**,** 407-10.

SHERR, C. J. & MCCORMICK, F. 2002. The RB and p53 pathways in cancer. *Cancer Cell,* 2**,** 103-12.

SHERR, C. J. & ROBERTS, J. M. 1999. CDK inhibitors: positive and negative regulators of G1-phase progression. *Genes Dev,* 13**,** 1501-12.

SHIN, K. H., BAE, S. D., HONG, H. S., KIM, R. H., KANG, M. K. & PARK, N. H. 2011. miR-181a shows tumor suppressive effect against oral squamous cell carcinoma cells by downregulating K-ras. *Biochem Biophys Res Commun,* 404**,** 896-902.

SHVARTS, A., BRUMMELKAMP, T. R., SCHEEREN, F., KOH, E., DALEY, G. Q., SPITS, H. & BERNARDS, R. 2002. A senescence rescue screen identifies BCL6 as an inhibitor of anti-proliferative p19(ARF)-p53 signaling. *Genes Dev,* 16**,** 681-6.

SIGOILLOT, F. D. & KING, R. W. 2011. Vigilance and validation: Keys to success in RNAi screening. *ACS Chem Biol,* 6**,** 47-60.

SIMMONDS, P. C., PRIMROSE, J. N., COLQUITT, J. L., GARDEN, O. J., POSTON, G. J. & REES, M. 2006. Surgical resection of hepatic metastases from colorectal cancer: a systematic review of published studies. *Br J Cancer,* 94**,** 982-99.

SIMON, J. A. & KINGSTON, R. E. 2009. Mechanisms of polycomb gene silencing: knowns and unknowns. *Nat Rev Mol Cell Biol,* 10**,** 697-708.

SLAMON, D. J., CLARK, G. M., WONG, S. G., LEVIN, W. J., ULLRICH, A. & MCGUIRE, W. L. 1987. Human breast cancer: correlation of relapse and survival with amplification of the HER-2/neu oncogene. *Science,* 235**,** 177-82.

SONG, G. & WANG, L. 2008. MiR-433 and miR-127 arise from independent overlapping primary transcripts encoded by the miR-433-127 locus. *PLoS One,* 3**,** e3574.

SONG, L., YANG, J., DUAN, P., XU, J., LUO, X., LUO, F., ZHANG, Z., HOU, T., LIU, B. & ZHOU, Q. 2013. MicroRNA-24 inhibits osteosarcoma cell proliferation both in vitro and in vivo by targeting LPAAT β . *Arch Biochem Biophys,* 535**,** 128-35.

SOUZA-RODRÍGUES, E., ESTANYOL, J. M., FRIEDRICH-HEINEKEN, E., OLMEDO, E., VERA, J., CANELA, N., BRUN, S., AGELL, N., HÜBSCHER, U., BACHS, O. & JAUMOT, M. 2007. Proteomic analysis of p16ink4a-binding proteins. *Proteomics,* 7**,** 4102-11.

STAMPFER, M., HALLOWES, R. C. & HACKETT, A. J. 1980. Growth of normal human mammary cells in culture. *In Vitro,* 16**,** 415-25.

STAUD, F. & PAVEK, P. 2005. Breast cancer resistance protein (BCRP/ABCG2). *Int J Biochem Cell Biol,* 37**,** 720-5.

STEFANSSON, O. A., JONASSON, J. G., OLAFSDOTTIR, K., HILMARSDOTTIR, H., OLAFSDOTTIR, G., ESTELLER, M., JOHANNSSON, O. T. & EYFJORD, J. E. 2011. CpG island hypermethylation of BRCA1 and loss of pRb as co-occurring events in basal/triple-negative breast cancer. *Epigenetics,* 6**,** 638-49.

STOTT, F. J., BATES, S., JAMES, M. C., MCCONNELL, B. B., STARBORG, M., BROOKES, S., PALMERO, I., RYAN, K., HARA, E., VOUSDEN, K. H. & PETERS, G. 1998. The alternative product from the human CDKN2A locus, p14(ARF), participates in a regulatory feedback loop with p53 and MDM2. *EMBO J,* 17**,** 5001-14.

SUBHAWONG, A. P., SUBHAWONG, T., NASSAR, H., KOUPRINA, N., BEGUM, S., VANG, R., WESTRA, W. H. & ARGANI, P. 2009. Most basal-like breast carcinomas demonstrate the same Rb-/p16+ immunophenotype as the HPV-related poorly differentiated squamous cell carcinomas which they resemble morphologically. *Am J Surg Pathol,* 33**,** 163-75.

SUN, L., MA, K., WANG, H., XIAO, F., GAO, Y., ZHANG, W., WANG, K., GAO, X., IP, N. & WU, Z. 2007. JAK1-STAT1-STAT3, a key pathway promoting proliferation and preventing premature differentiation of myoblasts. *J Cell Biol,* 179**,** 129-38.

SYNOLD, T. W., DUSSAULT, I. & FORMAN, B. M. 2001. The orphan nuclear receptor SXR coordinately regulates drug metabolism and efflux. *Nat Med,* 7**,** 584-90.

SZAKÁCS, G., PATERSON, J., LUDWIG, J., BOOTH-GENTHE, C. & GOTTESMAN, M. 2006. Targeting multidrug resistance in cancer. *Nat Rev Drug Discov,* 5**,** 219-34.

TAGUCHI, Y. H. & MURAKAMI, Y. 2013. Principal component analysis based feature extraction approach to identify circulating microRNA biomarkers. *PLoS One,* 8**,** e66714.

TAN, X., QIN, W., ZHANG, L., HANG, J., LI, B., ZHANG, C., WAN, J., ZHOU, F., SHAO, K., SUN, Y., WU, J., ZHANG, X., QIU, B., LI, N., SHI, S., FENG, X., ZHAO, S., WANG, Z., ZHAO, X., CHEN, Z., MITCHELSON, K., CHENG, J., GUO, Y. & HE, J. 2011. A 5-microRNA signature for lung squamous cell carcinoma diagnosis and hsa-miR-31 for prognosis. *Clin Cancer Res,* 17**,** 6802-11.

TAURINO, C., MILLER, W. H., MCBRIDE, M. W., MCCLURE, J. D., KHANIN, R., MORENO, M. U., DYMOTT, J. A., DELLES, C. & DOMINICZAK, A. F. 2010. Gene expression profiling in whole blood of patients with coronary artery disease. *Clin Sci (Lond),* 119**,** 335-43.

THIEBAUT, F., TSURUO, T., HAMADA, H., GOTTESMAN, M. M., PASTAN, I. & WILLINGHAM, M. C. 1987. Cellular localization of the multidrug-resistance gene product P-glycoprotein in normal human tissues. *Proc Natl Acad Sci U S A,* 84**,** 7735-8.

TOWBIN, H., STAEHELIN, T. & GORDON, J. 1979. Electrophoretic transfer of proteins from polyacrylamide gels to nitrocellulose sheets: procedure and some applications. *Proc Natl Acad Sci U S A,* 76**,** 4350-4.

TRIPATHI, V., ELLIS, J. D., SHEN, Z., SONG, D. Y., PAN, Q., WATT, A. T., FREIER, S. M., BENNETT, C. F., SHARMA, A., BUBULYA, P. A., BLENCOWE, B. J., PRASANTH, S. G. & PRASANTH, K. V. 2010. The nuclear-retained noncoding RNA MALAT1 regulates alternative splicing by modulating SR splicing factor phosphorylation. *Mol Cell,* 39**,** 925-38.

TSAI, C. J., SAUNA, Z. E., KIMCHI-SARFATY, C., AMBUDKAR, S. V., GOTTESMAN, M. M. & NUSSINOV, R. 2008. Synonymous mutations and ribosome stalling can lead to altered folding pathways and distinct minima. *J Mol Biol,* 383**,** 281-91.

TSAI, M. C., MANOR, O., WAN, Y., MOSAMMAPARAST, N., WANG, J. K., LAN, F., SHI, Y., SEGAL, E. & CHANG, H. Y. 2010. Long noncoding RNA as modular scaffold of histone modification complexes. *Science,* 329**,** 689-93.

VAN HELVOORT, A., SMITH, A. J., SPRONG, H., FRITZSCHE, I., SCHINKEL, A. H., BORST, P. & VAN MEER, G. 1996. MDR1 P-glycoprotein is a lipid translocase of broad specificity, while MDR3 P-glycoprotein specifically translocates phosphatidylcholine. *Cell,* 87**,** 507-17.

VOLPICELLI, E. R., LEZCANO, C., ZHAN, Q., GIROUARD, S. D., KINDELBERGER, D. W., FRANK, M. H., FRANK, N. Y., CRUM, C. P. & MURPHY, G. F. 2014. The multidrug-resistance transporter ABCB5 is expressed in human placenta. *Int J Gynecol Pathol,* 33**,** 45-51.

VREDEVELD, L. C., POSSIK, P. A., SMIT, M. A., MEISSL, K., MICHALOGLOU, C., HORLINGS, H. M., AJOUAOU, A., KORTMAN, P. C., DANKORT, D., MCMAHON, M., MOOI, W. J. & PEEPER, D. S. 2012. Abrogation of BRAFV600E-induced senescence by PI3K pathway activation contributes to melanomagenesis. *Genes Dev,* 26**,** 1055-69.

VÁSQUEZ-MOCTEZUMA, I., MERAZ-RÍOS, M. A., VILLANUEVA-LÓPEZ, C. G., MAGAÑA, M., MARTÍNEZ-MACIAS, R., SÁNCHEZ-GONZÁLEZ, D. J., GARCÍA-SIERRA, F. & HERRERA-GONZÁLEZ, N. E. 2010. ATP-binding cassette transporter ABCB5 gene is expressed with variability in malignant melanoma. *Actas Dermosifiliogr,* 101**,** 341-8.

WANG, F., ZHU, Y., GUO, L., DONG, L., LIU, H., YIN, H., ZHANG, Z., LI, Y., LIU, C., MA, Y., SONG, W., HE, A., WANG, Q., WANG, L., ZHANG, J., LI, J. & YU, J. 2014. A regulatory circuit comprising GATA1/2 switch and microRNA-27a/24 promotes erythropoiesis. *Nucleic Acids Res,* 42**,** 442-57.

WANG, H., WANG, L., ERDJUMENT-BROMAGE, H., VIDAL, M., TEMPST, P., JONES, R. S. & ZHANG, Y. 2004. Role of histone H2A ubiquitination in Polycomb silencing. *Nature,* 431**,** 873-8.

WANG, X., KHAIDAKOV, M., DING, Z., DAI, Y., MERCANTI, F. & MEHTA, J. L. 2013. LOX-1 in the maintenance of cytoskeleton and proliferation in senescent cardiac fibroblasts. *J Mol Cell Cardiol,* 60**,** 184-90.

WANG, X. Q., CRUTCHLEY, J. L. & DOSTIE, J. 2011. Shaping the Genome with Non-Coding RNAs. *Curr Genomics,* 12**,** 307-21.

WILSON, B. J., SCHATTON, T., ZHAN, Q., GASSER, M., MA, J., SAAB, K. R., SCHANCHE, R., WAAGA-GASSER, A. M., GOLD, J. S., HUANG, Q., MURPHY, G. F., FRANK, M. H. & FRANK, N. Y. 2011. ABCB5 identifies a therapy-refractory tumor cell population in colorectal cancer patients. *Cancer Res,* 71**,** 5307-16.

WILUSZ, J. E., SUNWOO, H. & SPECTOR, D. L. 2009. Long noncoding RNAs: functional surprises from the RNA world. *Genes Dev,* 23**,** 1494-504.

WITTENBERG, C. & REED, S. I. 2005. Cell cycle-dependent transcription in yeast: promoters, transcription factors, and transcriptomes. *Oncogene,* 24**,** 2746-55.

WOJTOWICZ, K., SZAFLARSKI, W., JANUCHOWSKI, R., ZAWIERUCHA, P., NOWICKI, M. & ZABEL, M. 2012. Inhibitors of N-glycosylation as a potential tool for analysis of the mechanism of action and cellular localisation of glycoprotein P. *Acta Biochim Pol,* 59**,** 445-50.

WOODWARD, O. M., KÖTTGEN, A. & KÖTTGEN, M. 2011. ABCG transporters and disease. *FEBS J,* 278**,** 3215-25.

XIE, P., XU, F., CHENG, W., GAO, J., ZHANG, Z., GE, J., WEI, Z., XU, X. & LIU, Y. 2012. Infiltration related miRNAs in bladder urothelial carcinoma. *J Huazhong Univ Sci Technolog Med Sci,* 32**,** 576-80.

YAMAGISHI, T., SAHNI, S., SHARP, D. M., ARVIND, A., JANSSON, P. J. & RICHARDSON, D. R. 2013. P-glycoprotein mediates drug resistance via a novel mechanism involving lysosomal sequestration. *J Biol Chem,* 288**,** 31761-71.

YANG, M., LI, W., FAN, D., YAN, Y., ZHANG, X., ZHANG, Y. & XIONG, D. 2012. Expression of ABCB5 gene in hematological malignances and its significance. *Leuk Lymphoma,* 53**,** 1211-5.

YANG, M., LIU, R., SHENG, J., LIAO, J., WANG, Y., PAN, E., GUO, W., PU, Y. & YIN, L. 2013. Differential expression profiles of microRNAs as potential biomarkers for the early diagnosis of esophageal squamous cell carcinoma. *Oncol Rep,* 29**,** 169-76.

YANG, W., CHENDRIMADA, T. P., WANG, Q., HIGUCHI, M., SEEBURG, P. H., SHIEKHATTAR, R. & NISHIKURA, K. 2006. Modulation of microRNA processing and expression through RNA editing by ADAR deaminases. *Nat Struct Mol Biol,* 13**,** 13-21.

YAP, K. L., LI, S., MUÑOZ-CABELLO, A. M., RAGUZ, S., ZENG, L., MUJTABA, S., GIL, J., WALSH, M. J. & ZHOU, M. M. 2010. Molecular interplay of the noncoding RNA ANRIL and methylated histone H3 lysine 27 by polycomb CBX7 in transcriptional silencing of INK4a. *Mol Cell,* 38**,** 662-74.

YASWEN, P. & STAMPFER, M. R. 2002. Molecular changes accompanying senescence and immortalization of cultured human mammary epithelial cells. *Int J Biochem Cell Biol,* 34**,** 1382-94.

YEGOROV, Y. E., AKIMOV, S. S., HASS, R., ZELENIN, A. V. & PRUDOVSKY, I. A. 1998. Endogenous beta-galactosidase activity in continuously nonproliferating cells. *Exp Cell Res,* 243**,** 207-11.

YI, R., QIN, Y., MACARA, I. G. & CULLEN, B. R. 2003. Exportin-5 mediates the nuclear export of pre-microRNAs and short hairpin RNAs. *Genes Dev,* 17**,** 3011-6.

ZABEL, A. & DEBUS, J. 2004. Treatment of brain metastases from non-small-cell lung cancer (NSCLC): radiotherapy. *Lung Cancer,* 45 Suppl 2**,** S247-52.

ZENG, Y. & CULLEN, B. R. 2004. Structural requirements for pre-microRNA binding and nuclear export by Exportin 5. *Nucleic Acids Res,* 32**,** 4776-85.

ZHANG, F., ZHANG, W., LIU, L., FISHER, C. L., HUI, D., CHILDS, S., DOROVINI-ZIS, K. & LING, V. 2000. Characterization of ABCB9, an ATP binding cassette protein associated with lysosomes. *J Biol Chem,* 275**,** 23287-94.

ZHU, J., WOODS, D., MCMAHON, M. & BISHOP, J. M. 1998. Senescence of human fibroblasts induced by oncogenic Raf. *Genes Dev,* 12**,** 2997-3007.

ZHU, M., NI, W., DONG, Y. & WU, Z. Y. 2013a. EGFP tags affect cellular localization of ATP7B mutants. *CNS Neurosci Ther,* 19**,** 346-51.

ZHU, Y., YOU, W., WANG, H., LI, Y., QIAO, N., SHI, Y., ZHANG, C., BLEICH, D. & HAN, X. 2013b. MicroRNA-24/MODY gene regulatory pathway mediates pancreatic β-cell dysfunction. *Diabetes,* 62**,** 3194-206.

ZOLNERCIKS, J. K., ANDRESS, E. J., NICOLAOU, M. & LINTON, K. J. 2011. Structure of ABC transporters. *Essays Biochem,* 50**,** 43-61.

ZOLNERCIKS, J. K., WOODING, C. & LINTON, K. J. 2007. Evidence for a Sav1866-like architecture for the human multidrug transporter P-glycoprotein. *FASEB J,* 21**,** 3937-48.

ZUKER, M. 2003. Mfold web server for nucleic acid folding and hybridization prediction. *Nucleic Acids Res,* 31**,** 3406-15.

ZUTZ, A., GOMPF, S., SCHÄGGER, H. & TAMPÉ, R. 2009. Mitochondrial ABC proteins in health and disease. *Biochim Biophys Acta,* 1787**,** 681-90.

ZÜCHNER, S., GILBERT, J. R., MARTIN, E. R., LEON-GUERRERO, C. R., XU, P. T., BROWNING, C., BRONSON, P. G., WHITEHEAD, P., SCHMECHEL, D. E., HAINES, J. L. & PERICAK-VANCE, M. A. 2008. Linkage and association study of late-onset Alzheimer disease families linked to 9p21.3. *Ann Hum Genet,* 72**,** 725-31.

Appendices

Appendix I. *ABCB5fl* and *ABCB5β* sequences submitted for TaqMan and siRNA generation.

A

```
1    TGTAGAGAGA GAAAGAGAAA ACACGCTCAT GTAATTGTGG TGACTGGCAC
51   TTCCAAAATC CACAAGCCAG ACTAGAAGGC TGGAAATTCT GGCAAAAAAT
101  TGATACCTTG TATCTGAAAG CTTTATCCTA TCCTCTTCAG AAGACTTCAG
151  TCTTTTCTCT TAAGGACTTC AACTGACTGG ATGGGGCCCA CTCAAAACAG
201  CATCTAAGGA ATTAAAAAGA AGTAAATTGT AAATAAGATG GAAAATTCAG
251  AAAGAGCTGA AGAAATGCAA GAAAATTATC AGAGAAATGG AACTGCAGAA
301  GAACAGCCAA AACTGAGAAA GGAAGCAGTT GGATCTATTG AGATATTCCG
351  CTTTGCTGAT GGACTGGACA TCACACTCAT GATCCTGGGT ATACTGGCAT
401  CACTGGTCAA TGGAGCCTGC CTTCCTTTAA TGCCACTGGT TTTAGGAGAA
451  ATGAGTGATA ACCTTATTAG TGGATGTCTA GTCCAAACTA ACACAACAAA
501  TTATCAGAAC TGTACTCAGT CTCAAGAGAA GCTGAATGAA GATATGACTC
551  TGTTGACCCT GTATTATGTT GGAATAGGTG TTGCTGCCTT GATTTTTGGT
601  TACATACAGA TTTCCTTGTG GATTATAACT GCAGCACGAC AGACCAAGAG
651  GATTCGAAAA CAGTTTTTTC ATTCAGTTTT GGCACAGGAC ATCGGCTGGT
701  TTGATAGCTG TGACATCGGT GAACTTAACA CTCGCATGAC AGATGACATT
751  GACAAAATCA GTGATGGTAT TGGAGATAAG ATTGCTCTGT TGTTTCAAAA
801  CATGTCTACT TTTTCGATTG GCCTGGCAGT TGGTTTGGTG AAGGGCTGGA
851  AACTCACCCT AGTGACTCTA TCCACGTCTC CTCTTATAAT GGCTTCAGCG
901  GCAGCATGTT CTAGGATGGT CATCTCATTG ACCAGTAAGG AATTAAGTGC
951  CTATTCCAAA GCTGGGGCTG TGGCAGAAGA AGTCTTGTCA TCAATCCGAA
1001 CAGTC
```

B

```
1   ATTGCTTCTC GGCCTTTTGG CTAAGATCAA GTGTAATCTG TGTTCTTTTT
51  TATTTGGTCA TATCTTCCAT TCTTTCTTAC CTAATTCCTC TAATATCTCT
101 CTGTGAGCCT AAACCAATAA TTATATATTA CATTCTATTG TCTTTCTTAT
151 ATAACTGCAG AAAGATAAAT ATCACTTTGT TTGTTCCTGT AG
```

Appendix I. *ABCB5fl* and *ABCB5β* sequences submitted for TaqMan and siRNA generation.

A. 1005 nt sequence unique to *ABCB5fl*. B. 193 nt sequence of *ABCB5β* not present in ABCB5fl.

Appendix II. Optimisation of HMEC seeding density

Due to the small area of 384-well plates (the surface area of each well is 0.087 cm^2), it is important that each step of the siRNA transfection protocol is precisely optimised. The first step was to establish the appropriate seeding density for the cells. The required seeding density is one at which the cells would still be sub-confluent after 120 h (the experiment endpoint), to allow for an increase in proliferation to be observed, but for there to be enough cells to also be able to measure reduction in cell proliferation. Unless otherwise stated, all of the following experiments were carried out in HMEC P6, at which stage there is a mixed population of both proliferative (p16 negative) and senescent (p16 positive) cells, allowing changes in their relative proportions to be measured.

Cells were seeded in 384-well format at five different densities (5,000 – 15,000 cm^{-2}), the media was changed after 48 h and the cells were fixed at the 120 h time point (Appendix II-I panel A). The 10,000 cm^{-2} seeding density was chosen for future experiments, as the resulting final cell number (2348 ± 283) allowed for measurement of both increase and decrease in cell proliferation following siRNA transfection.

To control for edge effects and thereby assess whether the entire plate could be used for experimental set-up, an entire plate was seeded at 10,000 cm^{-2} and the cells fixed and counted after 120 h. The data from a quarter of the plate is shown for row-to-row and column-to-column variability (Appendic II-I panel B). With the exception of the two outermost rows (A and B), and the two outermost columns (1 and 2), there was little variability found across the plate. The reduction in cell number in the outermost wells of

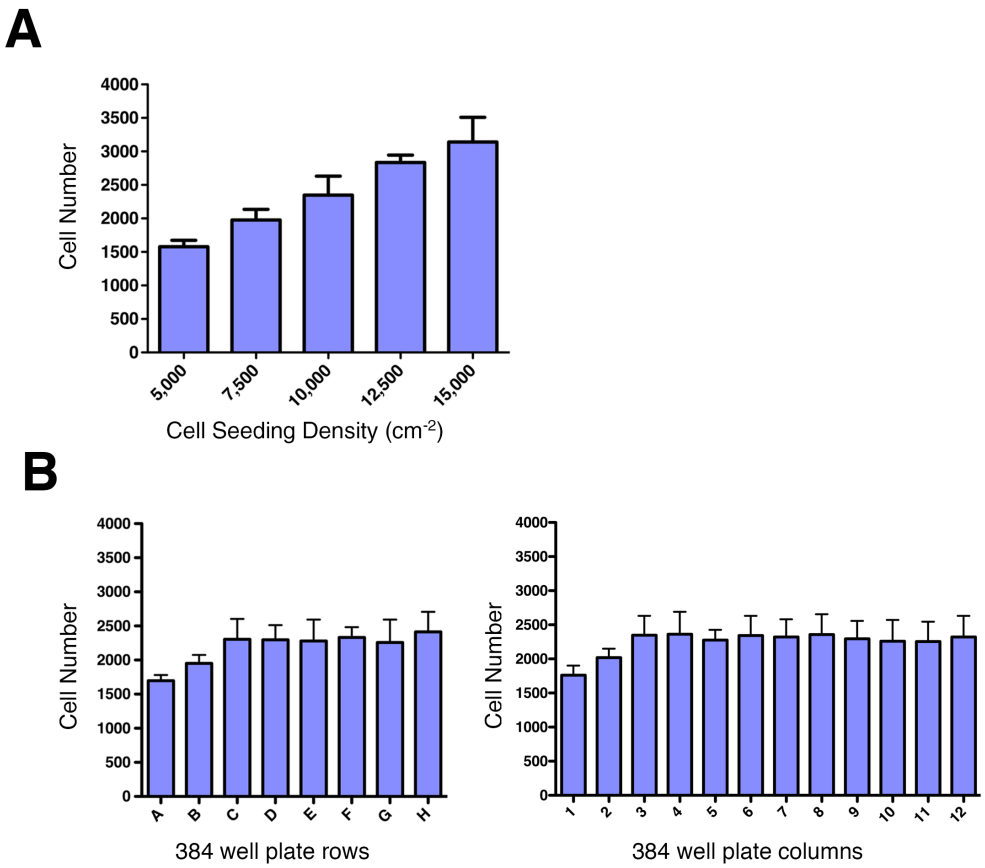

Appendix II-I. Seeding density optimisation for HMEC transfection in 384-well format.

A. HMECs seeded at increasing densities in wells of a 384-well plate were fixed, stained with DAPI and counted after 120 h. B. To assess well-to-well variability over the plate, cells seeded at 10,000 cm^{-2} were counted after 120 h in both the rows (A – H) and columns (1 – 12). Both rows A and B, and columns 1 and 2 were found to have a consistently lower cell number after 120 h than any other row or column. Error bars represent one SD. n = 2 biological repeats.

the plate can be explained by the edge effect, in which evaporation of medium from the edge of the plate can cause reduction in cell growth. Accordingly, the outer wells (rows A, B, O, P and columns 1, 2, 23, 24) were not used as experimental wells for the remainder of this study.

The next step of the optimisation procedure was to find the correct volume of transfection reagent to use per well to provide a significant knockdown of target gene

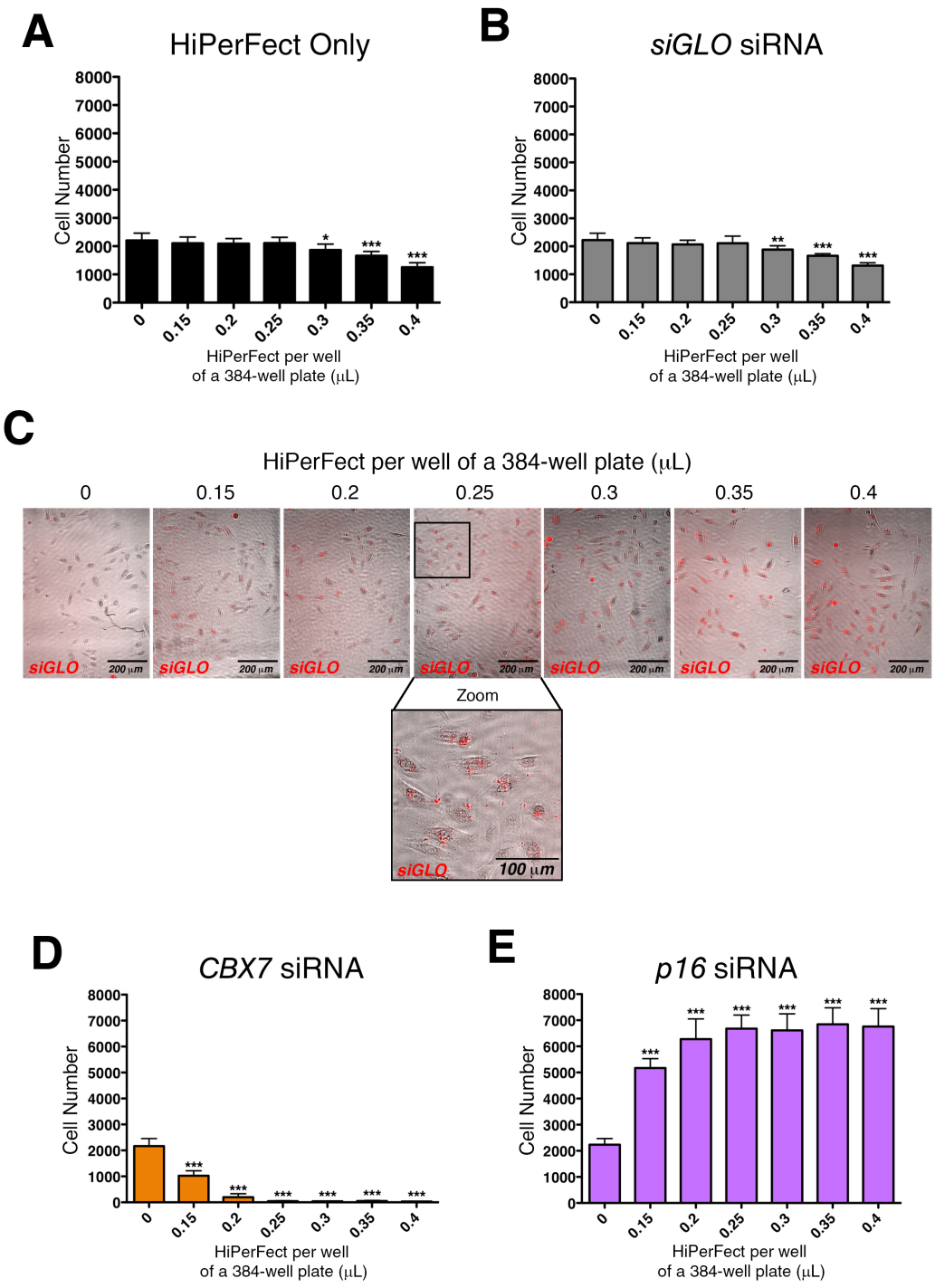

Appendix II-II Optimisation of transfection reagent volume for HMEC transfection.

A B D and E. HMECs were treated with transfection reagent as indicated (HiPerFect Only - black columns) or HiPerFect with 30 nM siRNA (*siGLO* – grey columns; *CBX7* – orange columns; *p16* – purple columns). Cells were fixed 120 h post transfection, stained with DAPI and imaged using an IN Cell 1000 microscope at 10x magnification (GE Healthcare, UK). Nuclei were counted from the resulting images using Developer Toolbox 1.7 (GE Healthcare, UK). C. Transfected cells were imaged 48 h post transfection using an IN Cell 1000 microscope to assess transfection efficiency. The black box represents the zoomed area. Brightfield images with red (siGLO) overlay. Error bars represent one SD. * $p < 0.05$, ** $p < 0.01$, *** $p < 0.001$. n = 3 biological repeats.

expression, without causing cellular cytotoxicity. To optimise the quantity of transfection reagent (HiPerFect; QIAGEN, NL) to be used, cells were treated with increasing amounts of HiPerFect, and a constant concentration of 30 nM siRNAs targeting three control genes (*Cyclophilin B, CBX7* and *p16*), alongside untransfected cells and cells treated with the transfection reagent alone (HiPerFect only), as negative controls.

Cytotoxicity as a consequence of excessive transfection reagent dose resulted in a reduction in cell number when the volume of transfection reagent was at 0.3 μL well^{-1} and above, with a stepwise increase in cytotoxicity with HiPerFect only ($p < 0.05$ to $p < 0.001$)[I] and *siGLO* ($p < 0.01$ to $p < 0.001$) between 0.30 μL well^{-1} and 0.40 μL well^{-1} (Appendix II-II panels A and B). Fluorescent *siGLO* siRNA was used to assess transfection efficiency in cells 48 h post transfection (Appendix II-II panel C). The number of fluorescent foci – *siGLO*-HiPerFect complexes – per cell were observed to increase with increasing volume of transfection reagent up to 0.3 μL well^{-1}, after which, all HiPerFect volumes were comparable. A stepwise increase in the predicted phenotypes following transfection with siRNAs targeting *CBX7* and *p16* was seen with volumes of transfection reagent between 0.15 μL well^{-1} and 0.25 μL well^{-1} (both $p < 0.001$), after which, increasing the amount of transfection reagent made no difference to the cell number (Appendix II-II panels D and E).

[I] Accurate p-values cannot be calculated when using a one-way ANOVA due to limitations in the software being used (Prism v5.0d; GraphPad Software Inc, CA). See Section 2.29.2.

The volume of 0.25 μL $well^{-1}$ of transfection reagent was chosen for all future siRNA transfections in HMECs because it was found to give the strongest knockdown phenotype with no measurable toxicity.

Appendix III. mRNA sequences submitted for RNA secondary structure prediction.

A

```
1    TGTAGAGAGA GAAAGAGAAA ACACGCTCAT GTAATTGTGG TGACTGGCAC
51   TTCCAAAATC CACAAGCCAG ACTAGAAGGC TGGAAATTCT GGCAAAAAAT
101  TGATACCTTG TATCTGAAAG CTTTATCCTA TCCTCTTCAG AAGACTTCAG
151  TCTTTTCTCT TAAGGACTTC AACTGACTGG ATGGGGCCCA CTCAAAACAG
201  CATCTAAGGA ATTAAAAAGA AGTAAATTGT AAATAAGATG GAAAATTCAG
251  AAAGAGCTGA AGAAATGCAA GAAAATTATC AGAGAAATGG AACTGCAGAA
301  GAACAGCCAA AACTGAGAAA GGAAGCAGTT GGATCTATTG AGATATTCCG
351  CTTTGCTGAT GGACTGGACA TCACACTCAT GATCCTGGGT ATACTGGCAT
401  CACTGGTCAA TGGAGCCTGC CTTCCTTTAA TGCCACTGGT TTTAGGAGAA
451  ATGAGTGATA ACCTTATTAG TGGATGTCTA GTCCAAACTA ACACAACAAA
```

B

```
1    TAAATGTGCG GCATTATCGA GACCATATTG GAGTGGTTAG TCAAGAGCCT
51   GTTTTGTTCG GGACCACCAT CAGTAACAAT ATCAAGTATG GACGAGATGA
101  TGTGACTGAT GAAGAGATGG AGAGAGCAGC AAGGGAAGCA AATGCGTATG
151  ATTTTATCAT GGAGTTTCCT AATAAATTTA ATACATTGGT AGGGGAAAAA
201  GGAGCTCAAA TGAGTGGAGG GCAGAAACAG AGGATCGCAA TTGCTCGTGC
251  CTTAGTTCGA AACCCCAAGA TTCTGATTTT AGATGAGGCT ACGTCTGCCC
301  TGGATTCAGA AAGCAAGTCA GCTGTTCAAG CTGCACTGGA GAAGGCGAGC
351  AAAGGTCGGA CTACAATCGT GGTAGCACAC CGACTTTCTA CTATTCGAAG
401  TGCAGATTTG ATTGTGACCC TAAAGGATGG AATGCTGGCG GAGAAAGGAG
451  CACATGCTGA ACTAATGGCA AAACGAGGTC TATATTATTC ACTTGTGATG
```

C

```
1    TATTTTACGG CAGAGCAGGG GAAATTTTAA CGATGAGATT AAGACACTTG
51   GCCTTCAAAG CCATGTTATA TCAGGATATT GCCTGGTTTG ATGAAAAGGA
101  AAACAGCACA GGAGGCTTGA CAACAATATT AGCCATAGAT ATAGCACAAA
151  TTCAAGGAGC AACAGGTTCC AGGATTGGCG TCTTAACACA AAATGCAACT
201  AACATGGGAC TTTCAGTTAT CATTTCCTTT ATATATGGAT GGGAGATGAC
251  ATTCCTGATT CTGAGTATTG CTCCAGTACT TGCCGTGACA GGAATGATTG
301  AAACCGCAGC AATGACTGGA TTTGCCAACA AAGATAAGCA AGAACTTAAG
351  CATGCTGGAA AGATAGCAAC TGAAGCTTTG GAGAATATAC GTACTATAGT
401  GTCATTAACA AGGGAAAAAG CCTTCGAGCA AATGTATGAA GAGATGCTTC
451  AGACTCAACA CAGAAATACC TCGAAGAAAG CACAGATTAT TGGAAGCTGT
```

Appendix III. mRNA sequences submitted for RNA secondary structure prediction.

A. Bases 1 – 500 of *ABCB5β*. B. Bases 1601 – 2100 of *ABCB5fl*. C. Bases 2501 – 3000 of *ABCB5fl*.

Appendix IV. Optimisation of MDA-MB-468 transfection

As previously described (see Appendix II), it is critical to optimise seeding of 384-well plates for RNA transfection. As the MDA-MB-468s already express *p16*, it was hypothesised that introduction of the miRNAs would have little or no effect upon the level of p16 and cell proliferation at the experiment end point (120 h), where as the antimiRs may reduce the level of p16 and alter cellular proliferation.

Cells were seeded in 384-well format at seven different densities (5,000 – 35,000 cells cm^{-2}), the media was changed after 48 h and the cells were fixed after 120 h (Appendix IV-I panel A). The 30,000 cells cm^{-2} seeding density was chosen for future experiments, as the final cell number (10655 ± 1381) would allow for changes in cell proliferation following miRNA transfection to be visualised. The two outermost rows (A and B) and columns (1 and 2) were omitted to eliminate the edge effect from the experiments (as described in Appendix II; Appendix IV-I panel B).

The next step of the transfection optimisation was to determine the ideal volume of transfection reagent to use per well to provide a significant knockdown of target gene expression without causing cellular toxicity. These experiments were carried out in MDA-MB-468 cells as previously described for HMECs (see Appendix II), although with both 60 nM and 90 nM concentrations of siRNA (Appendix IV-II).

In light of these optimisation experiments, 0.2 μL $well^{-1}$ of HiPerFect was chosen for all future si/miRNA experiments at both 60 nM and 90 nM in MDA-MB-468 cells, as it was found to give the strongest knockdown with no significant toxicity.

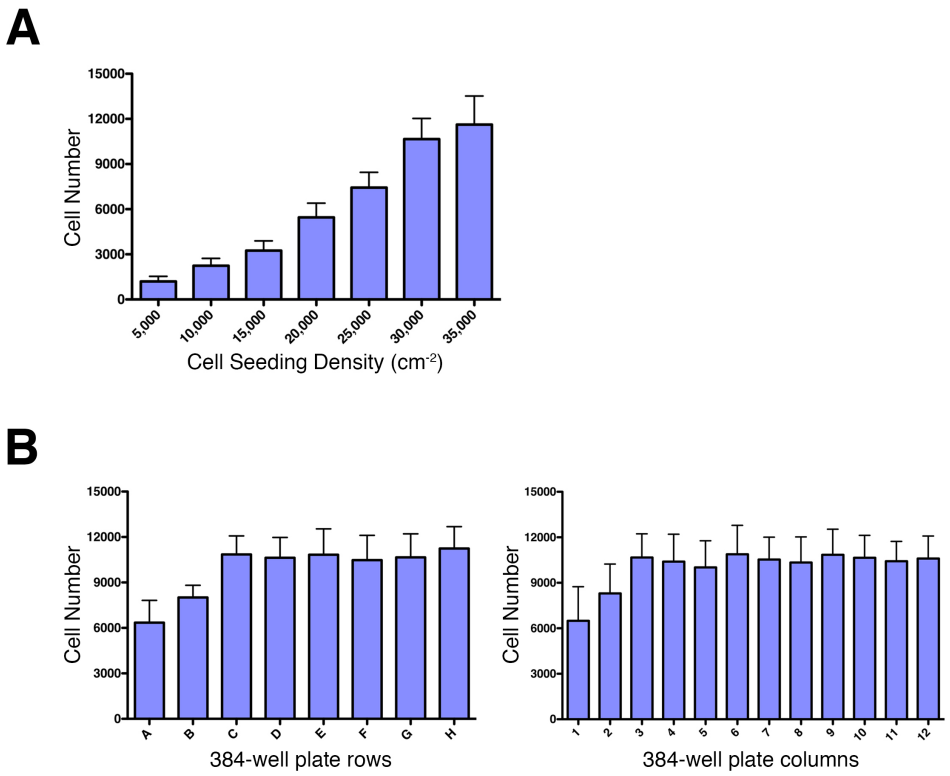

Appendix IV-I Seeding density optimisation for MDA-MB-468 transfection in 384-well format.

A. MDA-MB-468s seeded at increasing cell densities in wells of a 384-well plate were fixed and counted after 120 h. B. To assess well-to-well variability over the plate, cells seeded at 30,000 cm^{-2} were counted after 120 h in both the rows (A – H) and columns (1 – 12) of a quarter of the plate. The outer rows (A and B) and columns (1 and 2) were found to have consistently lower cell numbers after 120 h than any other row or column. Error bars represent one SD. n = 2 biological replicates.

As the transfection of siRNA targeting *p16* at 60 nM was found to cause an increase in cell number with lower concentrations of HiPerFect, it can be concluded that although the MDA-MB-468 cells proliferate whilst expressing p16 they remain responsive to changes in its expression level.

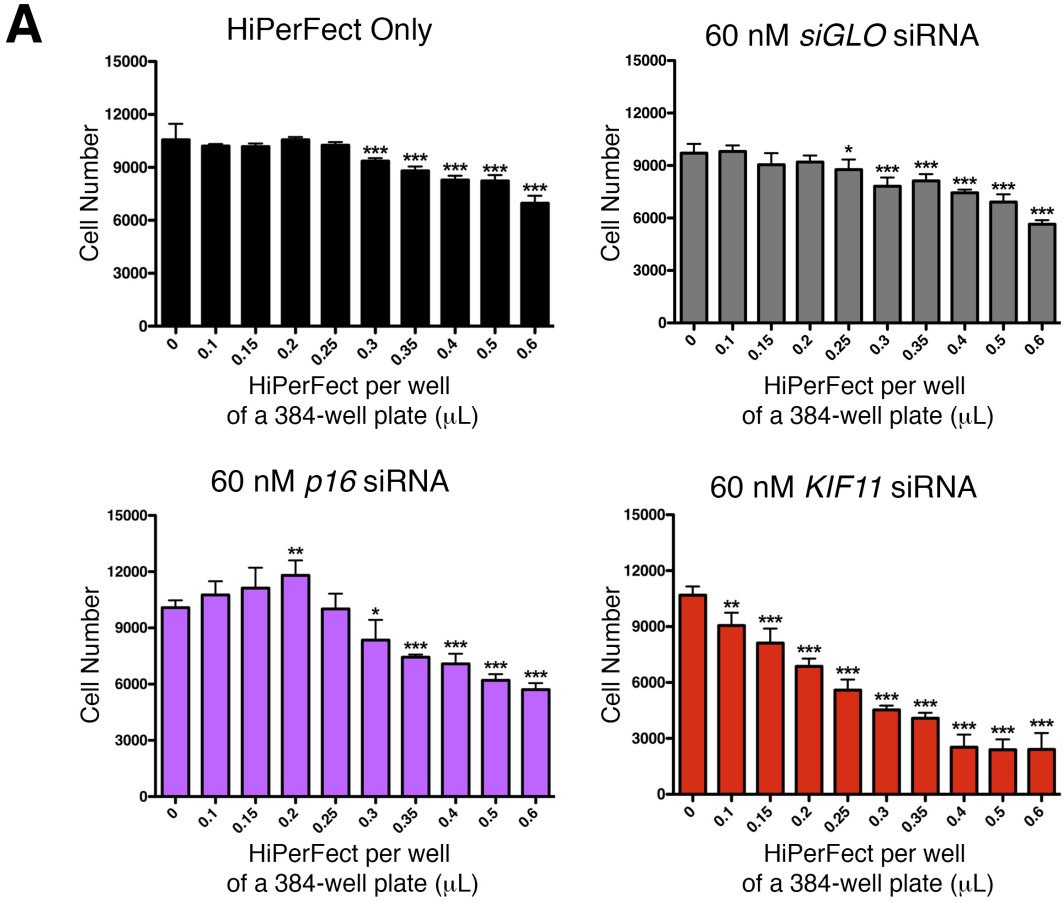

Appendix IV-II. Optimisation of transfection reagent volume for MDA-MB-468 transfection.

A. MDA-MB-468s were treated with transfection reagent as indicated (HiPerFect Only; black columns) or HiPerFect with 60nM siRNA (*siGLO* – grey columns; *p16* – purple columns; *KIF11* – red columns). Cells were fixed 120 h post transfection, stained with DAPI and imaged using an IN Cell 1000 microscope at 10x magnification (GE Healthcare, UK). Nuclei were counted from the resulting images using Developer Toolbox 1.7 (GE Healthcare, UK). Error bars represent one SD, * $p < 0.05$, ** $p < 0.01$, *** $p < 0.001$. n = 2 biological repeats.

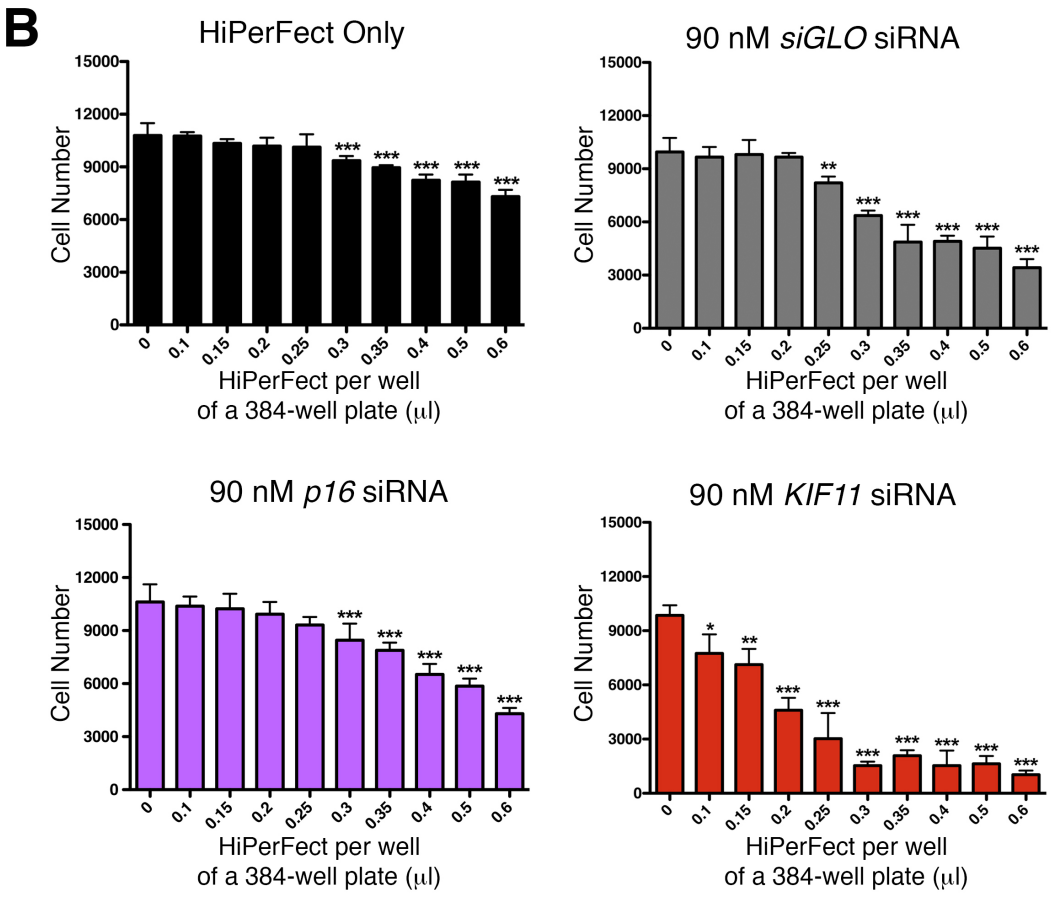

Appendix IV-II. (continued) Optimisation of transfection reagent volume for MDA-MB-468 transfection.

B. MDA-MB-468s were treated with transfection reagent as indicated (HiPerFect Only; black columns) or HiPerFect with 90nM siRNA (*siGLO* – grey columns; *p16* – purple columns; *KIF11* – red columns). Cells were fixed 120 h post transfection, stained with DAPI and imaged using an IN Cell 1000 microscope at 10x magnification (GE Healthcare, UK). Nuclei were counted from the resulting images using Developer Toolbox 1.7 (GE Healthcare, UK). Error bars represent one SD, * $p < 0.05$, ** $p < 0.01$, *** $p < 0.001$. n = 2 biological repeats.

Appendix V. Potential mRNA target genes linked to cellular proliferation and p16 by IPA Core Analysis.

Gene Symbol	Accession Number	Gene Name	p-value	Location	Type
AARS2	NM_020745	alanyl-tRNA synthetase 2, mitochondrial	2.74E-02	Cytoplasm	enzyme
AARS	NM_001605	alanyl-tRNA synthetase	1.98E-02	Cytoplasm	enzyme
ABCB9	NM_203444	ATP-binding cassette, sub-family B, member 9	1.42E-02	Cytoplasm	transporter
ABCG1	NM_207627	ATP-binding cassette, sub-family G, member 1	3.30E-03	Plasma Membrane	transporter
ABCG8	NM_022437	ATP-binding cassette, sub-family G, member 8	3.40E-02	Plasma Membrane	transporter
ABHD12	NM_001042472	abhydrolase domain containing 12	9.80E-03	unknown	enzyme
ACAD9	NM_014049	acyl-CoA dehydrogenase family, member 9	0.00E+00	Cytoplasm	enzyme
ACAD11	NM_032169	acyl-CoA dehydrogenase family, member 11	1.26E-02	Cytoplasm	enzyme
ACADS	NM_000017	acyl-CoA dehydrogenase, C-2 to C-3 short chain	3.46E-02	Cytoplasm	enzyme
ACOT13	NM_018473	acyl-CoA thioesterase 13	6.90E-03	Cytoplasm	enzyme
ADAL	NM_001012969	adenosine deaminase-like	2.40E-02	Cytoplasm	enzyme
ADAMTS5	NM_007038	ADAM metallopeptidase with thrombospondin type 1 motif, 5	1.50E-03	Extracellular Space	peptidase
ADAR	NM_001111	adenosine deaminase, RNA-specific	4.12E-02	Nucleus	enzyme
ADCY6	NM_015270	adenylate cyclase 6	3.62E-02	Plasma Membrane	enzyme
ADCY7	NM_001114	adenylate cyclase 7	1.00E-02	Plasma Membrane	enzyme
ADD2	NM_017488	adducin 2	2.48E-02	Cytoplasm	other
ADIPOR1	NM_015999	adiponectin receptor 1	4.51E-02	Plasma Membrane	transmembrane receptor
ADM	NM_001124	adrenomedullin	1.12E-02	Extracellular Space	other
ADRA1A	NM_033303	adrenoceptor alpha 1A	2.65E-02	Plasma Membrane	G-protein coupled receptor
AGPAT1	NM_006411	1-acylglycerol-3-phosphate O-acyltransferase 1	1.62E-02	Cytoplasm	enzyme
AGPAT2	NM_006412	1-acylglycerol-3-phosphate O-acyltransferase 2	9.70E-03	Cytoplasm	enzyme
AGPAT3	NM_020132	1-acylglycerol-3-phosphate O-acyltransferase 3	1.96E-02	Cytoplasm	enzyme
AGPAT9	NM_032717	1-acylglycerol-3-phosphate O-acyltransferase 9	4.20E-03	Cytoplasm	enzyme
AIM1	NM_001624	absent in melanoma 1	2.85E-02	Extracellular Space	other
AKIP1	NM_182901	A kinase (PRKA) interacting protein 1	3.59E-02	Nucleus	other
AMFR	NM_001144	autocrine motility factor receptor, E3 ubiquitin protein ligase	2.20E-02	Plasma Membrane	transmembrane receptor
ANGPT4	NM_015985	angiopoietin 4	5.20E-03	Extracellular Space	growth factor
ANKS1A	NM_015245	ankyrin repeat and sterile alpha motif domain containing 1A	2.70E-03	Cytoplasm	other
ANP32A	NM_006305	acidic (leucine-rich) nuclear phosphoprotein 32 family, member A	1.53E-02	Nucleus	other
ANPEP	NM_001150	alanyl (membrane) aminopeptidase	3.27E-02	Plasma Membrane	peptidase
AP1M2	NM_005498	adaptor-related protein complex 1, mu 2 subunit	2.37E-02	Cytoplasm	transporter
AP2A1	NM_014203	adaptor-related protein complex 2, alpha 1 subunit	2.14E-02	Cytoplasm	transporter
AP2B1	NM_001030006	adaptor-related protein complex 2, beta 1 subunit	1.03E-02	Cytoplasm	transporter
APH1A	NM_016022	anterior pharynx defective 1 homolog A	1.73E-02	Cytoplasm	peptidase
APH1B	NM_031301	anterior pharynx defective 1 homolog B	8.10E-03	Plasma Membrane	peptidase
APPL2	NM_018171	adaptor protein, phosphotyrosine interaction, PH domain and leucine zipper containing 2	1.63E-02	Cytoplasm	other
ARAF	NM_001654	v-raf murine sarcoma 3611 viral oncogene homolog	7.40E-03	Cytoplasm	kinase
ARHGAP1	NM_004308	Rho GTPase activating protein 1	2.98E-02	Cytoplasm	other
ARHGEF5	NM_005435	Rho guanine nucleotide exchange factor 5	9.00E-03	Cytoplasm	other
ATP13A2	NM_022089	ATPase type 13A2	4.00E-03	Cytoplasm	transporter
ATP2B1	NM_001001323	ATPase, Ca++ transporting, plasma membrane 1	4.82E-02	Plasma Membrane	transporter
ATXN10	NM_013236	ataxin 10	1.93E-02	Cytoplasm	other

Appendix V-I. Predicted target genes of hsa-miR-24 based upon miRWalk target comparison.

Gene Symbol	Accession Number	Gene Name	p-value	Location	Type
AURKA	NM_198433	aurora kinase A	4.63E-02	Nucleus	kinase
BBC3	NM_014417	BCL2 binding component 3	1.48E-02	Cytoplasm	other
BCL2	NM_000633	B-cell CLL/lymphoma 2	5.00E-03	Cytoplasm	transporter
BCL2L2	NM_004050	BCL2-like 2	4.20E-02	Cytoplasm	other
BCL2L11	NM_138621	BCL2-like 11 (apoptosis facilitator)	4.00E-03	Cytoplasm	other
BDKRB2	NM_000623	bradykinin receptor B2	4.22E-02	Plasma Membrane	G-protein coupled receptor
BLVRB	NM_000713	biliverdin reductase B	7.50E-03	Cytoplasm	enzyme
BNIP1	NM_013979	BCL2/adenovirus E1B 19kDa interacting protein 1	7.10E-03	Cytoplasm	other
BNIP3L	NM_004331	BCL2/adenovirus E1B 19kDa interacting protein 3-like	2.60E-03	Cytoplasm	other
C2	NM_000063	complement component 2	4.80E-03	Extracellular Space	peptidase
C1R	NM_001733	complement component 1, r subcomponent	5.30E-03	Extracellular Space	peptidase
CACNA1E	NM_000721	calcium channel, voltage-dependent, R type, alpha 1E subunit	4.12E-02	Plasma Membrane	ion channel
CALCR	NM_001742	calcitonin receptor	7.10E-03	Plasma Membrane	G-protein coupled receptor
CARD10	NM_014550	caspase recruitment domain family, member 10	4.82E-02	Cytoplasm	other
CBS	NM_000071	cystathionine-beta-synthase	4.23E-02	Cytoplasm	enzyme
CBX5	NM_001127322	chromobox homolog 5	6.00E-04	Nucleus	transcription regulator
CCNI	NM_006835	cyclin I	1.29E-02	unknown	other
CCT3	NM_005998	chaperonin containing TCP1, subunit 3	3.60E-03	Cytoplasm	other
CD74	NM_001025159	CD74 molecule, major histocompatibility complex, class II invariant chain	9.40E-03	Plasma Membrane	transmembrane receptor
CD3E	NM_000733	CD3e molecule, epsilon	9.90E-03	Plasma Membrane	transmembrane receptor
CDC34	NM_004359	cell division cycle 34	3.31E-02	Nucleus	enzyme
CDC73	NM_024529	cell division cycle 73	1.84E-02	Nucleus	other
CDC25A	NM_001789	cell division cycle 25A	2.68E-02	Nucleus	phosphatase
CDC42EP3	NM_006449	CDC42 effector protein 3	8.40E-03	Cytoplasm	other
CDH13	NM_001257	cadherin 13, H-cadherin (heart)	2.38E-02	Plasma Membrane	other
CDK5	NM_004935	cyclin-dependent kinase 5	1.23E-02	Nucleus	kinase
CDKN1B	NM_004064	cyclin-dependent kinase inhibitor 1B	5.10E-03	Nucleus	kinase
CDKN1C	NM_000076	cyclin-dependent kinase inhibitor 1C	4.28E-02	Nucleus	other
CGN	NM_020770	cingulin	5.20E-03	Plasma Membrane	other
CHCHD6	NM_032343	coiled-coil-helix-coiled-coil-helix domain containing 6	1.44E-02	Cytoplasm	other
CHDH	NM_018397	choline dehydrogenase	2.70E-03	Cytoplasm	enzyme
CHRNB4	NM_000750	cholinergic receptor, nicotinic, beta 4	4.99E-02	Plasma Membrane	transmembrane receptor
CHTF18	NM_022092	CTF18, chromosome transmission fidelity factor 18 homolog	6.40E-03	unknown	other
CITED4	NM_133467	Cbp/p300-interacting transactivator, with Glu/Asp-rich carboxy-terminal domain, 4	8.20E-03	Nucleus	transcription regulator
CLDN4	NM_001305	claudin 4	3.30E-03	Plasma Membrane	transmembrane receptor
CLTC	NM_004859	clathrin, heavy chain	4.63E-02	Plasma Membrane	other
CNTFR	NM_147164	ciliary neurotrophic factor receptor	3.92E-02	Plasma Membrane	transmembrane receptor
COPG2	NM_012133	coatomer protein complex, subunit gamma 2	6.60E-03	Cytoplasm	transporter
COPS4	NM_016129	COP9 signalosome subunit 4	2.44E-02	Cytoplasm	other
CSK	NM_004383	c-src tyrosine kinase	0.00E+00	Cytoplasm	kinase
CSTF1	NM_001324	cleavage stimulation factor, 3' pre-RNA, subunit 1, 50kDa	3.00E-03	Nucleus	other
CTSD	NM_001909	cathepsin D	3.20E-03	Cytoplasm	peptidase
CXCL16	NM_022059	chemokine ligand 16	1.50E-02	Extracellular Space	cytokine
CYTH2	NM_017457	cytohesin 2	4.63E-02	Cytoplasm	other
DDIT3	NM_004083	DNA-damage-inducible transcript 3	1.44E-02	Nucleus	transcription regulator
DEDD	NM_032998	death effector domain containing	1.77E-02	Nucleus	other
DEGS2	NM_206918	delta(4)-desaturase, sphingolipid 2	2.12E-02	Cytoplasm	enzyme
DGAT2	NM_032564	diacylglycerol O-acyltransferase 2	1.00E-04	Cytoplasm	enzyme

Appendix V-I. (continued) Predicted target genes of hsa-miR-24 based upon miRWalk target comparison.

Gene Symbol	Accession Number	Gene Name	p-value	Location	Type
DHCR24	NM_014762	24-dehydrocholesterol reductase	3.90E-02	Cytoplasm	enzyme
DIAPH1	NM_005219	diaphanous homolog 1	7.00E-03	Plasma Membrane	other
DLC1	NM_182643	deleted in liver cancer 1	2.30E-03	Cytoplasm	other
DNAJB2	NM_006736	DnaJ (Hsp40) homolog, subfamily B, member 2	2.88E-02	Nucleus	other
DNAJB12	NM_001002762	DnaJ (Hsp40) homolog, subfamily B, member 12	1.14E-02	Cytoplasm	other
DNAJC3	NM_006260	DnaJ (Hsp40) homolog, subfamily C, member 3	0.00E+00	Cytoplasm	other
DNAL4	NM_005740	dynein, axonemal, light chain 4	1.45E-02	Cytoplasm	enzyme
DSCR3	NM_006052	Down syndrome critical region gene 3	3.18E-02	Nucleus	other
DUSP8	NM_004420	dual specificity phosphatase 8	9.40E-03	Nucleus	phosphatase
ECSIT	NM_016581	ECSIT homolog (Drosophila)	1.78E-02	Nucleus	transcription regulator
EFHD1	NM_025202	EF-hand domain family, member D1	1.63E-02	Cytoplasm	other
EIF2AK2	NM_002759	eukaryotic translation initiation factor 2-alpha kinase 2	4.28E-02	Cytoplasm	kinase
EIF2AK4	NM_001013703	eukaryotic translation initiation factor 2 alpha kinase 4	3.19E-02	Cytoplasm	kinase
EIF3I	NM_003757	eukaryotic translation initiation factor 3, subunit I	6.20E-03	Cytoplasm	translation regulator
ELF3	NM_001114309	E74-like factor 3	7.10E-03	Nucleus	transcription regulator
ELOVL2	NM_017770	ELOVL fatty acid elongase 2	4.51E-02	Cytoplasm	enzyme
ELP5	NM_203413	elongator acetyltransferase complex subunit 5	1.76E-02	unknown	other
EMC9	NM_016049	ER membrane protein complex subunit 9	1.60E-03	Plasma Membrane	other
ENTPD1	NM_001776	ectonucleoside triphosphate diphosphohydrolase 1	4.07E-02	Plasma Membrane	enzyme
ENTPD6	NM_001247	ectonucleoside triphosphate diphosphohydrolase 6	1.74E-02	Cytoplasm	enzyme
EPAS1	NM_001430	endothelial PAS domain protein 1	3.13E-02	Nucleus	transcription regulator
EPHA4	NM_004438	EPH receptor A4	5.00E-02	Plasma Membrane	kinase
ERBB3	NM_001982	v-erb-b2 erythroblastic leukemia viral oncogene homolog 3	4.90E-03	Plasma Membrane	kinase
ERGIC1	NM_020462	endoplasmic reticulum-golgi intermediate compartment (ERGIC) 1	3.10E-03	Cytoplasm	other
ERP29	NM_006817	endoplasmic reticulum protein 29	3.41E-02	Cytoplasm	transporter
EXOC5	NM_006544	exocyst complex component 5	5.80E-03	Cytoplasm	other
FAM213B	NM_152371	family with sequence similarity 213, member B	3.08E-02	Cytoplasm	enzyme
FANCE	NM_021922	Fanconi anemia, complementation group E	4.59E-02	Nucleus	other
FASLG	NM_000639	Fas ligand	1.37E-02	Extracellular Space	cytokine
FBLN1	NM_006486	fibulin 1	1.04E-02	Extracellular Space	other
FBN1	NM_000138	fibrillin 1	4.01E-02	Extracellular Space	other
FCGRT	NM_004107	Fc fragment of IgG, receptor, transporter, alpha	1.49E-02	Plasma Membrane	transmembrane receptor
FDXR	NM_004110	ferredoxin reductase	5.40E-03	Cytoplasm	enzyme
FGF9	NM_002010	fibroblast growth factor 9	4.59E-02	Extracellular Space	growth factor
FGFBP1	NM_005130	fibroblast growth factor binding protein 1	2.39E-02	Extracellular Space	other
FKBP1B	NM_054033	FK506 binding protein 1B	3.81E-02	Cytoplasm	enzyme
FLOT1	NM_005803	flotillin 1	2.36E-02	Plasma Membrane	other
FNTB	NM_002028	farnesyltransferase, CAAX box, beta	1.30E-03	Cytoplasm	enzyme
FOS	NM_005252	FBJ murine osteosarcoma viral oncogene homolog	4.68E-02	Nucleus	transcription regulator
FST	NM_006350	follistatin	6.20E-03	Extracellular Space	other
FTL	NM_000146	ferritin, light polypeptide	9.80E-03	Cytoplasm	enzyme
FURIN	NM_002569	furin	2.38E-02	Cytoplasm	peptidase
FZD5	NM_003468	frizzled family receptor 5	1.67E-02	Plasma Membrane	G-protein coupled receptor
GAMT	NM_000156	guanidinoacetate N-methyltransferase	1.80E-02	Cytoplasm	enzyme
GATA2	NM_032638	GATA binding protein 2	2.42E-02	Nucleus	transcription regulator
GCAT	NM_014291	glycine C-acetyltransferase	1.15E-02	Cytoplasm	enzyme
GDI1	NM_001493	GDP dissociation inhibitor 1	4.88E-02	Cytoplasm	other
GFPT1	NM_002056	glutamine--fructose-6-phosphate transaminase 1	2.42E-02	Cytoplasm	enzyme

Appendix V-I. (continued) Predicted target genes of hsa-miR-24 based upon miRWalk target comparison.

Gene Symbol	Accession Number	Gene Name	p-value	Location	Type
GGT5	NM_001099781	gamma-glutamyltransferase 5	1.93E-02	Plasma Membrane	enzyme
GLG1	NM_012201	golgi glycoprotein 1	8.60E-03	Cytoplasm	other
GLIS2	NM_032575	GLIS family zinc finger 2	5.00E-04	Nucleus	transcription regulator
GM2A	NM_000405	GM2 ganglioside activator	4.39E-02	Cytoplasm	enzyme
GNE	NM_005476	glucosamine (UDP-N-acetyl)-2-epimerase/N-acetylmannosamine kinase	4.39E-02	Cytoplasm	kinase
GOSR2	NM_004287	golgi SNAP receptor complex member 2	3.90E-02	Cytoplasm	transporter
GOT1	NM_002079	glutamic-oxaloacetic transaminase 1,	4.12E-02	Cytoplasm	enzyme
GPR56	NM_201524	G protein-coupled receptor 56	2.30E-02	Plasma Membrane	G-protein coupled receptor
GRINA	NM_000837	glutamate receptor, ionotropic, N-methyl D-aspartate-associated protein 1	3.55E-02	unknown	ion channel
GSK3B	NM_002093	glycogen synthase kinase 3 beta	1.60E-03	Nucleus	kinase
GSTT1	NM_000853	glutathione S-transferase theta 1	1.81E-02	Cytoplasm	enzyme
GTF2H5	NM_207118	general transcription factor IIH, polypeptide 5	1.21E-02	Nucleus	other
H1FX	NM_006026	H1 histone family, member X	2.94E-02	Nucleus	other
H2AFX	NM_002105	H2A histone family, member X	1.73E-02	Nucleus	transcription regulator
HDAC1	NM_004964	histone deacetylase 1	3.47E-02	Nucleus	transcription regulator
HELLS	NM_018063	helicase, lymphoid-specific	3.26E-02	Nucleus	enzyme
HERC2	NM_004667	HECT and RLD domain containing E3 ubiquitin protein ligase 2	1.10E-02	Cytoplasm	enzyme
HEXA	NM_000520	hexosaminidase A	3.83E-02	Cytoplasm	enzyme
HIST1H4A	NM_003540	histone cluster 1, H4a	3.40E-03	Nucleus	other
HKR1	NM_181786	HKR1, GLI-Kruppel zinc finger family member	4.20E-02	Nucleus	other
HLA-E	NM_005516	major histocompatibility complex, class I, E	3.51E-02	Plasma Membrane	transmembrane receptor
HMGCL	NM_000191	3-hydroxymethyl-3-methylglutaryl-CoA lyase	3.57E-02	Cytoplasm	enzyme
HMOX1	NM_002133	heme oxygenase 1	3.61E-02	Cytoplasm	enzyme
HOMER3	NM_004838	homer homolog 3	1.72E-02	Plasma Membrane	other
HOXB7	NM_004502	homeobox B7	3.71E-02	Nucleus	transcription regulator
HS6ST2	NM_001077188	heparan sulfate 6-O-sulfotransferase 2	3.33E-02	Plasma Membrane	enzyme
HYAL1	NM_007312	hyaluronoglucosaminidase 1	2.30E-03	Cytoplasm	enzyme
IFNG	NM_000619	interferon, gamma	9.30E-03	Extracellular Space	cytokine
IGFBP5	NM_000599	insulin-like growth factor binding protein 5	1.79E-02	Extracellular Space	other
IKBKE	NM_014002	inhibitor of kappa light polypeptide gene enhancer in B-cells, kinase epsilon	1.13E-02	Cytoplasm	kinase
IKZF1	NM_006060	IKAROS family zinc finger 1	1.69E-02	Nucleus	transcription regulator
IL10RB	NM_000628	interleukin 10 receptor, beta	1.30E-02	Plasma Membrane	transmembrane receptor
IL15RA	NM_172200	interleukin 15 receptor, alpha	4.32E-02	Plasma Membrane	transmembrane receptor
IL1A	NM_000575	interleukin 1, alpha	1.76E-02	Extracellular Space	cytokine
IL1B	NM_000576	interleukin 1, beta	3.60E-02	Extracellular Space	cytokine
INPP5K	NM_130766	inositol polyphosphate-5-phosphatase K	1.91E-02	Cytoplasm	phosphatase
IP6K2	NM_016291	inositol hexakisphosphate kinase 2	4.30E-03	Cytoplasm	kinase
IRF3	NM_001571	interferon regulatory factor 3	4.70E-03	Nucleus	transcription regulator
ITGA2B	NM_000419	integrin, alpha 2b	2.80E-03	Plasma Membrane	transmembrane receptor
ITGB3	NM_000212	integrin, beta 3	3.75E-02	Plasma Membrane	transmembrane receptor
ITGB8	NM_002214	integrin, beta 8	5.50E-03	Plasma Membrane	other
ITPK1	NM_014216	inositol-tetrakisphosphate 1-kinase	6.50E-03	Cytoplasm	kinase
IVD	NM_002225	isovaleryl-CoA dehydrogenase	3.60E-02	Cytoplasm	enzyme
KCNK2	NM_001017424	potassium channel, subfamily K, member 2	7.40E-03	Plasma Membrane	ion channel
KLF6	NM_001300	Kruppel-like factor 6	1.90E-03	Nucleus	transcription regulator
KLF8	NM_007250	Kruppel-like factor 8	2.40E-03	Nucleus	other
KLF9	NM_001206	Kruppel-like factor 9	1.21E-02	Nucleus	transcription regulator
KRT7	NM_005556	keratin 7	3.30E-03	Cytoplasm	other

Appendix V-I. (continued) Predicted target genes of hsa-miR-24 based upon miRWalk target comparison.

Gene Symbol	Accession Number	Gene Name	p-value	Location	Type
L3MBTL2	NM_031488	l(3)mbt-like 2 (Drosophila)	1.56E-02	Nucleus	transcription regulator
LAIR1	NM_002287	leukocyte-associated immunoglobulin-like receptor 1	2.47E-02	Plasma Membrane	transmembrane receptor
LAMB3	NM_001017402	laminin, beta 3	6.50E-03	Extracellular Space	transporter
LAMC1	NM_002293	laminin, gamma 1	1.06E-02	Extracellular Space	other
LARS2	NM_015340	leucyl-tRNA synthetase 2, mitochondrial	5.00E-03	Cytoplasm	enzyme
LCOR	NM_032440	ligand dependent nuclear receptor corepressor	1.14E-02	Nucleus	transcription regulator
LIAS	NM_006859	lipoic acid synthetase	3.31E-02	Cytoplasm	enzyme
LIMK1	NM_002314	LIM domain kinase 1	4.70E-03	Cytoplasm	kinase
LIMK2	NM_016733	LIM domain kinase 2	2.47E-02	Cytoplasm	kinase
LIMS2	NM_017980	LIM and senescent cell antigen-like domains 2	3.30E-03	Cytoplasm	other
LIPG	NM_006033	lipase, endothelial	3.58E-02	Extracellular Space	enzyme
LMNB2	NM_032737	lamin B2	2.60E-03	Nucleus	other
LOX	NM_002317	lysyl oxidase	8.70E-03	Extracellular Space	enzyme
LPAR6	NM_005767	lysophosphatidic acid receptor 6	5.50E-03	Plasma Membrane	G-protein coupled receptor
LPIN2	NM_014646	lipin 2	4.93E-02	Nucleus	phosphatase
LPPR4	NM_014839	lipid phosphate phosphatase-related protein type 4	3.87E-02	Plasma Membrane	phosphatase
LTBP4	NM_001042544	latent transforming growth factor beta binding protein 4	1.74E-02	Extracellular Space	growth factor
LY6K	NM_017527	lymphocyte antigen 6 complex, locus K	1.25E-02	Nucleus	other
MAF	NM_001031804	v-maf musculoaponeurotic fibrosarcoma oncogene homolog	4.70E-03	Nucleus	transcription regulator
MAGI1	NM_015520	membrane associated guanylate kinase, WW and PDZ domain containing 1	4.25E-02	Plasma Membrane	kinase
MAP1LC3A	NM_032514	microtubule-associated protein 1 light chain 3 alpha	7.80E-03	Cytoplasm	other
MAP3K2	NM_006609	mitogen-activated protein kinase kinase kinase 2	4.50E-02	Cytoplasm	kinase
MAPK3	NM_001040056	mitogen-activated protein kinase 3	4.95E-02	Cytoplasm	kinase
MAPK7	NM_139033	mitogen-activated protein kinase 7	5.30E-03	Cytoplasm	kinase
MAPK12	NM_002969	mitogen-activated protein kinase 12	3.14E-02	Cytoplasm	kinase
MAPK8IP1	NM_005456	mitogen-activated protein kinase 8 interacting protein 1	4.61E-02	Cytoplasm	other
MAPKAPK2	NM_004759	mitogen-activated protein kinase-activated protein kinase 2	8.40E-03	Nucleus	kinase
MAPKAPK3	NM_004635	mitogen-activated protein kinase-activated protein kinase 3	4.70E-03	Nucleus	kinase
MAT1A	NM_000429	methionine adenosyltransferase I, alpha	2.97E-02	Cytoplasm	enzyme
MBOAT7	NM_024298	membrane bound O-acyltransferase domain containing 7	9.60E-03	Plasma Membrane	other
MBTPS2	NM_015884	membrane-bound transcription factor peptidase, site 2	4.15E-02	Cytoplasm	peptidase
MCM4	NM_005914	minichromosome maintenance complex component 4	4.36E-02	Nucleus	enzyme
MDM2	NM_002392	MDM2 oncogene, E3 ubiquitin protein ligase	3.51E-02	Nucleus	transcription regulator
MED12	NM_005120	mediator complex subunit 12	1.00E-03	Nucleus	transcription regulator
MLXIP	NM_014938	MLX interacting protein	3.95E-02	Nucleus	other
MMP10	NM_002425	matrix metallopeptidase 10	1.75E-02	Extracellular Space	peptidase
MMP11	NM_005940	matrix metallopeptidase 11	1.19E-02	Extracellular Space	peptidase
MMP14	NM_004995	matrix metallopeptidase 14	2.37E-02	Extracellular Space	peptidase
MMP24	NM_006690	matrix metallopeptidase 24	3.60E-02	Plasma Membrane	peptidase
MNT	NM_020310	MNT, MAX dimerization protein	4.28E-02	Nucleus	transcription regulator
MPI	NM_002435	mannose phosphate isomerase	7.50E-03	Cytoplasm	enzyme
MTMR14	NM_001077525	myotubularin related protein 14	2.91E-02	Cytoplasm	phosphatase
MYBBP1A	NM_014520	MYB binding protein (P160) 1a	8.10E-03	Nucleus	transcription regulator
MYC	NM_002467	v-myc myelocytomatosis viral oncogene homolog	2.93E-02	Nucleus	transcription regulator
MYD88	NM_002468	myeloid differentiation primary response 88	2.63E-02	Plasma Membrane	other
MYH11	NM_001040113	myosin, heavy chain 11, smooth muscle	1.51E-02	Cytoplasm	other
NCOA5	NM_020967	nuclear receptor coactivator 5	1.99E-02	Nucleus	other
NCSTN	NM_015331	nicastrin	4.12E-02	Plasma Membrane	peptidase

Appendix V-I. (continued) Predicted target genes of hsa-miR-24 based upon miRWalk target comparison.

Gene Symbol	Accession Number	Gene Name	p-value	Location	Type
NDUFV3	NM_021075	NADH dehydrogenase flavoprotein 3, 10kDa	3.97E-02	Cytoplasm	enzyme
NEK2	NM_002497	NIMA-related kinase 2	3.87E-02	Cytoplasm	kinase
NELL2	NM_006159	NEL-like 2	3.90E-02	Extracellular Space	other
NF1	NM_001042492	neurofibromin 1	1.34E-02	Cytoplasm	other
NFKBIE	NM_004556	nuclear factor of kappa light polypeptide gene enhancer in B-cells inhibitor, epsilon	0.00E+00	Nucleus	transcription regulator
NINL	NM_025176	ninein-like	4.51E-02	Cytoplasm	other
NME4	NM_005009	NME/NM23 nucleoside diphosphate kinase 4	2.79E-02	Cytoplasm	kinase
NOL3	NM_003946	nucleolar protein 3	4.11E-02	Nucleus	other
NR1D1	NM_021724	nuclear receptor subfamily 1, group D, member 1	1.78E-02	Nucleus	ligand-dependent nuclear receptor
NRP1	NM_003873	neuropilin 1	9.90E-03	Plasma Membrane	transmembrane receptor
NRP2	NM_201266	neuropilin 2	4.60E-02	Plasma Membrane	kinase
NSDHL	NM_001129765	NAD(P) dependent steroid dehydrogenase-like	1.60E-02	Cytoplasm	enzyme
P2RY6	NM_004154	pyrimidinergic receptor P2Y, G-protein coupled, 6	1.69E-02	Plasma Membrane	G-protein coupled receptor
PADI1	NM_013358	peptidyl arginine deiminase, type I	6.70E-03	Cytoplasm	enzyme
PADI4	NM_012387	peptidyl arginine deiminase, type IV	1.48E-02	Cytoplasm	enzyme
PAK4	NM_001014831	p21 protein (Cdc42/Rac)-activated kinase 4	1.25E-02	Cytoplasm	kinase
PARVA	NM_018222	parvin, alpha	2.91E-02	Cytoplasm	other
PCBP2	NM_005016	poly(rC) binding protein 2	2.61E-02	Nucleus	other
PCSK9	NM_174936	proprotein convertase subtilisin/kexin type 9	3.00E-04	Extracellular Space	peptidase
PDE6B	NM_000283	phosphodiesterase 6B, cGMP-specific, rod, beta	4.04E-02	Cytoplasm	enzyme
PDGFRA	NM_006206	platelet-derived growth factor receptor, alpha polypeptide	1.13E-02	Plasma Membrane	kinase
PDGFRB	NM_002609	platelet-derived growth factor receptor, beta polypeptide	2.90E-02	Plasma Membrane	kinase
PDXP	NM_020315	pyridoxal (pyridoxine, vitamin B6) phosphatase	1.71E-02	Plasma Membrane	phosphatase
PEA15	NM_003768	phosphoprotein enriched in astrocytes 15	2.84E-02	Cytoplasm	transporter
PER1	NM_002616	period circadian clock 1	3.63E-02	Nucleus	other
PER2	NM_022817	period circadian clock 2	8.90E-03	Nucleus	other
PFKFB4	NM_004567	6-phosphofructo-2-kinase/fructose-2,6-biphosphatase 4	3.12E-02	Cytoplasm	kinase
PIK3R5	NM_014308	phosphoinositide-3-kinase, regulatory subunit 5	3.26E-02	Cytoplasm	kinase
PIM1	NM_002648	pim-1 oncogene	2.08E-02	Cytoplasm	kinase
PIP4K2B	NM_003559	phosphatidylinositol-5-phosphate 4-kinase, type II, beta	1.00E-03	Cytoplasm	kinase
PKMYT1	NM_182687	protein kinase, membrane associated tyrosine/threonine 1	1.65E-02	Cytoplasm	kinase
PLCL2	NM_015184	phospholipase C-like 2	1.07E-02	Cytoplasm	enzyme
PLTP	NM_006227	phospholipid transfer protein	1.11E-02	Extracellular Space	enzyme
PML	NM_033238	promyelocytic leukemia	4.20E-02	Nucleus	transcription regulator
PNKP	NM_007254	polynucleotide kinase 3'-phosphatase	4.40E-03	Nucleus	kinase
PNPO	NM_018129	pyridoxamine 5'-phosphate oxidase	3.81E-02	Cytoplasm	enzyme
POLR2G	NM_002696	polymerase (RNA) II (DNA directed) polypeptide G	1.23E-02	Nucleus	enzyme
POLR2J	NM_006234	polymerase (RNA) II (DNA directed) polypeptide J, 13.3kDa	3.38E-02	Nucleus	enzyme
POLR3D	NM_001722	polymerase (RNA) III (DNA directed) polypeptide D, 44kDa	1.01E-02	Nucleus	transcription regulator
PPARD	NM_006238	peroxisome proliferator-activated receptor delta	8.00E-03	Nucleus	ligand-dependent nuclear receptor
PPARG	NM_138711	peroxisome proliferator-activated receptor gamma	3.20E-03	Nucleus	ligand-dependent nuclear receptor
PPCS	NM_024664	phosphopantothenoylcysteine synthetase	7.40E-03	Cytoplasm	enzyme
PPID	NM_005038	peptidylprolyl isomerase D	3.75E-02	Cytoplasm	enzyme
PPM1G	NM_177983	protein phosphatase, Mg2+/Mn2+ dependent, 1G	2.51E-02	Nucleus	phosphatase
PRKCA	NM_002737	protein kinase C, alpha	2.53E-02	Cytoplasm	kinase
PRKCH	NM_006255	protein kinase C, eta	1.76E-02	Cytoplasm	kinase
PRPF19	NM_014502	PRP19/PSO4 pre-mRNA processing factor 19 homolog	7.70E-03	Nucleus	enzyme
PRPF40A	NM_017892	PRP40 pre-mRNA processing factor 40 homolog A	4.50E-03	Nucleus	other

Appendix V-I. (continued) Predicted target genes of hsa-miR-24 based upon miRWalk target comparison.

Gene Symbol	Accession Number	Gene Name	p-value	Location	Type
PSG4	NM_002780	pregnancy specific beta-1-glycoprotein 4	4.16E-02	Extracellular Space	other
PSMB8	NM_004159	proteasome (prosome, macropain) subunit, beta type, 8	4.00E-03	Cytoplasm	peptidase
PSMD8	NM_002812	proteasome (prosome, macropain) 26S subunit, non-ATPase, 8	2.72E-02	Cytoplasm	other
PTDSS2	NM_030783	phosphatidylserine synthase 2	1.26E-02	Cytoplasm	enzyme
PTHLH	NM_002820	parathyroid hormone-like hormone	1.56E-02	Extracellular Space	other
PTK2	NM_153831	protein tyrosine kinase 2	1.61E-02	Cytoplasm	kinase
PTPDC1	NM_177995	protein tyrosine phosphatase domain containing 1	2.87E-02	Extracellular Space	phosphatase
PTPLAD1	NM_016395	protein tyrosine phosphatase-like A domain containing 1	2.97E-02	Cytoplasm	other
PTPMT1	NM_175732	protein tyrosine phosphatase, mitochondrial 1	8.00E-04	Cytoplasm	phosphatase
PTPRF	NM_002840	protein tyrosine phosphatase, receptor type, F	2.51E-02	Plasma Membrane	phosphatase
PTRF	NM_012232	polymerase I and transcript release factor	3.37E-02	Nucleus	transcription regulator
RAB4B	NM_016154	RAB4B, member RAS oncogene family	1.60E-03	Plasma Membrane	enzyme
RAB5B	NM_002868	RAB5B, member RAS oncogene family	3.79E-02	Cytoplasm	enzyme
RAB5C	NM_201434	RAB5C, member RAS oncogene family	3.10E-03	Cytoplasm	enzyme
RAP1A	NM_001010935	RAP1A, member of RAS oncogene family	1.63E-02	Cytoplasm	enzyme
RASD2	NM_014310	RASD family, member 2	1.90E-03	Cytoplasm	enzyme
RDH13	NM_138412	retinol dehydrogenase 13	4.47E-02	Cytoplasm	enzyme
RECQL	NM_002907	RecQ protein-like	1.96E-02	Nucleus	enzyme
RFC2	NM_181471	replication factor C (activator 1) 2,	3.74E-02	Nucleus	other
RHOJ	NM_020663	ras homolog family member J	4.86E-02	Cytoplasm	enzyme
RIPK1	NM_003804	receptor (TNFRSF)-interacting serine-threonine kinase 1	7.00E-03	Plasma Membrane	kinase
RNF41	NM_194358	ring finger protein 41	2.95E-02	Cytoplasm	enzyme
RPL13A	NM_012423	ribosomal protein L13a	3.05E-02	Cytoplasm	other
RPS20	NM_001023	ribosomal protein S20	3.20E-03	Cytoplasm	other
RRAS	NM_006270	related RAS viral (r-ras) oncogene homolog	4.70E-03	Cytoplasm	enzyme
RXRG	NM_006917	retinoid X receptor, gamma	1.00E-02	Nucleus	ligand-dependent nuclear receptor
S100B	NM_006272	S100 calcium binding protein B	1.13E-02	Cytoplasm	other
S1PR1	NM_001400	sphingosine-1-phosphate receptor 1	5.30E-03	Plasma Membrane	G-protein coupled receptor
S1PR2	NM_004230	sphingosine-1-phosphate receptor 2	9.20E-03	Plasma Membrane	G-protein coupled receptor
SAP130	NM_024545	Sin3A-associated protein, 130kDa	1.22E-02	Nucleus	transcription regulator
SARS2	NM_017827	seryl-tRNA synthetase 2, mitochondrial	2.11E-02	Cytoplasm	enzyme
SCAND1	NM_016558	SCAN domain containing 1	9.40E-03	Nucleus	transcription regulator
SCARB1	NM_005505	scavenger receptor class B, member 1	1.48E-02	Plasma Membrane	transporter
SCO2	NM_005138	SCO2 cytochrome c oxidase assembly protein	3.50E-03	Cytoplasm	other
SERPINB9	NM_004155	serpin peptidase inhibitor, clade B, member 9	4.34E-02	Cytoplasm	other
SERPINE2	NM_006216	serpin peptidase inhibitor, clade E, member 2	3.10E-03	Extracellular Space	other
SERPINH1	NM_001235	serpin peptidase inhibitor, clade H, member 1,	4.31E-02	Extracellular Space	other
SERTAD1	NM_013376	SERTA domain containing 1	0.00E+00	Nucleus	transcription regulator
SGCB	NM_000232	sarcoglycan, beta	4.88E-02	Plasma Membrane	other
SH2B3	NM_005475	SH2B adaptor protein 3	4.97E-02	Plasma Membrane	other
SIN3A	NM_015477	SIN3 transcription regulator homolog A	4.00E-03	Nucleus	transcription regulator
SIPA1	NM_153253	signal-induced proliferation-associated 1	1.32E-02	Cytoplasm	other
SIRT2	NM_012237	sirtuin 2	3.55E-02	Nucleus	transcription regulator
SIRT6	NM_016539	sirtuin 6	3.06E-02	Nucleus	enzyme
SLC16A2	NM_006517	solute carrier family 16, member 2	3.58E-02	Plasma Membrane	transporter
SLC7A1	NM_003045	solute carrier family 7, member 1	1.92E-02	Plasma Membrane	transporter
SLC7A5	NM_003486	solute carrier family 7, member 5	4.40E-02	Plasma Membrane	transporter
SLC9A3R1	NM_004252	solute carrier family 9, subfamily A, member 3 regulator 1	1.08E-02	Plasma Membrane	other

Appendix V-I. (continued) Predicted target genes of hsa-miR-24 based upon miRWalk target comparison.

Gene Symbol	Accession Number	Gene Name	p-value	Location	Type
SMARCA4	NM_001128844	SWI/SNF related, matrix associated, actin dependent regulator of chromatin, subfamily a, member 4	7.20E-03	Nucleus	transcription regulator
SNCAIP	NM_005460	synuclein, alpha interacting protein	9.20E-03	Cytoplasm	transcription regulator
SNRNP25	NM_024571	small nuclear ribonucleoprotein 25kDa (U11/U12)	3.26E-02	Nucleus	other
SNRNP200	NM_014014	small nuclear ribonucleoprotein 200kDa (U5)	1.04E-02	Nucleus	enzyme
SNTB1	NM_021021	syntrophin, beta 1 (dystrophin-associated protein A1, 59kDa, basic component 1)	4.67E-02	Plasma Membrane	other
SNX1	NM_003099	sorting nexin 1	2.49E-02	Cytoplasm	transporter
SOX6	NM_017508	SRY (sex determining region Y)-box 6	3.83E-02	Nucleus	transcription regulator
SPTAN1	NM_001130438	spectrin, alpha, non-erythrocytic 1	0.00E+00	Plasma Membrane	other
SREBF2	NM_004599	sterol regulatory element binding transcription factor 2	1.11E-02	Nucleus	transcription regulator
SRF	NM_003131	serum response factor (c-fos serum response element-binding transcription factor)	3.51E-02	Nucleus	transcription regulator
SRM	NM_003132	spermidine synthase	1.65E-02	Cytoplasm	enzyme
STAT5B	NM_012448	signal transducer and activator of transcription 5B	3.95E-02	Nucleus	transcription regulator
STC2	NM_003714	stanniocalcin 2	4.68E-02	Extracellular Space	other
STEAP2	NM_152999	STEAP family member 2, metalloreductase	1.91E-02	Plasma Membrane	transporter
SYNJ2	NM_003898	synaptojanin 2	3.26E-02	Cytoplasm	phosphatase
TAB1	NM_006116	TGF-beta activated kinase 1/MAP3K7 binding protein 1	2.52E-02	Cytoplasm	enzyme
TAB2	NM_015093	TGF-beta activated kinase 1/MAP3K7 binding protein 2	2.87E-02	Cytoplasm	other
TAF5	NM_006951	TAF5 RNA polymerase II, TATA box binding protein (TBP)-associated factor	1.30E-02	Nucleus	transcription regulator
TAF10	NM_006284	TAF10 RNA polymerase II, TATA box binding protein (TBP)-associated factor	1.20E-03	Nucleus	transcription regulator
TAGLN	NM_001001522	transgelin	2.71E-02	Cytoplasm	other
TCF7	NM_003202	transcription factor 7	0.00E+00	Nucleus	transcription regulator
TEP1	NM_007110	telomerase-associated protein 1	4.01E-02	Nucleus	enzyme
TFE3	NM_006521	transcription factor binding to IGHM enhancer 3	2.21E-02	Nucleus	transcription regulator
TFPI	NM_006287	tissue factor pathway inhibitor	4.06E-02	Extracellular Space	other
TGFB2	NM_003238	transforming growth factor, beta 2	4.87E-02	Extracellular Space	growth factor
TMEM55B	NM_001100814	transmembrane protein 55B	4.31E-02	Cytoplasm	phosphatase
TNF	NM_000594	tumor necrosis factor	4.75E-02	Extracellular Space	cytokine
TNFRSF19	NM_148957	tumor necrosis factor receptor superfamily, member 19	4.08E-02	Plasma Membrane	transmembrane receptor
TNFRSF1A	NM_001065	tumor necrosis factor receptor superfamily, member 1A	3.52E-02	Plasma Membrane	transmembrane receptor
TNK2	NM_005781	tyrosine kinase, non-receptor, 2	4.86E-02	Cytoplasm	kinase
TNNC1	NM_003280	troponin C type 1	1.17E-02	Cytoplasm	other
TNNI3	NM_000363	troponin I type 3	5.50E-03	Cytoplasm	transporter
TOP1	NM_003286	topoisomerase (DNA) I	4.50E-03	Nucleus	enzyme
TOR2A	NM_130459	torsin family 2, member A	6.40E-03	Extracellular Space	other
TPM2	NM_003289	tropomyosin 2	1.41E-02	Cytoplasm	other
TRAF1	NM_005658	TNF receptor-associated factor 1	1.00E-02	Cytoplasm	other
TRIM55	NM_033058	tripartite motif containing 55	1.53E-02	Cytoplasm	other
TST	NM_003312	thiosulfate sulfurtransferase	1.22E-02	Cytoplasm	enzyme
TWSG1	NM_020648	twisted gastrulation homolog 1	4.35E-02	Extracellular Space	other
TXNDC12	NM_015913	thioredoxin domain containing 12	4.87E-02	Cytoplasm	enzyme
U2AF1	NM_001025204	U2 small nuclear RNA auxiliary factor 1	2.50E-03	Nucleus	other
UBE2D4	NM_015983	ubiquitin-conjugating enzyme E2D 4	1.32E-02	unknown	enzyme
UCK1	NM_031432	uridine-cytidine kinase 1	1.90E-02	Cytoplasm	kinase
UCKL1	NM_017859	uridine-cytidine kinase 1-like 1	8.70E-03	Cytoplasm	kinase
UCP2	NM_003355	uncoupling protein 2	2.03E-02	Cytoplasm	transporter
USP40	NM_018218	ubiquitin specific peptidase 40	2.83E-02	unknown	peptidase
USP54	NM_152586	ubiquitin specific peptidase 54	1.71E-02	unknown	peptidase
VAV1	NM_005428	vav 1 guanine nucleotide exchange factor	1.53E-02	Nucleus	transcription regulator

Appendix V-I. (continued) Predicted target genes of hsa-miR-24 based upon miRWalk target comparison.

Gene Symbol	Accession Number	Gene Name	p-value	Location	Type
VGF	NM_003378	VGF nerve growth factor inducible	3.12E-02	Extracellular Space	growth factor
VPS25	NM_032353	vacuolar protein sorting 25 homolog	3.31E-02	Cytoplasm	other
VPS28	NM_183057	vacuolar protein sorting 28 homolog	2.22E-02	Cytoplasm	transporter
VPS9D1	NM_004913	VPS9 domain containing 1	4.45E-02	unknown	transporter
WDR33	NM_018383	WD repeat domain 33	3.16E-02	Nucleus	other
WDR45	NM_007075	WD repeat domain 45	2.41E-02	unknown	other
WDR46	NM_005452	WD repeat domain 46	2.90E-03	Nucleus	enzyme
WNT4	NM_030761	wingless-type MMTV integration site family, member 4	4.10E-02	Extracellular Space	cytokine
WNT7B	NM_058238	wingless-type MMTV integration site family, member 7B	3.75E-02	Extracellular Space	other
WNT8B	NM_003393	wingless-type MMTV integration site family, member 8B	1.25E-02	Extracellular Space	other
WWOX	NM_016373	WW domain containing oxidoreductase	3.40E-03	Cytoplasm	enzyme
YKT6	NM_006555	YKT6 v-SNARE homolog	1.90E-03	Cytoplasm	enzyme
ZCRB1	NM_033114	zinc finger CCHC-type and RNA binding motif 1	1.49E-02	Nucleus	other
ZNF217	NM_006526	zinc finger protein 217	3.35E-02	Nucleus	transcription regulator

Appendix V-I. (continued) Predicted target genes of hsa-miR-24 based upon miRWalk target comparison.

Gene Symbol	Accession Number	Gene Name	p-value	Location	Type
ABCA1	NM_005502	ATP-binding cassette, sub-family A (ABC1), member 1	8.00E-04	Plasma Membrane	transporter
ABHD2	NM_007011	abhydrolase domain containing 2	2.62E-02	unknown	enzyme
ABL1	NM_007313	c-abl oncogene 1, non-receptor tyrosine kinase	2.99E-02	Nucleus	kinase
ACAD8	NM_014384	acyl-CoA dehydrogenase family, member 8	1.37E-02	Cytoplasm	enzyme
ACAD11	NM_032169	acyl-CoA dehydrogenase family, member 11	4.96E-02	Cytoplasm	enzyme
ACP5	NM_001111035	acid phosphatase 5, tartrate resistant	2.30E-02	Cytoplasm	phosphatase
ACSL1	NM_001995	acyl-CoA synthetase long-chain family member 1	5.90E-03	Cytoplasm	enzyme
ADAM17	NM_003183	ADAM metallopeptidase domain 17	1.38E-02	Plasma Membrane	peptidase
AGL	NM_000028	amylo-alpha-1, 6-glucosidase, 4-alpha-glucanotransferase	3.55E-02	Cytoplasm	enzyme
AHCYL2	NM_015328	adenosylhomocysteinase-like 2	4.74E-02	unknown	enzyme
AKR1B1	NM_001628	aldo-keto reductase family 1, member B1	2.36E-02	Cytoplasm	enzyme
ALDH1A3	NM_000693	aldehyde dehydrogenase 1 family, member A3	7.10E-03	Cytoplasm	enzyme
AP2S1	NM_004069	adaptor-related protein complex 2, sigma 1 subunit	4.30E-03	Cytoplasm	transporter
APH1B	NM_031301	anterior pharynx defective 1 homolog B (C. elegans)	2.00E-03	Plasma Membrane	peptidase
ARF5	NM_001662	ADP-ribosylation factor 5	2.41E-02	Cytoplasm	enzyme
ARHGEF6	NM_004840	Rac/Cdc42 guanine nucleotide exchange factor (GEF) 6	3.73E-02	Cytoplasm	other
ARHGEF16	NM_014448	Rho guanine nucleotide exchange factor (GEF) 16	3.25E-02	Cytoplasm	other
ARL4C	NM_005737	ADP-ribosylation factor-like 4C	1.13E-02	Nucleus	enzyme
ARPC5L	NM_030978	actin related protein 2/3 complex, subunit 5-like	7.50E-03	unknown	other
ASAP1	NM_018482	ArfGAP with SH3 domain, ankyrin repeat and PH domain 1	3.92E-02	Plasma Membrane	other
ASIC1	NM_020039	acid-sensing (proton-gated) ion channel 1	2.96E-02	Plasma Membrane	ion channel
ATF2	NM_001880	activating transcription factor 2	2.04E-02	Nucleus	transcription regulator
ATR	NM_001184	ataxia telangiectasia and Rad3 related	1.22E-02	Nucleus	kinase
BACE1	NM_012104	beta-site APP-cleaving enzyme 1	3.70E-03	Cytoplasm	peptidase
BAG1	NM_004323	BCL2-associated athanogene	4.12E-02	Cytoplasm	other
BAG3	NM_004281	BCL2-associated athanogene 3	3.44E-02	Cytoplasm	other
BAHD1	NM_014952	bromo adjacent homology domain containing 1	3.20E-02	Nucleus	other
BCAS2	NM_005872	breast carcinoma amplified sequence 2	8.80E-03	Nucleus	other
BCL2	NM_000633	B-cell CLL/lymphoma 2	1.99E-02	Cytoplasm	transporter
BCL2L2	NM_004050	BCL2-like 2	4.20E-02	Cytoplasm	other
BET1L	NM_016526	Bet1 golgi vesicular membrane trafficking protein-like	3.83E-02	Cytoplasm	transporter
CABLES1	NM_001100619	Cdk5 and Abl enzyme substrate 1	1.18E-02	Nucleus	other
CALCR	NM_001742	calcitonin receptor	2.81E-02	Plasma Membrane	G-protein coupled receptor
CAND1	NM_018448	cullin-associated and neddylation-dissociated 1	2.75E-02	Cytoplasm	transcription regulator
CARD10	NM_014550	caspase recruitment domain family, member 10	4.82E-02	Cytoplasm	other
CCNG2	NM_004354	cyclin G2	1.57E-02	Nucleus	other
CCS	NM_005125	copper chaperone for superoxide dismutase	1.21E-02	Cytoplasm	enzyme
CD82	NM_002231	CD82 molecule	3.97E-02	Plasma Membrane	other
CD8A	NM_001768	CD8a molecule	2.17E-02	Plasma Membrane	other
CDC25A	NM_001789	cell division cycle 25A	2.68E-02	Nucleus	phosphatase
CENPA	NM_001809	centromere protein A	1.25E-02	Nucleus	other
CENPE	NM_001813	centromere protein E	2.61E-02	Nucleus	other
CHMP5	NM_016410	charged multivesicular body protein 5	4.09E-02	Cytoplasm	other
CHST2	NM_004267	carbohydrate (N-acetylglucosamine-6-O) sulfotransferase 2	2.10E-03	Cytoplasm	enzyme
CHST12	NM_018641	carbohydrate (chondroitin 4) sulfotransferase 12	1.09E-02	Cytoplasm	enzyme
CITED4	NM_133467	Cbp/p300-interacting transactivator, with Glu/Asp-rich carboxy-terminal domain, 4	2.10E-03	Nucleus	transcription regulator
CREB1	NM_134442	cAMP responsive element binding protein 1	2.71E-02	Nucleus	transcription regulator
CRY1	NM_004075	cryptochrome 1	3.91E-02	Nucleus	enzyme

Appendix V-II. Predicted target genes of hsa-miR-140-3p based upon miRWalk target comparison.

Gene Symbol	Accession Number	Gene Name	p-value	Location	Type
CSF1	NM_000757	colony stimulating factor 1	1.36E-02	Extracellular Space	cytokine
CTBP1	NM_001012614	C-terminal binding protein 1	4.77E-02	Nucleus	enzyme
CTBP2	NM_022802	C-terminal binding protein 2	6.30E-03	Nucleus	transcription regulator
CTNNA1	NM_001903	catenin (cadherin-associated protein), alpha 1	3.70E-03	Plasma Membrane	other
CTR9	NM_014633	Ctr9, Paf1/RNA polymerase II complex component, homolog	3.91E-02	Nucleus	other
CTSB	NM_147780	cathepsin B	3.89E-02	Cytoplasm	peptidase
CTSD	NM_001909	cathepsin D	4.96E-02	Cytoplasm	peptidase
CTSF	NM_003793	cathepsin F	2.93E-02	Cytoplasm	peptidase
DAB2	NM_001343	Dab, mitogen-responsive phosphoprotein, homolog 2	2.64E-02	Plasma Membrane	other
DDX5	NM_004396	DEAD (Asp-Glu-Ala-Asp) box helicase 5	4.70E-03	Nucleus	enzyme
DHFRL1	NM_176815	dihydrofolate reductase-like 1	4.53E-02	Cytoplasm	enzyme
DHX9	NM_001357	DEAH (Asp-Glu-Ala-His) box polypeptide 9	2.01E-02	Nucleus	enzyme
DIABLO	NM_019887	diablo, IAP-binding mitochondrial protein	1.12E-02	Cytoplasm	other
DNAJC3	NM_006260	DnaJ (Hsp40) homolog, subfamily C, member 3	0.00E00	Cytoplasm	other
DNAJC8	NM_014280	DnaJ (Hsp40) homolog, subfamily C, member 8	3.70E-03	Nucleus	other
DNAJC24	NM_181706	DnaJ (Hsp40) homolog, subfamily C, member 24	3.65E-02	unknown	other
DNM1	NM_001005336	dynamin 1	9.30E-03	Cytoplasm	enzyme
DOK5	NM_018431	docking protein 5	4.14E-02	Plasma Membrane	other
DPH5	NM_001077394	DPH5 homolog	4.79E-02	unknown	enzyme
DRAM1	NM_018370	DNA-damage regulated autophagy modulator 1	3.56E-02	Cytoplasm	other
E2F1	NM_005225	E2F transcription factor 1	1.20E-03	Nucleus	transcription regulator
ECE1	NM_001113347	endothelin converting enzyme 1	4.07E-02	Plasma Membrane	peptidase
EGR3	NM_004430	early growth response 3	4.21E-02	Nucleus	transcription regulator
ENC1	NM_003633	ectodermal-neural cortex 1	3.97E-02	Nucleus	peptidase
EPHX1	NM_000120	epoxide hydrolase 1, microsomal	1.29E-02	Cytoplasm	peptidase
EXTL2	NM_001439	exostosin-like glycosyltransferase 2	6.00E-03	Cytoplasm	enzyme
FADS1	NM_013402	fatty acid desaturase 1	4.18E-02	Plasma Membrane	enzyme
FAIM	NM_001033030	Fas apoptotic inhibitory molecule	4.60E-03	Plasma Membrane	other
FAM162A	NM_014367	family with sequence similarity 162, member A	1.71E-02	Cytoplasm	other
FANCD2	NM_033084	Fanconi anemia, complementation group D2	4.24E-02	Nucleus	other
FANCF	NM_022725	Fanconi anemia, complementation group F	3.23E-02	Nucleus	other
FARSB	NM_005687	phenylalanyl-tRNA synthetase, beta subunit	2.58E-02	Cytoplasm	enzyme
FBLN1	NM_006486	fibulin 1	4.11E-02	Extracellular Space	other
FCGRT	NM_004107	Fc fragment of IgG, receptor, transporter, alpha	3.70E-03	Plasma Membrane	transmembrane receptor
FGF7	NM_002009	fibroblast growth factor 7	4.22E-02	Extracellular Space	growth factor
FGF9	NM_002010	fibroblast growth factor 9	1.17E-02	Extracellular Space	growth factor
FKBP1A	NM_000801	FK506 binding protein 1A	1.75E-02	Cytoplasm	enzyme
FSTL3	NM_005860	follistatin-like 3	2.56E-02	Extracellular Space	other
FUT7	NM_004479	fucosyltransferase 7	2.10E-03	Cytoplasm	enzyme
FXYD5	NM_144779	FXYD domain containing ion transport regulator 5	1.62E-02	Plasma Membrane	ion channel
GALM	NM_138801	galactose mutarotase	4.99E-02	Cytoplasm	enzyme
GDI1	NM_001493	GDP dissociation inhibitor 1	1.24E-02	Cytoplasm	other
GGT7	NM_178026	gamma-glutamyltransferase 7	9.20E-03	Plasma Membrane	enzyme
GJB2	NM_004004	gap junction protein, beta 2	2.19E-02	Plasma Membrane	transporter
GLG1	NM_012201	golgi glycoprotein 1	2.20E-03	Cytoplasm	other
GNB4	NM_021629	guanine nucleotide binding protein (G protein), beta polypeptide 4	4.90E-03	Plasma Membrane	enzyme
GNRHR	NM_000406	gonadotropin-releasing hormone receptor	4.63E-02	Plasma Membrane	G-protein coupled receptor
GOT1	NM_002079	glutamic-oxaloacetic transaminase 1	1.05E-02	Cytoplasm	enzyme

Appendix V-II. (continued) Predicted target genes of hsa-miR-140-3p based upon miRWalk target comparison.

Gene Symbol	Accession Number	Gene Name	p-value	Location	Type
GPNMB	NM_001005340	glycoprotein nmb	3.40E-03	Plasma Membrane	enzyme
GRB2	NM_002086	growth factor receptor-bound protein 2	8.70E-03	Cytoplasm	other
GRB10	NM_001001555	growth factor receptor-bound protein 10	4.33E-02	Cytoplasm	other
GRHL2	NM_024915	grainyhead-like 2	1.15E-02	Nucleus	transcription regulator
GSK3A	NM_019884	glycogen synthase kinase 3 alpha	2.40E-03	Nucleus	kinase
GSTM3	NM_000849	glutathione S-transferase mu 3	4.68E-02	Cytoplasm	enzyme
GTF3C4	NM_012204	general transcription factor IIIC, polypeptide 4	1.72E-02	Nucleus	transcription regulator
GTF3C5	NM_001122823	general transcription factor IIIC, polypeptide 5	3.24E-02	Nucleus	transcription regulator
HBP1	NM_012257	HMG-box transcription factor 1	1.70E-02	Nucleus	transcription regulator
HENMT1	NM_144584	HEN1 methyltransferase homolog 1	1.74E-02	unknown	enzyme
HGS	NM_004712	hepatocyte growth factor-regulated tyrosine kinase substrate	3.09E-02	Cytoplasm	other
HIST1H2BK	NM_080593	histone cluster 1, H2bk	2.39E-02	Nucleus	other
HK2	NM_000189	hexokinase 2	9.20E-03	Cytoplasm	kinase
HKDC1	NM_025130	hexokinase domain containing 1	1.26E-02	unknown	kinase
HKR1	NM_181786	HKR1, GLI-Kruppel zinc finger family member	4.20E-02	Nucleus	other
HLA-DOB	NM_002120	major histocompatibility complex, class II, DO beta	2.82E-02	Plasma Membrane	transmembrane receptor
HMGCS1	NM_001098272	3-hydroxy-3-methylglutaryl-CoA synthase 1	2.62E-02	Cytoplasm	enzyme
HOXB7	NM_004502	homeobox B7	6.00E-04	Nucleus	transcription regulator
HOXD10	NM_002148	homeobox D10	4.31E-02	Nucleus	transcription regulator
HSF1	NM_005526	heat shock transcription factor 1	6.20E-03	Nucleus	transcription regulator
HSPG2	NM_005529	heparan sulfate proteoglycan 2	1.63E-02	Extracellular Space	enzyme
HYAL1	NM_007312	hyaluronoglucosaminidase 1	3.55E-02	Cytoplasm	enzyme
IDI1	NM_004508	isopentenyl-diphosphate delta isomerase 1	4.50E-03	Cytoplasm	enzyme
IDO2	NM_194294	indoleamine 2,3-dioxygenase 2	4.70E-02	Cytoplasm	enzyme
IFT57	NM_018010	intraflagellar transport 57 homolog	2.54E-02	Cytoplasm	other
IGFBP1	NM_000596	insulin-like growth factor binding protein 1	8.90E-03	Extracellular Space	other
IL8	NM_000584	interleukin 8	1.91E-02	Extracellular Space	cytokine
IL13RA1	NM_001560	interleukin 13 receptor, alpha 1	4.01E-02	Plasma Membrane	transmembrane receptor
IL15RA	NM_172200	interleukin 15 receptor, alpha	4.32E-02	Plasma Membrane	transmembrane receptor
IMPAD1	NM_017813	inositol monophosphatase domain containing 1	2.22E-02	Cytoplasm	enzyme
IPP	NM_005897	intracisternal A particle-promoted polypeptide	1.90E-02	Cytoplasm	other
IRAK1	NM_001569	interleukin-1 receptor-associated kinase 1	2.07E-02	Plasma Membrane	kinase
JAG2	NM_002226	jagged 2	1.45E-02	Extracellular Space	growth factor
KCTD6	NM_153331	potassium channel tetramerisation domain containing 6	7.00E-04	unknown	ion channel
KDM4B	NM_015015	lysine (K)-specific demethylase 4B	3.24E-02	unknown	other
KIF7	NM_198525	kinesin family member 7	7.10E-03	Extracellular Space	other
KLF8	NM_007250	Kruppel-like factor 8	3.70E-02	Nucleus	other
KYNU	NM_003937	kynureninase	9.70E-03	Cytoplasm	enzyme
L1CAM	NM_000425	L1 cell adhesion molecule	4.36E-02	Plasma Membrane	other
LOXL2	NM_002318	lysyl oxidase-like 2	1.73E-02	Extracellular Space	enzyme
MAFK	NM_002360	v-maf musculoaponeurotic fibrosarcoma oncogene homolog K	1.01E-02	Nucleus	transcription regulator
MAML2	NM_032427	mastermind-like 2	4.02E-02	Nucleus	transcription regulator
MAP1LC3A	NM_032514	microtubule-associated protein 1 light chain 3 alpha	3.06E-02	Cytoplasm	other
MAP2K4	NM_003010	mitogen-activated protein kinase kinase 4	9.40E-03	Cytoplasm	kinase
MAP2K6	NM_002758	mitogen-activated protein kinase kinase 6	3.51E-02	Cytoplasm	kinase
MARK3	NM_001128918	MAP/microtubule affinity-regulating kinase 3	9.40E-03	Cytoplasm	kinase
MBD1	NM_015846	methyl-CpG binding domain protein 1	3.90E-03	Nucleus	transcription regulator
MBTPS1	NM_003791	membrane-bound transcription factor peptidase, site 1	4.14E-02	Cytoplasm	peptidase

Appendix V-II. (continued) Predicted target genes of hsa-miR-140-3p based upon miRWalk target comparison.

Gene Symbol	Accession Number	Gene Name	p-value	Location	Type
MBTPS2	NM_015884	membrane-bound transcription factor peptidase, site 2	4.15E-02	Cytoplasm	peptidase
MCM6	NM_005915	minichromosome maintenance complex component 6	1.85E-02	Nucleus	enzyme
MED31	NM_016060	mediator complex subunit 31	1.75E-02	Nucleus	other
MEIS2	NM_170677	Meis homeobox 2	2.23E-02	Nucleus	transcription regulator
MINOS1	NM_001032363	mitochondrial inner membrane organizing system 1	3.42E-02	Cytoplasm	other
MLYCD	NM_012213	malonyl-CoA decarboxylase	1.08E-02	Cytoplasm	enzyme
MMP15	NM_002428	matrix metallopeptidase 15	2.22E-02	Extracellular Space	peptidase
MMP24	NM_006690	matrix metallopeptidase 24	2.30E-03	Plasma Membrane	peptidase
MOCS2	NM_004531	molybdenum cofactor synthesis 2	8.40E-03	Cytoplasm	enzyme
MT3	NM_005954	metallothionein 3	2.40E-03	Cytoplasm	other
MTAP	NM_002451	methylthioadenosine phosphorylase	1.50E-02	Nucleus	enzyme
MTMR3	NM_021090	myotubularin related protein 3	1.92E-02	Cytoplasm	phosphatase
MYB	NM_001130173	v-myb myeloblastosis viral oncogene homolog	4.60E-03	Nucleus	transcription regulator
MYD88	NM_002468	myeloid differentiation primary response 88	2.63E-02	Plasma Membrane	other
MYH11	NM_001040113	myosin, heavy chain 11, smooth muscle	1.51E-02	Cytoplasm	other
MYL12A	NM_006471	myosin, light chain 12A, regulatory, non-sarcomeric	2.01E-02	Cytoplasm	other
NAAA	NM_014435	N-acylethanolamine acid amidase	4.39E-02	Cytoplasm	enzyme
NAPB	NM_022080	N-ethylmaleimide-sensitive factor attachment protein, beta	4.27E-02	Cytoplasm	transporter
NAPG	NM_003826	N-ethylmaleimide-sensitive factor attachment protein, gamma	1.11E-02	unknown	transporter
NAT1	NM_000662	N-acetyltransferase 1	6.20E-03	Cytoplasm	enzyme
NCKAP1L	NM_005337	NCK-associated protein 1-like	2.69E-02	Plasma Membrane	other
NCL	NM_005381	nucleolin	7.00E-03	Nucleus	other
NDST1	NM_001543	N-deacetylase/N-sulfotransferase 1	1.84E-02	Cytoplasm	enzyme
NFKBIA	NM_020529	nuclear factor of kappa light polypeptide gene enhancer in B-cells inhibitor, alpha	3.09E-02	Cytoplasm	transcription regulator
NMNAT2	NM_015039	nicotinamide nucleotide adenylyltransferase 2	1.67E-02	Cytoplasm	enzyme
NOV	NM_002514	nephroblastoma overexpressed	1.97E-02	Extracellular Space	growth factor
NR2C2	NM_003298	nuclear receptor subfamily 2, group C, member 2	2.36E-02	Nucleus	ligand-dependent nuclear receptor
NR2F2	NM_021005	nuclear receptor subfamily 2, group F, member 2	1.85E-02	Nucleus	ligand-dependent nuclear receptor
NR5A2	NM_205860	nuclear receptor subfamily 5, group A, member 2	1.22E-02	Nucleus	ligand-dependent nuclear receptor
NRIP1	NM_003489	nuclear receptor interacting protein 1	1.32E-02	Nucleus	transcription regulator
NSF	NM_006178	N-ethylmaleimide-sensitive factor	2.48E-02	Cytoplasm	transporter
PAWR	NM_002583	PRKC, apoptosis, WT1, regulator	3.94E-02	Nucleus	transcription regulator
PDE6B	NM_000283	phosphodiesterase 6B, cGMP-specific, rod, beta	1.02E-02	Cytoplasm	enzyme
PDGFB	NM_002608	platelet-derived growth factor beta polypeptide	2.53E-02	Extracellular Space	growth factor
PDP1	NM_018444	pyruvate dehyrogenase phosphatase catalytic subunit 1	3.61E-02	Cytoplasm	phosphatase
PDPK1	NM_002613	3-phosphoinositide dependent protein kinase-1	2.05E-02	Cytoplasm	kinase
PDSS1	NM_014317	prenyl (decaprenyl) diphosphate synthase, subunit 1	2.32E-02	Cytoplasm	enzyme
PDSS2	NM_020381	prenyl (decaprenyl) diphosphate synthase, subunit 2	3.12E-02	Cytoplasm	enzyme
PGM1	NM_002633	phosphoglucomutase 1	3.51E-02	Cytoplasm	enzyme
PHKB	NM_001031835	phosphorylase kinase, beta	3.24E-02	Cytoplasm	kinase
PHLDB1	NM_015157	pleckstrin homology-like domain, family B, member 1	4.60E-03	Cytoplasm	other
PI4KB	NM_002651	phosphatidylinositol 4-kinase, catalytic, beta	1.39E-02	Cytoplasm	kinase
PICK1	NM_012407	protein interacting with PRKCA 1	3.51E-02	Cytoplasm	enzyme
PIK3C2B	NM_002646	phosphatidylinositol-4-phosphate 3-kinase, catalytic subunit type 2 beta	3.33E-02	Cytoplasm	kinase
PIK3R3	NM_003629	phosphoinositide-3-kinase, regulatory subunit 3	1.35E-02	Cytoplasm	kinase
PIP4K2C	NM_024779	phosphatidylinositol-5-phosphate 4-kinase, type II, gamma	2.49E-02	Cytoplasm	kinase
PKIB	NM_181795	protein kinase (cAMP-dependent, catalytic) inhibitor beta	1.82E-02	unknown	other
PMF1	NM_007221	polyamine-modulated factor 1	6.70E-03	Nucleus	transcription regulator

Appendix V-II. (continued) Predicted target genes of hsa-miR-140-3p based upon miRWalk target comparison.

Gene Symbol	Accession Number	Gene Name	p-value	Location	Type
PMVK	NM_006556	phosphomevalonate kinase	6.20E-03	Cytoplasm	kinase
PNPLA4	NM_004650	patatin-like phospholipase domain containing 4	1.80E-03	Cytoplasm	enzyme
POLR1B	NM_019014	polymerase (RNA) I polypeptide B	2.17E-02	Nucleus	enzyme
POLR2E	NM_002695	polymerase (RNA) II (DNA directed) polypeptide E	3.24E-02	Nucleus	enzyme
POSTN	NM_006475	periostin, osteoblast specific factor	2.90E-03	Extracellular Space	other
POU2F2	NM_002698	POU class 2 homeobox 2	4.55E-02	Nucleus	transcription regulator
PPAP2B	NM_003713	phosphatidic acid phosphatase type 2B	2.72E-02	Plasma Membrane	phosphatase
PPP2R2A	NM_002717	protein phosphatase 2, regulatory subunit B, alpha	4.41E-02	Cytoplasm	phosphatase
PPP2R5C	NM_002719	protein phosphatase 2, regulatory subunit B', gamma	3.72E-02	Nucleus	other
PPP3R2	NM_147180	protein phosphatase 3, regulatory subunit B, beta	2.70E-03	Cytoplasm	phosphatase
PPTC7	NM_139283	PTC7 protein phosphatase homolog (S. cerevisiae)	3.90E-02	Cytoplasm	phosphatase
PRKCI	NM_002740	protein kinase C, iota	4.26E-02	Cytoplasm	kinase
PSMD7	NM_002811	proteasome (prosome, macropain) 26S subunit, non-ATPase, 7	3.43E-02	Cytoplasm	other
PTDSS2	NM_030783	phosphatidylserine synthase 2	1.26E-02	Cytoplasm	enzyme
PTP4A2	NM_080391	protein tyrosine phosphatase type IVA, member 2	2.50E-03	Cytoplasm	phosphatase
PTPMT1	NM_175732	protein tyrosine phosphatase, mitochondrial 1	1.26E-02	Cytoplasm	phosphatase
PTRF	NM_012232	polymerase I and transcript release factor	3.37E-02	Nucleus	transcription regulator
PYCR1	NM_006907	pyrroline-5-carboxylate reductase 1	4.89E-02	Cytoplasm	enzyme
RAB1A	NM_004161	RAB1A, member RAS oncogene family	2.48E-02	Cytoplasm	enzyme
RAB3A	NM_002866	RAB3A, member RAS oncogene family	4.16E-02	Cytoplasm	enzyme
RAB5B	NM_002868	RAB5B, member RAS oncogene family	3.79E-02	Cytoplasm	enzyme
RAD23B	NM_002874	RAD23 homolog B (S. cerevisiae)	3.79E-02	Nucleus	other
RARB	NM_000965	retinoic acid receptor, beta	2.12E-02	Nucleus	ligand-dependent nuclear receptor
RDH13	NM_138412	retinol dehydrogenase 13	4.47E-02	Cytoplasm	enzyme
RHOBTB3	NM_014899	Rho-related BTB domain containing 3	4.76E-02	unknown	enzyme
RHOF	NM_019034	ras homolog family member F	2.65E-02	Cytoplasm	enzyme
RPTOR	NM_020761	regulatory associated protein of MTOR, complex 1	3.07E-02	Cytoplasm	other
RRAS2	NM_012250	related RAS viral (r-ras) oncogene homolog 2	2.14E-02	Plasma Membrane	enzyme
RSAD2	NM_080657	radical S-adenosyl methionine domain containing 2	3.43E-02	Cytoplasm	enzyme
RUVBL1	NM_003707	RuvB-like 1	4.70E-03	Nucleus	transcription regulator
SEMA3C	NM_006379	sema domain, immunoglobulin domain (Ig), short basic domain, secreted, (semaphorin) 3C	2.30E-03	Extracellular Space	other
SEMA5A	NM_003966	sema domain, seven thrombospondin repeats, transmembrane domain and short cytoplasmic domain, 5A	2.96E-02	Plasma Membrane	transmembrane receptor
SERPINA1	NM_001127701	serpin peptidase inhibitor, clade A, member 1	1.60E-03	Extracellular Space	other
SGCD	NM_000337	sarcoglycan, delta	8.00E-03	Cytoplasm	other
SHANK2	NM_012309	SH3 and multiple ankyrin repeat domains 2	1.89E-02	Plasma Membrane	other
SHC1	NM_001130040	SHC (Src homology 2 domain containing) transforming protein 1	2.29E-02	Cytoplasm	kinase
SIPA1	NM_153253	signal-induced proliferation-associated 1	1.32E-02	Cytoplasm	other
SIRT1	NM_012238	sirtuin 1	2.72E-02	Nucleus	transcription regulator
SLC19A1	NM_194255	solute carrier family 19), member 1	9.00E-04	Plasma Membrane	transporter
SLC1A4	NM_003038	solute carrier family 1 (glutamate/neutral amino acid transporter), member 4	4.12E-02	Plasma Membrane	transporter
SLCO4A1	NM_016354	solute carrier organic anion transporter family, member 4A1	6.40E-03	Plasma Membrane	transporter
SMARCA2	NM_003070	SWI/SNF related, matrix associated, actin dependent regulator of chromatin, subfamily a, member 2	1.34E-02	Nucleus	transcription regulator
SMPD1	NM_000543	sphingomyelin phosphodiesterase 1, acid lysosomal	2.43E-02	Cytoplasm	enzyme
SNAP25	NM_003081	synaptosomal-associated protein, 25kDa	4.60E-03	Plasma Membrane	transporter
SOCS5	NM_144949	suppressor of cytokine signaling 5	3.96E-02	Extracellular Space	cytokine
SP100	NM_001080391	SP100 nuclear antigen	3.97E-02	Nucleus	transcription regulator
SPARC	NM_003118	secreted protein, acidic, cysteine-rich (osteonectin)	3.24E-02	Extracellular Space	other
STAG2	NM_001042749	stromal antigen 2	3.10E-02	Nucleus	other

Appendix V-II. (continued) Predicted target genes of hsa-miR-140-3p based upon miRWalk target comparison.

Gene Symbol	Accession Number	Gene Name	p-value	Location	Type
SULF2	NM_018837	sulfatase 2	3.60E-03	Plasma Membrane	enzyme
SWAP70	NM_015055	SWAP switching B-cell complex 70kDa subunit	4.46E-02	Cytoplasm	other
TAB1	NM_006116	TGF-beta activated kinase 1/MAP3K7 binding protein 1	2.52E-02	Cytoplasm	enzyme
TAB2	NM_015093	TGF-beta activated kinase 1/MAP3K7 binding protein 2	2.87E-02	Cytoplasm	other
TAGLN	NM_001001522	transgelin	2.71E-02	Cytoplasm	other
TAP1	NM_000593	transporter 1, ATP-binding cassette, sub-family B (MDR/TAP)	2.36E-02	Cytoplasm	transporter
TFRC	NM_003234	transferrin receptor	4.00E-02	Plasma Membrane	transporter
TH	NM_199292	tyrosine hydroxylase	4.60E-03	Cytoplasm	enzyme
THRSP	NM_003251	thyroid hormone responsive	4.45E-02	Nucleus	other
TMEFF2	NM_016192	transmembrane protein with EGF-like and two follistatin-like domains 2	1.78E-02	Cytoplasm	other
TNFAIP6	NM_007115	tumor necrosis factor, alpha-induced protein 6	3.18E-02	Extracellular Space	other
TNIP1	NM_006058	TNFAIP3 interacting protein 1	1.17E-02	Nucleus	other
TNS3	NM_022748	tensin 3	4.46E-02	unknown	phosphatase
TOP2B	NM_001068	topoisomerase (DNA) II beta	1.95E-02	Nucleus	enzyme
TP73	NM_005427	tumor protein p73	4.90E-02	Nucleus	transcription regulator
TPM1	NM_001018004	tropomyosin 1	2.90E-03	Cytoplasm	other
TRAF2	NM_021138	TNF receptor-associated factor 2	4.39E-02	Cytoplasm	enzyme
TRPS1	NM_014112	trichorhinophalangeal syndrome I	2.09E-02	Nucleus	transcription regulator
UBE2C	NM_181802	ubiquitin-conjugating enzyme E2C	3.50E-03	Cytoplasm	enzyme
UNC13B	NM_006377	unc-13 homolog B (C. elegans)	2.01E-02	Cytoplasm	other
USP1	NM_003368	ubiquitin specific peptidase 1	1.26E-02	Cytoplasm	peptidase
USP13	NM_003940	ubiquitin specific peptidase 13	8.00E-04	unknown	peptidase
USP34	NM_014709	ubiquitin specific peptidase 34	3.97E-02	Extracellular Space	peptidase
USP54	NM_152586	ubiquitin specific peptidase 54	4.30E-03	unknown	peptidase
VARS2	NM_020442	valyl-tRNA synthetase 2, mitochondrial	1.49E-02	Cytoplasm	enzyme
VPS9D1	NM_004913	VPS9 domain containing 1	4.45E-02	unknown	transporter
WIPF1	NM_001077269	WAS/WASL interacting protein family, member 1	4.46E-02	Cytoplasm	other
WNT7B	NM_058238	wingless-type MMTV integration site family, member 7B	9.50E-03	Extracellular Space	other
YWHAB	NM_003404	tyrosine 3-monooxygenase/tryptophan 5-monooxygenase activation protein, beta polypeptide	7.90E-03	Cytoplasm	transcription regulator
YWHAZ	NM_145690	tyrosine 3-monooxygenase/tryptophan 5-monooxygenase activation protein, zeta polypeptide	3.19E-02	Cytoplasm	enzyme
ZFP36	NM_003407	ZFP36 ring finger protein	4.22E-02	Nucleus	transcription regulator
ZNF512B	NM_020713	zinc finger protein 512B	4.75E-02	Nucleus	other

Appendix V-II. (continued) Predicted target genes of hsa-miR-140-3p based upon miRWalk target comparison.

Gene Symbol	Accession Number	Gene Name	p-value	Location	Type
ACADM	NM_001127328	acyl-CoA dehydrogenase, C-4 to C-12 straight chain	1.39E-02	Cytoplasm	enzyme
ACOT11	NM_147161	acyl-CoA thioesterase 11	1.20E-03	Cytoplasm	enzyme
ACTR2	NM_001005386	ARP2 actin-related protein 2 homolog	3.79E-02	Plasma Membrane	other
ADAM11	NM_002390	ADAM metallopeptidase domain 11	7.90E-03	Plasma Membrane	peptidase
ADAM22	NM_021723	ADAM metallopeptidase domain 22	9.90E-03	Plasma Membrane	peptidase
ADAMTS6	NM_197941	ADAM metallopeptidase with thrombospondin type 1 motif, 6	1.18E-02	Extracellular Space	peptidase
ADHFE1	NM_144650	alcohol dehydrogenase, iron containing, 1	2.82E-02	Cytoplasm	enzyme
AGL	NM_000028	amylo-alpha-1, 6-glucosidase, 4-alpha-glucanotransferase	3.55E-02	Cytoplasm	enzyme
AKAP9	NM_147171	A kinase (PRKA) anchor protein 9	3.10E-02	Cytoplasm	other
AKAP13	NM_006738	A kinase (PRKA) anchor protein 13	1.77E-02	Cytoplasm	other
ALDH16A1	NM_153329	aldehyde dehydrogenase 16 family, member A1	2.20E-03	unknown	enzyme
ALG6	NM_013339	ALG6, alpha-1,3-glucosyltransferase	1.28E-02	Cytoplasm	enzyme
ANKRD32	NM_032290	ankyrin repeat domain 32	8.40E-03	Nucleus	transcription regulator
ANXA1	NM_000700	annexin A1	4.30E-03	Plasma Membrane	other
ANXA3	NM_005139	annexin A3	5.40E-03	Cytoplasm	enzyme
ARF1	NM_001024227	ADP-ribosylation factor 1	1.83E-02	Cytoplasm	enzyme
ARF4	NM_001660	ADP-ribosylation factor 4	1.31E-02	Cytoplasm	enzyme
ARHGAP10	NM_024605	Rho GTPase activating protein 10	4.25E-02	Cytoplasm	other
ARHGEF17	NM_014786	Rho guanine nucleotide exchange factor (GEF) 17	2.01E-02	Cytoplasm	other
ARID1A	NM_006015	AT rich interactive domain 1A	3.00E-04	Nucleus	transcription regulator
ATF3	NM_001040619	activating transcription factor 3	2.52E-02	Nucleus	transcription regulator
ATF6	NM_007348	activating transcription factor 6	6.20E-03	Cytoplasm	transcription regulator
ATG12	NM_004707	autophagy related 12	2.54E-02	Cytoplasm	other
ATP1A1	NM_000701	ATPase, Na+/K+ transporting, alpha 1 polypeptide	5.20E-03	Plasma Membrane	transporter
ATP2B3	NM_021949	ATPase, Ca++ transporting, plasma membrane 3	4.39E-02	Plasma Membrane	transporter
ATPBD4	NM_080650	ATP binding domain 4	1.92E-02	unknown	enzyme
AZI2	NM_022461	5-azacytidine induced 2	6.50E-03	Cytoplasm	other
BAG3	NM_004281	BCL2-associated athanogene 3	3.44E-02	Cytoplasm	other
BAG5	NM_001015049	BCL2-associated athanogene 5	4.87E-02	Cytoplasm	other
BLVRA	NM_000712	biliverdin reductase A	7.30E-03	Cytoplasm	enzyme
BNIP3L	NM_004331	BCL2/adenovirus E1B 19kDa interacting protein 3-like	4.07E-02	Cytoplasm	other
BRK1	NM_018462	BRICK1, SCAR/WAVE actin-nucleating complex subunit	1.39E-02	unknown	other
CACNA1H	NM_021098	calcium channel, voltage-dependent, T type, alpha 1H subunit	4.69E-02	Plasma Membrane	ion channel
CAMKK1	NM_032294	calcium/calmodulin-dependent protein kinase kinase 1, alpha	2.88E-02	Cytoplasm	kinase
CASP10	NM_032977	caspase 10, apoptosis-related cysteine peptidase	1.48E-02	Cytoplasm	peptidase
CASR	NM_000388	calcium-sensing receptor	1.99E-02	Plasma Membrane	G-protein coupled receptor
CAV2	NM_001233	caveolin 2	9.30E-03	Plasma Membrane	other
CCND2	NM_001759	cyclin D2	2.02E-02	Nucleus	other
CDK1	NM_001130829	cyclin-dependent kinase 1	1.35E-02	Nucleus	kinase
CDKN1C	NM_000076	cyclin-dependent kinase inhibitor 1C	4.28E-02	Nucleus	other
CDS1	NM_001263	CDP-diacylglycerol synthase 1	1.01E-02	Cytoplasm	enzyme
CENPA	NM_001809	centromere protein A	4.91E-02	Nucleus	other
CHD8	NM_020920	chromodomain helicase DNA binding protein 8	3.14E-02	Nucleus	enzyme
CHMP4B	NM_176812	charged multivesicular body protein 4B	1.29E-02	Cytoplasm	other
CLDN11	NM_005602	claudin 11	2.91E-02	Plasma Membrane	other
CLDN12	NM_012129	claudin 12	3.84E-02	Plasma Membrane	other
CNR1	NM_016083	cannabinoid receptor 1	1.52E-02	Plasma Membrane	G-protein coupled receptor
COX7A2L	NM_004718	cytochrome c oxidase subunit VIIa polypeptide 2 like	1.13E-02	Cytoplasm	enzyme

Appendix V-III. Predicted target genes of hsa-miR-221 based upon miRWalk target comparison.

Gene Symbol	Accession Number	Gene Name	p-value	Location	Type
CPT1A	NM_001876	carnitine palmitoyltransferase 1A	4.14E-02	Cytoplasm	enzyme
CREB1	NM_134442	cAMP responsive element binding protein 1	6.80E-03	Nucleus	transcription regulator
CREBZF	NM_001039618	CREB/ATF bZIP transcription factor	2.26E-02	Nucleus	transcription regulator
CSNK2A1	NM_177559	casein kinase 2, alpha 1 polypeptide	4.90E-03	Cytoplasm	kinase
CXCL12	NM_000609	chemokine (C-X-C motif) ligand 12	4.72E-02	Extracellular Space	cytokine
CYR61	NM_001554	cysteine-rich, angiogenic inducer, 61	3.50E-03	Extracellular Space	other
DBN1	NM_080881	drebrin 1	4.88E-02	Cytoplasm	other
DHTKD1	NM_018706	dehydrogenase E1 and transketolase domain containing 1	3.51E-02	unknown	enzyme
DNAJC5	NM_025219	DnaJ (Hsp40) homolog, subfamily C, member 5	3.77E-02	Plasma Membrane	other
DNAJC24	NM_181706	DnaJ (Hsp40) homolog, subfamily C, member 24	9.20E-03	unknown	other
DNM3	NM_015569	dynamin 3	1.85E-02	Cytoplasm	enzyme
DNMT3B	NM_006892	DNA (cytosine-5-)-methyltransferase 3 beta	2.22E-02	Nucleus	enzyme
DPYSL3	NM_001387	dihydropyrimidinase-like 3	1.23E-02	Cytoplasm	enzyme
DSCC1	NM_024094	defective in sister chromatid cohesion 1 homolog	1.42E-02	Nucleus	other
DVL2	NM_004422	dishevelled, dsh homolog 2	8.40E-03	Cytoplasm	other
DYRK1A	NM_130436	dual-specificity tyrosine-(Y)-phosphorylation regulated kinase 1A	4.25E-02	Nucleus	kinase
EFNB2	NM_004093	ephrin-B2	4.92E-02	Plasma Membrane	other
EIF1	NM_005801	eukaryotic translation initiation factor 1	1.24E-02	unknown	translation regulator
EIF2S3	NM_001415	eukaryotic translation initiation factor 2, subunit 3 gamma	3.07E-02	Cytoplasm	translation regulator
FAM208A	NM_001112736	family with sequence similarity 208, member A	1.38E-02	unknown	other
FANCG	NM_004629	Fanconi anemia, complementation group G	1.74E-02	Nucleus	other
FERMT2	NM_006832	fermitin family member 2	1.70E-02	Cytoplasm	other
FOS	NM_005252	FBJ murine osteosarcoma viral oncogene homolog	4.68E-02	Nucleus	transcription regulator
FRAT2	NM_012083	frequently rearranged in advanced T-cell lymphomas 2	2.10E-02	Cytoplasm	other
GDI2	NM_001494	GDP dissociation inhibitor 2	4.84E-02	Cytoplasm	other
GGCT	NM_024051	gamma-glutamylcyclotransferase	2.96E-02	Cytoplasm	enzyme
GLI2	NM_005270	GLI family zinc finger 2	2.99E-02	Nucleus	transcription regulator
GLTSCR2	NM_015710	glioma tumor suppressor candidate region gene 2	7.40E-03	Cytoplasm	other
GNAI2	NM_002070	guanine nucleotide binding protein (G protein), alpha inhibiting activity polypeptide 2	3.80E-03	Plasma Membrane	enzyme
GNG12	NM_018841	guanine nucleotide binding protein (G protein), gamma 12	1.52E-02	Plasma Membrane	enzyme
GNPAT	NM_014236	glyceronephosphate O-acyltransferase	2.64E-02	Cytoplasm	enzyme
GOSR1	NM_001007024	golgi SNAP receptor complex member 1	1.68E-02	Cytoplasm	transporter
GPAM	NM_020918	glycerol-3-phosphate acyltransferase, mitochondrial	1.40E-02	Cytoplasm	enzyme
GRB10	NM_001001555	growth factor receptor-bound protein 10	4.33E-02	Cytoplasm	other
GRIA4	NM_001077243	glutamate receptor, ionotropic, AMPA 4	9.60E-03	Plasma Membrane	ion channel
H1FX	NM_006026	H1 histone family, member X	2.94E-02	Nucleus	other
HARS2	NM_012208	histidyl-tRNA synthetase 2, mitochondrial	4.60E-02	Cytoplasm	enzyme
HDAC6	NM_006044	histone deacetylase 6	2.16E-02	Nucleus	transcription regulator
HEXIM1	NM_006460	hexamethylene bis-acetamide inducible 1	2.76E-02	Nucleus	transcription regulator
HLTF	NM_003071	helicase-like transcription factor	3.16E-02	Nucleus	transcription regulator
HMGB2	NM_002129	high mobility group box 2	4.21E-02	Nucleus	transcription regulator
HOXB7	NM_004502	homeobox B7	3.71E-02	Nucleus	transcription regulator
HS3ST3B1	NM_006041	heparan sulfate (glucosamine) 3-O-sulfotransferase 3B1	3.18E-02	Cytoplasm	enzyme
HSPA8	NM_006597	heat shock protein 8	1.56E-02	Cytoplasm	enzyme
IBSP	NM_004967	integrin-binding sialoprotein	3.26E-02	Extracellular Space	other
IFIT2	NM_001547	interferon-induced protein with tetratricopeptide repeats 2	2.87E-02	Cytoplasm	other
INPP4B	NM_003866	inositol polyphosphate-4-phosphatase, type II	1.17E-02	Cytoplasm	phosphatase
INSIG1	NM_198336	insulin induced gene 1	2.86E-02	Cytoplasm	other

Appendix V-III. (continued) Predicted target genes of hsa-miR-221 based upon miRWalk target comparison.

Gene Symbol	Accession Number	Gene Name	p-value	Location	Type
JAK3	NM_000215	Janus kinase 3	2.97E-02	Cytoplasm	kinase
JMY	NM_152405	junction mediating and regulatory protein, p53 cofactor	2.12E-02	Nucleus	transcription regulator
KCNH1	NM_172362	potassium voltage-gated channel, subfamily H (eag-related), member 1	1.88E-02	Plasma Membrane	ion channel
KCNK2	NM_001017424	potassium channel, subfamily K, member 2	5.00E-04	Plasma Membrane	ion channel
KIF20A	NM_005733	kinesin family member 20A	4.60E-03	Cytoplasm	transporter
KLC1	NM_005552	kinesin light chain 1	9.60E-03	Cytoplasm	other
KLF8	NM_007250	Kruppel-like factor 8	2.40E-03	Nucleus	other
KPNA2	NM_002266	karyopherin alpha 2	4.40E-03	Nucleus	transporter
KRT81	NM_002281	keratin 81	5.40E-03	Cytoplasm	other
LAMB3	NM_001017402	laminin, beta 3	2.59E-02	Extracellular Space	transporter
LBR	NM_002296	lamin B receptor	2.73E-02	Nucleus	enzyme
LIFR	NM_001127671	leukemia inhibitory factor receptor alpha	2.50E-02	Plasma Membrane	transmembrane receptor
MAGI1	NM_015520	membrane associated guanylate kinase, WW and PDZ domain containing 1	4.25E-02	Plasma Membrane	kinase
MAP4K5	NM_198794	mitogen-activated protein kinase kinase kinase kinase 5	2.28E-02	Cytoplasm	kinase
MAPK12	NM_002969	mitogen-activated protein kinase 12	3.14E-02	Cytoplasm	kinase
MAT2A	NM_005911	methionine adenosyltransferase II, alpha	2.30E-02	Cytoplasm	enzyme
MBD2	NM_003927	methyl-CpG binding domain protein 2	1.69E-02	Nucleus	transcription regulator
MDM2	NM_002392	MDM2 oncogene, E3 ubiquitin protein ligase	8.90E-03	Nucleus	transcription regulator
MED28	NM_025205	mediator complex subunit 28	4.85E-02	Nucleus	other
MEST	NM_002402	mesoderm specific transcript	1.20E-03	Cytoplasm	peptidase
MFN2	NM_014874	mitofusin 2	7.40E-03	Cytoplasm	enzyme
MMP1	NM_002421	matrix metallopeptidase 1	7.50E-03	Extracellular Space	peptidase
MORF4L1	NM_206839	mortality factor 4 like 1	4.14E-02	Nucleus	other
MSN	NM_002444	moesin	3.08E-02	Plasma Membrane	other
MTMR6	NM_004685	myotubularin related protein 6	4.53E-02	Cytoplasm	phosphatase
MYBL1	NM_001080416	v-myb myeloblastosis viral oncogene homolog-like 1	3.77E-02	Nucleus	transcription regulator
MYLIP	NM_013262	myosin regulatory light chain interacting protein	2.28E-02	Cytoplasm	enzyme
NAPA	NM_003827	N-ethylmaleimide-sensitive factor attachment protein, alpha	3.94E-02	Cytoplasm	transporter
NAT1	NM_000662	N-acetyltransferase 1	2.44E-02	Cytoplasm	enzyme
NCK1	NM_006153	NCK adaptor protein 1	4.16E-02	Cytoplasm	kinase
NDST3	NM_004784	N-deacetylase/N-sulfotransferase 3	2.80E-03	Cytoplasm	enzyme
NDUFA1	NM_004541	NADH dehydrogenase (ubiquinone) 1 alpha subcomplex, 1	9.00E-03	Cytoplasm	enzyme
NFATC4	NM_004554	nuclear factor of activated T-cells, cytoplasmic, calcineurin-dependent 4	2.93E-02	Nucleus	transcription regulator
NFYB	NM_006166	nuclear transcription factor Y, beta	1.01E-02	Nucleus	transcription regulator
NLK	NM_016231	nemo-like kinase	6.70E-03	Nucleus	kinase
NPR3	NM_024563	natriuretic peptide receptor C/guanylate cyclase C	7.50E-03	Plasma Membrane	G-protein coupled receptor
NRG1	NM_013960	neuregulin 1	4.93E-02	unknown	growth factor
NRK	NM_198465	Nik related kinase	4.52E-02	unknown	kinase
NTF3	NM_001102654	neurotrophin 3	1.96E-02	Extracellular Space	growth factor
NUDT9	NM_024047	nudix (nucleoside diphosphate linked moiety X)-type motif 9	2.05E-02	Cytoplasm	phosphatase
NXN	NM_022463	nucleoredoxin	6.10E-03	Nucleus	enzyme
ODC1	NM_002539	ornithine decarboxylase 1	2.07E-02	Cytoplasm	enzyme
PDCD6IP	NM_013374	programmed cell death 6 interacting protein	4.73E-02	Cytoplasm	other
PDGFD	NM_025208	platelet derived growth factor D	6.00E-04	Extracellular Space	growth factor
PGLS	NM_012088	6-phosphogluconolactonase	1.31E-02	Cytoplasm	enzyme
PIGF	NM_173074	phosphatidylinositol glycan anchor biosynthesis, class F	2.27E-02	Cytoplasm	enzyme
PLCL2	NM_015184	phospholipase C-like 2	4.21E-02	Cytoplasm	enzyme
POLR2G	NM_002696	polymerase (RNA) II (DNA directed) polypeptide G	1.23E-02	Nucleus	enzyme

Appendix V-III. (continued) Predicted target genes of hsa-miR-221 based upon miRWalk target comparison.

Gene Symbol	Accession Number	Gene Name	p-value	Location	Type
PPP3R1	NM_000945	protein phosphatase 3, regulatory subunit B, alpha	3.31E-02	Cytoplasm	phosphatase
PRKAR2A	NM_004157	protein kinase, cAMP-dependent, regulatory, type II, alpha	1.40E-02	Cytoplasm	kinase
PRPS1	NM_002764	phosphoribosyl pyrophosphate synthetase 1	1.51E-02	Cytoplasm	kinase
PSPH	NM_004577	phosphoserine phosphatase	4.39E-02	Cytoplasm	phosphatase
PTP4A3	NM_032611	protein tyrosine phosphatase type IVA, member 3	8.20E-03	Plasma Membrane	phosphatase
PTPRM	NM_001105244	protein tyrosine phosphatase, receptor type, M	1.10E-02	Plasma Membrane	phosphatase
RAB1A	NM_004161	RAB1A, member RAS oncogene family	2.48E-02	Cytoplasm	enzyme
RAB3A	NM_002866	RAB3A, member RAS oncogene family	4.16E-02	Cytoplasm	enzyme
RALA	NM_005402	v-ral simian leukemia viral oncogene homolog A	2.85E-02	Cytoplasm	enzyme
RBBP7	NM_002893	retinoblastoma binding protein 7	2.32E-02	Nucleus	transcription regulator
RBCK1	NM_031229	RanBP-type and C3HC4-type zinc finger containing 1	2.10E-03	Cytoplasm	transcription regulator
RGS7	NM_002924	regulator of G-protein signaling 7	3.87E-02	Cytoplasm	enzyme
RGS10	NM_001005339	regulator of G-protein signaling 10	1.77E-02	Cytoplasm	other
RNLS	NM_018363	renalase, FAD-dependent amine oxidase	1.66E-02	Extracellular Space	other
S100B	NM_006272	S100 calcium binding protein B	4.45E-02	Cytoplasm	other
SAFB	NM_002967	scaffold attachment factor B	1.32E-02	Nucleus	other
SAP130	NM_024545	Sin3A-associated protein, 130kDa	4.79E-02	Nucleus	transcription regulator
SCD5	NM_001037582	stearoyl-CoA desaturase 5	2.70E-02	Cytoplasm	enzyme
SEMA3C	NM_006379	sema domain, immunoglobulin domain, short basic domain, secreted, 3C	3.55E-02	Extracellular Space	other
SERPINA3	NM_001085	serpin peptidase inhibitor, clade A, member 3	1.68E-02	Extracellular Space	other
SF3B4	NM_005850	splicing factor 3b, subunit 4	1.48E-02	Nucleus	other
SHANK2	NM_012309	SH3 and multiple ankyrin repeat domains 2	1.89E-02	Plasma Membrane	other
SIGIRR	NM_021805	single immunoglobulin and toll-interleukin 1 receptor (TIR) domain	3.00E-03	Plasma Membrane	transmembrane receptor
SMARCA1	NM_003069	SWI/SNF related, matrix associated, actin dependent regulator of chromatin, subfamily a, member 1	4.90E-02	Nucleus	transcription regulator
SMC2	NM_001042550	structural maintenance of chromosomes 2	8.00E-03	Nucleus	transporter
SMC1A	NM_006306	structural maintenance of chromosomes 1A	2.25E-02	Nucleus	transporter
SMURF1	NM_020429	SMAD specific E3 ubiquitin protein ligase 1	4.68E-02	Cytoplasm	enzyme
SNAP23	NM_003825	synaptosomal-associated protein, 23kDa	2.38E-02	Plasma Membrane	transporter
SNF8	NM_007241	SNF8, ESCRT-II complex subunit, homolog	2.36E-02	Cytoplasm	enzyme
SNRNP48	NM_152551	small nuclear ribonucleoprotein 48kDa	4.61E-02	Nucleus	other
SOCS3	NM_003955	suppressor of cytokine signaling 3	2.49E-02	Cytoplasm	phosphatase
SOD2	NM_000636	superoxide dismutase 2, mitochondrial	1.17E-02	Cytoplasm	enzyme
SOX10	NM_006941	SRY (sex determining region Y)-box 10	1.82E-02	Nucleus	transcription regulator
SRGAP1	NM_020762	SLIT-ROBO Rho GTPase activating protein 1	1.68E-02	Cytoplasm	other
SSRP1	NM_003146	structure specific recognition protein 1	6.50E-03	Nucleus	other
STAT2	NM_005419	signal transducer and activator of transcription 2	2.73E-02	Nucleus	transcription regulator
STMN1	NM_203401	stathmin 1	3.50E-03	Cytoplasm	other
STRAP	NM_007178	serine/threonine kinase receptor associated protein	3.11E-02	Plasma Membrane	other
STYX	NM_145251	serine/threonine/tyrosine interacting protein	1.48E-02	Cytoplasm	phosphatase
T	NM_003181	T, brachyury homolog	1.09E-02	Nucleus	transcription regulator
TAF1A	NM_005681	TATA box binding protein (TBP)-associated factor, RNA polymerase I, A	2.12E-02	Nucleus	transcription regulator
TAPBP	NM_003190	TAP binding protein (tapasin)	3.17E-02	Cytoplasm	transporter
TARS2	NM_025150	threonyl-tRNA synthetase 2, mitochondrial	1.37E-02	Cytoplasm	enzyme
TARSL2	NM_152334	threonyl-tRNA synthetase-like 2	4.97E-02	unknown	enzyme
TCF12	NM_207037	transcription factor 12	3.58E-02	Nucleus	transcription regulator
TFRC	NM_003234	transferrin receptor	1.02E-02	Plasma Membrane	transporter
THBS1	NM_003246	thrombospondin 1	3.19E-02	Extracellular Space	other
THBS2	NM_003247	thrombospondin 2	3.09E-02	Extracellular Space	other

Appendix V-III. (continued) Predicted target genes of hsa-miR-221 based upon miRWalk target comparison.

Gene Symbol	Accession Number	Gene Name	p-value	Location	Type
TIMP4	NM_003256	TIMP metallopeptidase inhibitor 4	2.89E-02	Extracellular Space	other
TNF	NM_000594	tumor necrosis factor	4.75E-02	Extracellular Space	cytokine
TNFSF13B	NM_006573	tumor necrosis factor (ligand) superfamily, member 13b	4.80E-03	Extracellular Space	cytokine
TOPBP1	NM_007027	topoisomerase (DNA) II binding protein 1	4.05E-02	Nucleus	other
TP53BP2	NM_005426	tumor protein p53 binding protein, 2	1.00E-04	Nucleus	other
TRAF2	NM_021138	TNF receptor-associated factor 2	4.39E-02	Cytoplasm	enzyme
TRPC1	NM_003304	transient receptor potential cation channel, subfamily C, member 1	2.50E-02	Plasma Membrane	ion channel
TSC22D3	NM_198057	TSC22 domain family, member 3	5.10E-03	Nucleus	transcription regulator
TSEN54	NM_207346	tRNA splicing endonuclease 54 homolog (S. cerevisiae)	2.15E-02	Nucleus	enzyme
TUBA1A	NM_006009	tubulin, alpha 1a	1.35E-02	Cytoplasm	other
UBE2N	NM_003348	ubiquitin-conjugating enzyme E2N	2.62E-02	Cytoplasm	enzyme
USP5	NM_001098536	ubiquitin specific peptidase 5	3.47E-02	Cytoplasm	peptidase
USP21	NM_001014443	ubiquitin specific peptidase 21	1.71E-02	Cytoplasm	peptidase
USP39	NM_006590	ubiquitin specific peptidase 39	3.01E-02	Nucleus	peptidase
USP53	NM_019050	ubiquitin specific peptidase 53	3.48E-02	Extracellular Space	enzyme
USP6NL	NM_001080491	USP6 N-terminal like	2.90E-02	Plasma Membrane	other
VCAM1	NM_001078	vascular cell adhesion molecule 1	4.64E-02	Plasma Membrane	transmembrane receptor
VPS37A	NM_152415	vacuolar protein sorting 37 homolog A	8.40E-03	Cytoplasm	other
WWTR1	NM_015472	WW domain containing transcription regulator 1	3.47E-02	Nucleus	transcription regulator
YWHAG	NM_012479	tyrosine 3-monooxygenase/tryptophan 5-monooxygenase activation protein, gamma polypeptide	4.21E-02	Cytoplasm	other
ZCRB1	NM_033114	zinc finger CCHC-type and RNA binding motif 1	1.49E-02	Nucleus	other
ZEB2	NM_014795	zinc finger E-box binding homeobox 2	2.20E-02	Nucleus	transcription regulator
ZYX	NM_003461	zyxin	2.70E-02	Plasma Membrane	other

Appendix V-III. (continued) Predicted target genes of hsa-miR-221 based upon miRWalk target comparison.

Gene Symbol	Accession Number	Gene Name	p-value	Location	Type
ACACA	NM_198839	acetyl-CoA carboxylase alpha	3.53E-02	Cytoplasm	enzyme
ADAM10	NM_001110	ADAM metallopeptidase domain 10	1.87E-02	Plasma Membrane	peptidase
ADCK3	NM_020247	aarF domain containing kinase 3	4.86E-02	Cytoplasm	kinase
ADCY7	NM_001114	adenylate cyclase 7	3.93E-02	Plasma Membrane	enzyme
ADRA1A	NM_033303	adrenoceptor alpha 1A	2.65E-02	Plasma Membrane	G-protein coupled receptor
AKR1B1	NM_001628	aldo-keto reductase family 1, member B1 (aldose reductase)	5.90E-03	Cytoplasm	enzyme
ARHGEF3	NM_001128616	Rho guanine nucleotide exchange factor (GEF) 3	2.80E-02	Cytoplasm	other
ATF2	NM_001880	activating transcription factor 2	5.10E-03	Nucleus	transcription regulator
BARD1	NM_000465	BRCA1 associated RING domain 1	8.60E-03	Nucleus	transcription regulator
CAB39	NM_001130849	calcium binding protein 39	3.58E-02	Cytoplasm	enzyme
CAV1	NM_001753	caveolin 1, caveolae protein, 22kDa	2.84E-02	Plasma Membrane	transmembrane receptor
CDKN2B	NM_078487	cyclin-dependent kinase inhibitor 2B (p15, inhibits CDK4)	1.29E-02	Nucleus	transcription regulator
CDKN2D	NM_001800	cyclin-dependent kinase inhibitor 2D (p19, inhibits CDK4)	3.67E-02	Cytoplasm	transcription regulator
CERK	NM_022766	ceramide kinase	2.60E-03	Plasma Membrane	kinase
CRABP1	NM_004378	cellular retinoic acid binding protein 1	1.59E-02	Cytoplasm	transporter
CSE1L	NM_001316	CSE1 chromosome segregation 1-like (yeast)	3.18E-02	Nucleus	transporter
CYP27B1	NM_000785	cytochrome P450, family 27, subfamily B, polypeptide 1	4.90E-02	Cytoplasm	enzyme
EHF	NM_012153	ets homologous factor	3.89E-02	Nucleus	transcription regulator
EIF2AK3	NM_004836	eukaryotic translation initiation factor 2-alpha kinase 3	3.80E-03	Cytoplasm	kinase
ERCC2	NM_000400	excision repair cross-complementing rodent repair deficiency, complementation group 2	1.44E-02	Nucleus	enzyme
FDFT1	NM_004462	farnesyl-diphosphate farnesyltransferase 1	4.24E-02	Cytoplasm	enzyme
GDI1	NM_001493	GDP dissociation inhibitor 1	4.88E-02	Cytoplasm	other
GDI2	NM_001494	GDP dissociation inhibitor 2	4.84E-02	Cytoplasm	other
IL6R	NM_000565	interleukin 6 receptor	3.50E-02	Plasma Membrane	transmembrane receptor
KLF8	NM_007250	Kruppel-like factor 8	3.70E-02	Nucleus	other
LSS	NM_002340	lanosterol synthase (2,3-oxidosqualene-lanosterol cyclase)	3.00E-02	Cytoplasm	enzyme
MAP3K1	NM_005921	mitogen-activated protein kinase kinase kinase 1, E3 ubiquitin protein ligase	9.40E-03	Cytoplasm	kinase
MIF	NM_002415	macrophage migration inhibitory factor (glycosylation-inhibiting factor)	1.80E-03	Extracellular Space	cytokine
MPRIP	NM_201274	myosin phosphatase Rho interacting protein	4.70E-02	Cytoplasm	other
MST4	NM_016542	serine/threonine protein kinase MST4	6.80E-03	Nucleus	kinase
NEDD9	NM_006403	neural precursor cell expressed, developmentally down-regulated 9	2.82E-02	Nucleus	other
NSMAF	NM_003580	neutral sphingomyelinase (N-SMase) activation associated factor	9.30E-03	Cytoplasm	other
OXCT1	NM_000436	3-oxoacid CoA transferase 1	2.53E-02	Cytoplasm	enzyme
OXTR	NM_000916	oxytocin receptor	9.80E-03	Plasma Membrane	G-protein coupled receptor
PDXK	NM_003681	pyridoxal (pyridoxine, vitamin B6) kinase	1.50E-03	Cytoplasm	kinase
PLEKHG2	NM_022835	pleckstrin homology domain containing, family G (with RhoGef domain) member 2	4.70E-02	Cytoplasm	other
PRDX4	NM_006406	peroxiredoxin 4	3.80E-03	Cytoplasm	enzyme
PSMB8	NM_004159	proteasome (prosome, macropain) subunit, beta type, 8	1.58E-02	Cytoplasm	peptidase
PTGES2	NM_025072	prostaglandin E synthase 2	3.05E-02	Cytoplasm	transcription regulator
RPL13	NM_033251	ribosomal protein L13	6.40E-03	Cytoplasm	other
SLC16A3	NM_001042422	solute carrier family 16, member 3 (monocarboxylic acid transporter 4)	7.90E-03	Plasma Membrane	transporter
SMARCA2	NM_003070	SWI/SNF related, matrix associated, actin dependent regulator of chromatin, subfamily a, member 2	1.00E-04	Nucleus	transcription regulator
SNRNP48	NM_152551	small nuclear ribonucleoprotein 48kDa (U11/U12)	4.61E-02	Nucleus	other
STX4	NM_004604	syntaxin 4	1.72E-02	Plasma Membrane	transporter
SWAP70	NM_015055	SWAP switching B-cell complex 70kDa subunit	1.13E-02	Cytoplasm	other
TEAD2	NM_003598	TEA domain family member 2	4.68E-02	Nucleus	transcription regulator
TOP2B	NM_001068	topoisomerase (DNA) II beta 180kDa	1.95E-02	Nucleus	enzyme
TUBB3	NM_006086	tubulin, beta 3 class III	1.92E-02	Cytoplasm	other

Appendix V-IV. Predicted target genes of hsa-miR-451 based upon miRWalk target comparison.

Gene Symbol	Accession Number	Gene Name	p-value	Location	Type
ABAT	NM_000663	4-aminobutyrate aminotransferase	4.69E-02	Cytoplasm	enzyme
ABCG8	NM_022437	ATP-binding cassette, sub-family G, member 8	3.40E-02	Plasma Membrane	transporter
ABLIM1	NM_001003408	actin binding LIM protein 1	1.95E-02	Cytoplasm	other
ABR	NM_021962	active BCR-related	2.50E-03	Cytoplasm	other
ACACA	NM_198839	acetyl-CoA carboxylase alpha	3.53E-02	Cytoplasm	enzyme
ACADS	NM_000017	acyl-CoA dehydrogenase, C-2 to C-3 short chain	3.46E-02	Cytoplasm	enzyme
ACOT13	NM_018473	acyl-CoA thioesterase 13	4.00E-04	Cytoplasm	enzyme
ACTA1	NM_001100	actin, alpha 1, skeletal muscle	4.10E-03	Cytoplasm	other
ACTN1	NM_001130004	actinin, alpha 1	4.50E-02	Cytoplasm	other
ACTR3	NM_005721	ARP3 actin-related protein 3 homolog	1.74E-02	Plasma Membrane	other
ADAR	NM_001111	adenosine deaminase, RNA-specific	1.05E-02	Nucleus	enzyme
ADCY3	NM_004036	adenylate cyclase 3	1.18E-02	Plasma Membrane	enzyme
ADIPOR2	NM_024551	adiponectin receptor 2	3.92E-02	Plasma Membrane	other
AGPAT2	NM_006412	1-acylglycerol-3-phosphate O-acyltransferase 2	9.70E-03	Cytoplasm	enzyme
AHCYL1	NM_006621	adenosylhomocysteinase-like 1	7.80E-03	Cytoplasm	enzyme
AK5	NM_012093	adenylate kinase 5	2.00E-02	Cytoplasm	kinase
AKAP10	NM_007202	A kinase (PRKA) anchor protein 10	4.78E-02	Cytoplasm	other
ALDH3A2	NM_001031806	aldehyde dehydrogenase 3 family, member A2	3.12E-02	Cytoplasm	enzyme
ALPL	NM_000478	alkaline phosphatase, liver/bone/kidney	4.56E-02	Plasma Membrane	phosphatase
ARHGAP10	NM_024605	Rho GTPase activating protein 10	1.08E-02	Cytoplasm	other
ARHGAP22	NM_021226	Rho GTPase activating protein 22	1.50E-03	Cytoplasm	other
ARRB2	NM_004313	arrestin, beta 2	2.88E-02	Cytoplasm	other
ATP1A1	NM_000701	ATPase, Na+/K+ transporting, alpha 1 polypeptide	1.30E-03	Plasma Membrane	transporter
ATP2C2	NM_014861	ATPase, Ca++ transporting, type 2C, member 2	2.85E-02	Cytoplasm	enzyme
AXL	NM_021913	AXL receptor tyrosine kinase	2.81E-02	Plasma Membrane	kinase
BCAP31	NM_005745	B-cell receptor-associated protein 31	2.70E-02	Cytoplasm	transporter
BCL11A	NM_022893	B-cell CLL/lymphoma 11A	4.78E-02	Nucleus	transcription regulator
BCR	NM_004327	breakpoint cluster region	9.50E-03	Cytoplasm	kinase
BDKRB2	NM_000623	bradykinin receptor B2	4.22E-02	Plasma Membrane	G-protein coupled receptor
BDNF	NM_170735	brain-derived neurotrophic factor	4.39E-02	Extracellular Space	growth factor
BLOC1S6	NM_012388	biogenesis of lysosomal organelles complex-1, subunit 6, pallidin	3.10E-03	Cytoplasm	other
CABLES1	NM_001100619	Cdk5 and Abl enzyme substrate 1	4.65E-02	Nucleus	other
CACNA1E	NM_000721	calcium channel, voltage-dependent, R type, alpha 1E subunit	4.12E-02	Plasma Membrane	ion channel
CAMKK1	NM_032294	calcium/calmodulin-dependent protein kinase kinase 1, alpha	2.88E-02	Cytoplasm	kinase
CARD10	NM_014550	caspase recruitment domain family, member 10	1.23E-02	Cytoplasm	other
CCK	NM_000729	cholecystokinin	4.50E-03	Extracellular Space	other
CCL2	NM_002982	chemokine (C-C motif) ligand 2	2.33E-02	Extracellular Space	cytokine
CCR7	NM_001838	chemokine (C-C motif) receptor 7	1.50E-02	Plasma Membrane	G-protein coupled receptor
CD22	NM_001771	CD22 molecule	0.00E00	Plasma Membrane	transmembrane receptor
CD83	NM_004233	CD83 molecule	2.53E-02	Plasma Membrane	transmembrane receptor
CD151	NM_004357	CD151 molecule	1.01E-02	Plasma Membrane	other
CDC42BPB	NM_006035	CDC42 binding protein kinase beta	2.01E-02	Cytoplasm	kinase
CDK3	NM_001258	cyclin-dependent kinase 3	9.00E-03	unknown	kinase
CHMP3	NM_016079	charged multivesicular body protein 3	9.00E-03	Cytoplasm	other
CHST3	NM_004273	carbohydrate (chondroitin 6) sulfotransferase 3	1.93E-02	Cytoplasm	enzyme
CHST7	NM_019886	carbohydrate (N-acetylglucosamine 6-O) sulfotransferase 7	4.15E-02	Cytoplasm	enzyme
CREBBP	NM_004380	CREB binding protein	3.98E-02	Nucleus	transcription regulator
CSF1R	NM_005211	colony stimulating factor 1 receptor	1.21E-02	Plasma Membrane	kinase

Appendix V-V. Predicted target genes of hsa-miR-574 based upon miRWalk target comparison.

Gene Symbol	Accession Number	Gene Name	p-value	Location	Type
CTSD	NM_001909	cathepsin D	3.20E-03	Cytoplasm	peptidase
CTSL1	NM_001912	cathepsin L1	5.80E-03	Cytoplasm	peptidase
CXCL2	NM_002089	chemokine (C-X-C motif) ligand 2	4.47E-02	Extracellular Space	cytokine
DDR1	NM_013993	discoidin domain receptor tyrosine kinase 1	1.33E-02	Plasma Membrane	kinase
DDX58	NM_014314	DEAD (Asp-Glu-Ala-Asp) box polypeptide 58	1.70E-03	Cytoplasm	enzyme
DLG2	NM_001364	discs, large homolog 2	0.00E00	Plasma Membrane	kinase
DNAJA1	NM_001539	DnaJ (Hsp40) homolog, subfamily A, member 1	9.80E-03	Nucleus	other
DNASE1	NM_005223	deoxyribonuclease I	1.00E-04	Extracellular Space	enzyme
DPAGT1	NM_001382	dolichyl-phosphate (UDP-N-acetylglucosamine) N-acetylglucosaminephosphotransferase 1	7.60E-03	Cytoplasm	enzyme
DSCR3	NM_006052	Down syndrome critical region gene 3	3.18E-02	Nucleus	other
EBP	NM_006579	emopamil binding protein	4.50E-03	Cytoplasm	enzyme
ECE1	NM_001113347	endothelin converting enzyme 1	4.07E-02	Plasma Membrane	peptidase
ELK4	NM_021795	ELK4, ETS-domain protein	6.00E-04	Nucleus	transcription regulator
ELOVL6	NM_024090	ELOVL fatty acid elongase 6	1.00E-04	Cytoplasm	enzyme
EMP2	NM_001424	epithelial membrane protein 2	1.70E-02	Plasma Membrane	other
EXOC4	NM_021807	exocyst complex component 4	1.88E-02	Cytoplasm	transporter
FAAH	NM_001441	fatty acid amide hydrolase	1.71E-02	Plasma Membrane	enzyme
FANCE	NM_021922	Fanconi anemia, complementation group E	4.59E-02	Nucleus	other
FGF18	NM_003862	fibroblast growth factor 18	5.90E-03	Extracellular Space	growth factor
FHOD3	NM_025135	formin homology 2 domain containing 3	3.15E-02	Nucleus	other
FMO2	NM_001460	flavin containing monooxygenase 2	1.38E-02	Cytoplasm	enzyme
FSHB	NM_000510	follicle stimulating hormone, beta polypeptide	2.23E-02	Extracellular Space	other
G6PC3	NM_138387	glucose 6 phosphatase, catalytic, 3	1.82E-02	Cytoplasm	phosphatase
GABRA5	NM_000810	gamma-aminobutyric acid (GABA) A receptor, alpha 5	3.74E-02	Plasma Membrane	ion channel
GALK2	NM_001001556	galactokinase 2	2.48E-02	Cytoplasm	kinase
GAPDH	NM_002046	glyceraldehyde-3-phosphate dehydrogenase	3.00E-03	Cytoplasm	enzyme
GLG1	NM_012201	golgi glycoprotein 1	2.20E-03	Cytoplasm	other
GNPDA1	NM_005471	glucosamine-6-phosphate deaminase 1	2.07E-02	Cytoplasm	enzyme
GPNMB	NM_001005340	glycoprotein (transmembrane) nmb	3.40E-03	Plasma Membrane	enzyme
GTF3C2	NM_001521	general transcription factor IIIC, polypeptide 2, beta	4.97E-02	Nucleus	transcription regulator
HADH	NM_005327	hydroxyacyl-CoA dehydrogenase	4.97E-02	Cytoplasm	enzyme
HADHB	NM_000183	hydroxyacyl-CoA dehydrogenase/3-ketoacyl-CoA thiolase/enoyl-CoA hydratase, beta subunit	3.12E-02	Cytoplasm	enzyme
HHIP	NM_022475	hedgehog interacting protein	1.17E-02	Plasma Membrane	other
HIBADH	NM_152740	3-hydroxyisobutyrate dehydrogenase	4.77E-02	Cytoplasm	enzyme
HLTF	NM_003071	helicase-like transcription factor	8.00E-03	Nucleus	transcription regulator
HOXB4	NM_024015	homeobox B4	0.00E00	Nucleus	transcription regulator
HOXC6	NM_153693	homeobox C6	3.30E-03	Nucleus	transcription regulator
HS3ST3B1	NM_006041	heparan sulfate (glucosamine) 3-O-sulfotransferase 3B1	3.18E-02	Cytoplasm	enzyme
HTR3A	NM_213621	5-hydroxytryptamine (serotonin) receptor 3A, ionotropic	3.43E-02	Plasma Membrane	ion channel
HYAL1	NM_007312	hyaluronoglucosaminidase 1	3.55E-02	Cytoplasm	enzyme
IDH3B	NM_174856	isocitrate dehydrogenase 3 (NAD+) beta	2.24E-02	Cytoplasm	enzyme
IDH3G	NM_174869	isocitrate dehydrogenase 3 (NAD+) gamma	2.38E-02	Cytoplasm	enzyme
IL32	NM_001012631	interleukin 32	4.70E-03	Extracellular Space	cytokine
IL10RB	NM_000628	interleukin 10 receptor, beta	1.30E-02	Plasma Membrane	transmembrane receptor
IL22RA1	NM_021258	interleukin 22 receptor, alpha 1	4.00E-03	Plasma Membrane	transmembrane receptor
IRF2	NM_002199	interferon regulatory factor 2	1.59E-02	Nucleus	transcription regulator
KCNJ4	NM_152868	potassium inwardly-rectifying channel, subfamily J, member 4	7.10E-03	Plasma Membrane	ion channel
KLF8	NM_007250	Kruppel-like factor 8	9.40E-03	Nucleus	other

Appendix V-V. (continued) Predicted target genes of hsa-miR-574 based upon miRWalk target comparison.

Gene Symbol	Accession Number	Gene Name	p-value	Location	Type
LCOR	NM_032440	ligand dependent nuclear receptor corepressor	1.14E-02	Nucleus	transcription regulator
LETM1	NM_012318	leucine zipper-EF-hand containing transmembrane protein 1	4.39E-02	Cytoplasm	other
MAFK	NM_002360	v-maf musculoaponeurotic fibrosarcoma oncogene homolog K	1.01E-02	Nucleus	transcription regulator
MAML3	NM_018717	mastermind-like 3	4.38E-02	Nucleus	transcription regulator
MAP1LC3B	NM_022818	microtubule-associated protein 1 light chain 3 beta	2.55E-02	Cytoplasm	other
MEF2C	NM_002397	myocyte enhancer factor 2C	1.65E-02	Nucleus	transcription regulator
MKI67	NM_002417	antigen identified by monoclonal antibody Ki-67	9.60E-03	Nucleus	other
MLXIP	NM_014938	MLX interacting protein	3.95E-02	Nucleus	other
MMP3	NM_002422	matrix metallopeptidase 3	5.00E-03	Extracellular Space	peptidase
MMP25	NM_022468	matrix metallopeptidase 25	2.47E-02	Extracellular Space	peptidase
MNT	NM_020310	MNT, MAX dimerization protein	7.00E-04	Nucleus	transcription regulator
MORF4L1	NM_206839	mortality factor 4 like 1	2.60E-03	Nucleus	other
MPP5	NM_022474	membrane protein, palmitoylated 5	4.30E-02	Plasma Membrane	kinase
MPRIP	NM_201274	myosin phosphatase Rho interacting protein	1.20E-02	Cytoplasm	other
MX1	NM_002462	myxovirus resistance 1, interferon-inducible protein p78	2.73E-02	Cytoplasm	enzyme
MYBL1	NM_001080416	v-myb myeloblastosis viral oncogene homolog (avian)-like 1	3.77E-02	Nucleus	transcription regulator
NDUFA8	NM_014222	NADH dehydrogenase (ubiquinone) 1 alpha subcomplex, 8	1.20E-02	Cytoplasm	enzyme
NFIC	NM_205843	nuclear factor I/C	8.00E-04	Nucleus	transcription regulator
NGEF	NM_019850	neuronal guanine nucleotide exchange factor	4.78E-02	Cytoplasm	other
NME3	NM_002513	NME/NM23 nucleoside diphosphate kinase 3	2.13E-02	Cytoplasm	kinase
NMNAT2	NM_015039	nicotinamide nucleotide adenylyltransferase 2	0.00E00	Cytoplasm	enzyme
NOSTRIN	NM_001039724	nitric oxide synthase trafficker	6.60E-03	Cytoplasm	transcription regulator
NR3C2	NM_000901	nuclear receptor subfamily 3, group C, member 2	3.86E-02	Nucleus	ligand-dependent nuclear receptor
NRGN	NM_001126181	neurogranin	1.29E-02	Cytoplasm	other
NT5C3A	NM_001002009	5'-nucleotidase, cytosolic IIIA	9.10E-03	Cytoplasm	phosphatase
ORAI1	NM_032790	ORAI calcium release-activated calcium modulator 1	1.50E-03	Plasma Membrane	ion channel
PADI4	NM_012387	peptidyl arginine deiminase, type IV	3.70E-03	Cytoplasm	enzyme
PAX6	NM_000280	paired box 6	1.20E-03	Nucleus	transcription regulator
PFKFB4	NM_004567	6-phosphofructo-2-kinase/fructose-2,6-biphosphatase 4	7.90E-03	Cytoplasm	kinase
PGS1	NM_024419	phosphatidylglycerophosphate synthase 1	3.14E-02	Cytoplasm	enzyme
PIAS4	NM_015897	protein inhibitor of activated STAT, 4	1.77E-02	Nucleus	transcription regulator
PIN1	NM_006221	peptidylprolyl cis/trans isomerase, NIMA-interacting 1	2.90E-02	Nucleus	enzyme
PIP5K1C	NM_012398	phosphatidylinositol-4-phosphate 5-kinase, type I, gamma	2.80E-03	Plasma Membrane	kinase
PMVK	NM_006556	phosphomevalonate kinase	2.44E-02	Cytoplasm	kinase
POLR1D	NM_152705	polymerase (RNA) I polypeptide D	2.25E-02	Nucleus	enzyme
PPP2R5B	NM_006244	protein phosphatase 2, regulatory subunit B', beta	3.78E-02	Cytoplasm	phosphatase
PPP3R2	NM_147180	protein phosphatase 3, regulatory subunit B, beta	4.19E-02	Cytoplasm	phosphatase
PPT1	NM_000310	palmitoyl-protein thioesterase 1	2.08E-02	Cytoplasm	enzyme
PRKACB	NM_002731	protein kinase, cAMP-dependent, catalytic, beta	4.78E-02	Cytoplasm	kinase
PRKDC	NM_006904	protein kinase, DNA-activated, catalytic polypeptide	1.61E-02	Nucleus	kinase
PRMT2	NM_206962	protein arginine methyltransferase 2	3.79E-02	Nucleus	enzyme
PSMB7	NM_002799	proteasome (prosome, subunit, beta type, 7	9.80E-03	Cytoplasm	peptidase
PSMD9	NM_002813	proteasome (prosome, 26S subunit, non-ATPase, 9	2.37E-02	Cytoplasm	transcription regulator
PTP4A2	NM_080391	protein tyrosine phosphatase type IVA, member 2	3.95E-02	Cytoplasm	phosphatase
PTPN3	NM_002829	protein tyrosine phosphatase, non-receptor type 3	2.02E-02	Cytoplasm	phosphatase
PVRL1	NM_002855	poliovirus receptor-related 1	1.43E-02	Plasma Membrane	other
RAB3B	NM_002867	RAB3B, member RAS oncogene family	1.18E-02	Cytoplasm	enzyme
RAB5B	NM_002868	RAB5B, member RAS oncogene family	3.79E-02	Cytoplasm	enzyme

Appendix V-V. (continued) Predicted target genes of hsa-miR-574 based upon miRWalk target comparison.

Gene Number	Accession Number	Gene Name	p-value	Location	Type
RALB	NM_002881	v-ral simian leukemia viral oncogene homolog B	3.00E-04	Cytoplasm	enzyme
RALBP1	NM_006788	ralA binding protein 1	1.00E-04	Cytoplasm	enzyme
RBCK1	NM_031229	RanBP-type and C3HC4-type zinc finger containing 1	3.31E-02	Cytoplasm	transcription regulator
RHOU	NM_021205	ras homolog family member U	4.43E-02	Cytoplasm	enzyme
RNF19A	NM_183419	ring finger protein 19A, E3 ubiquitin protein ligase	5.80E-03	Nucleus	enzyme
SAP130	NM_024545	Sin3A-associated protein, 130kDa	4.79E-02	Nucleus	transcription regulator
SFN	NM_006142	stratifin	3.11E-02	Cytoplasm	other
SH3GLB2	NM_020145	SH3-domain GRB2-like endophilin B2	1.07E-02	Cytoplasm	other
SLC22A4	NM_003059	solute carrier family 22 (organic cation/ergothioneine transporter), member 4	2.37E-02	Plasma Membrane	transporter
SLC27A5	NM_012254	solute carrier family 27 (fatty acid transporter), member 5	3.10E-03	Cytoplasm	transporter
SLC7A1	NM_003045	solute carrier family 7 (cationic amino acid transporter, y+ system), member 1	1.20E-03	Plasma Membrane	transporter
SLC9A1	NM_003047	solute carrier family 9, subfamily A (NHE1, cation proton antiporter 1), member 1	4.00E-04	Plasma Membrane	ion channel
SLIT2	NM_004787	slit homolog 2 (Drosophila)	2.40E-03	Extracellular Space	other
SMAD4	NM_005359	SMAD family member 4	2.48E-02	Nucleus	transcription regulator
SMURF1	NM_020429	SMAD specific E3 ubiquitin protein ligase 1	4.68E-02	Cytoplasm	enzyme
SMYD3	NM_022743	SET and MYND domain containing 3	9.00E-04	Nucleus	enzyme
SNAP23	NM_003825	synaptosomal-associated protein, 23kDa	2.38E-02	Plasma Membrane	transporter
SNAP25	NM_003081	synaptosomal-associated protein, 25kDa	4.60E-03	Plasma Membrane	transporter
SOX2	NM_003106	SRY (sex determining region Y)-box 2	1.72E-02	Nucleus	transcription regulator
SOX6	NM_017508	SRY (sex determining region Y)-box 6	0.00E00	Nucleus	transcription regulator
SRD5A3	NM_024592	steroid 5 alpha-reductase 3	2.42E-02	Cytoplasm	enzyme
STAT4	NM_003151	signal transducer and activator of transcription 4	1.57E-02	Nucleus	transcription regulator
T	NM_003181	T, brachyury homolog (mouse)	4.28E-02	Nucleus	transcription regulator
TEAD1	NM_021961	TEA domain family member 1	1.00E-04	Nucleus	transcription regulator
TEAD3	NM_003214	TEA domain family member 3	4.00E-04	Nucleus	transcription regulator
TFAP2C	NM_003222	transcription factor AP-2 gamma	1.96E-02	Nucleus	transcription regulator
TGM2	NM_004613	transglutaminase 2	2.67E-02	Cytoplasm	enzyme
TIMP2	NM_003255	TIMP metallopeptidase inhibitor 2	1.03E-02	Extracellular Space	other
TIPARP	NM_015508	TCDD-inducible poly(ADP-ribose) polymerase	2.46E-02	unknown	other
TIRAP	NM_001039661	toll-interleukin 1 receptor (TIR) domain containing adaptor protein	1.88E-02	Cytoplasm	other
TNNI1	NM_003281	troponin I type 1 (skeletal, slow)	5.20E-03	Cytoplasm	other
TOLLIP	NM_019009	toll interacting protein	4.01E-02	Cytoplasm	other
TRADD	NM_003789	TNFRSF1A-associated via death domain	7.30E-03	Cytoplasm	other
TRAF2	NM_021138	TNF receptor-associated factor 2	4.39E-02	Cytoplasm	enzyme
TRIB2	NM_021643	tribbles homolog 2	2.92E-02	Plasma Membrane	kinase
TSEN15	NM_052965	tRNA splicing endonuclease 15 homolog	2.08E-02	Nucleus	enzyme
TUB	NM_003320	tubby homolog	4.30E-03	Cytoplasm	transcription regulator
UBA52	NM_001033930	ubiquitin A-52 residue ribosomal protein fusion product 1	3.48E-02	Cytoplasm	enzyme
UBE2A	NM_181777	ubiquitin-conjugating enzyme E2A	1.81E-02	Cytoplasm	enzyme
UBE2G1	NM_003342	ubiquitin-conjugating enzyme E2G 1	4.96E-02	Cytoplasm	enzyme
UCK1	NM_031432	uridine-cytidine kinase 1	4.80E-03	Cytoplasm	kinase
USP38	NM_032557	ubiquitin specific peptidase 38	5.80E-03	unknown	peptidase
VIM	NM_003380	vimentin	3.00E-04	Cytoplasm	other
VPS36	NM_016075	vacuolar protein sorting 36 homolog	0.00E00	Cytoplasm	other
VPS37C	NM_017966	vacuolar protein sorting 37 homolog C	2.39E-02	Cytoplasm	other
WASF1	NM_003931	WAS protein family, member 1	4.26E-02	Nucleus	other

Appendix V-V. (continued) Predicted target genes of hsa-miR-574 based upon miRWalk target comparison.

Appendix VI. Putative oncomiR target genes predicted by IPA

Gene Symbol	Accession Number	miRNAs Targeting Gene	p Value Scoring					Total Score	Score + miRNAs Targeting Gene
			miR-24	miR-140-3p	miR-221	miR-451	miR-574		
ABHD2	NM_007011	1		1				1	2
ABL1	NM_007313	1		1				1	2
ACSL1	NM_001995	1		2				2	3
ADAM10	NM_001110	1				1		1	2
ADM	NM_001124	1	1					1	2
AIM1	NM_001624	1	1					1	2
AKIP1	NM_182901	1	1					1	2
ALDH1A3	NM_000693	1		2				2	3
ANKS1A	NM_015245	1	3					3	4
ARL4C	NM_005737	1		1				1	2
ARRB2	NM_004313	1					1	1	2
ASAP1	NM_018482	1		1				1	2
ATF2	NM_001880	2		1		2		3	5
ATR	NM_001184	1		1				1	2
ATXN10	NM_013236	1	1					1	2
AURKA	NM_198433	1	1					1	2
BACE1	NM_012104	1		3				3	4
BAG1	NM_004323	1		1				1	2
BAG3	NM_004281	2		1	1			2	4
BARD1	NM_000465	1				2		2	3
BBC3	NM_014417	1	1					1	2
BCAS2	NM_005872	1		2				2	3
BCL11A	NM_022893	1					1	1	2
BCL2	NM_000633	2	2	1				3	5
BCL2L11	NM_138621	1	3					3	4
BCL2L2	NM_004050	2	1	1				2	4
BDKRB2	NM_000623	2	1				1	2	4
CAV1	NM_001753	1				1		1	2
CCK	NM_000729	1					3	3	4
CCL2	NM_002982	1					1	1	2
CCNG2	NM_004354	1		1				1	2
CCR7	NM_001838	1					1	1	2
CCT3	NM_005998	1	3					3	4
CD151	NM_004357	1					1	1	2
CD74	NM_001025159	1	2					2	3
CD82	NM_002231	1		1				1	2
CDC25A	NM_001789	2	1	1				2	4
CDC42BPB	NM_006035	1					1	1	2
CDC73	NM_024529	1	1					1	2
CDK3	NM_001258	1					2	2	3
CDK5	NM_004935	1	1					1	2
CDKN1B	NM_004064	1	2					2	3
CDKN1C	NM_000076	1	1					1	2
CDKN2B	NM_078487	1				1		1	2
CENPA	NM_001809	2		1	1			2	4
CENPE	NM_001813	1		1				1	2
CHTF18	NM_022092	1	2					2	3
CLDN4	NM_001305	1	3					3	4
CLTC	NM_004859	1	1					1	2
CREB1	NM_134442	2		1	2			3	5
CREBBP	NM_004380	1					1	1	2
CSE1L	NM_001316	1				1		1	2
CSF1	NM_000757	1		1				1	2

Appendix VI. Predicted oncomiR target genes linked to *p16* expression and cell proliferation by IPA.

Blue rows mark the top 116 genes selected for future study, based upon their score.

Gene Symbol	Accession Number	miRNAs Targeting Gene	p Value Scoring					Total Score	Score + miRNAs Targeting Gene
			miR-24	miR-140-3p	miR-221	miR-451	miR-574		
CSF1R	NM_005211	1					1	1	2
CSTF1	NM_001324	1	3					3	4
CTBP1	NM_001012614	1		1				1	2
CTBP2	NM_022802	1		2				2	3
CTR9	NM_014633	1		1				1	2
CTSB	NM_147780	1		1				1	2
CTSD	NM_001909	3	3	1			3	7	10
CTSF	NM_003793	1		1				1	2
CXCL2	NM_002089	1					1	1	2
DAB2	NM_001343	1		1				1	2
DDIT3	NM_004083	1	1					1	2
DDX5	NM_004396	1		3				3	4
DHCR24	NM_014762	1	1					1	2
DHX9	NM_001357	1		1				1	2
DIABLO	NM_019887	1		1				1	2
DIAPH1	NM_005219	1	2					2	3
DLC1	NM_182643	1	3					3	4
DNAJA1	NM_001539	1					2	2	3
DNAL4	NM_005740	1	1					1	2
DNMT3B	NM_006892	1			1			1	2
DSCR3	NM_006052	2	1				1	2	4
E2F1	NM_005225	1		3				3	4
EFHD1	NM_025202	1	1					1	2
EGR3	NM_004430	1		1				1	2
EHF	NM_012153	1				1		1	2
ELF3	NM_001114309	1	2					2	3
ELK4	NM_021795	1					4	4	5
EMC9	NM_016049	1	3					3	4
ENC1	NM_003633	1		1				1	2
EPAS1	NM_001430	1	1					1	2
ERBB3	NM_001982	1	3					3	4
ERCC2	NM_000400	1				1		1	2
ERGIC1	NM_020462	1	3					3	4
ERP29	NM_006817	1	1					1	2
FANCD2	NM_033084	1		1				1	2
FBLN1	NM_006486	2	1	1				2	4
FDFT1	NM_004462	1				1		1	2
FDXR	NM_004110	1	2					2	3
FGF7	NM_002009	1		1				1	2
FGF9	NM_002010	2	1	1				2	4
FHOD3	NM_025135	1					1	1	2
FMO2	NM_001460	1					1	1	2
FOS	NM_005252	2	1		1			2	4
FST	NM_006350	1	2					2	3
FSTL3	NM_005860	1		1				1	2
FURIN	NM_002569	1	1					1	2
FXYD5	NM_144779	1		1				1	2
GFPT1	NM_002056	1	1					1	2
GOT1	NM_002079	2	1	1				2	4
GPR56	NM_201524	1	1					1	2
GRB10	NM_001001555	2		1	1			2	4
GRB2	NM_002086	1		2				2	3
GRHL2	NM_024915	1		1				1	2
GRINA	NM_000837	1	1					1	2
GSK3B	NM_002093	1	3					3	4
GSTM3	NM_000849	1		1				1	2
GTF3C4	NM_012204	1		1				1	2
H2AFX	NM_002105	1	1					1	2

Appendix VI. (continued) Predicted oncomiR target genes linked to *p16* expression and cell proliferation by IPA.

Blue rows mark the top 116 genes selected for future study, based upon their score.

Gene Symbol	Accession Number	miRNAs Targeting Gene	p Value Scoring					Total Score	Score + miRNAs Targeting Gene
			miR-24	miR-140-3p	miR-221	miR-451	miR-574		
HBP1	NM_012257	1		1				1	2
HDAC1	NM_004964	1	1					1	2
HENMT1	NM_144584	1		1				1	2
HGS	NM_004712	1		1				1	2
HIST1H2BK	NM_080593	1		1				1	2
HK2	NM_000189	1		2				2	3
HKDC1	NM_025130	1		1				1	2
HMGCS1	NM_001098272	1		1				1	2
HMOX1	NM_002133	1	1				5	6	7
HOXB4	NM_024015	1					5	5	6
HOXB7	NM_004502	3	1	4	1			6	9
HOXC6	NM_153693	1					3	3	4
HOXD10	NM_002148	1		1				1	2
HSF1	NM_005526	1		2				2	3
IDI1	NM_004508	1		3				3	4
IFNG	NM_000619	1	2					2	3
IGFBP5	NM_000599	1	1					1	2
IL1A	NM_000575	1	1					1	2
IL1B	NM_000576	1	1					1	2
IL6R	NM_000565	1				1		1	2
IL8	NM_000584	1		1				1	2
IPP	NM_005897	1		1				1	2
IRF2	NM_002199	1					1	1	2
ITGB3	NM_000212	1	1					1	2
KCNK2	NM_001017424	2	2		4			6	8
KCTD6	NM_153331	1		4				4	5
KDM4B	NM_015015	1		1				1	2
KLF6	NM_001300	1	3					3	4
KLF8	NM_007250	5	3	1	3	1	2	10	15
KLF9	NM_001206	1	1					1	2
KRT7	NM_005556	1	3					3	4
KYNU	NM_003937	1		2				2	3
L1CAM	NM_000425	1		1				1	2
L3MBTL2	NM_031488	1	1					1	2
LAMB3	NM_001017402	2	2		1			3	5
LCOR	NM_032440	2	1				1	2	4
LOX	NM_002317	1	2					2	3
LOXL2	NM_002318	1		1				1	2
LY6K	NM_017527	1	1					1	2
MAP1LC3B	NM_022818	1					1	1	2
MAP3K1	NM_005921	1				2		2	3
MAPK12	NM_002969	2	1		1			2	4
MAPK3	NM_001040056	1	1					1	2
MAPK7	NM_139033	1	2					2	3
MBD1	NM_015846	1		3				3	4
MBD2	NM_003927	1			1			1	2
MBOAT7	NM_024298	1	2					2	3
MCM6	NM_005915	1		1				1	2
MDM2	NM_002392	2	1		2			3	5
MEIS2	NM_170677	1		1				1	2
MIF	NM_002415	1				3		3	4
MINOS1	NM_001032363	1		1				1	2
MKI67	NM_002417	1					2	2	3
MLXIP	NM_014938	2	1				1	2	4
MMP1	NM_002421	1			2			2	3
MMP10	NM_002425	1	1					1	2
MMP14	NM_004995	1	1					1	2
MMP25	NM_022468	1					1	1	2

Appendix VI. (continued) Predicted oncomiR target genes linked to *p16* expression and cell proliferation by IPA.

Blue rows mark the top 116 genes selected for future study, based upon their score.

Gene Symbol	Accession Number	miRNAs Targeting Gene	p Value Scoring					Total Score	Score + miRNAs Targeting Gene
			miR-24	miR-140-3p	miR-221	miR-451	miR-574		
MYB	NM_001130173	1		3				3	4
MYBBP1A	NM_014520	1	2					2	3
MYBL1	NM_001080416	2			1		1	2	4
MYC	NM_002467	1	1					1	2
MYD88	NM_002468	2	1	1				2	4
NAT1	NM_000662	2		2	1			3	5
NCOA5	NM_020967	1	1					1	2
NDUFV3	NM_021075	1	1					1	2
NEDD9	NM_006403	1				1		1	2
NEK2	NM_002497	1	1					1	2
NELL2	NM_006159	1	1					1	2
NFIC	NM_205843	1					4	4	5
NFKBIA	NM_020529	1		1				1	2
NFKBIE	NM_004556	1	5					5	6
NINL	NM_025176	1	1					1	2
NOL3	NM_003946	1	1					1	2
NR1D1	NM_021724	1	1					1	2
NR2C2	NM_003298	1		1				1	2
NR5A2	NM_021005	1		1				1	2
NRG1	NM_013960	1			1			1	2
NRIP1	NM_003489	1		1				1	2
NRP1	NM_003873	1	2					2	3
NRP2	NM_201266	1	1					1	2
OXTR	NM_000916	1				2		2	3
PADI4	NM_012387	2	1				3	4	6
PAK4	NM_001014831	1	1					1	2
PARVA	NM_018222	1	1					1	2
PCBP2	NM_005016	1	1					1	2
PDGFRB	NM_002609	2	1	1				2	4
PDP1	NM_018444	1		1				1	2
PDPK1	NM_002613	1		1				1	2
PEA15	NM_003768	1	1					1	2
PGM1	NM_002633	1		1				1	2
PHLDB1	NM_015157	1		3				3	4
PIK3C2B	NM_002646	1		1				1	2
PIM1	NM_002648	1	1					1	2
PIN1	NM_006221	1					1	1	2
PKIB	NM_181795	1		1				1	2
PKMYT1	NM_182687	1	1					1	2
PLEKHG2	NM_022835	1				1		1	2
PML	NM_033238	1	1					1	2
POU2F2	NM_002698	1		1				1	2
PPARD	NM_006238	1	2					2	3
PPARG	NM_138711	1	3					3	4
PRKCA	NM_002737	1	1					1	2
PRKDC	NM_006904	1					1	1	2
PSG4	NM_002780	1	1					1	2
PTHLH	NM_002820	1	1					1	2
PTK2	NM_153831	1	1					1	2
PTP4A2	NM_080391	2		3			1	4	6
PTPRF	NM_002840	1	1					1	2
PTRF	NM_012232	2	1	1				2	4
RAB5C	NM_201434	1	3					3	4
RALB	NM_002881	1					5	5	6
RAP1A	NM_001010935	1	1					1	2
RBCK1	NM_031229	2			3		1	4	6
RFC2	NM_181471	1	1					1	2
RHOBTB3	NM_014899	1		1				1	2

Appendix VI. (continued) Predicted oncomiR target genes linked to *p16* expression and cell proliferation by IPA.

Blue rows mark the top 116 genes selected for future study, based upon their score.

Gene Symbol	Accession Number	miRNAs Targeting Gene	p Value Scoring					Total Score	Score + miRNAs Targeting Gene
			miR-24	miR-140-3p	miR-221	miR-451	miR-574		
RIPK1	NM_003804	1	2					2	3
RNF41	NM_194358	1	1					1	2
RPTOR	NM_020761	1		1				1	2
RRAS	NM_006270	1	3					3	4
RUVBL1	NM_003707	1		3				3	4
SAFB	NM_002967	1			1			1	2
SCARB1	NM_005505	1	1					1	2
SERPINA1	NM_001127701	1		3				3	4
SERPINH1	NM_001235	1	1					1	2
SERTAD1	NM_013376	1	5					5	6
SFN	NM_006142	1					1	1	2
SH3GLB2	NM_020145	1					1	1	2
SHC1	NM_001130040	1		1				1	2
SIN3A	NM_015477	1	3					3	4
SIRT1	NM_012238	1		1				1	2
SLC7A5	NM_003486	1	1					1	2
SLC9A1	NM_003047	1					5	5	6
SLC9A3R1	NM_004252	1	1					1	2
SLCO4A1	NM_016354	1		2				2	3
SMAD4	NM_005359	1					1	1	2
SMARCA2	NM_003070	2		1		5		6	8
SMARCA4	NM_001128844	1	2					2	3
SMPD1	NM_000543	1		1				1	2
SNX1	NM_003099	1	1					1	2
SOD2	NM_000636	1			1			1	2
SOX2	NM_003106	1					1	1	2
SP100	NM_001080391	1		1				1	2
SPARC	NM_003118	1		1				1	2
SPTAN1	NM_001130438	1	5					5	6
SREBF2	NM_004599	1	1					1	2
SRF	NM_003131	1	1					1	2
STAT5B	NM_012448	1	1					1	2
STC2	NM_003714	1	1					1	2
SULF2	NM_018837	1		3				3	4
SWAP70	NM_015055	2		1		1		2	4
TAB1	NM_006116	2	1	1				2	4
TAB2	NM_015093	2	1	1				2	4
TAGLN	NM_001001522	2	1	1				2	4
TAP1	NM_000593	1		1				1	2
TEAD1	NM_021961	1					5	5	6
TEAD2	NM_003598	1				1		1	2
TEAD3	NM_003214	1					5	5	6
TEP1	NM_007110	1	1					1	2
TFAP2C	NM_003222	1					1	1	2
TFPI	NM_006287	1	1					1	2
TGFB2	NM_003238	1	1					1	2
TGM2	NM_004613	1					1	1	2
TIMP2	NM_003255	1					1	1	2
TNF	NM_000594	2	1		1			2	4
TNFRSF1A	NM_001065	1	1					1	2
TNK2	NM_005781	1	1					1	2
TOP1	NM_003286	1	3					3	4
TP73	NM_005427	1		1				1	2
TPM1	NM_001018004	1		3				3	4
TRADD	NM_003789	1					2	2	3
TRAF1	NM_005658	1	1					1	2
TRAF2	NM_021138	3		1	1		1	3	6
VAV1	NM_003378	1	1					1	2

Appendix VI. (continued) Predicted oncomiR target genes linked to *p16* expression and cell proliferation by IPA.

Blue rows mark the top 116 genes selected for future study, based upon their score.

Gene Symbol	Accession Number	miRNAs Targeting Gene	p Value Scoring					Total Score	Score + miRNAs Targeting Gene
			miR-24	miR-140-3p	miR-221	miR-451	miR-574		
VGF	NM_003378	1	1					1	2
WDR45	NM_007075	1	1					1	2
WDR46	NM_005452	1	3					3	4
WNT4	NM_030761	1	1					1	2
WWOX	NM_016373	1	3					3	4
YWHAB	NM_003404	1		1				1	2
YWHAZ	NM_145690	1		1				1	2
ZFP36	NM_003407	1		1				1	2
ZNF217	NM_006526	1	1					1	2

Appendix VI. (continued) Predicted oncomiR target genes linked to *p16* expression and cell proliferation by IPA.

Blue rows mark the top 116 genes selected for future study, based upon their score.